DIRECT REDUCTION OF IRON ORE IN A ROTARY KILN

A thesis submitted for the

degree of Doctor of Philosophy

by

Seyed Kazem Taheri

Department of Metallurgy,

Brunel University, Great Britain

August 1982

ABSTRACT

Brazilian hematite iron ore was reduced successfully in a rotary kiln with a gaseous reactant which was prepared by reforming butane within the kiln, using the beneficial effect of iron/iron oxide as an autocatalyst. The optimum ratio of the gaseous reactants, $H_2/CO_2/C_4H_{10}$, was used to prevent undesirable soot formation.

The effects of variation in temperature, gas composition, residence time, ore particle size and particle volume were examined. The variation of each of these, or a function thereof, on the percentage reduction or function of it showed a straight line relationship, from which the percentage of reduction can be determined for any chosen value of that variable, when all the other variables were held constant. Also the effect of reducing capacity (flow rate of gas) and the oxidant in the input gas were examined. When all these operating variables were held constant, the usage of the kiln without chokes in position gave less carbon deposition on the ore, less poisoning of the autocatalytic effect and also a higher extent of reduction than when using the kiln with chokes.

For the particle size range (1.7 - 4.75 mm) examined a mode of uniform internal reduction was predominant up to the temperature at which surface sintering became significant and above that temperature a limiting mixed control checked the extent of reduction. These observations were in accord with microstructural examination of the sponge iron, porosimeter measurements and the results of percentage reduction obtained at different temperatures.

Sulphur and phosphorus were partially removed in gaseous form from the ore. Within the temperature range examined, sulphur removal increased with increase in temperature, whereas phosphorus removal was favoured at lower temperatures.

The carbon content of the sponge iron was not in the form of pearlite or cementite. From the microprobe observations it was concluded that the carbon was in the form of soot in the pores of the sponge.

A precise study of the progress of reduction from ore to a desirable sponge iron for the different stages of reduction was made including the removal of sulphur and phosphorus and carbon deposition, which was in agreement with the above observations.

CONTENTS

CHAPTER 1

INTRODUCTION

INTRODUCTION

1. The investigation of the reduction of iron oxides has been studied extensively because of its industrial importance. Most of the publications on this subject have dealt with the evaluation of the reduction of various ores by different reducing agents in solid or gaseous form. The majority of the studies have been concerned with the reduction of single particles or compacts. Much of this work has been reviewed by E.T. Turkdogan[1], Bogdandy[2], Szekely et al[3], and more recently there is a comprehensive up-to-date review in the book "Direct Reduced Iron"[4].

Modern blast furnace developments and in particular the increase in blast furnace size have been possible due to the availability of uniform and strong metallurgical coke. This coke has required for its production a carefully chosen blend of coals because the rapid growth of world steelmaking has led to some shortage of high quality coking coal. This scarcity has meant that prices of metallurgical coal and coke rose much faster than the prices of oil, natural gas and electricity in the ten years up to 1977[5]. So, despite the benefits of saving in operating costs from huge blast furnaces, the search for reliable lower investment methods of making iron has intensified in recent years.

What is known as direct reduction appears to offer the advantages being sought, namely a lower capital cost per annual tonne and a smaller minimum economic size.

Considered in terms of reducing agents, the direct reduction processes can be divided into two groups, one which uses a gaseous reductant obtained by reforming natural gas or higher hydrocarbons in a catalytic reformer, and the other group which uses noncoking coal.

The types of apparatus used for direct reduction can be divided into four groups:

(i) retort (HyL),

(ii) shaft furnaces (Midrex - Armco - HyL III),

(iii) rotary kilns (SL/RN, D.R.C.),

(iv) fluidised bed processes (Fior, H.I.B.).

A solid reductant is usually employed in the rotary kiln processes, but in the other processes hematite iron ore is reacted with a hydrogen-carbon monoxide mixture.

The reduction of iron ore to iron without melting was the first iron making method. This was clearly described in 1556 in De Re Metallica[5]. Over the years hundreds of direct reduction methods for producing sponge iron or similar products have been patented, as shown recently in "Direct Reduction of Iron Ore: a bibliographical Survey"[6], but only a few have been used commercially (some of them named above).

The first process actually used on a full commercial scale was developed in Mexico by Hojalata y Lamina and started operation in Monterrey in 1957, where there was available natural gas, a relatively rich iron ore and a market for steel, but little coking coal. Until 1965, the only commercial scale direct reduction plants used for carbon steel production were two HyL units in Mexico, with a capacity of 350,000 tonnes per year. Notably, the world DRI output of 7.9 million tons in 1980 was up sharply from the 1975 level of 3.0 million tons. Of the 17.1 million tons of world capacity in place at the end of 1980, 72% was completed after 1975. It is obvious that the wide acceptance of direct reduction has been achieved

in a short time and development is being continued for increasing capacity and further improvements. Especially nowadays the new coal based processes have found new motivation as a result of the escalating price of natural gas.

As mentioned before, rotary kilns use mainly solid fuel reactants, thus facing the inherent process difficulties of generating heat from one solid reactant (fuel combustion) and transferring it to another (ore reduction); this involves local overheating of the solid reactants and of the kiln wall, leading to stickiness of the ore. In processes using a mixture of gaseous reducing agents, a catalytic reformer is needed for preparation of the gaseous reductants. A shaft furnace cannot handle fine ores but a rotary kiln can as well as fluidised bed.

In the present investigation Brazilian iron ore was successfully reduced in a rotary kiln with reducing gases prepared within the kiln, using the beneficial effect of the auto-catalytic reactions of hydrocarbons, which take place on the ore surface and eventually increase the rate of reduction. A study was made of the effects upon the extent of reduction of different operating variables, identified as the reduction temperature, the ore particle size, the residence time, the amount and ratio of hydrocarbon (C_4H_{10}) and oxidant (CO_2) in the mixture of inlet gases, and the reducing capacity. The effect of the reducing condition upon the impurities content of the sponge iron was also examined.

CHAPTER

2

LITERATURE SURVEY

2. LITERATURE SURVEY

2.1. Definition and Objectives of Direct Reduction.

Direct reduction can be defined as reduction in the solid state at oxygen potentials which allow reduction of iron oxides, but not of MnO, SiO_2 etc., to the corresponding elements. Since reduction is in the solid state there is very little chance of these elements dissolving (at low thermodynamic activity) in the reduced iron, so the oxides which are more stable than iron remain essentially unreduced.

A good example of reaction in liquid-solid states is found in the conventional blast furnace process. A brief study of the rates of reactions from the top to the bottom of the furnace shows that the rate of reaction between the ascending gases and the descending iron ore increases as the temperature is increased, until a limiting temperature is reached at which slag formation begins. Thereafter, gaseous reduction is impeded and reduction occurs via the direct reaction between coke and iron oxide. Thus the rate of reduction decreases for a time. As the temperature continues to increase the rate of reduction again increases to a maximum in molten iron. From the above consideration, it is obvious that the overall rate of reaction in the liquid-solid state is lower than in the gas-solid state.

2.2. Liquid State Reduction: The blast furnace.

The blast furnace can be divided structurally into three sections or zones: hearth, bosh and stack (Fig. 1). Fundamentally, the blast furnace is a counter-current apparatus in which descending iron oxide, coke and slag-making materials remove heat from an ascending stream of hot reducing gases, composed mainly of nitrogen, carbon monoxide and carbon dioxide. Chemical reduction of the iron oxide also occurs as the charge

descends and, finally, in the bosh, fusion takes place of the reduced iron, some unreduced iron oxide and slag-making materials. In the hearth of the furnace the liquid slag and metal collect and also carbon is burnt at the tuyeres to produce heat and carbon monoxide which, together with solid carbon, serves as the reducing agent.

The essential functions of the metallurgical coke in the blast furnace are three-fold[7, 8]. Firstly, it supports the column of the burden. Secondly, in keeping steady movement of the gas and burden. Thirdly, providing carbon and producing carbon monoxide, and the heat required for reduction and melting the charge, thus allowing differences in density to cause a separation into a layer of slag, containing most of the unwanted non-metallic components, which floats on top of the liquid metal.

The final products tapped from an iron blast furnace are an impure iron and a liquid slag. The metal contains a high proportion of carbon, although it is seldom if ever saturated with carbon at the tapping temperature. The other solutes are mainly silicon, phosphorus, manganese and sulphur in varying proportions. Silicon, manganese and phosphorus are reduced from the burden and come mainly from the ore gangue materials, while sulphur comes mainly from the coke. There is a distribution of silicon, manganese and sulphur between metal and slag and the concentration of these elements is to some extent controlled by furnace operation. Under the conditions operating in the iron blast furnace all of the phosphorus charged finds its way into the metal, and the phosphorus content of the iron depends primarily on the phosphorus content of the ore charged.

Vast advances have been made in blast-furnace technology during the past two decades, through plant trials and plant developments, assisted

by research, to provide better understanding of the physical and chemical workings of the blast furnace[9]. The fields of research have included factors affecting heat and mass transfer in the stack, reducibility of the burden, resistance of the burden to swelling, breakage and sticking, alkali recycle, reactivity of coke and slag-metal reactions. The advanced knowledge acquired in each of these fields has contributed to the present realisation of large-capacity blast furnaces with high production capabilities at low coke rates. Much like a chain reaction, any change in the design or operation of any part of the furnace has to be accompanied by many other changes in order to maintain the delicate balance in the optimization of the blast-furnace practice. For example, the modern blast furnace operating with low coke rate is the result of a sequence of many developments, such as high top pressure, high temperature air blast, oxygen enrichment, oil, gas or coal injection[10, 11, 12]; usage of dolomite fluxed-pellets[13] and many developments in the burden preparation.

It is already ten years since the first mammoth blast furnaces of 400 m^3 inner volume were constructed[5, 14] at Nippon Kokan's Fukuyama works and Nippon Steel's Kimitsu works. Following the construction of these two furnaces, large blast furnaces were built one after another in Europe[15, 16] and Japan[5, 14]. To date these blast furnaces have been operated with good results, as anticipated.

In Japan, nine large blast furnaces are now in operation[5]. All of these are being operated stably, bringing about better productivity, fuel rate and coke rate than in conventional blast furnaces. It is anticipated that enlargement of furnaces will bring about various merits in the management of the steel industry. On the other hand, it demands enormous capital investment and great loss in incurred when the equipment breaks down

or furnace operation is disturbed for some reason. It has been found that no reduction in the construction cost of the blast furnace can be achieved if its inner column exceeds 3000 m^3 or hearth diameter exceeds 12.5 meters. The construction cost of large blast furnaces increases in proportion to the increase in its size.

Over the years numerous problems in the fields of raw materials, coke, various facilities of blast furnaces and operation of them,[15, 17, 18] have been solved, thus achieving the stable operation of present-day large blast furnaces. It may not be too much to say that the age of large blast furnaces has been perfected. At present they are under construction all over the world to meet the ever increasing demand for steel. In spite of the continuing rise in steel demand in the Third World and Comecon Countries, total world steel demand was predicted to fall[19] from 756 x 10^6 tonnes in 1979 to about 755 x 10^6 tonnes in 1980. The actual production of International Iron and Steel Institute members'[20] production in 1980, 1981 respectively were 453.256 x 10^6, 448.064 x 10^6 metric tonnes. The 29 member countries covered 63.2 per cent of 1980 world production and for approximately 97.9 per cent of world production excluding that of the USSR and other Eastern block countries, China and North Korea. This is the first decline since 1975. Predictions for the whole decade[21], however, given in the table below show that the underlying trend is a brisk growth in the demand for steel so that by 1990 it will be about 30% above the 1980 level.

Steel Production by Type of Country (Million tpy)

Country Type	1980	(%)	1985	(%)	1990	(%)	Growth rate
Industrial*	358	50	396	48	419	45	1.6%
Non-Industrial	102	14	140	17	197	21	6.8%
Communist	257	36	287	35	317	34	2.1%
Total	717	100	823	100	933	100	2.7%

* USA, Canada, EEC and Japan.

2.3. Elred, Inred, Plasmamelt, as alternatives for Molten Iron Producing Processes.

SKF has developed metallurgical pilot plant processes[22, 23] based on plasma technology, as an alternative to the blast furnace for producing the hot-metal. These processes are Elred, Inred, Plasmamelt (Fig. 2) which use powdered ores (concentrates) and ordinary non-coking coal. Fluidized beds, high temperature oxygen burners, plasma arc torches and injection techniques are typical new metallurgical tools. It is claimed that there is a potential possibility of lowering production cost by £10 - £15 per ton, mainly due to the use of cheaper raw materials preparation and lower capital cost at smaller tonnages and also a good environmental control using these processes. However, a full economic consideration could be made only when the processes were shown to work technically on a production scale. The high working temperature of these processes (about 2000^{o}C) can bring numerous problems on a commercial scale.

2.4. Direct Reduction Processes.

Hundreds of direct reduction methods for producing sponge iron products have been patented[6] over the years, but only a few are being used commercially. A brief description of the more important and more recent processes follows, in which the processes are divided into four basic types:

(i) Static bed: The HyL.

(ii) Moving bed: The Midrex - The Armco - The HyL III.

(iii) Rotary Kiln: The SL/RN, The DRC.

(iv) Fluidised bed: The Fior, The HIB

2.4.1. The HyL Process.

The HyL process[24, 25, 26, 27] which was the second largest producer of DRI in the world in 1980[28] involves a static bed in which batches of ore remain stationary in a chamber through which hot reducing gases are circulated (Fig. 3). The heart of a HyL plant is a gas reforming section and a reduction section of four vertical shaft furnaces. Natural gas enters the gas reforming furnace, is mixed with superheated steam and raised to reaction temperature. The steam-hydrocarbons mixture is then passed over a nickel/ceramic catalyst where it is converted to hydrogen and carbon monoxide. Sulphur is removed from the feed stock prior to entering the furnace to prevent poisoning of the reformer catalyst. The reformed product, after cooling, includes approximately 74% H_2, 13% CO, 5% CH_4, 8% CO_2. The four reduction reactors contain a fixed charge of 6 - 13 mm iron ore lumps or pellets. Every reactor is operated in a sequence of stages:

(i) Preheating of the raw ore by recirculated secondary (spent) gas.

(ii) Reducing the preheated ore to sponge iron with primary (fresh) gas.

(iii) Cooling the sponge iron.

(iv) Discharging the cooled sponge and charging raw ore.

The full cycle takes approximately 12 hours. Rated capacity is based on a three hour cycle in each reactor. This can be varied at will, dependent upon the reducibility of the charge, metallisation desired and the time required to load and unload the reactor. The reaction temperature can be varied between 850 and 1050°C. The HyL process can operate satisfactorily at any metallisation degree desired from levels of 82% up to 94%. The

original operation of the steel works at Monterrey found its economic optimum at about 85% metallisation. The variation in the different degrees of metallisation controls the plant productivity. In general, the gas consumption and operation costs increase as the degree of reduction increases. Since the gas flows downward through the bed, the ore on top is reduced more than the ore at the bottom. Therefore, the degree of reduction within each reactor is not completely uniform at the end of the operation. As a result blending of the sponge iron before it is used in steelmaking becomes essential. Fresh reformed gas is cooled ($380^{o}C$)[25] and dried before entry into the top of the cooling reactor which contains hot, metallised sponge iron. On its passage through the reactor this gas cools the sponge, whilst also giving between 1.0 and 2.5% carbon within the sponge, carburisation occurring in the neighbourhood of $550^{o}C$. At such temperature, carbon deposits as Fe_3C, forming a cementite shell which, among other advantages, protects the product from re-oxidation.

2.4.2. The Midrex Process.

The Midrex direct reduction plants continued to produce more DRI (56% of world output) than all the other plants combined in 1980[28]. The largest Midrex plant, currently in operation, is the Midrex (TM) series 600 plant with capacity of 600,000 tonnes per year, but designs exist for a 1 M tonne per annum module.

Iron oxide in the form of pellets and/or natural lump ore with a size range of +5 - 30 mm is automatically fed into the vertical shaft furnace with a reduction zone in the upper region and a cooling zone in the lower region. When metallised iron material is withdrawn from the bottom of the furnace, oxide feed flows through the upper seal leg into

the furnace, in response to level control devices, such as are used for feeding blast furnaces. The iron oxide is heated and reduced to iron in the reduction zone by counter-flow contact with hot reducing gases. The reduction temperature employed is up to 875°C, which depends on the type of oxide feed. The hot reduced iron is cooled in the cooling zone of the furnace by counter-flow contact with recycled cooling-zone gas to about 40°C to 50°C before being discharged from the furnace. The furnace geometry achieves isolation of the reduction and cooling zones, which enables the gas composition in the reduction zone and in the cooling zone to be controlled independently (Fig. 4)[26, 29, 30]. The composition of the cooling zone gas is controlled to avoid the formation of soot on the reduced product during cooling. The carburizing potential of the reducing gas is automatically controlled to achieve the desired level of carbon in the reduced iron. In Midrex metallised iron material, the carbon is present essentially as iron carbide, which favours subsequent melting. The midrex direct-reduction iron processes achieve 92 - 95% metallisation with controlled carbon of 1 - 2%. The gas reformer developed by Midrex is of the tube (multiple-alloy tubes) type. For converting natural gas to the reducing gas, oxygen from the ore is continuously recycled as CO_2 and H_2O vapour in the top gases to be used for cracking the natural gas. Therefore, no additional oxygen carriers are required which in turn reduces the investment and operating costs. The catalysts developed specially for this method of gas reforming convert the natural gas almost completely at about 900°C to a reducing gas composed mainly of carbon monoxide and hydrogen. The approximate composition of reductant gases are: H_2, 60 - 40%; CO, 24 - 36%; CO_2, 0.5 - 3%; CH_4, 3 - 6%; N_2, 12 - 15%. The total energy requirements

per metric ton of DRI are about 3.0 (G cal) as natural gas and 125 (kWh) of electricity and 2.0 (m^3) of water.

More recently Midrex Corporation introduced[31] a concept for constructing a floating direct reduction plant in a shipyard, towing it to the plant site and beaching.

2.4.2.1. Midrex Electrothermal Direct Reduction Process.

Midrex has recently introduced its Electrothermal Direct Reduction (E.D.R.) process[32], which is based entirely on coal and electricity rather than on liquid or gaseous fuels. It is a continuous process and is carried out in a furnace with a rectangular shaft (Fig. 5). Coal and iron oxide (as pellets or sized ore lumps) with limestone and recycled char are charged into the top of the furnace. The heat for the process is generated by passing an electric current through the charge from conductive panels permanently mounted on opposite sides of the furnace. The total energy requirements per metric ton of DRI for EDR are claimed to be about 2.25 G cal as coal and 850 kWh of electricity. It is claimed also that about 1 G cal of medium calorific value gas is recovered and can be used for other purposes.

2.4.3. The Armco Process.

In 1972 a plant with a design rating of 1,000+ tonnes/day was started up in Houston using two Foster Wheeler reformers, each used to 60% capacity. Armco's shaft furnace[32] (Fig. 6) is, essentially, a vertical tube with both ends "open", the maximum inside diameter is 5 metres and height from charging to discharging points is 27 metres. Lump ore 20% and pellets 80% have been set as the standard burden practice. The burden is metallised at about 850°C while moving continuously downward through the shaft furnace counter current to hot reducing gases. The

product is cooled to 60°C or less before discharge.

The fresh hot reducing gas, used in the Armco process, is produced by reforming natural gas with steam in a catalytic reformer. There are 96 catalyst tubes (15.24 cm dia.) in each reformer. Natural gas flows through an activated carbon bed for desulphurization to 0.2 ppm. It is preheated and mixed with steam. This mixture, having a steam-to-carbon ratio of 1.5:1, is then heated to 538°C before entering the reformer. The mixture flows down through reformer tubes containing a Ni catalyst. Reformed gas is blended with cooled compressed top gas and introduced into the shaft furnace through 12 symmetrically placed tuyeres. With a reformer outlet temperature of 857°C, the analysis of reformed gas is:

H_2	CO	CO_2	CH_4	N_2	H_2O
68.3%	20.2%	2.0%	1.1%	0.1%	8.4%

Furnace top gases are cooled and partially cleaned by water sprays. About 60% of the cooled, top gas is burned in the reformer burners and serves to heat the reformer. The balance after it has been compressed and recooled, is used for mixing with the reducing gas to control its temperature and a measured amount of this after adjustment of the desired CO_2/CH_4 enters at the bottom of shaft furnace to cool the reduced pellets, then the cooling gas flows upward into the centre region of the reduction zone, where it mixes with the reducing gas. The reduced pellets contain about 2.4% carbon, with a metallization of 92%.

2.4.4. The HyL III Process.

In early May, 1980, HyL introduced its continuous countercurrent process (HyL III).[23, 34] The process profits from advantages of economy

and efficiency attributable to continuous processing, while overcoming some of the problems in some existing continuous processes. The HyL III plants consist fundamentally of three sections, the reduction reactor, the systems for material handling and the gas reformer, which is essentially the same as the one used at fixed-bed HyL plants. The HyL III continuous reduction reactor (Fig. 7) is made up of a reduction zone in the upper part and a cooling and carburization zone in the lower part. They are separated by an isobaric zone that keeps the mixing of gases from the reduction and cooling loops to a minimum. The reactor is designed to permit a mass flow of solids by gravity through the reactor, with good gas-solids contact and low fines generation. There are no moving parts in the interior of the reactor, so a minimum of fines is generated. The reactor is operated with different types of pellets and with a mixture of pellets and lump ore. The operating pressure varies from 3.3 to 4.5 kg per square centimetre and inlet gas temperature ranges from 820°C to 940°C. In commercial operation the product metallization ranges from 85% to 93%, the carbon content ranges from 1.5 to 2.8% and the product temperature is held to less than 50°C.

2.4.5. Rotary Kiln Processes.

When the charge materials are not melted the poor intimacy of contact between ore and reducing agent, results in very much lower rates of reduction with solid carbon than with a reducing gas mixture, and longer times are required to achieve the necessary degree of reduction. Some improvement in the reaction rate is obtained if the ore and the solid reducing agent are agitated so that the contact zones between the particles are changing continuously. One method of achieving this

condition is to effect the reduction in a rotary kiln.

2.4.5.1. The SL/RN Process.

The SL/RN process[35, 36, 37] is used in several parts of the world in commercial operations, including the largest yet built for producing 400,000 net tons per year of reduced pellets at the Griffith Mine of the Steel Company of Canada.

The kiln is mounted with a slope downward from the feed end to the discharge end (Fig. 8). The transport rate of materials through the kiln can be controlled by the slope of the kiln and the speed of rotation. There are inlet and outlet cones at opposite ends of the kiln. The dimensions of the refractory-lined rotary kiln range from 4 to 6 metres in diameter and from 60 to 125 metres in length.

The charge to the SL/RN kiln consists of iron oxide pellet, (however, lump ores can also be used and iron sands are used commercially in the plant in New Zealand), coal, recycled char together with dolomite and/or limestone if sulphur needs to be scavenged from the coal. Air is blown with shell fans into the counter currently flowing freeboard gas through burner tubes, located at several positions along the length of the kiln. The kiln is usually operated with a slightly positive pressure to prevent the intrusion of unregulated air. Provision is also made for the supply of natural gas if required as auxiliary fuel. The hot products, consisting of sponge iron, unreacted coal char and gangue, exit the kiln at about 1000^{o}C via a transfer chute into a rotary cooler. There the hot products are cooled to roughly 90^{o}C and upon discharge from the cooler are magnetically separated into sponge iron and nonmagnetic tailings. The

amount of coal fed into the kiln is adjusted so that there is always a slight excess of unreacted carbon in the product. This procedure minimizes the possibility that the reduced iron could become reoxidised before exiting the kiln.

From a processing stand point, the kiln can be divided (Fig. 8) conveniently into two sections: a preheat zone, and a reduction zone. In the preheat zone the solids are heated by the freeboard gases from the charging temperature to a temperature where CO reduction can proceed. Heat is generated in the freeboard by the combustion of any CO carried over from the reduction zone, together with the volatiles from the coal and natural gas, if injected. For efficient use of the rotary kiln the preheat zone is made as small as possible, which is usually 40 to 50 % of the kiln length. As the solids reach a temperature in excess of 900^{o}C the carbon gasification, or Boudouard reaction, sets in and reduction of the iron oxide commences. Owing to the highly endothermic nature of the Boudouard reaction, the temperature of the solids ceases to rise any further, and throughout the reaction zone it is essentially constant. The temperature at which the solids bed stabilizes depends on a number of factors, the most important among them being the reactive nature of the coal and oxide pellets and the heat transfer rates from the freeboard gas and wall to the bed. An important point to note is that the gaseous atmosphere inside the solids bed is reducing in nature as opposed to freeboard gas which is slightly oxidising. Heat is generated in the freeboard by the combustion of CO which evolves from the bed at a rate depending on the rate of the Boudouard reaction. The process is controlled via the amount of air introduced through the air inlet tubes. By this direct reduction method it is claimed that the metallization achieved is more than 95% and the carbon content is 0.5%.

2.4.5.2. The DRC Process.

The equipment for the DRC process is similar to that of the other rotary-kiln (e.g. SL/RN) reduction processes, but this process uses only coal as both the fuel and reductant, which recently attracted considerable world-wide interest.

In the operation of the DRC process[38], a mixture of ore, limestone, coal and recycled char are continuously fed at the kiln feed end and a proportion of the coal is blown into the discharge end. The precise distribution of air supplies to the individual air tubes and of the proportion of coal blown into the discharge end of the kiln control the actual operating factors, bed and gas temperature profiles for stable operation. The resultant product has metallizations in excess of 92% with sulphur below 0.02% and carbon content of 0.25%.

2.4.6. Fluidised Bed Processes.

Several fluidised bed systems have reached the pilot plant or production plant stage of development, but they have all been bedevilled with a variety of operating problems such as:

(i) The settling of the ore is dependent on the particle size and the charge must be sieved within close size limits if the process is to operate efficiently. The size is usually selected within the range 0.5 - 3 mm diameter, for it is difficult to maintain a fluidised bed with smaller particles. The settling rate is determined also by the density of the ore. This is one of the major problems, for the density of the particles increases by 20 - 30% during the course of reduction, hence one of the solutions was usage of the multiple stage reduction.

(ii) Since the fine particles tend to sinter or become sticky in the normal direct reduction temperature range, the fluidised bed processes have to be operated at low temperatures. The rate of reduction is then low at atmospheric pressure and a more rapid rate is obtained by operating at high pressures.

(iii) The finely divided sponge iron product is strongly pyrophoric and has to be consolidated, usually by briquetting before exposure to air.

2.4.6.1. The FIOR Process.

In 1976, a commercial size FIOR plant with an annual capacity of 400,000 metric tons of DRI briquettes started operation at Puerto Ordaz, Venezuela[39, 4] and it is the only fluidized-bed process producing DRI grade for steelmaking (i.e. with about 92% metallization).

Pressurised, dried ore (mainly in the size range 0.05 to 5 mm) is metered from the lock hoppers into the uppermost of the four reactors (Fig. 9)[39, 4] in the structure. In this reactor the ore is preheated to a reduction temperature of 880^{o}C by combustion of natural gas and preheated air in the fluidised iron ore bed.

Fluidised, preheated iron ore flows from this burning bed reactor into a stand pipe, where it is steam stripped to remove entrained air, and metered by a cycling slide valve into the uppermost reducing reactor.

There are three fluid bed reducing reactors in series in the reactor structure. The ore reduction system operates at about 10 atmospher

The iron ore flows downward through them by gravity, overflowing from the highest reactor to the lowest reactor. The flowing ore is maintained in a fluidised state and, at the same time, reduced by the circulating hydrogen-rich reducing gas. The reducing gas is sent through a reheat furnace to the lower reducing reactor to flow upward through each of the reducing reactors, counter current to the descending ore.

The hydrogen-rich reducing gas is produced by steam reforming of natural gas over a nickel catalyst packed into the reforming furnace tubes. Prior to reforming, the natural gas feed is desulphurized over zinc oxide beds. The product gas from the reformer is shift reacted using an iron oxide catalyst that converts carbon monoxide to carbon dioxide and hydrogen in the presence of steam. The carbon dioxide is then removed from the gas stream by contact with a circulating hot carbonate solution. The final hydrogen rich gas stream is then added as make-up gas to the recycling reducing gas stream. The recycling reducing gas is the spent reducing gas leaving the upper reducing reactor after being quenched and scrubbed to remove the water produced by reduction and to remove ore fines carried in the gas from the cyclones.

Reduced iron fines are depressurized from the lower reducing reactor through a product let-down system into the briquetter feed drum operating at atmospheric pressure. Briquetting is done hot, close to reduction temperature, using double roll presses. The hot briquettes are cooled and air passivated on a circular grate cooler and then conveyed to open storage piles. The FIOR briquettes are 92 - 94% metallized. The energy consumption is 4.0 G cal of natural gas, 180 kWh of electricity and 5.5 m^3 of water, per metric ton of DRI.

2.4.6.2. The HIB Process.

The HIB (High Iron Briquette) direct reduction process, which is now in commercial operation at Puerto Ordaz, Venezuela, is a modified version of the Nu-iron process. The plant[40], which has a design capacity of one million tons of HIB per year comprises three separate trains, each with a capacity of one third of a million tons per year.

In the HIB process, fine iron ore is reduced in a counter current two-stage fluidized-bed reactor (Fig. 10) and then briquetted hot. From an operating point of view the plant can be divided into four sections:

(i) The reducing gas is provided by a mixture of superheated steam and natural gas in a ratio of approximately 3 to 1. This mixture is heated to about 600°C in the convection section of the reformer. The mixture then passes through direct fired, catalyst-filled reformer tubes and is reformed to hydrogen and CO by heating to about 850°C. The reformed gas is cooled to remove water vapour and then reheated in a heat exchanger and a fired gas heater to the desired temperature for reduction.

(ii) There is an ore preparation section where the ore is dried in a rotary kiln and then ground to minus 10 mesh. An inert gas pneumatic lift transports the fine ore to the first stage of the two-stage fluidized-bed preheating system, in which the ore is heated to about 320°C, using the off gas from the second preheater In the second preheater the ore is heated to 870°C (reduction temperature) by the combustion of natural gas with air.

(iii) The reduction reactor is divided into two stages. Reduction of

Fe_2O_3 to FeO is accomplished in the first stage by contact with spent gas from the second (lower) stage. Reduction of FeO to Fe is accomplished in the second stage by contact with fresh reducing gas. The reduction reactor is operated at a pressure of about 2 Kg/cm^2 (2 atm) gauge.

(iv) The reduced iron ore fines are transported to a surge bin by means of an inert gas lift and briquetted hot. The briquettes are then cooled with inert gas in a shaft cooler.

Because of the compaction, the briquettes are oxidation resistant and can be stored and transported without appreciable oxidation. A representative chemical analysis of a briquette gave 62.5% metallization and 0.19% carbon. It was found that it would be more economic to produce a briquette that was only 75% reduced. The HIB process was designed for the product to be used in ironmaking (blast furnace) rather than steelmaking.

2.4.7. Alternative Energy Sources for Gaseous Direct Reduction Processes.

As natural gas prices have approached prohibitive levels, the possibility of utilizing substitute reducing gases has received increasing attention in industrial nations. These alternative processes for producing reducing gases are use of coke-oven gas[41], coal gasification[37] and plasmared generators[42, 43].

The economic consideration of the efficiency of hot uncleaned coke oven gas for the production of reducing gas to be used in the direct reduction processes indicated that it is certainly one alternative for the production of reducing gas, where coke oven gas is readily available.

Coal with poor coking properties can be used for the direct reduction via coal gasification. Generally, the coal gasification consists of two basic processes in a reactor (Fixed bed, Fluidized bed, Entrained bed) as i) Partial combustion reactions, 2) steam gasification. In the first stage the carbon reactions with injected oxygen serve as heat-generating for the second stage of the endothermic water gas reaction. The basic reactions to be considered in coal gasification processes are:

Combustion

$$C + \tfrac{1}{2}O_2 \rightarrow CO$$

$$C + O_2 \rightarrow CO_2$$

Steam gasification

$$C + H_2O \rightleftarrows H_2 + CO$$

$$CO + H_2O \rightleftarrows H_2 + CO_2$$

$$CO + 3H_2 \rightleftarrows CH_4 + H_2O$$

Hydrogasification

$$C + 2H_2 \rightarrow CH_4$$

The composition of the crude gas leaving the gasifiers depends on the coal used and the gasification process. The Midrex process based on lurgi[28] coal gasification uses subbituminous coal, the crude gas leaving the gasifier passes through a spray cooler and waste heat boiler to remove tars and dust and cool the gas. A shift converter catalytically reduces the CO content of the gas via the water gas shift reaction. The gas is further cooled to condense out any remaining oils and finally passes through a methanol wash absorber to remove carbon dioxide and hydrogen sulphide. A typical gas composition consists of 78% H_2, 16% CH_4, 3% CO, 2% CO_2 and

1% N_2. This gas receives the same treatment as natural gas before use in a shaft reduction furnace. But in the Midrex plant based on Texaco coal gasification, the crude gas passes through waste heat boiler scrubbers and an acid gas (CO_2, H_2S) absorption tower and subsequently after heating the purified gas is used directly in the shaft reduction furnace, without reforming.

2.4.7.1. The plasmared process.

SKF introduced more recently the plasmared process[42, 43] (Fig. 11), which incorporates with a plasma gas generator, a gas cleaning unit, a sulphur-filtering unit (calcined dolomite[44] was used for desulphurization) and a shaft furnace for the direct reduction. The plasmared process prepares the reducing gas from coal or other fuels outside of the reduction unit, which distinguishes it from the new technologies for direct coal use already described. The interaction of gases and solids (either pellets or lump ore) in the reduction shaft is designed to occur in the same general manner as in other continuous feed/vertical-shaft processes. The most significant feature, the plasma gas generator (using an electric arc heater), is potentially adaptable to almost all gas-based, direct reduction processes as a means of providing acceptable substitutes for reformed natural gas. In 1978 the direct reduction facility at Hofors, based on the Wiberg process, which generated its reducing gas by the electric heating of coke, was forced to shut down by high energy costs and low productivity. In February, 1981 the facility was restarted, its Wiberg gas generator having been replaced by a plasmared generator. Operations to-date have utilized LPG as the principal fuel, with plans calling for a change to powdered coal later this year.

2.5. Blast Furnace versus Direct Reduction

As is obvious, blast furnace metal and scrap are the major sources of iron for steelmaking. Firstly, the rapid growth of world steelmaking[45, 46] and changes in the geographical distribution of the steel industry have led to some shortages of high quality coal, and hence scarcity of uniform, strong, metallurgical coke which is essential for the modern blast furnace. Secondly, the price of scrap fluctuates widely[47, 26] (compared with ore and pellets price) depending on availability and world trade conditions; it creates problems in the raw material situation. Also the problem of residual elements[48] in scrap is well known, and their adverse effect on steel quality is of long standing and occurs in all industrially advanced countries of the world.

Thus attention has been confused on the development of alternative routes for producing iron, of which the most promising is that of direct reduction.

There are many reviews[46, 49, 50, 51, 52] on plant progress and production prediction, but as a result of regional high energy costs (of natural gas), raw materials supplies and the political situation, some processes have been shut down, or there is a delay in their construction. Thus, the earlier estimates differed considerably from actual production. The latest prediction[21] of steel production by processes for the decade 1980 - 1990 indicated the highest growth rate for electric arc furnace (EAF), and eventually a higher need for direct

reduced iron (DRI):

Steel Production by Process (Million tpy)

Process	1980	(%)	1985	(%)	1990	(%)	Growth Rate
EAF	155	22	209	25	288	31	6.4%
BOF	373	52	442	54	515	55	3.3%
OH	189	26	172	21	130	14	(3.8)%
Total	717	100	823	100	933	100	2.7%

A general economic judgement between different steelmaking routes has been made by a few authors,[51, 52, 53, 54] but these are of limited value, because hardly ever could be found a similarity between the variables involved such as: various plants, capacity, location and the market price of raw materials, in actual practice.

The summarised advantages of direct reduction are as follows:

(i) Direct reduction permits iron production without the use of coke or coking coal, which are not readily available in some parts of the world, but uses natural gas, heavy oil or non coking coal.

(ii) Steel production with the electric arc furnace becomes independent of scrap and thus independent of price and quality fluctuations associated with this raw material.

(iii) Direct reduction[55] cuts the capital equipment cost per annual tonne capacity nearly in half. Just the deletion of coke in the process accomplished much toward this end. This allows developing countries, which could not consider constructing large integrated steel plants, to go into steel production without having to spend billions of dollars, which would be out of line, in any case, with local market

requirements.

(iv) Communication with and organization of a labour force in a steel enterprise with 1,000 - 1,200 employees (the DR/EAF plant)[56], the standard manning for 500,000 - 1,000,000 ton per year plant, is simpler to manage than in a mammoth blast furnace - steelmaking complex with 20,000 - 30,000 employees.

(v) Produced from ore or pellet, sponge iron contains ore or pellet gangue but is free from foreign tramp elements in solution in the iron.

(vi) It is possible to reduce ores which could not be reduced in the blast furnace, such as[57] titaniferrous iron sands and V_2O_5 bearing ore in rotary kilns.

(vii) Fine iron ores can be reduced without preliminary treatment in a fluidised bed or in rotary kilns.

(viii) Both round and flat products[56] can be produced economically with an annual capacity of 500,000 metric tons or greater in an integrated steelmaking and rolling plant based on direct reduction. More recently, a new method[58] has been developed for producing strip, bar and light sections, which involves purification and direct reduction of iron ore followed by direct rolling of the sponge iron pellets.

The developing confidence in the reliability of direct reduction processes and acceptable economics in many parts of the world lead to the conclusion that by 1985 the world capacity for this form of iron making will be over 50,000,000 tonnes per year[5, 59].

2.6. The Iron - Oxygen System.

The iron-oxygen system is perhaps one of the most extensively studied systems. The thermodynamics of the system is well understood and a great deal is known about the kinetics of gaseous reduction involving iron oxides.

The thermodynamically stable solid phases which occur between 400 and 1400^{o}C in the iron-oxygen system, at a total pressure of one atmosphere, are shown in the binary diagram (Fig. 12), based on the data of Darken and Gurry[60], Phillips and Muan[61] and Salmon[62]. This diagram shows that iron forms with oxygen the three stable, solid compounds; hematite (Fe_2O_3), magnetite (Fe_3O_4), and wustite (Fe_xO, where x is a little lower than 1). The non-stoichiometric FeO phase (wustite) is unstable below 570^{o}C and decomposes into a mixture of metallic iron and Fe_3O_4. Thus, reading from right to left across the phase diagram at constant temperature, below 570^{o}C the phase sequence is Fe_2O_3 - Fe_3O_4 - Fe, whereas above 570^{o}C the sequence is Fe_2O_3 - Fe_3O_4 - FeO - Fe.

The negligible solubility of oxygen in solid α and γ-iron determined by Sifferlen[63] is less than 0.01% O_2 by weight. Therefore, the oxygen content has no effect on the transition temperatures of the solid iron modifications and is disregarded in the diagram.

2.7. Equilibrium Considerations.

The reduction of iron oxides involves one or more of the following steps:

Hematite	——>	magnetite	Fe_2O_3	——> Fe_3O_4
Magnetite	——>	iron	Fe_3O_4	—— Fe
Magnetite	——>	wustite	Fe_3O_4	——> FeO
Wustite	——>	iron	FeO	——> Fe

Wustite is stable only above 570°C.

The thermodynamic equilibria for these reactions are well established for the two major gaseous reducing agents used, viz., hydrogen and carbon monoxide, as shown below.

2.7.1. Iron - Oxygen - Carbon System.

The equilibria of iron and iron oxides with a mixture of the gases CO and CO_2 and with solid carbon[64, 65, 66] is shown in (Fig. 13). From this figure it is inferred that, at temperatures above 710°C and at a total pressure of 1 atmosphere all the iron oxides can be reduced by mixtures of CO/CO_2 which are in equilibrium with carbon, and can, therefore, be reduced by carbon itself. At lower temperatures only those mixtures which are super-saturated with carbon and which, therefore, according to the Boudouard equilibrium, should react towards carbon deposition have a reducing action on wustite.

2.7.2. Iron - Oxygen - Hydrogen System.

The equilibrium diagram for iron and iron oxides with a mixture of the gases H_2 and H_2O is shown in (Fig. 14)[64, 65, 66]. The major difference between this system and the iron - oxygen - carbon system is the absence of a "sooting line" or corresponding phenomena. Thus it is theoretically possible to reduce hematite (and magnetite) to iron with

hydrogen at any temperature.

2.7.3. Comparison between Reducing Agents (CO, H_2).

From the iron-oxygen-carbon and iron-oxygen-hydrogen systems (Fig. 15)[67] it appears that above 815°C hydrogen is a more efficient reducer than carbon monoxide (i.e., the equilibrium H_2/ H_2O ratios are lower than the corresponding CO/CO_2 ratios), whilst the converse applies at lower temperatures. These equilibria are rarely, if ever, attained in industrial practice, because the rate of reduction becomes very slow as equilibrium is approached. When conditions deviate markedly from equilibrium the respective reaction rates for reduction with hydrogen and carbon monoxide are in the reverse order to those which would normally be expected from the equilibrium consideration. Thus, hydrogen is actually a more efficient reducer for a non equilibrium process which is designed to operate at temperatures below 815°C and carbon monoxide is more efficient at higher temperatures. This interpretation was based upon experimental results of Edstrom[65] and Tenebaum[68]. Recently the effect of gas composition mixture[69, 70, 71, 72] $(CO + H_2)$ for different temperatures indicates that as the hydrogen content of the reducing gas mixture increases the rate of reaction increases. This relationship was found to be markedly nonlinear.

The reduction of iron oxides to metallic iron with hydrogen is endothermic and an external source of heat is necessary to maintain the charge at the required temperature. The corresponding reactions with carbon monoxide are exothermic and under suitably controlled conditions the reactions are thermally self-sustaining. In fact, it may be necessary to dilute the carbon monoxide with hydrogen or other heat-absorbing gas

to avoid overheating the charge. Some processes have been designed to take advantage of CO - H_2 thermal balance and use mixtures of these gases to increase the amount of reduction obtained during the heating of the ore, from the ambient temperature up to the maximum reaction temperature of about 1100°C.

Figure 15 indicates that for all temperatures within the range where gaseous reduction is economically possible, the equilibrium gas mixtures contain at least 60 per cent of carbon monoxide and/or hydrogen. When equilibrium is not attained the unreacted concentrations of these gases are even higher and the great part passes unchanged through the reducing chamber. If the process is to be economical provision must be made for utilising the gas which remains after the reduction of wustite to metallic iron, for reduction of the higher oxides of iron to wustite and/or for the regeneration of the gas mixture and the removal of the gaseous reaction products.

2.8. Gas-Solid Reaction and Solid-Solid Reaction.

Gas-solid reactions play a major role in technology, and encompass a very broad field including the extraction of metals from their ores (iron oxide reduction, etc.). A common feature of all gas-solid reaction systems[3] is that the overall process may involve several intermediate steps. Typically, these intermediate steps involve the following:

(i) Gaseous diffusion (mass transfer) of reactants and products from the bulk of the gas phase to the external surface of the reacting solid particle.

(ii) Diffusion of gaseous reactants or gaseous products through the pores of a solid reaction product or through the pores of a

partially reacted solid.

(iii) Adsorption of the gaseous reactants on and desorption of reaction products from the solid surfaces.

(iv) The actual chemical reaction between the adsorbed gas and the solid.

In studying gas-solid reactions there are several other phenomena that may affect the progress of reaction and the performance of industrial equipment in which gas-solid reactions are carried out. These other phenomena include heat transfer, changes in the solid structure (such as sintering) that accompany the reaction, and the flow of gases and solids through equipment in which gas-solid reactions are taking place. The rate of reduction is controlled by these factors depending on the process used.

The reactions between solids may be divided into the following main groups:

(i) True solid-solid reactions which take place in the solid state between two species in contact with each other, or through the migration of species in the solid state, (e.g. formation of metal carbides through the reaction between metal oxides and carbon).

(ii) Reactions between solid reactants, which take place through gaseous intermediates (e.g. reduction of iron oxides with carbon at atmospheric pressure).

The reduction of metal oxides with solid carbon could also be a true solid-solid reaction, provided it is carried out at very low

absolute pressures. Yun[73] investigated the reaction of mixtures of finely powdered graphite and hematite under a vacuum of 5.10^{-4}mm Hg. At temperatures of up to 900°C the reaction took place very slowly, and in 18 hours only Fe_3O_4 and FeO had formed, but no iron. Only at higher temperatures was an appreciable transformation observed. Yun concluded that the rate of reaction is determined by the diffusion of the iron ions within the oxide phase. A deduction made by Baukloh and Durrer[74] from corresponding investigations, that the carbon diffuses in the iron oxide, is perhaps only of historical interest. A comparison of the experimental results of Yun[73] and Baukloh[74] shows that the rate of reaction distinctly increases when the gas pressure above the powdered mixture increases. In experiments of similar type, in which a stream of nitrogen was passed through the mixture of carbon and oxide, Baldwin[75] observed a marked decrease in the reaction rate as the flow of nitrogen was increased. A comparison of the observed values in all the experimentions mentioned, whether carried out in vacuum or under nitrogen [73, 75], with the rate of reduction of similar powdered oxides[76] in CO or H_2, proves that the direct, solid-state reaction of carbon and ore (which is sometimes regarded as the actual mechanism of the true direct reduction) is of no importance for the progress of industrial reduction processes.

2.9. Pore Structure of Reduced Iron.

The reducibility tests[77] on several natural ores show that the porosity of iron ore particles is one of the most important factors controlling reducibility. The reducibility expressed as the reciprocal of the time required for 90% reduction, varied directly with the porosity.

The relative reducibility increased with an increase in porosity as:

$$\text{Relative reducibility} = (\text{porosity} \times 0.75) + 8.0 \qquad \text{(Fig. 16)}$$

The reduction of iron oxides will always yield a porous reaction product. The nature of the oxide and the reduction conditions affect the structure of pores in reduced iron. This is because the reduction progresses from the surface of a particle inwards. The volume occupying space defined by the original wustite surface is diminished. This can only be accomplished by developing porosity.

More recently a scanning electron micrograph study of this porosity has been reported by Turkdogan and Vinters and typical micrographs for hydrogen reduction are reproduced in Figure (17)[78]. At the top left is the fracture surface of synthetic Fe_2O_3 pellet (sintered in air at 1300°C, ~ 5% porosity) revealing a well-defined hexagonal crystal form of hematite; upon reduction in hydrogen at 900°C, porous iron is formed (top right). The outside surface of a dense wustite strip as viewed by the scanning electron microscope is shown at the bottom left; upon reduction to iron, pores are developed. In general, H_2 reduction has given a finer pore structure than that obtained by CO reduction (Fig. 18)[78].

From the scanning electron micrographs in Fig. (19)[79] it is apparent that the pore structure becomes coarser as the temperature of reduction in hydrogen is increased progressively from 600 to 1200°C. The top left micrograph is for natural hematite (Venezuelan blend ore) which consists of an agglomeration of ore grains 2 to 5 μm diameter. Although each grain appears to be relatively dense, fine pores are present within these grains, as indicated by the measured relatively large pore surface

area (18 $^{m^2}/g$); this is much greater than the area of the intergranular surface (0.6 to 1.5$^{m^2}/g$ for 5 to 2 μm diameter granules).

In addition to microscopic examination, the characteristics of porous media should be qualified by measurements of pore volume, pore surface area and effective gas diffusivity. A hard lump ore, (Venezuelan crustal ore) with average bulk density of 3.6 $^{g}/cm^3$, the connected pore volume of about 0.1 $^{cm^3}/g$, and 29% oxygen as iron oxides, was reduced by hydrogen[79]. Upon complete reduction the average connected pore volume of iron was about 0.26 $^{cm^3}/g$, which was essentially the same as the total pore volume. Therefore, the reduction temperature (from 600 - 1200^{o}C) did not change significantly the average fractional porosity.

The initial pore surface area of the iron oxide affects the pore surface area of the iron formed by gaseous reduction. A decrease in the initial pore surface area of the iron oxide decreases the pore surface area of the iron.

The pore surface area(s) of iron reduced from hematite ore in hydrogen measured by BET[80] technique indicated that it decreases with increasing reduction temperature, e.g. S = 39 sq, m, per, gram at 200^{o}C and 0.1 sq, m, per, gram at 1200^{o}C.

A relationship between the reduction temperature and average critical pore size and the smallest pore radius has been obtained from the pore size distribution[79]. The pore size was found to increase slowly with reduction temperature up to 900^{o}C, but increased rapidly with further increases in temperature. These results are in accordance with the observation of fracture surfaces by scanning electron microscopy,

Fig. (19), which showed the distinct coarsening of the pore structure at reduction temperatures above 900°C.

The pore surface area of the reduced hematite ore is affected by reduction temperature and gas composition, as is shown in Fig. (20)[78]. The pore surface area obtained from hematite reduced in CO - CO_2 mixture, curve c, is about 2/3 of that for reduction in H_2 - H_2O, curve b. This is consistent with the coarser pore structure of CO - CO_2 reduced iron observed under the microscope (Fig. 18).

The gas diffusion in the pores of reduced iron has been measured [80, 81]. The diffusive flux in porous media occurs via two diffusion processes, as follows:

(i) Knudsen diffusion, independent of pressure and proportional to $T^{\frac{1}{2}}$.

(ii) Molecular diffusion, inversely proportional to pressure and proportional to $T^{3}/2$.

The effective He-CO_2 diffusivity measured at 20°C at various gas pressures, in iron reduced from hematite ore in hydrogen at 800 and 1000°C, is shown in Fig. (21)[80] as a function of gas pressure. The approach to molecular diffusion at high pressure causes the curves to approach linearity with a slope of -1 in the log-log plot. The molecular-diffusion mechanism for iron reduced at 800 to 1000°C prevails at pressures above 5 and 1 atm., respectively. Decreasing gas pressure and reduction temperature increases the Knudsen diffusion[80]. An increase in Knudsen diffusion effect is consistent with microscopic observations and also confirms that the pore structure becomes finer with decreasing reduction temperature (Fig. 19)[79].

The average effective diffusivity, De, for binary gas mixture is given by:

$$\frac{1}{De} = \frac{1}{(D_{12})e} + \frac{1}{(\bar{D}_k)e} \qquad (1)$$

where $(D_{12})e$ is the effective molecular diffusivity and

$(\bar{D}_k)e$ is the effective average Knudsen diffusivity for the average molecular weight of the gas mixture.

The limiting ideal structure was assumed to have pores of uniform size that are all inter-connected and intersect each other with an angle of 45 degrees, as approximately seen in the pore structure of reduced iron[80], for which the effective diffusivities are given by:

$$(D_{12})e = \frac{\varepsilon}{2} D_{12} \qquad (2)$$

$$(\bar{D}_k)e = \frac{\varepsilon}{2} \bar{D}k \qquad (3)$$

where ε is the average fractional porosity.

The effective diffusivity varies for a given porous medium with temperature and pressure and is different for different binary gas pairs, that is for different values of D_{12}. However, the diffusivity ratio De/D_{12} is a property of a given porous material and characterizes the pore structure. The pore structure becomes finer with decreasing reduction temperature. This is consistent with observation of pore structures under the microscope and the decreasing value of De/D_{12}.

2.10. Modes of Reduction.

The reduction of natural iron ore particles or sintered hematite pellets results in the formation of product layers. This

well known phenomenon has been studied by many investigators. More recently Turkdogan and Vinters[79] have studied the reduction of sintered hematite pellets by hydrogen. They have shown a typical example of layer formation in polished section of a partially reduced hematite pellet, Fig. (22). Relatively smooth interfaces between the layers usually appear at low magnifications; however, such an appearance can be misleading. A diffuse iron/wustite interface is shown on the left in Fig. (23) and less irregular interfaces of magnetite with wustite and hematite are shown on the right. These observations indicate that gas diffusion is sufficient in the wustite layer to give some internal reduction ahead of the advancing iron/wustite interface.

The zone of internal reduction is extended as:

(a) The temperature is lowered,

(b) The porosity is raised,

(c) The particle size becomes smaller.

All of these effects are expected from the kinetics factors discussed earlier.

The reduction of porous hematite particles less than about 1mm diameter indicates that the reduction is almost completely internal and uniform. This is demonstrated in Fig. (24)[78] which is a micrograph of the 60 per cent reduced central part of a 1mm diameter hematite granule, reduced at 800^{o}C and shows white platelets of iron particles embedded in a matrix of porous wustite.

The effect of particle size on the time needed to achieve a given percentage of reduction depends on the mode of reduction and hence

on the type of rate-controlling process. Consideration of the modes of reduction of porous metal oxides by gaseous reduction showed[79] three limiting rate controlling processes: uniform internal reduction; limiting mixed control; and diffusion in the porous metal layer. If the reduction were controlled solely by one of these, then the time, t, of reduction would be related to the particle (spheroidal) diameter, d, in one of the following ways:

(i) Uniform internal reduction : t in independent of d

(ii) Limiting mixed control : $t \alpha d$

(iii) Diffusion in porous iron : $t \alpha d^2$.

The dotted curves in Fig. (25) show schematically the relationship between t-d for these individual limiting rate processes. The curve drawn[79] corresponds to the experimental observation. The rate-controlling process becomes relatively simple only when

(i) there is uniform internal reduction, hence a small particle size required, or

(ii) the ultimate rate control by gas diffusion in the pores of the iron layer predominates, since the particle size is large.

It should also be realised that there may be a transition from one limiting rate-controlling process to another as the reduction progresses, depending on temperature, gas composition, particle size and type of oxide.

The reduction of iron oxides also shows some unexplained and unusual behaviour. For example, Edstorm[65, 79] demonstrated an unusual temperature effect on the time of reduction in Fig. (26), where the temperature of reduction is plotted against the logarithm of time for

1 and 15mm diameter particles. For 15mm diameter particles the time of reduction decreases smoothly with increasing temperature, and the time for 95 per cent reduction is about twice that for 75 per cent reduction for the range 500 to 1200°C. But with decreasing particle size a peculiar temperature effect manifests itself within range 500 to 800°C. This anomalous temperature effect becomes more pronounced at a later stage of reduction and with decreasing particle size. For example, the time for 95 per cent reduction of 1mm diameter ore at 680°C is about the same as that at 480°C. So far there is no satisfactory explanation for this unusual behaviour which, incidentally, larger ore particles did not show.

2.11. Rate of Reduction of Porous Ore Granules.

The porosity and pore structure of the ore has a marked effect on the extent and uniformity of internal reduction. Turkdogan and Vinters[78] studied the reduction of Venezuelan ore with an average pore surface area of 14 m^2/g and about 30 per cent porosity.

Typical examples of rate data for reduction of hematite granules in H_2 at atmospheric pressure are shown in Fig. (27), where F is the fraction of oxygen removed. At temperatures above 900°C and below 500°C, log (1 - F) is a linear function of time up to about 96 to 98 per cent oxygen removal. For intermediate temperatures the curves are basically linear up to about 80 per cent oxygen removal, after which reduction becomes sluggish, as shown in the previous section (Fig. 26). The data of reduction in a 90 per cent CO - 10 per cent CO_2 mixture at various temperatures are shown in Fig. (28). There was no unusual

temperature effect on reduction in CO at 800^{o}C and above, unlike the case for H_2 reduction.

The effect of particle size on the rate of reduction of hematite ore for a mixture of 90 per cent CO and 10 per cent CO_2; and H_2 at 1000^{o}C showed[78, 79] with increasing particle size the internal reduction is confined to the outer regions of the granules, hence the decrease in the overall rate of reduction with increasing particle size.

In the early stages of reduction of porous hematite granules, there is rapid conversion to wustite followed by internal reduction of wustite to iron. In the limiting case of almost perfect gas diffusion in the pores of the oxide, the internal reduction predominates and the rate is controlled primarily by a gas-solid reaction on the pore walls. An iron layer, a few atoms thick is assumed to cover the pore walls of wustite. The reduction rate is presumed to be controlled jointly by rapid diffusion of oxygen through the coating of the iron layer on the pore walls and by the chemical reaction of H_2 or CO with the oxygen on the surface of this very thin iron layer.

The effect of particle size on the rate of reduction, $\partial Ln(1-F)/\partial t$, by hydrogen and carbon monoxide is shown in Fig. (29). Small extrapolation to the hypothetical zero particle size gives rates for essentially uniform internal reduction. The particle size effects show that the rate of reduction increases with decreasing size of the granules.

It should be emphasised that the concept of internal reduction is used in a general sense relative to the dimensions of the granules

of the order of 500 to 1000 μm. The typical micrograph in Fig. (24) indicated that the mode of reduction varies from one grain to another within the particle; this is because of the local differences in the porosity of the oxide grains. Because of variations in pore size and faster gas diffusion in larger pores, most of the reaction will occur on the walls of larger pores. That is, only a fraction of the total pore surface area is expected to be used for reaction. The rate of H_2 reduction at 800°C achieved with various types of hematite granules increased non-linearly with increasing pore surface area of the iron (or wustite) formed. These results substantiate the foregoing discussion that, the larger the pore surface area the smaller the fraction of the total pore wall used in the reaction.

The rate of internal reduction in H_2 - CO mixtures has been explained in terms of the sum of the two individual rates of reduction with H_2 and CO. Both the reduction data and carbon deposition observed indicate that, below 1000°C, gas reactions leading to water-gas equilibrium are slow.

2.12. Rate of Reduction of Lump Ore or Sintered Oxide Pellets.

The rate of reduction of lump ore or sintered pellets is complex in a stream of reducing gas in a packed bed, because the overall rate of the reduction is controlled by several reaction processes in series, such as heat and mass transfer through the gas film boundary layer, gas-solid reactions and gas diffusion in porous product layers. Through mathematical analyses, facilitated by computer calculations, numerous equations have been derived to describe the rate of reduction of large oxide particles for various modes of reduction[82].

In most experiments with single pellets or ore particles, heat transfer is relatively fast and, with sufficiently high-velocity gas streams, the gas-film mass-transfer resistance is small enough to be neglected. Therefore, there are primarily two major reaction steps in series which influence the rate of reduction: gas-oxide reactions, and gas diffusion in porous oxide and porous product layers. The relative effects of these rate processes depend on the particle size, gas composition, temperature and mode of reduction, and they change with the progress of reduction.

2.13. Gas Diffusion in the Porous Iron Layer.

Turkdogan and Vinters[79] have made unidirectional reduction experiments to demonstrate the effect of gas diffusion in the pores of iron layers. Long cylinder specimens were made from big pieces of the lump hematite ore and were packed inside a closely fitting nickel tube. After reduction in hydrogen for the required time, the sample was sectioned axially and polished, and the thickness of the iron layer was determined. Experimental results in Fig. (30) indicated that, when the thickness of the reduced iron layer obtained about 1 mm, the subsequent reduction proceeds in agreement with the parabolic rate law, thus substantiating the discussion for pore diffusion control.

Since the nominal iron/wustite interfacial area remains unchanged in this unidirectional reduction, from Fick's Law the limiting parabolic rate equation for gas diffusion in the porous iron layer is:

$$X^2 = Kt \qquad (4)$$

where X is the thickness of the iron layer at time t and K is the

parabolic rate constant, which is proportional to the effective gas diffusivity in the porous iron layer. Assuming that the total pressure is essentially constant and the ideal gas law is obeyed, for the equimolar counterflux of H_2 - H_2O,

$$K = \frac{2D_e}{\rho} \left(\frac{\Delta P_{H_2}}{RT} \right) \qquad (5)$$

Where De is the effective diffusivity for H_2 - H_2O in porous iron and ρ is the concentration of oxygen in wustite. In computing ΔP_{H_2} across the iron layer, equilibrium was supposed at the iron/wustite interface, and the gas-film resistance to gas diffusion at the outer surface was ignored, for the gas flow rates employed. The values of De obtained from the slopes of the lines in Fig. (30) give, for the diffusivity ratio De/D_{12} (H_2 - H_2O) = 0.021 and 0.11 for reduction temperatures of 600 and 800°C, respectively. These values of De/D_{12} are in good agreement with those measured directly. Thus, these tests demonstrate that as the thickness of the porous iron layer grows, the rate of reduction is ultimately controlled by gas diffusion in the pores of the iron layer.

In the reduction of spheroidal oxide particles or pellets with a porous outer iron shell surrounding the unreacted oxide core, the limiting rate equation is obtained for pore diffusion control by relating the equimolar counterflux of H_2O and H_2 (or CO_2 and CO) at essentially constant total pressure, through the reduced iron shell at any time, t, the relative thickness of the reduced layer as represented in terms of the fractional mass of oxygen loss, F, and the material balance for oxygen

removal accompanying hydrogen flux as follows:

$$\left[\frac{1}{2} - \frac{F}{3} - \frac{(1 - F)^{2/3}}{2}\right] = \frac{De}{\rho r^2}\left(\frac{Po - Pi}{RT}\right)t + C \qquad (6)$$

In the equation, r is the initial radius of the spheroidal pellet, assumed to undergo little or no dimensional change during reduction, Po is the hydrogen partial pressure on the surface of the sphere (the same as that in the gas stream for fast flow rates) and Pi is that for the metal/metal oxide equilibrium. C is a constant (a negative number) and takes account of all early time departures from the assumed boundary conditions. The value of C depends on particle size, gas composition, and temperature. Only in the limiting case of very fast interfacial reactions does C approach zero.

Typical experimental data for reduction of 15 mm diameter spheroids of natural hematite are plotted in Fig. (31) for the hydrogen reduction in accordance with Equation (6). The middle parts of the elongated S - shaped curves are well represented by straight lines from 50 to 60 per cent to 95 or 99 per cent reduction. Deviation from a parabolic relationship, as given by Equation (6), in the early and final stages of reduction can be explained by the following factors. As specified in the derivation[79], equation (6) is applicable only after the establishment of certain boundary conditions. Partial internal reduction preceding the main advancing front of the iron layer may lead to the entrapment of some wustite in the reduced layer. This situation could lead to sluggish oxygen removal in the final stages of reduction. For reduction of hematite particles less than about 7mm diameter, the data do not fit Equation (6) even for a limited range of reduction where mixed control predominates.

The rate data observation by McKewan[83], indicated in Fig. (32), for sintered Fe_2O_3 pellets, may also be represented by straight lines beyond about 60 per cent reduction. Turkdogan and Vinters[79] derived the effective diffusivity H_2 - H_2O, from Equation (6) and the slopes of the lines in Fig. (31) (and from similar plots for other temperatures and particle sizes). The values of De/D_{12} thus obtained from the H_2 reduction experiments are indicated in Fig. (33) as a function of reduction temperature. These values were in good agreement with those measured directly or calculated from structural considerations. As the reduction temperature decreases the pore structure becomes much finer, presumably with many narrow channels and bottlenecks on connected capillaries, when Knudsen diffusion predominates, hence low values of De/D_{12}. The pore structure becomes coarser with increasing reduction temperature, bringing about easy passage of gas through the pores, hence, higher De/D_{12}.

The effect of gas composition on the time to achieve 50, 75, 90 and 95 per cent reduction for sintered hematite and magnetite ore pellets reduced at 900°C by H_2 - CO - CO_2 mixtures (with CO/CO_2 = 9) to suppress soot deposition)[71], is that as hydrogen is replaced by carbon monoxide the time of isothermal reduction to achieve a given percentage of oxygen removal increases gradually up to about 50 per cent CO: with further addition of CO there is a marked increase in the time of reduction. The time of reduction for 100 per cent (CO/CO_2 = 9), is about ten times more than in hydrogen at the same temperature. The molecular gas diffusivity in a binary system, such as H_2 - H_2O or CO - CO_2, as derived from the kinetic theory of gases, is an invariant for the system and essentially independent of the gas composition. However in ternary and

multi component systems, each species has a different diffusivity and varies with the gas composition. Furthermore, the rate equation for diffusive flux is complicated. For these reasons the interpretation of the data for reduction in the H_2-CO mixtures for the limiting case of pore diffusion control becomes complicated. For an approximate solution of the problem, the gas mixture is supposed to be a pseudo-binary system consisting of (H_2/H_2O) - (CO/CO_2) with a pseudo-binary diffusivity $\bar{D}_{12}$ that varies linearly with the mole fraction of $N(H_2 + H_2O)$ and $N(CO + CO_2)$ in the free gas stream outside the pellet; that is

$$\bar{D}_{12} = D_{12}(H_2/H_2O)\cdot N(H_2 + H_2O) + D_{12}(CO/CO_2)\cdot N(CO + CO_2)$$

On the basis of this approximation and the assumption of equal molar H_2 - H_2O and CO - CO_2 diffusions, the limiting rate Equation (6) is rearranged to give approximately

$$Y = 3 - 2F - 3(1 - F)^{2/3} \simeq \frac{6\bar{D}e}{\rho r_o^2 RT}\{[(P_{H_2})_o - (P_{H_2})_i] + [(P_{CO})_o - (P_{CO})_i]\}t + c' \qquad (7)$$

For iron-wustite equilibrium at 900°C, $(P_{H_2})_i = 0.632(P_{H_2} + P_{H_2O})_o$ and $(P_{CO})_i = 0.685\ (P_{CO} + P_{CO_2})_o$ where the subscript $_o$ indicates partial pressures in the free gas stream. The values of effective diffusivities $\bar{D}e$, thus obtained from the diffusion plots for reduction in H_2 - CO/CO_2 (=9) are plotted in Fig. (34) as a function of the average molecular diffusivity D_{12}. The slope of the line drawn gives $De/D_{12} = 0.13$ for porous iron formed by reduction at 900°C.

The reduction behaviour of hematite pellets in the H_2 - CO mixtures indicated a pattern similar to that observed in the H_2 and CO, that is the rate of reduction beyond about 50 per cent oxygen removal

is controlled by gas diffusion in the pores of the iron layer.

From the limiting rate Equation (7) for diffusion control, it appears that it is the interplay of two basic parameters, effective diffusivity and gas composition, which cause the non-linear change of rate with composition of H_2 - CO mixtures. The rate of reduction is a linear function of the product $\bar{D}e\{[(P_{H_2})_o - (P_{H_2})_i] + [(P_{CO})_o - (P_{CO})_i]\}$, for a given particle size and temperature. When the relative rates of reduction are compared in H_2 and CO for a given temperature and particle size, the ratio $D_{12}(H_2 - H_2O)[(P_{H_2})_o - (P_{H_2})_i]/D_{12}(CO - CO_2)[(P_{CO})_o - (P_{CO})_i]$ should be considered where D_{12} is molecular gas diffusivity for the indicated binary mixture. For 900°C, this ratio is 10, which is in general agreement with the ratio of rates of reduction in H_2 and in CO observed experimentally.

In a more recent communication, Szekely and El-Tawil[72] reported findings on the reduction kinetics of hematite pellets with CO + H_2 mixtures which were very similar to the data presented earlier by Turkdogan and Vinters[71]. Within the temperature range of 800 - 900°C the overall rate of reduction increased with increasing hydrogen content of the reducing gas mixture.

2.14. Limiting Mixed Control in Initial Rate.

In the early stages of the reduction, the rate of reduction is controlled jointly by,

(i) gas diffusion in the pores of the wustite (solid state diffusion in wustite can be ignored), and

(ii) reaction on the pore walls of the wustite.

This implies a thin porous iron layer and a rapid gas diffusion therein. Depending on the porosity of wustite and the gas diffusivity therein, there will be partial internal reduction ahead of the nominal iron/wustite interface. The reaction of hydrogen with porous wustite will be confined to the pore mouths close to the nominal iron/wustite interface.

Tien and Turkdogan[84] derived a rate equation for partial internal reduction of metal oxides controlled simultaneously by gas diffusion into the pores of the oxide and chemical reaction of gas on the pore walls of the oxide. For the initial rate of reduction of relatively large oxide particles, the special case of "limiting mixed control", the rate equation for fractional oxygen mass removal per unit time for a spheroidal particle and binary gas mixtures (H_2 - H_2O) or (CO - CO_2) at constant pressure reduced to

$$\frac{dF}{dt} = \frac{3}{ro}\left(\frac{SkDe}{\rho}\right)^{1/2}\left(\frac{1 + K}{K}\right)^{1/2}\frac{P_i^s - P/(1 + K)}{RT} \qquad (8)$$

Where k is the specific rate constant, $cm/_S$, which is in terms of $\emptyset'$, the specific rate constant per unit area of useable pore surface, $k = RT\emptyset_i'(1 - \Theta)$, $\emptyset_i'(1 - \Theta)$ is specific rate constant for the formation of CO_2 or H_2O on the surface of iron in equilibrium with wustite, which can be derived from the reduction data, where $\Theta = \frac{De}{D_e'}$ (D_e' and De are respectively effective gas diffusivity in the porous iron layer and oxide phase), P is the total pressure, P_i^s is the partial pressure of the reducing gas at the outer surface of the spheroidal particle and K is the equilibrium constant for coexistence of metal and oxide phases, e.g.

$K = (P_{H_2O}/P_{H_2})_e$ or $(P_{CO_2}/P_{CO})_e$.

Where K>>1 equation (8) reduced to

$$\frac{dF}{dt} = \frac{3}{ro}\left(\frac{SkDe}{\rho}\right)^{1/2}\frac{P_i^S}{RT} \qquad (9)$$

This was derived by Thiele[85] for the limiting case of a gas reacting on the pore walls close to the outer surface of the porous pellet under conditions such that the reverse reaction was negligible. The log-log plot in Figure (35)[79] shows the variation of the initial rate of reduction in hydrogen with the radius (ro) of spheroidal hematite particles. The slopes of the curves for ro < 1mm decrease markedly with decreasing particle size, approaching the condition of uniform internal reduction. The lines drawn with a slope of - 1 for ro > 1mm are in accord with Equation (8) for the limiting mixed control.

The values of (dF/dt)ro are calculated from Equation (8) with the rate constant Sk (product of total pore surface area and the specific rate constant) derived from the rate of internal reduction of hematite granules, extrapolated to zero particle size, as shown in Fig. (29); and the effective diffusivity, H_2 - H_2O in wustite, supposed to be the same as in porous iron, shown in Fig. (33). The calculated initial rates of reduction are compared in Fig. (36) with those measured[79]. The calculated rates are about twice those measured experimentally. This discrepancy may be attributed to differences in the values of S and De for porous wustite in the early stages of reduction in comparison with those measured after completion of reduction. The slope of the experimental line in Fig. (36) gives 50.2 KJ for the apparent activation energy of this mixed control reaction.

The foregoing discussion indicated that a better understanding of the rate phenomena encountered in gaseous reduction of metal oxides can be developed by studying the limiting cases of rates of reduction and by experimental evaluation of the pore characteristics of the reaction products.

2.15. Partial Internal Reduction.

Depending on gas composition, temperature, pellet size and total gas pressure, there will be mixed rate control during some period of the reduction within the framework of the limiting rate laws discussed above. The rate equation obtained for the partial internal reduction depends on the model considered. Such complex rate expressions usually involve second order differential equations and, therefore, the rate expression cannot be given a closed analytical form; numerical solutions are derived through computer calculations.

Szekely and Evans[86,87] considered a so-called shrinking-core mode of reduction shown in Fig. (37) for a mathematical study of partial internal reduction of porous metal oxides. The rate equation they obtained was based on the assumption that the gaseous reduction of the pellet is controlled jointly by slow counter-current diffusion of gas through the inter particle pores of the pellet, and by slow chemical reaction of the gas with the oxide at the oxide-metal interface of the grains. The appropriate parameters determined in special experiments were used to calculate the rates, which were found to be in reasonable agreement with the experimentally determined rate of reduction of porous nickel oxide pellets in hydrogen. The shrinking-core model has two major shortcomings:

(i) The important postulate of "topochemical reaction", i.e. the existence of a sharp boundary between the reacted and unreacted zones. Gray and Henderson's[88] experimental evidence does not support such a postulation.

(ii) The structural effects, such as porosity, grain size, and so forth, are implicitly incorporated in the chemical rate constant.

The topochemical models by McKewan[89] and Spitzer[90] et al; which postulated the existence of sharp interfaces between the progressively receding hematite-magnetite-wustite and iron layers in the course of the reduction, are different from the above so-called shrinking-core model.

Tien and Turkdogan[84] considered a model of reduction for mathematical analysis of partial internal reduction, shown in Fig. (38) which indicated partial internal reduction ahead of the nominal metal/oxide interface for two situations classified as

(a) partial internal reduction - two-zone model and

(b) limited partial internal reduction - three-zone model.

From their studies of gaseous reduction of iron oxides, they have found that the two-zone model is appropriate for small pellets, 1 to 3 mm diameter, and the three-zone model for larger pellets. The rate equations obtained involve slow counter current diffusion of gas in the porous metal shell and the porous oxide-metal two-phase zone, and slow chemical reaction on the pore walls of wustite.

Tien and Turkdogan[84] assumed that the pore surface area per unit mass of wustite remained unchanged during reduction, i.e. surface

area α mass of oxide, and independent of the particle size in the pellet.

Fig. (39) indicates the results comparing the reduction of 10mm diameter hematite pellets with the rate of reduction calculated for the three-zone model. In this graph ro is the radius of the pellets, and De is the effective diffusivity of H_2 - H_2O mixtures in the porous iron and wustite layers. There is negligible temperature effect on the relationship indicated in Fig. (39), because the temperature sensitive, De, is incorporated in this correlation. This observation implies that the gas diffusion in the porous iron layer has a decisive influence on the rate of reduction of iron oxide pellets.

Seth and Ross[91] and Spitzer[90] in their mathematical model analysis assumed a sharp interface between the iron and wustite layers, which does not agree with the findings of Turkdogan et al[79]. They have found that, whether the hematite that was reduced was dense or porous, the wustite formed was always porous; consequently, the iron wustite "interface" was diffuse because of the partial internal reduction of the wustite.

2.15. The Water-gas Shift Reaction.

The water gas shift reaction plays a significant role in the direct reduction processes which use reformed hydrocarbons as reductant in the reduction of iron oxides.

It is generally agreed,[2] from the different rates of reduction of iron ore by CO and by H_2 and the marked effect which even

slight amounts of H_2 contained in a CO/CO_2 mixture have on the reduction rate, that the hydrogen is the actual reducing component in such gas mixtures. The CO is considered to serve mainly to reduce the resultant steam back to hydrogen:

$$H_2 + FeO \longrightarrow H_2O + Fe \qquad (1)$$

$$H_2O + CO \longrightarrow H_2 + CO_2 \qquad (2)$$

The second sub-process of this reaction is known as the water-gas shift reaction. It is well known that this process needs a catalyst. In iron ore reduction all of the products (Fe_3O_4, FeO, Fe) come under consideration as possible catalysts; particularly active is solid iron.

The process of reduction of iron ores in CO/CO_2 mixtures containing H_2 is, therefore, to be understood, when metallic iron is present, as a reaction sequence; subreaction (1) the reduction proper, takes place at the oxide surface; sub-reaction (2), the regeneration of the hydrogen by the water-gas reaction, takes place at the iron surface.

The spatial separation of the two sub-reactions requires their connection by a transport process, which must take place as a gaseous diffusion or surface diffusion by one of the participants in the reaction. The optimal conditions occur at the three-phase boundary metal/oxide/gas.

E.T. Turkdogan and J.V. Vinters[78] indicated that during reduction of iron oxides in H_2 - CO - CO_2 mixtures at 900°C and below, there is a slow approach to gas equilibrium. However, it appears that at 1100°C the water-gas shift equilibrium has nearly been established while reducing the iron oxide.

2.17. Swelling During Reduction.

The apparent volume of iron ore or pellets usually increases during reduction. This is called swelling. Broadly speaking, three categories of swelling[92] behaviour can be distinguished. These are known as "normal" swelling; "catastrophic" swelling in which sudden volume expansion is exhibited with the conversion of wustite to iron, the iron appearing in the form of filamentary growths, known as whiskers[93] wires,[94] or fibrous iron[95], and lastly "bursting expansion", a typical behaviour[92] of iron-rich materials containing small quantities of alkalis. This latter kind of behaviour is different to "catastrophic" swelling (although it is no less serious) in that a major part of the expansion takes place before the appearance of iron as a reaction product.

It should be pointed out that neither lump ore nor sinter[96] are known to swell abnormally or catastrophically, whereas certain types of pellets do, and give rise to operational problems by reducing the permeability of the burden as abnormally swollen pellets are soft, spongy and tend to disintegrate.

From the specific volumes of different iron oxides and iron reported by Edstrom[65]:

0.272 c.c. Fe_2O_3 per gramme of iron (at room temperature)
0.270 c.c. Fe_3O_4 per gramme of iron
0.231 c.c. FeO per gramme of iron (23.5% oxygen)
0.128 c.c. Fe per gramme of iron

it is expected that the volume would decrease during each stage of reduction. However, according to Edstrom[65], the main cause of swelling of ores is caused by the transformation of the hexagonal hematite into cubic magnetite and the resulting lattice disturbances. Lattice

disturbances cause pore formation, whereby there is a considerable increase in the apparent volume of the samples during the transformation from hematite to magnetite.

In general, during reduction in CO-rich gas the swelling is much greater than in H_2-rich gas[71, 97]. The reason given for this behaviour is that metal dusting occurs during carbon deposition in CO-containing gas mixtures. However, it is difficult to explain swelling that may occur during reduction in CO-CO_2 mixtures when there is no carbon deposition.

The cause and effect of swelling or shrinkage accompanying reduction have not, as yet, been resolved. Turkdogan and Vinters[71] indicated that the pellets made from reagent grade Fe_2O_3 undergo dramatic dimensional changes upon sintering and reduction. A 14 mm diameter green pellet shrank (~ 63 vol.%) to 10 mm diameter upon sintering in air for 40 minutes at 1300°C. When the pellet was reduced in hydrogen at 900°C, there was further shrinkage (~ 38 vol.%). However, there was extensive swelling when the pellet was reduced in CO/CO_2 = 9/1; after reduction the size of the reduced pellet exceeded the initial size of the pellet in the green state.

The crystal growth during sintering and H_2 reduction caused the shrinkage. However, the swelling accompanying reduction CO - CO_2 mixtures cannot readily be explained. There was no carbon deposition with the gas composition employed. The iron formed upon reduction contained 0.2 per cent carbon (equilibrium value at 900°C is 0.3%). In contrast to this behaviour, when pellets made from Venezuelan ore were sintered and reduced in H_2 or in CO/CO_2 = 9/1, only a small dimensional

change resulted (<15 vol.%). A number of commercial pellets and pellets made from a high grade taconite ore concentrate showed similar behaviour. However, at reduction temperatures above 900°C there was some swelling (~ 25 vol.%) when these pellets were reduced in CO - CO_2 mixtures (without carbon deposition).

The variations in the experimental observations of different investigators[65, 71, 92], in which the extent of swelling or shrinkage varies from one type of iron oxide pellet to another, could be because of the change in duration temperature, pore volume and limited sintering of the reduced oxide and impurities content of the pellets.

In general there are two types of impurities in pellets:

(i) Impurities with a hindering effect on swelling, e.g. silica; it was found[71] that reagent-grade Fe_2O_3 pellets containing silica (up to 5%) do not swell when reduced in CO (with CO_2 added). It was also found[98] that a certain amount of silica is necessary in acid pellets to maintain strength and to prevent catastrophic swelling.

(ii) Impurities with an enhancement effect on swelling, e.g. alkalies. It was demonstrated[99] that small (0.1 - 1%) additions of alkalis (Na_2CO_3 or K_2CO_3) can result in the catastrophic swelling (in H_2 or CO) of otherwise normal pellets. The effect of alkalies becomes more pronounced with increasing CaO/SiO_2 ratio in the pellet. The adverse effect could be prevented by the addition of a fine-grained acid gangue to form stable alkali silicates.

There are some contradictory observations of the effect of impurities in pellets (e.g. lime content). A small (< 0.1% CaO) amount of lime[92] addition to hematite ore pellets caused considerable swelling during reduction and this suggested that calcium oxide[100] was a cause of catastrophic swelling. On the other hand it was found [101, 102] that about 1% CaO addition to hematite pellets suppressed swelling during reduction. These variations in the observed effect of lime on swelling may be due, in part, to the presence or absence of other impurities in the ore, such as alkalies.

2.18. Reduction of Hematite by Carbon.

The reaction between hematite and carbon is of fundamental importance in the preparation of metallised pellets. Much of the new interest has been stimulated by the development of the SL/RN process [35, 36] which uses solid carbon as the reductant in the production of sponge iron.

It is generally accepted that reduction of iron oxide by carbon [103] occurs through gaseous intermediates CO and CO_2, except under a very high vacuum where the true solid-solid reaction is the predominant mechanism.

The reaction mechanism through gaseous intermediates may be written as follows:

$$C_{(s)} + {}^{1}/_{2}O_2 \longrightarrow CO_{(g)} \qquad (1)$$

$$Fe_xO_{y(s)} + CO_{(g)} \longrightarrow Fe_xO_{y-1(s)} + CO_{2(g)} \qquad (2)$$

$$CO_{2(g)} + C_{(s)} \longrightarrow 2CO_{(g)} \qquad (3)$$

The initial formation of carbon monoxide is an important step in the overall reaction rate. Oxygen of the entrapped air together with oxygen gas released by the dissociation of iron oxides reacts with carbon to yield carbon monoxide gas (reaction 1). In addition, some carbon monoxide may also be formed by "true" direct reduction occurring at the points of contact between the carbon and oxide particles. Carbon monoxide gas thus produced readily reacts with hematite particles (reaction 2), (refer to Fe - O - C system page 28).

The Boudouard or the solution-loss reaction between CO_2 gas and carbon particles regenerates CO gas (reaction 3) and thereby tends to restore the reducing potential of the gas-phase contained within the pores of the sample. The oxidation of certain types of carbon in CO_2 is catalysed in the presence of certain metals and metal compounds. The rate enhancement of the process has been observed with the addition of Li_2O and the inhibiting effect has been reported with addition of FeS[104] Metallic iron has been found[104 - 107] to be a good catalyst for the gasification of graphite. There is no evidence of catalytic oxidation when coconut charcoal is used[108]. Because of this unpredictable catalytic reaction in the mixture, equations derived through mathematical modelling[109,110] to describe the overall rate of the reaction are of limited value and may be applicable only to systems where reactions are not catalysed.

At moderately high temperatures (ca. 1000°C) the rates of the iron oxide reactions (at T > 570°C sequence is Fe_2O_3, Fe_3O_4, FeO, Fe refer Fe - O - C) are much greater than that of the Boudouard reaction.

In other words the overall process becomes limited by the availability of CO gas according to the Boudouard reaction. Thus at steady-state the composition of this gas-phase would closely correspond to the equilibrium gas-phase composition for Fe_xO_y/Fe_xO_{y-1} "x" and "y" having the values as specified earlier.

2.19. Iron Oxides Reduction with Hydrocarbons

Hydrocarbons can be used in two ways as a reducing agent for the production of reduced iron ores:

(i) direct use of hydrocarbons or a mixture of gas containing hydrocarbons,

(ii) use of the reformed hydrocarbon products (CO, H_2), by reforming within the reduction reactor (it was found that autocatalytic reforming of some hydrocarbons within the reducing reactor provided an access of macro and micro porosity which led to more extensive reduction and, on the economic side, a deletion of the capital cost of gas reformer and processing. More details will be discussed further) or in a separate catalytic reformer.

There are a few investigations[111 -113] using directly hydrocarbons or a mixture of gas containing hydrocarbons as reductant for direct reduction of iron ores. Two important points emerge from these reports. Firstly, the rate of reduction with hydrocarbons is slow and production of a high quality of sponge iron is troublesome and non economic. Secondly, these investigations were carried out under isothermal conditions in a thermogravimeter with single particle or powder compact, thus the results are of only theoretical value.

2.19.1. The theoretical importance of investigations with hydrocarbons.

The kinetics of ferric oxide reduction by pure methane[111, 112] were studied in the three temperature ranges of: low (500 - 600°C), medium (650 - 750°C) and high (800 - 950°C) temperature. At the low temperature reduction proceeded only from Fe_2O_3 to Fe_3O_4; a prolonged holding of the specimen in a stream of methane did not lead to any process extension beyond this stage. The rate became appreciable at 650°C. In special experiments after the Fe_3O_4 composition had been reached, the sample was reduced further by hydrogen and methane. It was shown that methane reduction in the low temperature range beyond the Fe_3O_4 stage occurs only if a sufficient quantity of metallic iron has been built up. In this case the reducing agent was not methane, but its decomposition product, hydrogen. Carbon formed by methane decomposition took almost no part in the reduction and accumulated in the sample.

In the medium temperature range the conversion of Fe_3O_4 to FeO took place but at low rates. A sharp rise in reduction rate was observed on going from 750°C to 800°C. Starting from 800°C, the process became very sensitive to temperature changes and accelerated considerably in the high temperature range, when metallic iron appeared in the sample. The appearance of metallic iron at the FeO to Fe stage, at comparatively high temperatures indicated a decisive role of metallic iron as a catalyst for reforming methane by the reduction products (CO_2, H_2O). In the absence of a catalyst the decomposition of methane and its reforming by the reduction products (CO_2, H_2O) did not occur to any substantial extent and no carbon accumulation in the sample was observed. When the iron catalyst was present, methane dissociation into the elements occurred only

at very late stages of reduction, when there was insufficient carbon dioxide and water vapour to convert all the methane diffused into the sample. Carbon build-up in the sample started from that stage.

In the two stage production of sponge iron[113] with methane, it was found that the complete decomposition of methane in the presence of iron bearing material occurred at temperatures of 850 - 900°C, which is 400 - 450°C lower than on an inert surface (e.g. fire clay), while the reaction rate, conversely, was ten times greater. The products of the first stage were a sooty iron containing 30 - 50% carbon (by weight) and technically pure hydrogen.

In the second stage, the product of the first stage (that means sooty iron with highly dispersed carbon in the pores of sponge iron and on the surface of the iron particles) was used as an active reducing agent and mixed with millscale or concentrate; the mixture was reduced in the temperature range 1050 - 1100°C with a make-up reducing agent of hydrogen or reformed natural gas. The results of industrial trials showed that the use of sooty iron instead of soot, petroleum coke and the other known carbonaceous reducing agents considerably intensified the iron-oxide reduction process. As is well known, the direct reduction of iron oxides with carbon is directly related to the rate of reaction between the carbon and carbon dioxide. The sooty iron may have intensified the rate of Boudouard reaction.

The isothermal reduction of hematite[114] pellets (with 10 to 15 per cent porosity) in a thermobalance with a mixture of methane-hydrogen (containing 4.5 per cent methane) within the temperature range 700 - 1000°C indicated that the reduction was chemical - controlled initially and diffusion - controlled in the later stages. It was shown that

reduction in pure hydrogen was faster than in the methane-hydrogen mixture. This difference was attributed to carbon deposition in the outer reduced layers of the pellet, causing resistance to gas diffusion when the reducing gas contained methane. It was shown that the excess residual carbon may be removed from the reduced iron at lower temperature by its hydrogenation. In another study[115] it was also demonstrated that it was possible to hydrogenate residual carbon in reduced sponge products to methane.

The carbon formed[116] as a result of the reduction of iron oxide in a mixture of CH_4 and H_2 (containing 20 per cent CH_4) reacted with steam according to the water gas reaction to regenerate hydrogen and produce carbon monoxide.

Pure ferric oxide briquettes[117] were reduced at temperatures ranging from 800 - 1050°C, in gas mixtures containing H_2, CO, CH_4, N_2 and CO_2, which was obtained by partial oxidation of natural gas with air. The CH_4 content of the reformed gas mixture was between 13 and 16 per cent. The over-all reduction rate again was controlled initially by chemical reaction and the gaseous diffusion was applicable during the latter stages. It was shown that the hematite briquettes swell and considerable porosity was developed during reduction. The normal topochemical patterns were shown in the metallographic studies, and hence the solid-state diffusion rates increased more rapidly with temperature than did interfacial or gaseous diffusion reaction rates.

The reduction of porous (30 per cent porosity) iron ore[118] in methane indicated that the reaction proceeded stepwise from hematite

to magnetite, wustite and iron. The iron catalyzed the methane cracking reaction. Optimum conditions for methane utilization occurred at about 1000^{o}C.

The above findings are not consistent with the earlier discussion on the understanding of high-grade porous (about 30 per cent) or dense hematite reduction kinetics, which showed that the rate of reduction may be considered to fall between three limiting cases, namely uniform internal reduction, limiting mixed control and diffusion in porous iron layer, respectively the rate of reduction corresponding to, chemical control, the overall chemical control and diffusion control, and diffusion control. The overall rate of reduction is not controlled by only one of these rate controlling mechanisms and would be changed from one limiting case to another during the course of reduction.

2.19.2. <u>The practical importance of investigation with hydrocarbons.</u>

2.19.2.1. The processes using a separate catalytic reformer were explained earlier (refer to 2.4).

2.19.2.2. The reduction of iron oxides with the products of reformed hydrocarbons (using CO_2 or H_2O oxidant) within the reduction reactor.

2.19.2.2.1 Reduction of iron oxides with a mixture of H_2, CO_2, and hydrocarbons.

Prefluxed consett sinter was reduced by a mixutre of H_2, CO_2 and hydrocarbons using the benefits of autocatalytic reforming of hydrocarbons on the ore surface, in a laboratory rotary kiln[119 -123] which was developed in Sussex University. It was found that the most

important factors controlling the extent of reduction were:

(i) the temperature.

(ii) the composition of gas, presence of unreacted hydrocarbons in the reducing gas, the ratio of hydrogen:carbon in it, and reducing capacity.

(iii) the ore particle size.

(iv) the residence time for reduction.

The effect of the above factors on the extent of reduction showed that the plot of each factor in question against the percentage reduction gave either a straight line relationship or could be put in a form which gave one. Thus the effect of varying one operating variable on the percentage reduction of the ore, when all the other operating parameters are fixed, can be readily calculated for each variable from an equation in the form $y = a + bx$, where x is a function of the percentage reduction, y that of a variable, and a and b are constants.

Two different hydrocarbons (i.e. methane or butane) were reformed within the kiln. When methane was used the reduction fell off rapidly as the temperature decreased below 950°C, since much of the hydrocarbon passed through the kiln unchanged. In the case of butane usage, above 920°C it was completely converted to $CO-CO_2-H_2-H_2O$ but below 920°C some methane left the kiln without reaction. In closely related experiments with H_2-CO and with a chemically equivalent mixture of $H_2-CO_2-C_4H_{10}$ better reductions were achieved and stickiness was more readily avoided, with the gas feeds containing butane. It may be that the butane assists in the preservation of the pore structure of the partially reduced particles, since any local hot spots induce

endothermic reactions with the hydro carbons, catalysed on the surface of the ore. Above 950°C, the reductions achieved were independent of the way in which the reducing gas was generated; similar results were obtained for CO:H_2 mixtures and for chemically equivalent mixtures (i.e. with the same proportions of C, H, O) in which some methane or butane was reformed within the kiln. The reason may be that the sintering tendency of the ore, which was confirmed by a decrease in measured surface area, becomes significant at high (above 930°C) temperatures.

The reducing gas feed was diluted with nitrogen so that the N:O ratio in the gases entering the kiln was the same as in air. Surprisingly, the reductions achieved were similar to those in experiments in which the nitrogen was omitted. Dilution with nitrogen has been reported to decrease the rate of reduction of iron oxide by hydrogen[124, 125], and so it may be that, in the kiln operated as described here[119], the conditions are particularly favourable for the establishment of equilibrium. This point merits further examination.

2.19.2.2.2. Reduction of iron oxides with the products of methane reformed with H_2O within the reduction reactor.

In early 1981 a commercial method[126] was introduced, using gaseous mixtures containing up to about 30% by volume of methane (e.g. coke oven gas), for the direct gaseous reduction of iron ore in a counter current moving bed shaft reactor. The reactor contained a reduction zone, a cooling zone and an intermediate reforming zone. A hot mixture of coke oven gas and steam was fed to the intermediate zone and reduced ore therein catalyzed the reforming of the methane to carbon monoxide and hydrogen. The reformed gas flowed upward into the reduction zone for the reduction of iron ore.

CHAPTER 3

EXPERIMENTAL

3. EXPERIMENTAL

3.1. The Kiln Description.

The kiln used for this work was a rotary kiln bench unit. The details of the rotary kiln are given in Figure 40. As will be seen from the figure the rotary kiln is in general an upscaled version of the original kilnused at Sussex University[119], having a stainless steel tube of the following dimensions:

Overall length of kiln tube	127.0 cm
I.D. of kiln tube	4.12 cm
O.D. of kiln tube	4.44 cm

The heated length of the tube (furnace length) was 87.0 cm and was inclined at an angle of $1^{o}9''$ (with changing angle availability) and was driven by a spring-mounted and water-cooled Citenko KQt/19 electric motor. Gas-tight connections were made at either end by air-cooled stuffing glands (A and R) packed with graphite-impregnated (Asbestos) cord and the tube was centralised by two 2 inch plumbers blocks S and T.

The tube was heated by three separate heating windings along the length, which were made with Kanthal, A.I. wire, wound around a straight alumina refractory tube (I.D. 64 mm and O.D. 74 mm) and controlled by three temperature controllers. The left hand winding was monitored by a platinum-platinum/13% rhodium sensor and the right hand and middle windings by chromel-alumel sensors.

The ore feed hopper, N, was made from a one litre conical glass flask having a B57 quick fit socket as the neck. The surface of the hopper was dimpled to facilitate tumbling of the ore. A 8 cm length of

glass tubing (wall thickness 3.0 mm, outside diameter 46 mm) with a B57 cone was sealed with araldite into the hopper neck and the connection to the stainless steel tube was made using reinforced rubber tube hose securely fastened by jubilee clips. The hopper was heavily taped to prevent injury in the event of an explosion. Additional heating at the outlet was provided by a Dimplex electric heater above the hopper and by electrically heated tape, L, in order to prevent water condensation. The hopper was further supported by the smaller stuffing gland,R. A sliding chromel-alumel thermocouple, Tc, inside the tube, and held at one end by means of a standard quickfit screw thread stuffing gland, Q, allowed accurate monitoring of temperature along the length of the tube throughout an experiment under actual run conditions. The thermocouple was protected from the reducing gases by a thin-walled stainless steel sheath (v).

Chokes: These were used for controlling the ore flow rate and residence time and comprised chokes fixed inside the main kiln tube, preferably one at the ore outlet end (furnace) and the other in the upper end of the tube not far below the ore entry point from the ore feed hopper (B, C). The reduced ore was collected in 100 ml conical flasks attached to a standard fractionating pig, so that receivers could be changed without interruption of the gas flow.

After several series of runs it was observed that a more suitable ore inventory distribution was obtained when the kiln was operated without chokes (i.e. the slope and the amount of inventory held in the tube was reversed towards the kiln outlet) hence the sponge iron was held for a short time in the outlet part and the ore was kept for a longer time in the inlet part of the kiln.

Window: A special glass stub was attached to the pig assembly equipped with a perspex viewing window, P, which permitted viewing inside the kiln tube, giving a view of the ore flow rate and warning of the possible onset of stickiness.

3.2. Gas Feeding System.

A schematic flow diagram of the gas system is shown in Fig. (41). Each of the feed gases, hydrogen, carbon dioxide and butane was taken from the cylinder, through the needle valves, A, F (Fig. 41) drying columns B and C (except for carbon dioxide, which was only passed through B), a pressure controlling bubbler, D, with the blow off, E, and the calibrated flow meter G to the mixing chamber K, an upstream pressure stabiliser H (differential bubbler) and manometer J.

The bubbler and differential bubbler in the gas system were filled with high flash diesel oil. The diesel oil was assumed to be saturated with the hydrocarbons which are slightly soluble in it. Di-n-butyl phthalate was used as the fluid in the calibrated flowmeters and manometers.

The drying column, B, was charged with magnesium perchloride for water absorption, and in column, C, soda-asbestos was charged for carbon dioxide adsorption.

Gas Measurements: These are done preferably[119,127] by using an inclined manometer (flow meter), which has to be calibrated for each gas, each flow meter and each jet installed in it, by running a series of calibration measurements for each gas. The flow meter reading was held steady while a determined gas volume was collected (by

water displacement) over a suitable time. The water (head) was measured for each measurement in the water displacement apparatus, and the atmospheric pressure (barometer) noted. The collected gas volume was converted to $0^{o}C$ and 1 atm pressure (incl. water vapour content) and the results plotted for a series of inclined manometer readings, giving a straightline graph.

The equation[127] and constants of the graph were determined by plotting $\Delta P/Q_m$ against $Q^{\ominus}$ where:

P = pressure difference across the flowmeter jet.

Q_m = gas flow at a temperature T and any average pressure $\frac{P_1 + P_2}{2}$ where P_1 and P_2 are the inlet and outlet pressures.

$Q^{\ominus}$ = gas flow at a standard temperature and pressure, $T^{\ominus}$, $P^{\ominus}$ (which for convenience were $0^{o}C$ and 1 atm respectively)

The equation of the line is

$$\Delta P/Q_m = a\mu + b\rho^{\ominus} Q^{\ominus} \quad (127) \qquad (10)$$

where:

$\rho^{\ominus}$ is the gas density at $T^{\ominus}$, $P^{\ominus}$

a and b are flowmeter constants independent of the gas properties

μ = viscosity.

Once the constants a and b are known the equation can be adapted to use the flowmeter for any other gases of known density and viscosity.

$$\text{Since } Q_m = Q^{\ominus} \left(\frac{T}{T^{\ominus}}\right) \left(\frac{2P^{\ominus}}{P_1 + P_2}\right) \qquad (11)$$

combining equation (10) with equation (11) yields the general formula (12).

$$Q^{\Theta} = [{}^{1}/_{4}(\frac{a\mu}{b\rho^{\Theta}})^{2} + \frac{\Delta P}{b\rho^{\Theta}}(\frac{\Delta P + 2P_2}{2P^{\Theta}})(\frac{T^{\Theta}}{T})]^{1}/_{2} - {}^{1}/_{2}(\frac{a\mu}{b\rho^{\Theta}}) \qquad (12)$$

Q^{Θ} is the gas flow at a standard temperature T^{Θ} and a standard pressure P^{Θ} which for convenience were taken as $0^{o}C$ and 1 atm (101325 Pa) respectively.

A typical gas measurement calculation and calibration is given in Appendix No. 1.

3.3. Reducing Capacity.

Provided that direct reactions between hydrocarbon and iron ore may be ignored, the maximum efficiency for the process is achieved when a reduction of 100% is obtained with a reducing capacity $P = 1.058t$ (119) (t = mole per hour Fe in iron ore and P = mole per hour gaseous reducing agent). Feeds with $P < 1.058t$ have insufficient reducing capacity to convert all the wustite in the ore to metallic iron. Since the reduction of wustite to iron is the controlling reaction it is advantageous to reduce iron ore in a continuous counter current reactor (like the rotary kiln) and to use the sufficient remaining reducing capacity of gas after the reduction of wustite to iron for reduction of higher iron ore oxides (i.e. hematite ⟶ magnetite ⟶ wustite).

Our experiments have nearly all been made with feed gases having reducing capacities 15 - 25% greater than 1.058t to ensure that the reaction is limited by kinetic rather than thermodynamic factors.

The best reducing capacity and the gas compositions, which included unreacted butane, hydrogen and carbon dioxide, were found experimentally to give 100% reduction of the Brazilian iron ore without any soot formation, and with a very small content of unreformed hydro-

carbons in the off gases. From the equation P = 1.058t the theoretical reducing capacity for 100 (grams) hourly ore feed was calculated as follows:

The total iron in the iron ore feed was 67.5 per cent.

Then:

67.5 grams of iron = 1.2085 mole/hour

Therefore:

P = 1.058t = 1.058 x 1.2085 = 1.2786 mole/hour.

A formula was found for reducing capacity[119] in which hydrocarbons were reformed within the kiln as follows:

$$P = {}^{1}/_{3}[a + c - 2(b + d)] + 2e + 7f \qquad (13)$$

Where

P = reducing capacity mole per hour

a = CO;

b = CO_2;

c = H_2;

d = H_2O;

e = CH_4;

f = C_4H_{10} in mole per hour.

From the above theoretical reducing capacity the best experimental reducing capacity (for 1.2085 grams mole/hour iron feed rate) to use had a value of about 1.52. The average total amount of hydrocarbons left in the off gases (expressed as methane) was found to be approximately 0.18 mole per hour, which depended on the temperature and is assumed as negative value in the equation (13). For example, when the inlet gas composition and amount was: hydrogen 2.44 mole/hour, carbon dioxide

0.91 mole/hour and butane 0.24 mole/hour, then the practical reducing capacity was as follows:

$$P = {}^{1}/_{3}\,[2.44 - 2(0.91)] + (7 \times 0.24) - (2 \times 0.18)$$

$$= 1.5266 \text{ mole/hour.}$$

3.4. Preparation of Iron Ore.

The lump ore was crushed by a rotary crusher which crushed ore more uniformly than did a jaw crusher. The ore used in these series of runs was taken between two sieve sizes; for the small size 1.7 to 2.36 mm, medium size 2.36 - 3.35 mm and large sizes 3.35 - 4.75 mm, 4.75 - 6.7 mm respectively.

The ore was roasted at 600 - 650^{o}C in a muffle furnace for 48 hours, 1.7% of moisture being removed. The crushed ore was not perfectly uniform and there was a fair proportion of flat lenticular particles.

The average volume of one particle of each of the three sized ores was found by displacement of liquid paraffin. For each measurement fifty particles were selected by coning and quartering and the measured volume divided by fifty was taken as the average volume for each size. The volumes were, 0.03947, 0.0153 and 0.00705 cm^3 respectively for the large, the medium and the small sizes.

3.5. Sampling of Sponge Iron and Off Gases.

The best time for sampling was when the steady state was reached and the gas and ore samples should be taken together. The composition of sponge iron produced was not perfectly uniform and individual grains with high gangue content and/or low prosity could be

easily picked out visually. Therefore, samples taken for analysis were selected as far as possible by the pyramiding/quartering technique to obtain a good average sample. The sample was crushed to less than 72 mesh for all types of analysis. This was assumed to give a good average uniformity of composition throughout the sample from the run. If the part analysed had more than average gangue it gave a low reduction and vice versa.

3.6. Chemical Analysis.

The sponge iron was analysed for determination of total iron, metallic iron, carbon, sulphur, phosphorus content using standard procedures[128 - 130] (refer to Appendix No. 2).

3.7. Off Gas Analysis and Gas Balance.

When steady state was reached, analysis of the outlet gases was made as follows. Water and carbon dioxide were determined gravimetrically in standard calcium chloride and sofnolite tubes attached to M (Fig. 40). Meantime the residual gases (CO, H_2, C_nH_m) were collected in a two litre water displacement apparatus and the time for collection was measured accurately. A series of samples were analysed for hydrocarbon content by gas chromatography. Inlet gas compositions were calculated from the calibrated flow meter readings. As some carbon was deposited within the sponge produced, the amount of carbon formed was measured by the combustion method. A gas balance could then be calculated. A typical illustration of a gas balance is given in Appendix 3.

The reduction could be checked independently by analysis of the metallic iron in the sponge and finding the per cent reduction using equations Nos. (14) and (15). The results by the two methods were,

in general, found to be in good agreement with one another. There is a small error in the gas balance reduction calculation, because the small amount of hydrocarbons found in the off gas was assumed to be methane. In fact, complete analysis identified the presence also of other hydrocarbons, but methane was found to be the major hydrocarbon in the off gases.

3.8. Feed Rate.

This was regulated normally by the rotational speed of the kiln tube and by its angle of inclination to the horizontal, and particularly by the hopper level which was determined by the rate of addition (g/hour) of ore to the hopper. At steady state flow the input rate in g/hour of ore added to the hopper must equal the rate of output g/hour.

During the runs with chokes, the angle of inclination of the kiln, rate of hourly feed and speed of rotation were maintained constant respectively at 1 degree 9 minutes to 1 degree 20 minutes, 100 grams per hour and twentynine seconds per revolution (residence time was changed by altering the I.D of the exit choke). When these parameters were fixed it was found experimentally that a very constant feed rate was obtained once steady state conditions had been reached. For example, with a feed rate to the hopper of 100 grams/hour of fresh sized ore, in a blank experiment at 900^{o}C, under a nitrogen atmosphere the delivery rates (unreduced) measured over five successive hourly periods after reaching steady state were, 100.9, 99.9, 101.2, 100.5 and 99.5 grams/hour.

The successful operating conditions found for the kiln working without chokes (refer to 3.1) are as follows:

(i) The speed of rotation - 47 seconds per revolution.

(ii) The angle of the kiln - $1^{o}.20'' - 1.^{o}30''$

A blank run was performed with ore size 3.35 - 4.75 mm at $900^{o}C$ under a nitrogen atmosphere. After reaching the steady state four successive outputs of, 103.5, 99.5, 101.5 and 99.8 grams were found for 100 grams hourly input.

It was confirmed that the rate of ore flow remained steady under normal operating conditions by carrying out checks of the ore discharge rate (iron sponge) under steady conditions during test run periods. The rate of iron sponge delivery can be disturbed by the onset of stickiness which may be due to the use of high reduction temperatures. A further reason could be damage to the winding, caused by partial oxidation of the wire at a point (Max. Temp.) which thins the wire and increases its resistance, so that part of the wire is overheated, causing a hot spot and stickiness in the kiln tube at that point. The only solution then is to replace the winding. However, after suitable working conditions had been defined, in all of the run series there was a good agreement between feed rate and output, which checked with the weight of sponge iron and its degree of reduction. By analysis, the error was found to be within 1 - 2%.

3.9. The Temperature in the Reduction Zone.

The heated section of the kiln consisted of three different windings on the one straight refractory tube (Fig. 40 D, E, F.) each winding being controlled by an independent temperature controller. The main reason for this sort of winding was to control the temperature profile to give a uniform steady temperature along the hot zone, with

ability to control the middle section temperature. Secondly, on the left hand side of the kiln the ore feed is preheated while the ore has a relatively low degree of reduction - calling for careful control as at the start of the run the ore is prone to stickiness. The right hand winding preheats the feed gas. If a higher percentage reduction was required without raising the residence time, all three controllers were increased in step to give a good temperature profile. The interior kiln temperature was measured accurately by a moveable axial thermocouple TC (Fig. 40), inserted through a stuffing gland, so that temperature measurement could be made at points along the kiln tube axis under actual operating conditions. Temperature profiles were determined at the end of each run under actual steady state operating conditions. The kiln hot zone temperature was found as the average of the three maximum temperatures of the three sections for each run.

3.10. Residence Time.

This is a most important operating parameter, as time and temperature are the basic controlling factors for the reduction. The time which the ore takes to move from one end of the hot-zone to the other is called the residence time. The hot zone is defined as the heated length of the kiln, which has as uniform a temperature as possible, with the average reaction temperature required. The temperature profile clearly varies along the heated length of the kiln so the average reaction temperature along the heated length of the kiln (hot-zone) was estimated as follows:

(i) The average of the maximum temperatures of the three sections of the tube (coil winding) was taken as the average run temperature.

(ii) The temperature at which the temperature profile becomes steep (see Fig. 42) due to the heating up of the ore and gas feeds and where the rate of reduction is low, was found to be about 700°C; hence 700°C was taken as the base temperature line.

(iii) With relation to the average run temperature line AB (see Fig. 42) and the base temperature line CD, there are found some positive areas outside the area enclosed by the lines GE - EH - HJ and some negative areas inside it, when a hot zone GJ is established for the kiln. These areas have to be balanced to integrate approximately the residence time corresponding to the average reaction temperature for the run. To achieve this, two parallel lines EFG and HIJ were drawn and located at equal distances from the line SNR, at the centre of the hot zone, in such positions that the sum of the positive areas FCG, IJD, OPQ and KLM balanced the sum of the negative areas FEK, MNO, IHQ. From this graphical integration the length of hot-zone corresponding to the average run temperature (average of the maximum temperatures of the three coil winding sections) is given by the length GJ, which for each individual run has to be calculated from the temperature profile in the same manner as above.

The residence time of the ore was based on the measured inventory of ore held in the hot zone. As it was impossible to measure the amount of inventory for each run separately, a series of runs were made and at the end of each set of runs, or when the operation had to be interrupted for maintenance, the amount of ore inventory was measured. The amount of inventory measured in the hot zone is expressed empirically

as the equivalent of unreduced ore. Because of the kiln angle and the presence of the chokes the ore was not distributed uniformly along the length of the hot zone, so the inventory is best expressed as the average equivalent grams of unreduced ore per cm. of the length of the kiln which is termed the standard inventory. This was calculated by dividing the total amount of ore in the tube (on the unreduced basis) by the heated length of the tube (from choke to choke when using chokes). The total amount of inventory in the hot-zone was calculated by multiplying the length of the hot-zone (cm) by the standard inventory (on the basis of grams of unreduced ore per cm.) for each run. This total amount of inventory divided by the hourly feed rate gave the residence time. The residence time for each curve (in a series of runs) was expressed as the average for all the runs in the series. The calculated residence time was slightly higher than the true figure, because of the empirical assumption that the average percentage reduction of ore in the tube (hot-zone) was that of the ore leaving it, but the results were all comparable. The desired residence time was achieved by changing the I.D. of the exit choke in the case of kiln with chokes and by changing the angle of the kiln when chokes were not used.

3.11. Steady State Condition.

It was found by experience that when full steady state was reached the percentage reduction for every individual run calculated by the three independent methods was in good agreement.

Metallization was calculated directly from the chemical analytical determination of metallic iron and total iron found in the

sponge iron and is defined as:

$$\% \text{ Metallization} = \frac{\text{Metallic iron in sponge}}{\text{Total iron in sponge}} \times 100$$

The degree of reduction is defined by:

$$\%R = \frac{\text{Amount of oxygen removed from the ore per hour}}{\text{Amount of oxygen entering kiln in the ore per hour}} \times 100$$

Three procedures were used to calculate the degree of reduction:

Method 1 by chemical analysis: The percentage reduction was expressed as percentage of oxygen content removed from the ore, calculated from the metallic iron content, which was determined by chemical analysis (refer 3.6) and the total iron content of its ore feed using the formulas:

$$m = [n - 0.30257(Z - 100\ q)] / (1 + 0.30257\ q) \qquad (14)$$

and $$\%R = (m/n) \times 100 \qquad (15)$$

where,

m = grams of oxygen removed per 100 grams of ore.

n = grams of oxygen contained in 100 grams of unreduced ore.

z = grams of total iron contained in 100 grams of unreduced ore.

q = percentage of metallic iron found by analysis in reduced ore/100 (i.e. proportion by weight).

0.30257 = weight ratio oxygen:iron in wustite ($Fe_{0.947}O$)

This formula assumes that for the % reduction normally used for iron sponge production any unreduced oxygen in the iron sponge is present as the iron oxide wustite. Thus, the calculation only applies to ores which have been reduced at least to that degree. It is assumed, also, that all the oxygen removed from the ore is derived from iron oxides, and none from the gangue.

Method 2 by oxygen balance: An oxygen balance was made for the gaseous feed and products. The error or results were within 1 - 5% compared with the first method which was attributed to hydrocarbon measurement in off gases (refer 4.1.9).

Method 3 by the weight of sponge discharged: The measured rate of sponge iron production checked well with the calculated weight determined from the ore feed rate and the measured degree of reduction. Results obtained by this method were within ± 3% of the results obtained by methods one and two. This difference may partly be due to small differences in the level and amount of ore in the hopper during heating up and cooling down and hence affects the hourly feed pass from the hopper to the tube. (Ref. 3.12). The apparent steady state approaches more closely to the true steady state conditions for a run when the run is prolonged. However, the percentage of reduction determined by method one is considered to be more reliable than the methods two and three.

3.12. Experimental Procedure.

First the operating parameters were determined (Refer 3.8). Under these conditions a constant flow of ore was established through the reaction zone, giving a steady flow of the sized ore particles so that they behaved as a fluid flowing over a weir (i.e. choke). Each set of runs had to be terminated if any condition occurred which could disturb the constant flow rate of the ore, because the inventory is affected by variations, such as changes in the feed rate of ore, speed of rotation, angle of kiln tube and stickiness occurrence as well as by the flow rate of ore. Changes in any of these conditions upset the steady state and made it impossible to obtain a good sample. When a kiln thermocouple,

kiln winding or hopper had to be replaced, it was advisable to determine the ore inventory for that set of runs and terminate the series.

The hopper was charged with a weighed amount of ore, the weight being based on previous experience of the steady state (in these run series around 1000 grams). The tube was charged with partly reduced ore from earlier experiments which allowed steady state to be obtained faster and also shortened the time the ore was held in the critical stickiness range during reduction (generally, sticking occurs in the 20 - 50%[124] metallization range so that excessive temperatures should be avoided when the material passes through this range of reduction). The kiln was tested for leaks by passing nitrogen at a metered rate whilst it was hot and rotating, and noting any difference in the rate at the entry and exit. This procedure was also carried out at the conclusion of a run.

The temperature of the kiln was raised slowly in 100°C steps to reach 500°C. The kiln was flushed with nitrogen and rotation was begun at a low speed while the temperature was raised in further steps of 100°C up to 800°C. Thereafter it was raised in 10°C steps to minimise the risk of over-shooting and damage to the heating elements.

The hopper auxiliary heater and tape heater were switched on to prevent water condensation before the reducing gases were injected in the following order: carbon dioxide, hydrogen and butane and their flow rates were stabilised. The speed of rotation was then set at 29 seconds per revolution.

At the end of each hour 100 grams of ore was added to the hopper, while the kiln was momentarily stopped. At regular intervals

(each hour) throughout the run, the speed of rotation, temperature of the kiln, weight of reduced ore and flow rates of reducing gases were carefully recorded and adjusted when necessary. In addition, the inside of the kiln was viewed frequently through the perspex window (P) (Fig. 40) in order to check whether it was necessary to counter the onset of stickiness or soot formation.

When steady state was reached, analysis of the exit off gases was made and the temperature was checked at every 5 cm of the kiln tube length by an axial thermocouple to determine and record the temperature profile for the run. The sponge iron output during the last hour of equilibrium operation (when the gas sample was also taken) was set aside as the sponge iron sample for the run. At the end of each run the kiln was cooled down while nitrogen was flushed through and rotation was maintained at a low speed to prevent tube distortion, until the kiln had cooled to 500^{o}C. Thereafter, all gas and power supplies were closed. A typical run report sheet is given in Appendix IV.

3.13. Sampling along the Length of the Kiln.

A sliding stainless steel scoop, held at one end by means of a standard quickfit screw thread stuffing gland attached to the pig assembly, allowed accurate monitoring position of the scoop along the length of the tube throughout an experiment under actual run conditions. Rotation of the scoop thus facilitated collection of a sample from any chosen position along the length of the kiln.

The contact between the red hot sponge samples with the carburising atmosphere in the cooling zone (toward the discharge end) caused a change

in the composition of the samples during withdrawal and invalidated analyses obtained under actual run conditions. An attempt was made to sample under a nitrogen atmosphere. For multiple sampling the pigs had to be changed shortly after a set of samples had been collected. It was found that the samples were still hot at this stage and surface oxidation occurred when the pigs were opened to air. Hence, the best solution was found to be to cool the kiln under nitrogen overnight and take the samples on the following day. It was recognised that some oxidation might occur during the cooling period, but samples collected from the discharge end of the kiln after cooling showed no significant difference from the composition of the last sample taken from the discharged ore before the termination of the run.

3.14. Metallography of Particles.

The structure of particles of original iron ore and sponge iron produced at different temperatures, were studied by standard scanning electronmicroscopy. Also cross sections of some samples were prepared by mounting in bakelite or resin and polished samples after etching in 2% nital were studied by optical microscopy.

3.15. Chromatography Analysis of Off Gases.

Samples of the residual off gases, after absorption of CO_2 and H_2O, were analysed by standard chromatography, to identify the hydrocarbons contained.

3.16. Porosity Measurements.

The total connected pore volume was measured by a mercury penetration porosimeter over the pressure range of 1 - 2000 Kg/Cm^2.

It should be noted that the chromatography and porosity meter measurement equipment was located in the chemistry department and access was limited.

CHAPTER 4

RESULTS

4. RESULTS.

A major modification in the design of the kiln was made during the experimental work (i.e. removal of the chokes). The results are separated accordingly into Part One (operation with chokes) and Part Two (operation without chokes).

For the sake of simplicity in considering the results and avoiding too many equations and figures in the text, most of the results are tabulated.

4.1. Results - (RP_1)(Experiments with chokes in position in the kiln).

These series of runs were performed to study the relationship between temperature and percentage reduction and also the effect of particle size and residence time on the percentage reduction. In the first three and the fifth series the particle size and residence time were treated as variables, whilst in series 4 and 6 the residence time was held constant as the particle size was varied.

4.1.1. Series I (Code No. RP_1S_1)

Particle size 2.36 - 3.35 mm.

Temperature range 743 - 903^{o}C

The results of the 10 runs in the series are given in Tables (1, 2, 3, 4) and are shown in Fig. (43, 44).

Paired values of the variables, i.e. temperature (x) and percentage reduction (y) were used to derive a mathematical relation, using the linear regression technique based on the method of least squares. Two different equations were found for reduction versus temperature, one for runs with temperature below 887^{o}C and the other above that, as follows:

$$R = 0.267\ Tc^{o} - 136.73 \text{ (for runs below } 887^{o}C) \qquad (16)$$

where T = temperature in degree centigrade

The coefficient of determination = $r^2 = 0.983$

$$R = 0.091\ Tc^{o} + 16.34 \text{ (for runs above } 887^{o}C) \qquad (17)$$

The coefficient of determination = $r^2 = 0.991$

When the values of $LogR_{10}$ were plotted against $\frac{10^4}{T_K{}^o}$

a straight line relationship emerged for the whole of the range of temperatures. The equation is as follows:

$$Log\%R = - 0.1571\left(\frac{10^4}{T_K{}^o}\right) + 3.3440 \qquad (18)$$

Where T = temperature in degrees Kelvin

The coefficient of determination = $r^2 = 0.977$

The data which were taken to calculate the equations are given in Tables 1 and 2.

NOTE: The coefficient of determination for the two individual equations (16, 17) proved to be higher than the one for equation (18), but for a curve covering the whole range of temperatures, the coefficient of determination for the combined equations (16, 17) will be lower. In the light of this series examined, the nonlinear effect of percentage of reduction vs temperature in the high temperature range (i.e. > 90% reduction) for the other series of runs were not examined and this is the reason why the coefficient of determination for percentage vs temperature is higher than the one calculated for Log $\underset{10}{R}$ vs. $\frac{10^4}{T_K{}^o}$.

4.1.2. The residence time calculation for the Series I.

The residence time for the first series of runs was found as follows: the last run of the first series was run No. 10; from its temperature profile the length of the hot zone was 56.5 cm and the amount of

inventory measured in this length (hot-zone) was 295.60 grams (as reduced ore). This quantity was converted to an unreduced ore basis as follows.

The rate of feeding ore into the furnace could not be measured accurately but an accurate measurement could be made, over relatively short time intervals, of the rate of discharge of reduced iron. Because of the non uniformity of distribution within the kiln, it was assumed the inventory had the same percentage reduction as the sponge iron leaving the kiln. The percentage reduction in run No. 10 was 98.93. The amount of oxygen in 100 grams of the iron ore was 29.087 grams. Thus the inventory, when converted to an unreduced ore basis, was 414.99 grams. If the amount of inventory in the hot-zone is divided by the hourly feed rate, which was 100 grams of ore per hour, the residence time would be 4.14 hours (249.0 minutes) for this run.

The residence time was calculated (for more details refer to 3.10) as above for the other runs of this series. The average residence time for all the runs was 220 minutes. The results are shown in Table (3).

4.1.3. <u>The carbon contents in the sponge iron determined for each run of the first series</u>.

The results are shown in Table No. 5 and in Fig. (45).

4.1.4. (See Page 88).

4.1.4. The corresponding data for the other series of experiments made with chokes in position in the kiln are presented as follows:

Series & Code No.	Particle size mm	Temp. ^{o}C	Average Residence Time Minutes	Results		Equations		Residence Time, Tables.
				Tables	Figures	%R Vs. T (Table 28)	log% R Vs. $\frac{1}{T}$ (Table 29)	
II(RP_1S_2)	3.35-4.75	804-931	107	6,7,8,9	46,47	19	20	8, 30
III(RP_1S_3)	1.7-2.36	756-867	164	12,13,14,15	51,52	21	22	14,30
IV(RP_1S_4)	1.7-2.36	756-855	228	16,17,18,19	43,44	23	24	18,30
V(RP_1S_5)	3.35-4.75	754-828	290	20,21,22,23	46,47	25	26	22,30
VI(RP_1S_6)	3.35-4.75	761-831	202	24,25,26,27	43,46,47	27	28	26,30

4.1.5. The carbon, sulphur, phosphorus content in the sponge iron determined for the second series.

The amount of carbon and the sulphur content in the sponge iron was determined for each run of the second series. The results are given in Table No. 10 and are shown in Figs. (48 and 49) respectively for carbon and sulphur.

The phosphorus content found in the sponge iron at three different temperatures is shown in Table No. 11 and in Figure (50).

4.1.6. The effect of Size of Particles on the Reduction.

The results for percentage reduction versus temperature for Series I, IV and VI with the three different particle sizes, but with the other variables the same, are represented by equations 16, 23 and 27. The equations showed that these relationships approximately parallel over the limited temperature range to which the equations apply. Therefore, at any chosen temperature within this range a relationship between the size and the percentage of reduction can be extracted, using the above equations, that could be fitted in linear form.

Some examples for the above statement are given as follows:

For a temperature of $830^{o}C$:

$$R = 4.255\ x + 97.1738 \qquad (29)$$

where R is the percentage reduction and x is the average particle size (between two sieve sizes)

Coefficient of determination = $r^2 = 0.997$.

For a temperature of $800^{o}C$:

$$R = -4.1519\ x + 89.0429 \qquad (30)$$

with $r^2 = 0.993$

For a temperature of 770^{o}C

$$R = -4.0489\ x + 80.9119 \qquad (31)$$

with $r^2 = 0.985$

The graphs of these equations are given in Fig. (53) and results in Tables (31, 32, 33).

4.1.7. The Effect of the Volume of Particles on the Reduction

The average volume of a particle of ore, corresponding to each of the sieve size ranges was determined as described in section 3.4. Using equations 16, 23 and 27 corresponding relationships were derived between particle volume and percentage of reduction at constant temperature. Some examples are:

For a temperature of 830^{o}C

$$Y = 63.83 - 5.01X \qquad (32)$$

Where Y = R is the percentage reduction and

X = LnV, V is the average volume of one particle.

Coefficient of determination = $r^2 = 0.99$

For a temperature of 800^{o}C

$$Y = 56.47 - 4.901\ x \qquad (33)$$

$r^2 = 0.99$

For a temperature of 770^{o}C

$$Y = 49.113 - 4.788\ x \qquad (34)$$

$r^2 = 0.99$

The graphs of these equations are given in Fig. (54) and results in Tables (34, 35, 36).

4.1.8. The Effect of Residence Time on the Reduction

The results of the three series of runs with ore size 3.35 - 4.75 mm but with different residence time indicated by equations 19, 25 and 27, showed that the lines are approximately parallel (in the limited temperature) and a straightline relationship was found for percentage reduction versus residence time, when all the other variables were held constant. The relationship was studied at only one temperature (831^{o}C) and could be expressed numerically for that temperature in the form:

$$R = 0.0415\ (R.t.) + 71.48 \qquad (35)$$

Where R.t. is residence time and R is percentage reduction.

Coefficient of determination = $r^2 = 0.999$.

The results are given in Table (37) and the graph is given in Fig. (55).

From the results of the two series of runs with ore size 1.7 - 2.36 mm, with different residence time, (but the other variables steady), a straightline relationship was also found for percentage reduction versus residence time at about 831^{o}C. This line was approximately parallel to the residence time graph for size 3.35 - 4.75 mm. It was of limited use because it had just two points.

4.1.9. Chromatography Analysis of Off Gases.

The analysis showed that at a low reduction temperature a quantity of CH_4, C_2H_6, C_3H_8, C_4H_{10} and the other non identified hydrocarbons left the kiln. The amount decreased as the reaction temperature increased and in the high temperature runs only CH_4 and C_2H_6

were found in the off gases. The complete results are given in Table (38) and Fig. (48).

4.1.10. Metallography of Particles.

Micrographs A, B, C, D, E, F, G and H indicate the features observed by scanning electron microscopy and optical microscopy of an original iron ore particle and of sponge iron produced at temperatures ranging from 829 to 903^{o}C.

4.2. Experiments without Chokes in the Kiln.

Six series of runs were performed to study the following:

(i) After the essential conditions were established for steady state working of the kiln without using the chokes, the seventh series of runs was made to study the progress of reduction, the removal of impurities (i.e. P, S) and carbon deposition as the ore traversed the reducing zone.

(ii) The eighth series of runs was performed to study the relationship between temperature and percentage reduction and also carbon deposition in the sponge iron.

(iii) The ninth series of runs examined the effect of different oxidant (CO_2) amount and ratio in the mixture of the input gases upon percentage reduction and carbon content of the sponge iron.

(iv) The tenth series of runs studied the effect of reducing capacity upon percentage reduction.

(v) The eleventh and twelth series of runs were performed to study the effect of different amount and ratio of hydrocarbon (C_4H_{10}) in the mixture of the input gases upon percentage reduction.

In these series of runs always one factor (affecting the progress of reduction) was varied whilst the others were held constant.

4.2.1. Series VII (Code No. RP_2S_7)

Particle size 3.35 - 4.75 mm

Run temperature 900°C.

The results of run No. 38 in the seventh series are given in Table No. (39) and (40). The residence time was found for the first series (Code No. RP_2T_1RT) and is shown in Table No.(55).

4.2.1.1. The Progress of the Metallisation along the Kiln Length.

The progress of the metallisation along the kiln length (i.e. reducing zone and cooling zone) was studied by analysing samples taken at invervals of 10 cm from the discharge end of the kiln. The analytical results and the corresponding kiln temperature for each sample are given in Table No. (40) and are shown in Fig. No. (56).

4.2.1.2. Carbon Content in the Sponge Iron.

The carbon content in the sponge iron found in the samples (i.e. the average of every 10 cm of the kiln length), are given in Table No. (40) and in Fig. No. (57) with the relative temperature profile.

4.2.1.3. Sulphur Content in Sponge Iron Samples.

The sponge iron samples were analysed for the sulphur content and the results are given in Table No. (40) and are shown in Fig. No. (58). The calculated sulphur content, assuming zero sulphur lost for the respective samples are also shown in the Figure.

4.2.1.4. Phosphorus Content in Sponge Iron.

The phosphorus content in the sponge iron was determined for three samples at different distances along the kiln (i.e. 90, 60, 40). The analyses are given in Table No. (41) and are shown in Fig. No. (59). The relationship between the phosphorus removal and the percentage of total iron content in the samples was measured for the same samples; the results are given in Table (41) and Fig. No. (60).

4.2.1.5. Cross Section of Sponge Iron Samples.

The cross section of the sponge iron samples (i.e. No. 10, 60, 80, 90) was studied by optical microscopy, shown in microphotographs I, J, K, L.

4.2.2. Series II

See Page 95.

4.2.2. The corresponding data for the other series of experiments made without chokes are presented as follows:

Series & Code No.	Particle size mm	Temp. ^oC	Average Residence Time Minutes	Results		Residence Time, Tables.	Equations Number (Table 57)
				Tables	Figures		
VIII (RP_2S_8)	3.35 - 4.75	752-902	97	42,43,44,45	61,62,63	44,55,56	%R vs. T ^oC No. 36 %R vs. $\frac{1}{T_K{}^o}$ No. 37
IX (RP_2S_9)	3.35-4.75	867	103	47,48	64	55,56	-
X (RP_2S_{10})	3.35-4.75	875	99	49,50	65	55,56	-
XI (RP_2S_{11})	3.35-4.75	849	97	51,52	67,66	55,56	%R vs. $V_{C_4H_{10}}$ No. 38 %R vs. $\%H_2$ No. 39
XII (RP_2S_{12})	4.75-6.7	900	63	53,54	68,66	55,56	%R vs. $V_{C_4H_{10}}$ No. 40 %R vs. $\%H_2$ 41

4.2.2.1. Total Pore Volume and Pore Radius

The total pore volume and pore radius were measured for four runs (No. 45, 44, 42, 40) of the series VIII (RP_2S_8) and also for the original hematite ore and are given in Table No. (46) and shown in Figure (No. 69). The percent of swelling is also given in Table No. (46).

4.2.2.2. Chromatographic Analysis of Residual Off-Gases.

The chromatographic analysis of the residual off-gases (CO, H_2) for runs in Series VIII (RP_2S_8) in the temperature range from 820°C to 900°C showed approximately 2% hydrocarbon (mainly methane) to be present.

4.2.2.3. Metallography of Particles.

Microphotographs M, N, O, and P indicate the features observed by scanning electron microscopy of sponge iron (size 3.35-4.75 mm) produced at temperatures ranging from 819 to 899°C in Series VIII (RP_2S_8).

4.2.3. Comparison of Ore Inventory Distribution.

A comparison of the ore inventory distribution along the length of the kiln was made for two series (II(RP_1S_2) and VIII(RP_2S_8)) respectively using the kiln with and without chokes, which is given in Table (58) and in Fig. (70).

CHAPTER

5

DISCUSSION

5. DISCUSSION

5.1. Usage of the Rotary Kiln for Studying the Rate of Reduction.

The determination of the progress with the time of the reduction of oxides depends in every case on measuring the progress of oxygen removal from the oxides, or measuring the value of some quantity which is uniquely determined by the extent of oxygen removal. Methods of investigation entailing discontinuous working are of limited value, because in a discontinuous method the course of the reaction is disturbed. Changes also occur in the test material by its being heated up and cooled and by being taken out of the reaction gas into the atmosphere. The desirable method is continuous, in which a solid pellet is suspended within a controlled temperature environment (e.g., a furnace) where it is reacted with a moving gas stream. The progress of the reaction may be measured by the following techniques:

(i) Measurement of some change in the properties of the pellet.

(ii) Measurement of some change in the properties of the gas downstream from the pellet.

The most popular techniques in group (i) include the continuous measurement of the changes in weight (by thermobalance) caused by the removal of oxygen of the pellet (gravimetric methods), the microscopic examination of a partially reacted pellet[131] and the chemical analysis of (partially) reacted pellets[132]. This procedure relies on being able to maintain exactly the same conditions (of temperature, etc.) for all the pellets (used one at a time), which is a difficult task. The gravimetric methods so far mentioned are particularly, or only, suitable for dealing with individual specimens of the oxides (pellets) under observation.

The most frequently used methods in group (ii) involve the analysis of the gas stream for gaseous reaction products and volumetric measurement methods.

Experimentally, in the thermobalance, the gas composition is usually held constant and the specimen progressively approaches equilibrium with the gas, i.e. the driving force for reduction is decreased progressively. This can be controlled to relate to batch reduction processes such as the HyL.

In continuous counterflow processes such as Midrex the fresh gas is in contact with almost completely reduced ore. The reducing potential of the gas decreases as it travels through the kiln and contacts ore which has experienced progressively less reduction. Hence the reduction behaviour of an ore may be very different here to that displayed in a thermobalance experiment.

The rotary kiln which was used in this investigation has some of the specific values of the apparatus for the different methods mentioned with a flexibility of working with multiparticles and control of the different factors affecting the rate of reduction such as temperature, residence time, amount and composition of gaseous reactant and handling different ore sizes. The main features of the kiln are as follows:

(i) It operates on multiparticles and as a small pilot plant for the proposed Sussex direct reduction process.

(ii) The extent of reduction was measured with three individual routes for every experiment (after attaining the steady

state condition), which were in good agreement (refer to Chapter 2). The three routes are as follows:

(a) Chemical analysis of the sponge out.

(b) Oxygen balance of inlet and outlet gases.

(c) Difference between weight of the hourly input of ore and the weight of output sponge.

(iii) The progress of reduction from iron ore to a desirable sponge iron could be studied by taking samples from the bed at selected points along the length of the kiln whilst operating under conditions simulating commercial practice.

(iv) The limitations of working with the kiln are as follows:

(a) The residence time recorded for an ore particle is the average measured residence time.

(b) The gas variation and composition is unknown within the kiln and only the composition of the inlet and outlet gases are known. This could be modified by replacing the axial thermocouple tube (Fig. No. 40) with a gas sampling tube for the time when sampling is necessary. This would give a good flexibility for taking gas samples from the kiln at selected points along the length of the kiln whilst operating under conditions simulating commercial practice. The findings could be combined with the bed sampling observation for a more precise interpretation of results.

5.2. The Usage of Iron Ore as a Catalyst.

The gaseous reactants were produced within the kiln from reaction between butane and carbon dioxide on the surface of the iron ore. When chokes were positioned at the kiln inlet and outlet, chromatography analysis indicated that as the temperature increased the number and the amount of unreformed hydrocarbons was decreased in the off gases but, even at high temperatures (about 930^{o}C), there was no achievement of complete conversion of the hydrocarbons (Table No. 38). When the kiln was operated without chokes in position chromatographic analysis showed substantially less unreformed hydrocarbons left the kiln (refer 4.2.2.2.).

In another study[119, 120], butane was reformed within a kiln with CO_2 on the surface of prefluxed sinter. It was found that above 920^{o}C butane was completely converted to (CO - CO_2 - H_2 - H_2O). When butane was used below 920^{o}C, some methane left the kiln without reaction, but no other hydrocarbon was found in the exit gas.

It is common practice to use a mixture of oxides including iron ores as catalysts for reforming hydrocarbons. For example, Voge and Morgan [133], examined the effect of the particle size of a Shell 205 catalyst (62.5% Fe_2O_3, 2.2% Cr_2O_3, 35.5% K_2CO_3) on the selectivity of the dehydrogenation, at 620^{o}C, of but-2-ene in the presence of steam. Some dependence on particle size was observed and it was concluded that the process studied provided an example of the diffusional control of selectivity.

In early 1981 a commercial method[126] was introduced for reforming the methane content (about 30% by volume) of a mixture of gases (e.g. coke oven gas) by steam using the autocatalytic effect of reduced

iron in the reactor.

Nickel metal is the catalytic species[134] in many commercial catalysts and has been found to be the most effective metal for the reforming of hydrocarbons. It is an active component in most of the catalyst formulations which are available. However, it is not possible to put nickel inside the rotary kiln. Using a catalyst reformer needs an external heat supply and regeneration of the catalyst after a period of time, thus increasing both the operating and investment costs. Therefore, the usage of an autocatalyst has an economic advantage in comparison with a catalytic reformer.

There are two serious problems that decrease the catalyst efficiency. Firstly, in common with other metallic catalysts, nickel steam-reforming catalysts are readily poisoned by the sulphur compounds present in natural gas. It is, therefore, necessary to pretreat the feedstock to eliminate sulphur poisoning of the catalyst. Secondly, carbon deposition in the reformer is a further serious problem that can destroy the active centres, cause catalyst breakage and concomitant bed plugging and eventually less reforming of the hydrocarbon feedstock. In contrast, the autocatalytic reforming of the gas within the kiln, on the surface of the partially reduced iron, can tolerate the above problems, because the sponge iron (the auto catalyst) would be replaced regularly by the fresh partially reduced ore.

Furthermore, the shorter dwell time of the ore in the low temperature regions of the discharge zone when the kiln was operated without chokes in position prevented a high carbon deposition in the sponge iron from the dissociation of carbon monoxide, thus reducing poisoning of the catalytic surfaces. When chokes were in position the

dwell time in the cooler discharge zone was increased and, correspondingly, the carbon content of the sponge iron was increased. This reduction of the catalytic activity explains the higher unreformed hydrocarbon content when the kiln was operated with chokes in position.

From the above considerations it may be concluded that in the case of prefluxed sinter, probably the gangue elements and the size of the sinter caused a better conversion of butane than in the present case, using Brazilian iron ore (the iron ore analysis is given in Table 59), while the kiln was operated with chokes in position. In contrast as discussed earlier this was improved by using the kiln without chokes in position.

5.3. Structural Characteristics of the Iron Ore and Sponge Iron Particles.

The performance of a commercial plant depends to a great extent on the characteristics of the iron ore; as the tendency towards disintegration, swelling, cracking and sintering is increased the ore is pronounced as more undesirable.

The Brazilian iron ore was chosen for this investigation because of its good resistance against decrepitation and fragmentation during rapid heating and in the early stages of reduction. It had a rich iron content with little gangue (Refer Table 59) and was selected commercially as suitable for direct reduction.

For reduction experiments the ore particles should ideally be of uniform shape and size. Where solid state diffusion is important, for example, the ideal form would be spheres of uniform diameter. In the

present study the ore used deviated markedly from regular dimension. After crushing it was in the form of non uniform, elongated particles with cross section varying from tabular to triangular. Thus an attempt to characterise the mean particle size of a sieved sample in terms of the physical dimensions of the particles would be virtually meaningless. For designative purposes, therefore, the particle size was expressed in terms of either the average sieve size or the average apparent volume. The former was expressed as the average linear dimensions of two adjacent sieve sizes (i.e. the - 2.36 mm and + 1.7 mm fraction was classed as $\frac{2.36 + 1.7}{2}$). The average apparent volume, corresponding to this dimension, was obtained by measuring the volumetric displacement of a known number of particles retained on the smaller of the two sieve sizes.

It is recognised that both forms of measurements are very approximate. During sieving a long, thin specimen, of length significantly greater than a particular aperture, could pass through the aperture if suitably oriented. In the case of volumetric measurement, as the number of particles of ore increased the error in the results decreased.

The reduction of iron oxide will always yield a porous reaction product. The structure of the sponge particles is much affected by the nature of the iron oxide, gas composition and temperature. It is important because the structure of the reduced iron affects the rate of reduction.

In this investigation the Brazilian hematite iron ore was reduced with gas mixtures initially comprising C_4H_{10}, CO_2 and H_2 at different temperatures. The ore and the product (sponge iron) produced

using the kiln with and without chokes in position were examined by optical and scanning electron microscopy and, in the latter case, also by porosimeter measurements. The following points were observed. A dehydrated iron ore sized 2.36 - 3.35 mm particle (micrograph A) revealed a well-defined hexagonal crystal form of hematite. Upon reduction at 773^{o}C a porous iron was formed (micrograph B) in which the pores were finer than after reduction at 829^{o}C (micrograph C). Some of the macro cracks (in micrograph B) probably occurred during the preparation and crushing of the iron ore. There was evidence of whisker growth of iron crystals in some of the specimens examined and examples can be seen in micrograph (C). The micrographs of ore reduced at 878^{o}C (D, E) and at 899^{o}C (F) showed that the pore structure became progressively coarser with increasing temperature. A comparison of micrographs (D) amd (E) obtained from two samples taken from the same run showed the differences between the pore structures caused by the sintering effect in high temperature reduction. The sintering effect was also revealed in micrograph (F).

The pore structure was also studied for a larger ore size (3.35 - 4.75 mm) while using the kiln without chokes in position. The micrograph (G) (reduced at 819^{o}C) showed smaller macropores and microcracks than the micrograph (H) (reduced at 845^{o}C). Micrograph (I) (reduced at 872^{o}C) and (J) (reduced at 899^{o}C) proved that the pore structure became progressively coarser with increasing temperature. Micrograph (I) clearly showed some whisker growth of iron and the effect of sintering can be seen from the micrograph (J).

Sintering in this context implies the phenomenon by which a porous particle increases its density on being held at an elevated

temperature, but below that at which it agglomerates and clusters with the other particles. The term sintering is also used to describe the agglomeration of ores as a means of feed preparation for the iron blast furnace, but this operation is not the one discussed here. The effect of sintering on reducibility for both sizes of sponge iron can also be seen from Figs. (No. 43, 46, 61) which indicates percentage reduction versus temperature. The appearance of sintering eventually decreased the rate of reduction (refer to temperature effect upon reduction).

For a more precise study of the porosity of the Brazilian hematite ore during the reduction a series of total pore volume measurements were carried out for different run temperatures (Table 46 - Fig. 69). It was found that, within the accuracy of the mercury porosimeter used, the original ore was non porous. After reduction a porous sponge iron was produced; the content of micropores and macropores respectively (pores diameter below and above ~ 50 nm) is shown in Fig. (69).

It was observed that as the temperature increased the macropore diameter increased regularly, but the volume of micropores for the lower temperature (i.e. 819°C) was higher than for the high temperature (i.e. 899°C). This resulted in a higher total pore volume for the sponge iron reduced at 819°C. For the run temperatures of 845°C and 872°C the pore volume was less than at 819°C, but the diameter of the pores increased for both micropores and macropores and eventually the total pore volume increased with respect to the increased temperature.

The percentage of swelling was calculated (Table 46) using the equation $S = \left(\frac{V_t - V_o}{V_o}\right) \times 100$ (where S = % swelling, V_o = specific volume

of original ore (0.218 $^{c.c.}/_{g.}$) V_t = specific volume of the sponge produced) and the total pore volume measurements for different run temperatures. It was found that as the temperature increased the percentage of swelling decreased. Maximum swelling was found for the run temperature of 819^{o}C as 25.64% and minimum swelling was found for the run temperature of 899^{o}C as 14.67%. From the above, it is obvious that the sintering effect at higher temperatures caused some shrinkage of the produced sponge iron. These observations were in good agreement with the scanning electron micrographs produced and also with the Fig. No. 61 which indicated per cent reduction versus temperature and clearly showed a decrease in the extent of reduction above the sintering temperature range.

As is clear from the micrographs, reduction of hematite iron ore yields a porous product. Reforming of the hydrocarbons by the autocatalysed reaction on the surface of the partly reduced ore particles would give less local pressure with decreasing reduction temperature; thus only micropores and microcracks occurred at low temperatures and at high temperatures (until limited by sintering) both micropores and macropores/macrocracks appeared in the micrographs. Above the limited sintering temperature, the micropores tended to sinter and only macropores/ macrocracks were seen in the micrographs. The further influence of the hydrocarbon feedstock on the rate of reaction will be determined by the diffusion of oxygen through the solid to the gas/solid interface. The diffusion path of oxygen will be influenced by the number, the size and the distribution of the micropores and the macrocracks induced by the reaction of the hydrocarbon.

It was observed that the temperature at which sintering started increased with increase in the size of the ore particles. This may be because of the smaller surface area or a lower metallic iron content in the case of the larger ore size. This behaviour is of particular importance in the reduction of iron oxides, where sintering of the porous metal product layer may markedly reduce the overall rate of reaction by limiting access by the reactant gas. Sintering is a complex phenomenon and, in spite of much careful investigation[135-137], it is still not possible to predict the rate at which the various structural characteristics (e.g. porosity, surface area) change under a given set of circumstances. Activation energies for sintering are high; that is, the rate of sintering increases rapidly with increasing temperature. The increase is so rapid, in fact, that for a particular solid there is a temperature (known as the Tammann temperature[3]) below which sintering is negligibly slow but above which it takes place quite rapidly.

A few growths of iron in the form of whiskers can be observed in the micrographs. This is related essentially to the non stoichiometric composition of wustite. A mechanism has been proposed by C. Wagner [138, 139] for the reduction of non stoichiometric compounds. It takes into account the simultaneous effects of the chemical reaction at the surface and of iron transport in the bulk, which results in an accumulation of iron in the super saturated wustite. For a whisker to be formed it is necessary that this accumulation be large, but it is also required that the iron activity threshold for nucleation at the surface be high, with only a few favourable sites. A model has been proposed by R. Nicolle

and A. Rist[139] which defines these conditions and accounts for the observed variations in the morphology of iron.

In another study[120] when butane, CO_2 and H_2 were used to generate the reducing gas the hydrocarbon was reformed within the kiln on the surface of the prefluxed sinter, it was found that the surface area was nearly trebled to a mximum of about 1.38 m^2g^{-1} at about 880°C, and then fell off rapidly as the temperature increased further. The formation of both micropores and macropores was stimulated by the reacting hydrocarbon. Probably at low temperatures, up to about 880°C, micropores and macropores were the dominating features and above that temperature the micropores tended to sinter progressively as the temperature increased, so that the surface area attributable to them decreased. This phenomena is confirmed by the present porosity measurements and micrographic study.

From studies of the reduction of natural hematite Venezuelan ore, Turkdogan and Vinters[79] indicated that the pore structure of iron reduced by hydrogen becomes progressively coarser with increase in reduction temperature from 600 to 1200°C (Fig. 19). This was in accord with observations of fracture surfaces by scanning electron microscopy which indicated distinct coarsening of the pore structure at reduction temperatures above 900°C. Clearly the structure of the iron depends markedly on the reduction temperature and this is reflected in the measurements of effective diffusivities carried out by Turkdogan and co-workers[80].

It has to be mentioned that, for a precise interpretation of the structural characteristics of reduced iron, it is not enough just

to interpretate the observation of the fracture surfaces by scanning electron microscopy. Close attention must be given also to the total pore volume and pore surface area. It was shown[80] (Fig. 71, 72) that both pore volume and pore surface area decreased as the temperature increased.

The above observations are in agreement with the present work up to the maximum temperature of about 950°C. None of the commercial direct reduction plants can work above the limiting stickiness temperature, which is about 1000°C, dependent on the nature of the ore, the gas composition and the conditions of operating the plants. The high temperature (1200°C) observations of Turkdogan and Vinters are of limited practical value.

5.4. The Mode of the Reduction for the Hematite Ore.

As mentioned before, the reduction of iron ore by a reducing gas generated from a mixture of H_2, CO_2 and C_4H_{10} yields a high by porous product, in which the gas diffusion is rapid (until the limiting sintering temperature is reached). Hence, with small particle sizes, it may be expected that uniform internal reduction predominates throughout the oxide particles. This was confirmed by microscopical examination for both experimental modes (i.e., using the kiln with and without chokes in position). The micrographs (G, H, I, J, K, L) show several islands of wustite surrounded by iron and iron islands in just one grain particle size. The curves (Fig. 43, 46, 61) which show percentage reduction versus temperature indicated that the uniform internal reduction was predominant until the limited temperature range was reached in which the ore became prone to sinter. This was also confirmed by the micrograph (E, F, P) observation. The mode of reduction for this region was probably

limiting mixed control.

The formation of the product layers during reduction of the hematite iron ore particles to wustite was very rapid in the early stages of reduction. This rapid conversion of Fe_2O_3 to Fe_3O_4, with increasing porosity during this stage, caused a faster reduction of Fe_3O_4 to FeO. Observations indicated that the product, wustite, was sufficiently porous to allow rapid gas diffusion in the wustite layer; hence internal reduction occurred ahead of the advancing iron/wustite interface. These observations were confirmed by measurements of the metallic iron content and the percentage metallisation (Fig. 56 and Table 40) for the progressive reduction of iron ore to sponge iron at different stages along the kiln. These measurements showed that some metallic iron was produced even in the very early stages of reduction. The nature of the internal reduction was shown also by microscopical examination (micrographs I, J, K, L) of the progressive change from iron ore to a desired sponge iron. In the completely internal reduction reaction the rate is controlled primarily by a gas-solid reaction on the pore walls. The pore walls of wustite are assumed to be covered with a thin porous layer of iron, which effectively increases the extent of reduction.

At higher temperatures where the reduced ore was prone to sinter and the porosity decreased the rate of reduction was controlled jointly by (1) gas diffusion in the pores of the wustite (solid diffusion in wustite may be ignored) and (2) reaction on the pore walls of the wustite.

Theoretical considerations[79] show that the relative depth of internal reduction increases with

(i) decreasing particle size,

(ii) decreasing temperature,

(iii) increasing porosity of the oxide, and

(iv) the progress of reduction.

However, the non-uniformity of the particle size used in this investigation and, hence the variations in the porosity and the surface area of the ore particles, made it too difficult to express precisely just one mode for the rate of reduction. As the porosity decreased the uniform internal reduction decreased and rate of reduction became controlled jointly by the uniform internal reduction and the limiting mixed control.

5.5. Calculation of One Variable from the Other and One Curve from Another.

In another study[120], the original kiln was used to reduce prefluxed sinter; the results obtained determined that the plot of each operating variable examined (except for the reducing capacity of the gas) against the percentage reduction, either gave a straightline relationship, or could be put in a form which gave one. The kiln used in this investigation was a larger version of the original one and the mathematical model was suitable for these results too. This specific model would help to up-scale the Sussex direct reduction pilot plant.

Using this approach, the effect of varying one operating variable on the percentage reduction of the ore, when all the other

operating parameters were fixed, was readily calculated for each variable from an equation in the form $y = a + bx$, where y was the percentage reduction, x was the chosen variable and a and b were constants. These curves were inter-related when plotted using identical co-ordinates, and, therefore, one curve can be calculated from another, once a base curve and the constants for each variable have been determined.

The effect of the change in the different variables was studied upon the percentage reduction. The variables were:

(i) The reducing capacity of the inlet gases,

(ii) The oxidant content of the inlet gases,

(iii) The temperature,

(iv) The particle size and the volume,

(v) The Residence time,

(vi) The gas composition (eventually the H_2/CO in the gas mixture)

5.5.1. Reducing Capacity.

One problem common to every gas-solid reduction investigational technique is the determination of the so-called "critical" flow-rate [132, 140] of reducing gas, above which the over-all reaction rate is not limited by the supply of reducing gas and to ensure that reduction is not inhibited by the presence of too high a concentration of product gas in the bulk gas phase.

It is well known that in the reduction of iron oxides the controlling reaction is reduction of wustite to iron[67, 119]. The Fe-C-O and Fe-H-O systems show that, for all temperatures within the range where gaseous reduction is economically feasible, the

equilibrium gas mixtures contain at least 60 per cent of carbon monoxide and/or hydrogen. When equilibrium is not attained the unreacted concentrations of these gases are even higher and the greater part passes unchanged through the reducing reactor. If the process is to be economical, provision must be made for utilising the gas which remains after the reduction of wustite to metallic iron for the reduction of the higher oxides of iron to wustite. This is adopted in the continuous counterflow processes such as Midrex. Thus the estimation of the "critical" flow rate in experiments using single particles in a thermobalance is different from the conditions which apply in commercial practice.

The optimum flow rate (above the critical flow rate) of the gas measured in this investigation using the rotary kiln was measured under conditions similar to those which apply in real practice and was called the reducing capacity of the gas.

A series of runs was made at a temperature of 875^{o}C with ore size 3.35 - 4.75 mm, using the kiln without chokes in position, to study the effect of reducing capacity upon percentage of reduction. As mentioned earlier, the maximum efficiency for the process is achieved when a reduction of 100% is obtained with a reducing capacity P = 1.058t (t = mole per hour Fe in iron ore, 1.058 = the atomic ratio of oxygen to iron in wustite and P = mole per hour of gaseous reducing agent). Gas feeds with P < 1.058t have insufficient reducing capacity to convert all the wustite in the ore to metallic iron. Provided that direct reactions between hydrocarbon and iron ore may be ignored, an optimum hydrocarbon to oxidant ratio (C_4H_{10}/CO_2) has been found to prevent undesirable carbon deposition (refer to 5.5.2.).

Thus in this series the reducing capacity was altered by keeping the C_4H_{10}/CO_2 steady and changing the hydrogen content in the inlet gases. Hence, the ratio of H_2/CO changed and that may be one of the factors affecting the percentage of reduction (refer to 5.5.6.). All the experiments were made with feed gases having reducing capacities 15 - 40% greater than (P = 1.058t) to ensure that the reaction was limited by kinetic rather than thermodynamic factors. Fig. (65) shows that as the reducing capacity was increased progressively toward the optimum flow rate the extent of reduction increased. However, the usage of reducing capacity above the optimum flow rate should have no effect on the percentage of reduction if the H_2/CO ratio is kept steady.

5.5.2. The Oxidant Content of the Input Gases.

It is perhaps surprising that in contrast to the large volume of work done on the reduction of various forms of iron oxides with pure hydrogen (and, to a lesser extent, with pure CO) much less information is available in the open references on the reduction kinetics with reducing gas mixtures[2]. It was part of the task of the present work to find some understanding of the goal of reforming hydrocarbons within the reduction reactor using the benefit of the autocatalytic effect of the partially reduced iron ore (sponge iron). Thus the best oxidant ratio in the mixture of the gas had to be found which would partially oxidise the hydrocarbon with the optimum carbon deposition on the sponge iron.

A series of runs was made using the kiln without chokes in position at a temperature of about 870^{o}C and with ore size 3.35 - 4.75 mm.

The hydrogen and hydrocarbon (C_4H_{10}) content in the mixture of the gas was kept steady. The only variable was the oxidant (CO_2) content in the in-put gases so the effect of this variation could be examined upon the extent of reduction (Fig. 64, Tables 47, 48). As there exists a continuous variation in the concentration of the gaseous agents and in the composition of the iron oxides and metallic iron within the kiln, it would be difficult to advance a precise interpretation of the end results without any hpothesis and/or taking into consideration the findings of the run series in which samples of the sponge iron were taken along the length of the kiln (refer run series VII code No. RP_2S_7).

It is assumed that direct reactions between hydrocarbon and iron ore may be ignored. In the case of run (47) in this series, which had the lowest amount of oxidant (CO_2), a series of reactions may be proposed between the gases and the iron ore (proceeding to sponge iron) travelling along the kiln.

(1) $C + 2H_2 \overset{Fe}{\rightleftarrows} CH_4$

(2) $C_4H_{10} + 4CO_2 \overset{Fe}{\leftarrow} 8CO + 5H_2$

(3) $2CO \overset{Fe}{\rightarrow} Fe_xO_y + C + CO_2$

(4) $C_4H_{10} \overset{Fe}{\rightleftarrows} 4C + 5H_2$

(5) $FeO + H_2/CO \rightarrow Fe + H_2O/CO_2$

(6) $(C_4H_{10} + 4H_2O \overset{Fe}{\rightarrow} 4CO + 9H_2$

$(C_4H_{10} + 4CO_2 \rightarrow 8CO + 5H_2$

(7) $C + H_2O \rightarrow CO + H_2$

(8) $C + CO_2 \rightarrow 2CO$

(9) $Fe_3O_4 + CO/H_2 \rightarrow 3FeO + H_2O/CO_2$

(10) $3Fe_2O_3 + CO/H_2 \rightarrow 2Fe_3O_4 + H_2O/CO_2$

(11) $2CO \overset{Fe}{\rightarrow} Fe_xO_y + C + CO_2$

As the inlet gases ($C_4H_{10}/H_2/CO_2$) travelled over the sponge iron bed they absorbed some of the heat. In the lower temperature region of the discharge end, there would be some methanation (reaction 1) of the carbon in the sponge iron with the input hydrogen in the cooling zone. It has been reported[114] that the metallic iron acts as a catalyst and increases the rate of the reaction, which depends on the availability of the active carbon. In this experiment carbon is in the form of soot (refer to 5.6), which could react with hydrogen (reaction 1). As the travelling hydrocarbon (C_4H_{10}) enters the heating zone, it would be reacted with the available CO_2 (reaction 2) of the input gases on the surface of sponge iron (acts as autocatalyst) and give CO and H_2. Some of the CO would be broken down (reaction 3) in the lower temperature region of the discharge end and would cause carbon deposition. Some of the remaining (C_4H_{10}) (which did not react with oxidant for the reforming) would be thermally cracked (reaction 4) and deposit some carbon and create some more hydrogen. This hydrogen, collectively with the reforming gases (CO, H_2), would reduce FeO to metallic iron (reaction 5), (reaction of solid carbon with FeO may be ignored, because of the slow rate of reaction). The gaseous products (CO_2 and H_2O) would react with the remaining unreformed/uncracked C_4H_{10} (reaction 6); also these oxidants would react with the carbon (reaction 7, 8) of the sponge iron (mainly created from cracking of the hydrocarbon, reaction 4) and produce extra reducing agents. The gasification of the carbon can be seen from the analysis of the carbon content (Table 47) of the sponge iron produced compared with the theoretical amount of carbon which should have been created from the cracking of the hydrocarbon (C_4H_{10}) in the sponge iron. These reducing agents (CO, H_2) would reduce the higher iron ore oxides

(reaction 9, 10), with the remaining reducing agents from the earlier stage. When the gases leave the kiln in the inlet ore region of the kiln there would be some Boudouard reaction (reaction 11) and carbon deposition.

As the amount of input oxidant (CO_2) in the mixture of the input gases increased, the cracking reaction of hydrocarbon (reaction 4) would be less, and the probability of the carbon reactions (reaction 7 and 8) would be decreased (less carbon available from the cracking). The over-all ratio of H_2/CO would be decreased also.

From the reducing capacity point of view, when the amount of CO_2 in the mixture of inlet gases is not enough to reform all the hydrocarbon, some of the hydrocarbon would be cracked and provide hydrogen and carbon. This carbon would be reacted (reaction 7, 8) with some of the oxidants (CO_2/H_2O) produced from the iron oxide reduction. Thus some extra reducing capacity would be provided and this makes it difficult to calculate a precise reducing capacity.

In the runs with the lower (CO_2) content, for the complete reforming of the butane, the ratio of H_2/CO would be higher (refer Table 47). This would be favourable from the reducing capacity usage point of view since the H_2/H_2O ratio in equilibrium with Fe and FeO is lower than the corresponding CO/CO_2 ratio (refer Fig. 16) at the temperature used (870^oC). It is also known that (refer to 5.5.6.) hydrogen is a more effective reducing agent than carbon monoxide.

This means that a higher extent of reduction should be found for a higher ratio of H_2/CO mixture (with the other variables the same,

e.g. reducing capacity, etc.). Hence the travelling sponge iron would be reduced to a greater extent before reaching the zone in which the cracking of the hydrocarbon (C_4H_{10}) and ultimate carbon deposition occurred. This is clear from a comparison of the effect of reducing capacity upon percentage reduction, run series X (Fig. 65 and Table 49), and the reducing capacity calculated for these run series (Table 47). For example, the reducing capacity for Run No. 47 (Series X) was 1.38 (mole/h) with the overall H_2/CO ratio of 6.38, which gave 92.57% reduction and a carbon deposition of 7.004% in the sponge. In contrast, in Run No. 51 (Series IX) with a higher reducing capacity of 1.45 (mole/h) and overall H_2/CO ratio of 1.33 a reduction of 78.07 was obtained and a carbon deposition of 0.224% in the sponge iron. In summary, with approximately constant reducing capacity, as the H_2/CO ratio increased the percentage reduction increased.

5.5.3. The Temperature Variable.

Two different curves were found for each series of runs (using the kiln with chokes in position) which showed the effect of temperature variation on the percentage reduction when the other variables were constant. The curves, (Fig. 43, 46, 51) which were plotted as the temperature in degree centigrade versus the percentage of the reduction, indicated that linearity predominated until the limited temperature range was reached at which the reduced ore tended to sinter. Thereafter, further increase in the temperature caused non-linearity of the curves. This was due to the decreasing porosity and hence changing the mode of reduction from uniform internal reduction to the limited mixed control.

It was found that if the function of the reciprocal of the temperature in degree Kelvin was plotted against the logarithm of the percentage reduction, the experimental results could be fitted adequately by a straightline for the full range of temperatures (Fig. 44, 47, 52). From these and their related equations, the temperature needed for a desired percentage reduction is readily calculated. For example, from the curve (Fig. 43) and the equation (R = 0.260 T^{o}C - 127.71, where R = percentage reduction and T = temperature in degree centigrade) for an 80 per cent reduction the temperature required was 798.8^{o}C for the small size of ore. In the same manner the temperature can be calculated for any desired percentage reduction and vice-versa (until the limited sintering range up to the temperature at which sintering occurs and above that from the logarithmic equations). Similar calculations can also be made for the other two ore sizes from the equations (see Chapter 4). The equations show that as the temperature increased the percentage reduction increased for a steady ore size.

Two different curves (Fig. 61, 62) also were found for a series of runs using the kiln without chokes in position which showed the effect of temperature variation on the percentage of the reduction when the other variables were constant. The nature of the curves was similar to the above curves, but a comparison of the results for two series of runs (Fig. 61 and 46) in which the variables had similar values indicated that when the kiln was used without chokes in position a higher reduction was obtained than when the kiln was used with chokes.

These differences may be caused by the differences in the inventory distribution along the kiln for the two different experimental modes (i.e. using the kiln with and without chokes in position)

In contrast to operating with an unrestricted kiln, when chokes were used the ore stopped for a lesser time in the ore charge part of the kiln (i.e. toward the hopper) (Fig. 70 and Table 58). Thus a less time was available for the transformation of the hexagonal hematite into cubic magnetite and the resulting lattice disturbances which cause some swelling. This could give a low gas utilization in this region, which could not be compensated by stopping for a longer time in the active part of the kiln (with highest rate of metallisation Fig56). Fig (70) showed also that the partially reduced ore stopped for a longer time in the lower temperature region behind the choke in the discharge end. This also caused a higher carbon deposition (refer 5.6) on the surface of the sponge iron, which decreased the autocatalytic effect of the sponge as well as a retardation of the gas diffusion to the surface of the sponge, where carbon had been deposited. Thus a lesser extent of reduction was obtained in these regions and a lesser overall reduction resulted for otherwise comparable conditions. When the kiln was used without chokes in position a better gas utilization was obtained by the reverse inventory distribution (compared with the time when chokes were used) and also by a lesser carbon deposition (Figs. 63, 48 and Tables 42, 10) on the surface of the sponge. This resulted in a higher overall extent of reduction.

5.5.3.1. The Temperature Effect upon the Sintering.

The effects of temperature upon the reduced iron structure and eventually upon the percentage reduction above the sintering temperature range are two-fold, i.e. a combination of the effects of temperature and per cent metallic iron (available in the sample) has to

be considered for the sintering effect. The comparison of the results for two different series of runs for the same iron ore size (3.35 - 4.75 mm) and with the other variables the same indicated that, without chokes in position, the sintering started at a lower temperature range (i.e. 870 - 902^{o}C) for a higher range of metallic iron content (84 - 90.90%), whereas with chokes in position sintering started in a higher temperature range (i.e. 912 - 930^{o}C) but at a lower range of metallic iron content 83.1 - 84.2%). Thus it may be concluded that as the metallic iron content in a sample increased the temperature range in which sintering occurred decreased and vice versa.

5.5.4. The Particle Size Variable.

The effect of particle size (expressed as average sieve aperture) on the temperature required for a given percentage reduction could be evaluated from the curves and their relative equations, for percentage reduction versus temperature for each of the particle sizes examined and knowledge of the temperature required to achieve this percentage reduction for one of the three particle sizes. These equations should be applicable up to the limiting size for uniform internal reduction.

For example, from the equation R = 0.260 T^{o}C - 127.71 for the small ore size, when the percentage reduction is assumed to be 80, the temperature required for this reduction was 798.8^{o}C. Hence the temperature required for 80 per cent reduction for the medium size and the large size, with respective equations of R = 0.267 T^{o}C - 136.73 and R = 0.255 T^{o}C - 131.45, can be calculated from the above figures for the small size and using a general formula. The general formula was

found from equations (A) and (B) as:

$Y_1 = a_1 + b_1x_1$ (A) and $Y_2 = a_2 + b_2x_2$ (B)

where Y_1 and Y_2 = percentage reduction and x_1 and x_2 = temperature in degree centigrade and a_1, b_1 and a_2, b_2 are constant for each particular size. The subscripts 1 and 2 are used to present two different particle sizes.

Two equations (D) and (C) were found from rearrangement of the equations (A) and (B) as:

$$x_1 = \frac{Y_1}{b_1} - \frac{a_1}{b_1} \qquad (C)$$

$$x_2 = \frac{Y_2}{b_2} - \frac{a_2}{b_2} \qquad (D)$$

subtracting the equation (C) from (D) and assuming

$Y_1 = Y_2 = Y$ gave the general formula as:

$$x_1 - x_2 = \frac{Y(b_2 - b_1) + (a_2b_1 - a_1b_2)}{b_2b_1} \qquad (F)$$

From the general formula (F) the temperature for the medium ore size was 811.6^{o}C and for the large size was 829.1^{o}C. The equations (23, 16, 27) show that for a constant percentage reduction, as the ore size increased the temperature needed increased.

A straight line relationship was found between the percentage reduction and the ore particles size (the average size between two sieved sizes) at constant temperature, which is shown by the curves (Fig. 53) and equations (29, 30, 31) as:

$$R = -4.255\,x + 97.1738 \text{ for a temperature of } 830^{o}C$$

(where R = percentage of reduction and x = the average particle size between two sieve sizes) and $R = -4.1519\,x + 89.0429$ for a temperature of $800^{o}C$ and $R = -4.0489\,x + 80.9119$ for a temperature of $770^{o}C$. Similar equations and curves can be found for any temperatures desired (up to the limited temperature) from the three equations (16, 23, 27) which show the percentage reduction versus temperature for the three different sizes with the other variables steady. From the above equation any ore particle size can easily be found for a desired percentage reduction or vice versa. For example, for a 70% reduction, the size required was 6.38 mm at $830^{o}C$, 4.58 mm at $800^{o}C$ and 2.69 mm at $770^{o}C$. In a similar manner, at constant temperature, it is possible to calculate the percentage of reduction of an ore of known size and, from this, the percentage of reduction for other size fractions within the size range amenable to the uniform internal reduction mechanism. The equations show that as the size increased the percentage reduction decreased for a constant temperature, and as the temperature decreased the reduction decreased for a steady particle size.

The plot of (Fig. 61) percentage reduction against temperature for ore size 3.35 - 4.75 mm, when the kiln was used without chokes is similar (with a steady shift up of the per cent reduction) to the one (Fig. 43) with chokes usage. It is expected, therefore, that for a different ore size the configuration of the plots are similar also and, for similar conditions, (with just ore particles size variation) parallel plots could be found for operation with and without chokes. Thus similar

equations with changes only in the values of the constants could be used to relate percentage reduction to the operating variables for operation without chokes.

5.5.4.1. The Volume Size Variable.

From the equations of (16, 23, 27), which show the percentage reduction versus temperature for the three different sizes and their respective average volume, a straight line relationship was found also between the percentage reduction and the logarithm of the average volume of a particle size at constant temperature. This is shown with the curves (Fig. 54) and equations (32, 33, 34) as:

$Y = 63.83 - 5.01\ x$ for a temperature of $830^{o}C$ (where Y = R = percentage of reduction and x = Lnv, v = average volume of one particle size (cm^3). $Y = 56.47 - 4.901\ x$ for a temperature of $800^{o}C$, and $Y = 49.113 - 4.788\ x$ for a temperature of $770^{o}C$. Similar equations and curves can be found from the equations (16, 23, 27) for any temperatures desired (up to the limited temperature). From the above equations can easily be found any average particle volume required for a desired percentage of reduction, or vice versa, e.g. for a 70% of reduction the volume required was 0.2918 cm^3 for $830^{o}C$, 0.632 cm^3 for $800^{o}C$ and 0.0127 cm^3 for $770^{o}C$. In the same way the volume can be found for the other percentage reduction and vice versa. The equations show that as the volume increased the percentage of reduction decreased for a constant temperature and also as the temperature decreased the reduction decreased for a steady volume.

5.5.5. The Residence Time Variable.

The effect of the residence time upon the percentage of

reduction was studied for just one size of the ore with the size of 3.35 - 4.75 mm. It was shown that for a given temperature the percentage reduction increased with increase in the residence time. The straight line relationship equation was found for three different residence times and their relative percentage reduction at the temperature of 831°C. From the curve (Fig. 55) and the equation (R = 0.0415 (R.t.) + 71.48 where R = percentage of reduction and R.t. = residence time) the residence time required can be found for any desirable percentage reduction at a temperature of 831°C. For example, 80 per cent reduction required a residence time of 205.3 minutes at 831°C for ore size 3.35 - 4.75 mm.

Fig. (46) shows that the plots of percentage reduction against temperature for the three residence times were approximately parallel. Hence, from the above considerations it is expected that these variables are related linearly for any constant temperature below the onset of sintering.

5.5.6. The Hydrocarbon content of the Inlet Gases.

The effect of different amounts of hydrocarbon in the mixture of input gases (C_4H_{10}, CO_2, H_2) upon the extent of reduction for ore size 3.35 - 4.75 mm was studied at 849°C, with steady reducing capacity in the kiln without chokes in position. As the amount of butane input decreased (for a steady reducing capacity by adjusting the hydrogen input) the ratio of CO to H_2 decreased. It was found that the extent of reduction varied linearly with the H_2 content of the gas mixture (Fig. 66, 67 and Tables 51, 52). The maximum reduction was observed for a gas with 100 per cent hydrogen. Because of the practical importance of the findings, it was decided to examine the effect of gas composition

in more detail. Hence another series of runs was performed with ore size 4.75 - 6.7 mm at 900°C and using a higher reducing capacity. The findings (Figs. 66, 68, Tables 53, 54) confirmed the above results; as the hydrogen ratio content of the reducing gases (after reforming) increased, the extent of reduction increased too and a pure hydrogen gas inlet gave the maximum extent of reduction.

The residence times for these two series of runs were selected to compensate approximately for the differences in particle size and reaction temperature. In fact, the higher temperature runs showed slightly higher percentage reduction for any chosen CO/H_2 ratio. Both sets of data could be represented by lines of similar slope, however, when plotted as per cent reduction versus % CO (or ratio CO/H_2) (Figs. 67, 68). The linear equations (39, 41) fitting these lines could thus be used, together with the preceding data, to determine the gas composition required to obtain any desired percentage reduction for any chosen set of operating variables within the limits investigated.

It has been shown[120, 123] that a more extensive pore structure is caused by the autocatalytic reforming of butane within the kiln. As the concentration of C_4H_{10} in the mixture of inlet gases is increased the amount per unit weight of ore of auto catalytic reforming of C_4H_{10} on the surface of the ore is increased. Thus the porosity of the ore should be increased, but a higher CO concentration is obtained in the mixture of the gas after reforming. As the concentration of carbon monoxide is higher, a higher carbon deposition would be expected, which is one of the factors causing retardation of contact between reducing gases and the ore surface (where carbon is deposited). Additionally, as the carbon monoxide concentration in the mixture of the gas is increased,

the actual gas mixture, through which the reactants and products must diffuse, has a high molecular weight, resulting in a low effective diffusivity in the pores. In contrast, if the hydrogen concentration is increased (by decreasing the C_4H_{10} content of the inlet gases) the pore structure of the reduced ore becomes finer, but the effective diffusivity must be higher because of the lower mean molecular weight of the gas mixture. This is why the extent of reduction increased with increasing hydrogen content of the mixture of the gases.

The above findings are in good agreement with the observation of E.T. Turkdogan et al[71], J. Szekely et al[72], Q.T. Tsay[70], and N. Towhidi et al[69] which indicated that the overall rate of reaction of iron oxides by H_2 + CO increased with increasing hydrogen content of the reducing gas mixture.

In another study,[120, 123] prefluxed consett sinter was reduced to study the effect of gas composition upon the extent of reduction. Below 930°C, a high extent of reduction was found for a gas mixture of H_2 - CO_2 - C_4H_{10}, when butane was reformed autocatalytically on the surface of the ore. In contrast a chemically equivalent mixture of CO - H_2 (i.e. with the same proportion of C, H, O) gave a significantly lower extent of reduction.

Thus better reductions were achieved with the gas feeds containing butane. Since any local hot spots induce endothermic reactions with the hydrocarbon, catalyzed on the surface of the ore, stickiness was more readily avoided and butane reforming assisted in the preservation of a higher pore volume in the partially reduced particles. These factors

contributed to the improved reduction with butane than with the corresponding synthetic mixtures.

On the basis of these results it might be concluded that pure hydrogen is to be preferred as the reducing medium, but economic factors must be considered also. The FIOR plant is the only commercial process (refer 2.4.6.1.) that uses a hydrogen stream as reductant. This hydrogen is produced by steam reforming of natural gas over a nickel catalyst. The reformed products gas is shift reacted using an iron oxide catalyst that converts carbon monoxide to carbon dioxide and hydrogen in the presence of steam. The carbon dioxide is then removed from the gas stream by contact with a circulating hot carbonate solution. The stage processes (after reforming of natural gas to H_2, CO), to produce a highly pure hydrogen as reductant needed extra energy compared with a CO-H_2 mixture as reductant, which is in use in the other gaseous plants. This can be seen[4] from comparison of the energy consumption for different plants:

Consumption per metric ton of DRI	FIOR	Midrex	Armco
Natural Gas (G Cal)	4.0	3.0	3.2
Electrical Power (K wh)	180.0	125.0	33
Water (m^3)	5.5	2.0	2.32

The price of the sponge iron produced has to be competitive with the other steelmaking materials (i.e. scrap or hot metal) in the plant locality and the price and consumption of energy are the main decisive factors on the price of sponge iron. Some of the well established processes (e.g. purofer in West Germany and the Midrex OSM plant in U.S.A.) were forced to shut down because of high energy prices in the region. In the case of the FIOR process, probably the usage of cheap dust iron ore or cheap natural gas available in some locations has facilitated the continuation of the process. This has been shown in an economic consideration[141] of direct reduction process (with the same fuel and power price) as:

Process	Materials & Fuel Cost$/Short tonne of Product			Selling Price $/NT-DRI
	Materials		Fuel and Power Price	
	Sort	Price		
Midrex	Pellets	62.43	38.85	146.50
Armco	Pellets	62.43	40.25	147.30
FIOR	Fine ore	31.66	54.85	145.50

These data show that the usage of pure hydrogen as reducing agent in the gaseous shaft processes is uneconomic; it is also known that the fluidized processes have inherent operational difficulties.

5.6. Carbon Formation and Deposition in the Sponge Iron.

As mentioned before, the heat of the sponge during discharge was used to heat the mixture of inlet gases (C_4H_{10}, CO_2, H_2) and the butane was reformed within the kiln on the surface of the partially reduced iron. From the temperature profile (Fig. 42) it is clear that

as the mean reaction temperature increased, the thermal gradient became steeper at the ends of the kiln. This indicated that the time available for reaching the average run temperature for the cold gases is less at higher temperatures than at lower ones and hence the probability of soot formation is less than at lower temperatures too.

The optimum ratios of $CO_2/C_4H_{10}/H_2$ were found carefully to prevent any soot formation and to give carbon deposition in a range desired for alternative steelmaking. It is assumed that all the carbon dioxide in the inlet gas was used to reform the butane and the products were CO and H_2, together with a small amount of unreacted hydrocarbons, and there was no direct reaction between hydrocarbons and the iron oxide. It is considered that the hydrogen acted as an inert gas in the region in which reforming occurred. In this case the experimental conditions were in the top region of the Fe - C - O diagram (Fig. 13). Any carbon dissolved in the iron would be in the form of cementite at low temperatures and in the form of solution in austenite at high temperatures.

The analysis of the carbon content of the sponge iron for ore size 2.36 - 3.35 mm (Fig. 45) indicated that, with chokes in position, as the temperature increased the amount of carbon decreased up to about 800^{o}C. With further increase in temperature the carbon content increased rapidly and then started to fall again. The variation with temperature of the carbon content of the sponge iron for ore size 3.35 - 4.75 mm (Fig. 48) was similar to that for the ore size 2.36 - 3.35 mm with only a difference in the limited temperature range of about 855^{o}C at which

the carbon content increased rapidly. In this series of experiments, the hydrocarbon contents in the off gases were found by chromotography analysis (Ref. 4.1.9). As the temperature increased the total amount of hydrocarbons in the off gases decreased. The maximum rate of change of residual hydrocarbon content with temperature occurred in the temperature regions in which the rapid carbon deposition was shown to occur.

The catalytic decomposition of carbon monoxide and the occurrence of carbon deposition has been the subject of much study[142]. The consensus is that iron, cobalt and nickel are the most effective catalysts for this decomposition. The important finding[143, 144] was that carbon deposition ultimately ceased when most of the iron was converted to cementite. Upon hydrogen treatment cementite was decomposed to iron and graphite but the regenerated iron lost most of its reactivity as a catalyst. It is generally agreed the rate of carbon deposition on an iron catalyst in CO - H_2 mixtures is a complex function of temperature and gas composition and iron is the only catalyst, not cementite.

The decrease in the amount of carbon deposition with increasing temperature is in good agreement with the Boudouard reaction, until a limited range of temperature is reached, at which there is a maximum efficiency of creating porosity (refer to 5.3) from the reforming of butane on the surface of the sponge. This caused a higher rate of carbon deposition in the pores (a higher surface area as a catalytic site). After this limited temperature range, as the temperature increased, the sponge iron tended to sinter. Thus the amount of microporosity was decreased (a lesser surface area as a catalytic site) and the

probability of better distribution and contact between the gases caused less carbon deposition.

An attempt was made to study the distribution of the carbon by microscopic examination of the sponge particles (ref 4.1.9.). Micrograph (G, H) indicated that there is no carbon in the form of pearlite nor as cementite and so it was concluded that the carbon must be in the form of soot. This was confirmed by finding a layer of carbon floating on the top of the solution when samples of sponge were dissolved in the hydrochloric acid.

The narrow filaments of iron surrounding the wustite particles extended only a short distance along the pores from the outer surface. Hence, it was concluded that the hydrocarbon molecules penetrated only a short distance into the pores before reacting with the oxygen from the ore or the CO_2 in the inlet gas. Beyond this zone, the pore surfaces were not contaminated with a soot deposit and were available to take part in the reduction reactions. In this region the rate of the reduction reaction would be determined by the rate of arrival of CO and H_2 molecules and/or the rate of removal of the reaction products.

However, carbon deposition and distribution could be affected by the temperature and the particle size (i.e., catalytic surface available). Thus, for the larger size ore the maximum porosity appeared at a higher temperature (until the limited sintering temperature) and hence more carbon was deposited at the higher temperature.

The carbon deposition situation was examined also, using the kiln without chokes in position during the different stages of reduction from

iron ore to sponge. The samples taken at 10 cm intervals along the length of the kiln were analysed as shown in (Fig. 57 and Table 40). The carbon content decreased from a peak value, 20 cm from the discharge end to a lower value at 10 cm and still lower in the run sample. As the temperatures in these regions (cooling zone) are low (from the hot sponge discharge about 600 - 300^{o}C), the cold mixture of inlet gases (CO_2, C_4H_{10}, H_2) did not absorb the necessary heat for reforming. Thus it may be concluded that the hydrogen in the inlet gases reacted with the carbon in the sponge iron discharge to form methane. It is known that the rate of the methanation reaction is slow but it is probable that the metallic iron present in the sponge iron acted as a catalyst and that low temperature increased the rate of reaction. This behaviour agreed with observations[114, 115], which demonstrated that it was possible to hydrogenate residual carbon in the reduced metallic iron products to form methane and so control the carbon content of the sponge iron.

After sample 20, as the temperature increased to the average run temperature, the reforming progressively was completed and the amount of CO in the gases increased. While the temperature was high the break down of CO (Boudouard reaction) to give carbon deposition would be decreased, which is in good agreement with the carbon content of the samples 30 and 40. Samples 50 and 60 showed a lower carbon content compared with samples 70 - 110 (carbon content of these samples came from original ore and the additional carbon caused by the Boudouard reaction in the region of sample 110). It may be concluded that some of the carbon had been gasified by the oxidants available (CO_2, H_2O). From samples 60 - 100 the carbon contents within the experimental error are steady, which indicated that the gas mixtures tended toward the equilibrium. Sample 110 showed an increase in the carbon content. The low temperature in this region was in favour of the Boudouard reaction.

There was no appreciable metallic iron available here to act as catalyst, but the definite identity of the catalyst (as iron or iron oxides) is a subject of some controversy[145, 146]; there is no doubt that iron is involved in one form or another - whether as oxide or elemental iron.

The carbon content of the sponge iron (Fig. 63 and Table 42) made in the kiln without chokes in position was less than in the sponge iron made in the kiln with the chokes under similar experimental conditions, i.e., similar ore size, gas composition, average residence time and temperature. The reasons for this difference are that, in the case of chokes usage, the sponge iron stopped a longer time in front of the discharge end choke. Thus it contacted with a higher carbon monoxide concentration in the gas (from the reforming of the hydrocarbon) during passage in the lower region of temperature profile, and also provided a higher amount of catalyst available. These factors are in favour of the Boudouard reaction. On the other hand, the sponge iron would travel through the choke region at a faster rate (as the diameter of the choke was smaller than the kiln tube). Thus less methanation of the deposited carbon occurred. In contrast to the above, in the case of kiln usage without chokes a better operating condition caused less carbon deposition and less poisoning of the autocatalytic effect of partially reduced ore (sponge iron).

5.7. Removal of the Sulphur from the Hematite Iron Ore.

Sulphur is undesirable in the majority of steels, so direct reduction processes should be capable of producing a low-sulphur product. This is one of the advantages of reduction in the solid state, in comparison with the liquid state (the blast furnace). In liquid state

reduction most of the sulphur is picked up from the coke, which supplies most of the reducing gas and heat for ore reduction and smelting. The solid state reduction processes use reformed natural gas or other reformed hydrocarbons (except the SL/RN type) which usually contain little or no sulphur. Thus the only source of sulphur in the product (sponge iron) would be the amount of sulphur content in the original iron ore, which would be different from ore to ore and is usually very small. Some of this small quantity of sulphur may be removed by the reducing agent. In the SL/RN process, which uses fine coal or coke for supplying the reducing agent, dolomite or limestone is used to combine with sulphur released from the coke, but the sulphur content of the sponge iron is higher than in the sponge produced from the solid state, gaseous reduction processes.

There is little or no work reported on the study of the removal of sulphur during reduction of iron ore by gaseous reductants. It was decided, therefore, that sulphur removal from the ore would be included in the present study.

Firstly, the off gases were examined for any sulphur content. The presence of hydrogen sulphide was identified by passing the gases over lead acetate paper; the colour of the paper changed to dark black. Secondly, the sulphur content of the sponge iron was analysed for the eleven runs (Fig. 49 and Table 10) of the series with ore size 3.35 - 4.75 mm (refer 4.1.5.). The results were examined from the thermodynamic viewpoint as below.

The sulphur content of iron ore is usually in the form of pyrite (FeS_2) or pyrrhotite ($Fe\ S_{1+x}$) where x ranged from (0 to 0.13). (147)

From examination of the free energy of formation of sulphides it is clear that FeS_2 is only slightly more stable than CuS (which CuS has the lowest value of - ΔG^o and the probability of trace of this compound in the iron ore may be ignored). Pyrite (FeS_2) can be easily thermally decomposed at a low temperature (i.e. < 500^oC) as:

$$2FeS_2 \rightarrow 2FeS + S_2$$

Thus from direct reduction temperature interest point of view the sulphur compound in iron ore would be $FeS_1 + x$. In this consideration x was taken as zero. Two equations were found for ΔG^o_T at two different ranges of temperatures as follows:[148]

$$\langle FeS\rangle_{\beta Solid} + (H_2)_{gas} = \langle Fe\rangle_{\alpha\ solid} + (H_2S)_{gas}$$

$$\therefore K = \frac{P_{H_2S} \times a_{Fe}}{P_{H_2} \times a_{FeS}}$$

For the temperature range 412 - 1179^oK;

ΔG^o_T = 15805 - 13.165T + 3.625T Log T Cal and, for the temperature range 1179 - 1261^oK;

$$\langle FeS\rangle_{\beta\ solid} + (H_2)_{gas} = \langle Fe\rangle_{\gamma} solid + (H_2S)_{gas}$$

$$\therefore K = \frac{P_{H_2S} \times a_{Fe}}{P_{H_2} \times a_{FeS}}$$

$$\Delta G^o_T = 15965 - 13.345T + 3.625T \log T \text{ cal.}$$

From the relation ΔG^{Θ}_T = - 19.147 T log K, and knowledge of the partial pressure of hydrogen (the composition of the outlet off gases were taken

as the gases at equilibrium), assuming $a_{FeS} = 1$, the partial pressure of H_2S in the gas and hence the amount of sulphur removed per hour could be calculated (Table 60).

The values of the equilibrium constant (K) indicated that the stability of H_2S increased as the temperature increased. The results of the chemical analysis of the residual sulphur content in the sponge iron for different temperatures were in good agreement with the equilibrium condition and all were above the equilibrium value. The amount of sulphur removal was compared with the amount of sulphur contained in 100 grams of the sponge, assuming zero sulphur removed for each individual run. The calculation was as follows for run No. 16.

The sulphur content of the iron ore is 0.009%

The oxygen content of the iron ore is 29.087%

The percentage of reduction for this run is 93.38%

The oxygen removal from 100 grams ore is 27.16 grams.

Therefore 0.009 grams sulphur is in 72.84 grams of the sponge; hence the amount of sulphur in 100 grams of sponge is 0.01235 grams. In the same manner, the amount of sulphur was calculated for the other runs with different percentage reduction.

The sulphur situation was examined for a run series, without chokes in position for the different stages of reduction, by taking samples at 10 cm intervals along the length of the kiln. The observations (Fig. 58 and Table 40) indicated that the amount of the sulphur in the iron ore (Samples 110 - 100) decreased sharply in the very early stage of reduction and in the low temperature range (385 - 740^{o}C). There is a probability of sulphur as pyrite (FeS_2) as well as pyrrhotite (FeS_{1+X}) as mentioned earlier, the decomposition of pyrite to pyrrhotite could be

caused by the rapid removal of sulphur in the early stage of reduction. The availability of hydrogen in the pores created during the reduction of hematite to magnetite facilitated the formation of hydrogen sulphide. After this region the sulphur variation was steady within the experimental analysis error, 'til the region of samples 60 - 40, where the extent of reduction was highest (because of the autocatalytic reforming of hydrocarbon and creation of extra porosity). The FeS reacted with hydrogen and formed more hydrogen sulphide. After this region the amount of sulphur increased. This sulphur pick-up was from the mercaptan sulphur content of the hydrocarbon (C_4H_{10}). It is reported[149] that the amount of mercaptan sulphur is (0.004 - 0.005% m/m). Thus the hourly input of sulphur with butane gas is in good agreement with the average sulphur increase in the samples in this region.

From consideration of the results it is clear a significant amount of the sulphur content in the iron ore was removed as H_2S in the off gases. If the off gases were recirculated to the kiln the sulphur would have to be removed from the off gas or removal of sulphur from the ore would cease when the gas became saturated.

If a nickel catalyst was used for reforming the gas, more or less complete sulphur removal would be essential to prevent poisoning the catalyst. Reforming the gas within the kiln would not suffer from this problem and hence a higher H_2S content could be tolerated in the recirculating gas stream.

5.8. Removal of the Phosphorus from the Hematite Iron Ore.

The phosphorus content of the iron ore usually is in the form of P_2O_5 and the iron ore is normally the only source of phosphorus

in both the liquid state and the solid state reduction processes. There is no thermodynamic information about solid P_2O_5 nor any work reported about the removal of phosphorus during reduction of iron ores in the solid state, so changes in the phosphorus content of the sponge iron were measured in the present study.

All of the phosphorus present in the gases from a phosphorus shaft furnace can be converted to phosphine by blowing steam through the furnace[150]; it is suggested that reaction occurs between the phosphorus and active hydrogen. Phosphine has also been produced[151] by passing phosphorus vapour and steam through a bed of coke at 700 - 1000°C. It is further suggested[152] that phosphine is formed in the thermal decomposition of calcium phosphite by the reduction of phosphite or phosphate with hydrogen. It is known that one of the most stable compounds of phosphorus with hydrogen is phosphine.

The phosphorus content of the sponge iron product was analysed for the three different temperatures of the run series (Fig. 50, Table 11) with ore size 3.35 - 4.75 mm (refer 4.1.5.). The results indicated that as the temperature increased the amount of phosphorus removal decreased. These results were examined with respect to the thermodynamic data of formation of phosphine as follows:

The equation for the dissociation of phosphine[151] is given as:

$$(PH_3)_{gas} \longrightarrow \tfrac{1}{4} \langle P_4 \rangle_{solid} + \tfrac{3}{2} (H_2)_{gas}$$

$$\therefore K = \frac{P_{H_2}{}^{3/2} \times a P_4^{\frac{1}{4}}}{P_{PH_3}}$$

and $\log K = 387/T_K o + 0.272 \log T_K o + 1.32 \times 10^{-3} T_K o$

Hence the equilibrium constant for the formation of phosphine, $K' = \frac{1}{K}$. From the equilibrium constant and knowledge of partial pressure of hydrogen (assuming that the outlet gases were in equilibrium, the gas analysis was used for calculation of the partial pressure of hydrogen for each run) the amount of phosphine at equilibrium and, therefore, the equilibrium phosphorus content in the outlet gases were found for the three different run temperatures. The results of the equilibrium calculations (Table 61) indicated that as the temperature increased the stability of formation of phosphine decreased, which is in good agreement with the chemical analysis results of the sponge iron products. However, the increasing divergence between the equilibrium and the actual phosphorus contents of the sponge iron, as the temperature increased, could arise from the sintering tendency at high temperature, which reduced the pore area and hence decreased the surface area available for phosphine formation.

The change in the phosphorus concentration during the reduction of the iron ore to a desirable sponge iron in the different stages of reduction, studied by taking the samples along the kiln length without chokes in position, are shown in Figs. 59, 60 and Table 41. It is observed that the rate of the removal of phosphorus decreased as the ore travelled along the length of the kiln toward discharge end. This is a two-fold effect, of the residence time and the total iron content of the partially reduced ore in the different stages of reduction. Firstly, the kiln inventory profile (Fig. 70 and Table 58) showed that the partially reduced ore stopped for a longer time in the hopper end part of the kiln, which means that the residence time for the interval samples decreased as the ore travelled nearer toward the discharge end. Secondly, it was noted that the extent of reduction increased rapidly as the ore travelled toward the discharge end; hence a higher total iron content

was found for the samples closer to the discharge end, this in turn resulted in a lower surface area (because of the sintering effect) available for phosphine formation in the samples with the higher total iron content. Thus the low surface area and less residence time available caused collectively a decrease in the usage of gas efficiency and a decrease in the rate of phosphine formation in the travelling samples toward the discharge end. In contrast, for the samples closer to the hopper regions a higher residence time and surface area allowed a better contact of the gas with the phosphorus in the ore and hence a higher rate of phosphorus removal for the samples taken in these regions. It may be concluded that the removal of the phosphorus depended on the residence time and the surface area. A higher surface area and residence time available would cause a higher rate of phosphorus removal and vice versa. The overall removal of the phosphorus in this series (RP_2S_7) is in good agreement with the results of the series (RP_1S_2), which indicated that a lower temperature favours the phosphorus removal as phosphine.

5.9. Viability of the SDR Process.

A consideration of the future place of directly reduced iron has been discussed under three general headings:[153]

(i) Manufacture, i.e. the processes description.

(ii) Location of the Plant.

(iii) Utilisation of the DRI.

(i) Manufacture of directly reduced iron (D.R.I.). The description of the plants are given for the available commercial direct reduction processes in Chapter 1.

(ii) Location and operating costs of direct reduction plants: The optimum location of a direct reduction plant is an economic exercise involving

considerations of raw material supplies, transport, capital and operating costs, taxation policy and politics. A full discussion of the above factors has been published[4]. A comparison of the cost of producing D.R.I. shows clearly the importance of each of these factors. An estimate of the cost of making DRI at the rated capacity of a 400,000 - ton - per - year plant in the U.S. Great Lakes area using a process based on reformed natural gas was $115 per metric ton of D.R.I. (including financial charges). The major elements of cost were 50 per cent for ore, 20 per cent for natural gas, and 20 per cent for financial charges. An estimate of the production cost of D.R.I. at the same rate in the same type of plant as above but located in Latin America at a site where ore, natural gas and labour are less expensive was about $55 per ton. The major elements of cost in this case were 44 per cent for ore, 36 per cent for financial charges and 6 per cent for natural gas. For the general situation, the relative costs for the two locations show the decisive role of natural gas (which is the energy and reducing agent after reforming) in the production cost of D.R.I.

(iii) Uses of directly reduced iron. By far the greatest enthusiasm for using directly reduced iron has been shown by those who want a raw material for electric arc furnace steelmaking. The product either in pellet, sinter, lump or briquette form, has several distinct advantages compared with scrap:

(a) consistency of chemical analysis,

(b) low and known residual elements,

(c) uniformity of size,

(d) not subject to such a wide fluctuation in price.

So far scrap is the main feed for the electric arc furnace, (scrap and D.R.I. consumption[154] in 1980 were respectively 334.76 and 7.15

million tonnes). Thus the production cost of D.R.I. has to be competitive with scrap in the locality of the plant. The current depressed cost of scrap metal has caused the shut down of some well known processes such as: Midrex (OSM plant) in U.S.A., Purofer (Oberhausen plant) in West Germany[21] and SL/RN plants in Korea and Canada[4].

(141)

More recently Midrex and HyL (batch) gaseous processes have exercised an alternative way to compensate the high cost of natural gas and energy by using the available coke oven gas in the industrial countries, but the Midrex process still uses a separate reformer to reform the hydrocarbons in the coke oven gas, which needs some operating and investment cost for the separate reformer. In the HyL batch process, tests showed that cleaned and desulphurized coke oven gas can be fed directly into the batch reactor in the cooling stage. The gas, serving as the sponge coolant, increased in temperature and the excess methane was reformed, with metallic iron in the sponge acting as the catalyst for the reforming reaction. The reducing gas then followed the cyclical cooling and heating steps of the batch-type HyL process. It is obvious that the absence of the necessary oxidant to reform the methane in the coke oven gas would cause some extra carbon deposition (by direct cracking of the methane) in the sponge produced by this manner.

As discussed earlier, the objective of the present research was to extend the study of the proposed SDR (Sussex Direct Reduction) process. The process has two major economic and practical advantages over existing direct reduction plants.

(i) The auto-catalytic reforming of hydrocarbons within the reducing kiln, whereby hydrocarbon reacts with carbon dioxide/water vapour (from recycling gas) on the surface of the partially reduced ore

to regenerate reducing gases which react with the iron oxide, coupled with recycle regeneration of the kiln off-gases avoids the cost of a separate plant (i.e. reformer) for the catalytic production of reducing gases. Also it was shown experimentally that at temperatures below 930°C a consistently higher[120, 123] extent of reduction was obtained using hydrogen-carbon dioxide-butane mixture, which resulted in the development of extra porosity in the ore when the hydrocarbon was reformed within the kiln, than when a chemically equivalent CO, H_2 mixture was used. This would give a higher plant capacity for the proposed SDR process, which is another economic advantage relative to the existing gaseous direct reduction plants.

(ii) As a result of the absence of solid-fuel reactant (in the SDR), which is a poor heat conductor compared with iron ore[2], and by employing a high hydrogen/carbon monoxide ratio in the reducing gases, in which hydrogen greatly promotes heat transfer because of its high thermal conductivity and diffusion[155], a higher rate of reduction would be given by the SDR process compared with the other solid-fuel rotary kilns. Also the effect of the absence of solid fuel[120] in the bed would almost double the residence time for the reacting ore for any given kiln loading factor, which is another factor to give a higher rate of reduction for the SDR process.

The higher rate of reduction achieved as a result of the above factors would give a higher plant capacity for the SDR compared with the other rotary-kiln processes. This would compensate for some of the high cost of using a gaseous reactant compared with the use of solid fuel.

In the present investigation it was found that hydrogen is a more effective reducing agent compared with a carbon monoxide and hydrogen mixture created from autocatalytic reforming (refer run series XI, XII). This means that, for a given degree of metallisation, the kiln can be operated with a shorter ore residence time and/or at a lower temperature when pure hydrogen is used as the reductant. The sponge iron product is also carbon free, which may or may not be beneficial, dependent on the degree of metallisation and the subsequent usage.

These changes in the kiln operating parameters reduce the thermal losses from the kiln (and hence the energy consumption) per tonne of iron ore which is reduced. These savings will be partially offset by the replacement of the exothermic reduction with CO by the endothermic reactions with hydrogen.

The substitution of hydrogen for a mixed ($CO + H_2$) reducing gas can only be justified economically if the overall energy savings and increased productivity are equal to, or greater than, the cost of production of the hydrogen. The cost of producing hydrogen depends on a number of factors, the most important of which are the total capital investment, the cost of the feedstock for the process and, since the process involves the conversion of one form of energy into another, the thermal efficiency of the process. There are a few commercial processes[156] which can be used to produce hydrogen:

(i) Reforming natural gas or other hydrocarbon with steam.

(ii) Coal gasification.

(iii) Heavy fuel oil partial oxidation.

(iv) Conventional electrolysis.

A consistent set of capital costs and production costs[156] have been produced, which show that if natural gas is available at a price of about 1.0£/GJ (approximately the price of North Sea gas to the U.K. petrochemical industry), then steam reforming of natural gas is claimed as the preferred process compared to the others. The following flow diagram shows the production of hydrogen from naphtha or natural gas by reforming with steam.

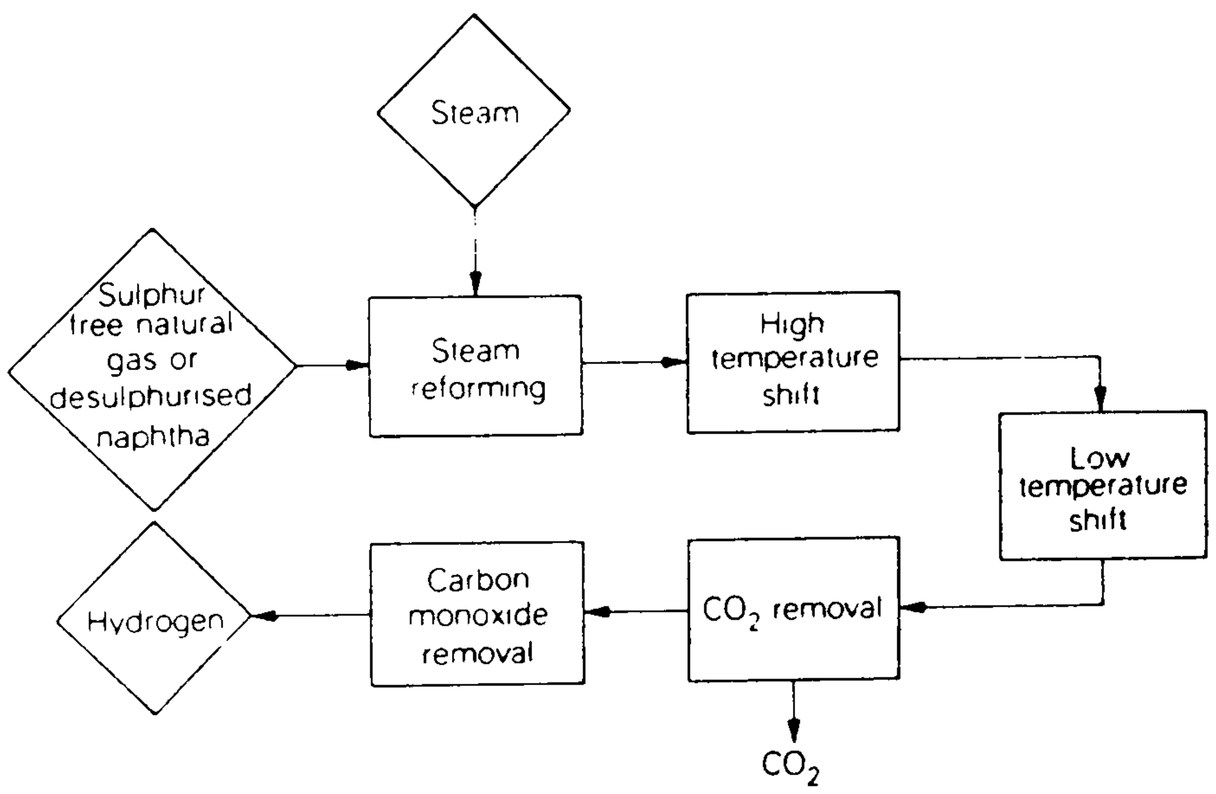

The production of hydrogen from naphtha or natural gas.

The flow diagram shows that after the reforming process several other stages are required in the manufacture of the hydrogen. But in the gaseous direct reduction plant the gas mixture ($CO + H_2$) from the reformer can be fed directly to the reducing plant. In the proposed SDR process there is no need for a separate reformer and steam generation system, which is economically advantageous.

From the sponge iron manufacturing point of view, the overall reaction of hydrogen and carbon monoxide with iron oxides are respectively endothermic and exothermic. The overall heat change from the reduction reaction can be controlled by varying the H_2/CO ratio to supply heat to the kiln but prevent overheating and stickiness problems in the reducing reactors. In the proposed SDR process the recycle gases have to be heated up somehow so that, after mixing with the make up hydrocarbon (hydrocarbon would be injected preferably preheated) within the kiln, they contain sufficient heat to compensate for the endothermic autocatalytic reforming reaction.

To simplify the experimental procedure in order to study the main theoretical aspects of the process, the laboratory experimental pilot plant tube was heated up externally by electricity (refer 3.1), iron ore and input gases (C_4H_{10}, CO_2, H_2) were fed cold and the recycling of the off gases was eliminated. The heat losses from the equipment are unknown, but it is expected that they would be greater than in commercial production. A full heat balance, therefore, is meaningless but, for a comparison of the effect of the operating variables on the heat requirements, a simplified heat balance is given for 100 grams hourly hematite iron ore input, with the assumption that the iron ore is pure hematite (the amount of impurities are very low, which may be neglected), and also there are no heat losses. Thus it may be assumed that the amount of heat given up to the ore from the gases leaving the kiln is equal to the amount which has to be supplied to the off gases to bring the temperature to the required recycling temperature. In other words, it is assumed that there is no heat transfer from gas to solid and the off gas temperature remained constant during the recycling. After starting the run, the quantities of make-up hydrocarbon (C_4H_{10}) and recycle

gases have to be adjusted. In the example shown, 1/3 of the off gases are bled-off and sufficient hydrocarbon is injected to restore the full reducing capacity of the remaining 2/3 of recycled gas, giving a reducing capacity for 100 per cent reduction of the hourly inputs. The gaseous conditions, which were taken for the heat balance example were as follows:

(i) The input gases composed H_2, CO_2, and C_4H_{10} with the respective amounts of 2.470, 0.920 and 0.247 mole/hour.

(ii) The analysed off gases showed H_2O, CO_2, CH_4, CO, H_2 with the respective amounts of 1.250, 0.555, 0.069, 1.251 and 2.13 mole/hour.

The composition of the off gases (analysed at room temperature) was converted to the high temperature equilibrium condition (at average run temperature of 1200K) by using the water shift reaction. Thermodynamic data were taken from references Nos. 157, 4 to calculate the heat balance shown:

No.	The various items making up the heat balance.	Available KJ	Required KJ
1	Heating 100 grams of Fe_2O_3 298 - 1200K		80.47
2	Heating (0.3) mole of C_4H_{10} 298 - 1200K		50.48
3	Auto catalytic reforming of (0.094 mole) C_4H_{10} to CO, H_2 with CO_2 at 1200K		78.11
4	Auto catalytic reforming of (0.206 mole) C_4H_{10} to CO, H_2 with H_2O at 1200K		144.12
5	Reduction of Fe_2O_3 to Fe with Hydrogen (60.95%)		22.65
6	Reduction of Fe_2O_3 to Fe with carbon monoxide (39.05%)	9.55	
	Total	9.55	375.83

Thus, if the heat of reforming is zero, the heat requirement on the above basis is reduced to less than 150 KJ/100 g of ore. It is further reduced if the endothermic hydrogen reduction reaction is partially replaced by CO reduction in consequence of the higher C/H ratio in the hydrocarbon. This additional heat could be supplied by combustion of the 1/3 off gases not recycled to preheat the ore feed and/or by heating the recycle gases to an appropriate temperature above 1200K.

Butane was only used in the laboratory experiments because of easy handling. In a full scale industrial process a more desirable hydrocarbon would be used from the so-called X-type[158] fuels (i.e. naptha, $C_1H_2 \cdot 167$, cycle oil, benzene, ethylene), which have either an exothermic heat of decomposition or only a zero or very small endothermic heat of decomposition. The SDR process is integrated with the SS (Sussex Steel) process and a combined and detailed heat balance for the process has been published[122].

The mathematical modelling of the kiln can be used for finding one operating variable from another and of course can be used for the up scaling of the pilot plant[120]. The following example shows experimentally how the higher rate of reduction with pure hydrogen could be compensated by raising the temperature when using C_4H_{10}, CO_2, H_2 mixture within the kiln. The reduction of the ore size 3.35 - 4.75 mm, with pure hydrogen at 849^oC and an average residence time of 97 minutes, when the kiln was used without chokes (refer run series XI, Code No. RP_2S_{11}) can be found from the equation $\%R = -23.79\ V_{C_4H_{10}} + 96.17$ ($r^2 = 0.978$), which gives a value of 96.17 per cent reduction. Alternatively by altering the operating temperature, this reduction can be achieved using

a mixture of C_4H_{10}, CO_2, H_2, with the respective amount of about 0.247, 0.929, 2.48 mole/hour and a ratio of H_2/CO of about 1.88 after reforming, if the other operating variables are unchanged. The equation $\%R = 0.2683(T_C^O) - 139.45$, ($r^2 = 0.994$), (refer run series VIII, Code No. RP_2S_8) gives the required temperature of 878^{O}C, which is 29^{O}C higher than with pure hydrogen. The required temperature to give the same extent of reduction (96.17% when pure hydrogen used) also can be found from the run series results (refer run series II, Code No. RP_1S_2) with chokes in position, ore size 3.35 - 4.75 mm, an average residence time of 106 minutes, and gas composed of C_4H_{10}, CO_2, H_2 with the respective amounts of about, 0.245, 0.920, 2.44 and a H_2/CO ratio of about 1.87 after reforming. The equation $\%R = 0.234\ T_C^O - 119.4$ ($r^2 = 0.955$) gives the required temperature of 921^{O}C, which is 72^{O}C higher than with pure hydrogen and also 43^{O}C higher than when experiments were made in the kiln without chokes (with the similar operating variables). This shows the substantial improvement for the experiments made in the kiln without chokes.

Alternatively, the lower rate of reduction with the reformed hydrocarbon gas could be compensated by decreasing the size of ore used, or with increasing residence time. This can be seen from the results for the experiments which were made in the kiln with chokes. But the operating variables were not all identical with those used with pure hydrogen (the measurements of the effect of change in gas composition were made only in the kiln without chokes), so more than one operating variable always had to be changed to compensate the higher rate of reduction with hydrogen. The following examples illustrate this.

The value of 96.17 per cent reduction, which was achieved at 921^{O}C (when the kiln was used with chokes and the mixed gases) with ore size 3.35 - 4.75 mm and average residence time of 106 minutes can be

found with the ore size 1.7 - 2.36 mm (refer run series IV Code No. RP_1S_4) and an average residence time of 228 minutes. The equation $\%R = 0.260\ T_C^O - 127.71$ ($r^2 = 0.992$) gives the required temperature of 861^OC. The above value (96.17 per cent reduction) can be achieved also from the results of runs (refer run series V Code No. RP_1S_5) with the higher average residence time of 290 minutes, but the same size ore (3.35 - 4.75 mm). The equation $\%R = 0.243\ T_C^O - 116.9$ ($r^2 = 0.985$) gives the required temperature of 877^OC. From these comparisons also may be concluded the substantial effect of using the kiln without chokes, which provided a better reducing condition and a higher extent of reduction.

From the data obtained, however, it is readily apparent that the required compensation, relative to hydrogen reduction, could be achieved by decreasing ore size, increasing residence time, increasing temperature, decreasing make up hydrocarbons in the mixture of inlet gases, or using a high hydrogen to carbon ratio hydrocarbon as make up gas. Consideration of the effect of each of the above factors on the operation and product cost show that:

(i) Decreasing the ore size would increase the cost, if this involved additional ore crushing.

(ii) Increasing the residence time would decrease the plant capacity and also increase the heat losses per tonne of product, which would result in a higher product cost.

(iii) Increasing the temperature has a three fold effect. Firstly, the process cannot work above the sintering temperature, which gives a lower extent of reduction and exacerbates the operating problems too. Secondly, the experimental results showed that at a lower temperature

a better phosphorus removal was achieved; in contrast it was found that sulphur removal was more effective at higher temperature. Thirdly, the increase in temperature would result in a higher energy requirement and eventually a higher cost for the product.

(iv) Lowering the make up hydrocarbon (but to not less than required to give a desirable reducing capacity with the recycling gases) would decrease or diminish the effect of the autocatalytic reforming reaction on the surface of partially reduced ore (sponge) and eventually give a lower rate of reduction.

(v) Using a higher hydrogen to carbon ratio hydrocarbon (e.g. C_4H_{10} compared with $C_1H_{2.167}$) Methane has the highest H/C ratio, but its higher stability needs a higher temperature for reforming. As the H/C ratio of the make up gas is increased, it requires a higher heat for the endothermic autocatalytic reaction within the kiln and a higher temperature for the input gases. In contrast using a lower H/C ratio increases the heat available from reduction and also the hydrocarbons are generally less expensive. On the other hand a lower H/C ratio gives a higher carbon deposition in the sponge (this may be advantageous in the alternative process, but would cause some poisoning of the sponge iron lowering any autocatality effect) and also gives a lower extent of reduction as the carbon monoxide increases in the mixture of gases.

The selection of the optimum operating conditions for full scale production would be dependent on the above factors and could be adjusted

to be competitive with the other processes.

In summary, it is concluded that, although the rate of gaseous reduction is most rapid with pure hydrogen, the process is unlikely to be viable generally on economic grounds (it might become viable when cheap electricity is available from an atomic plant[159] for electrolysis of water to produce hydrogen and oxygen) and the reforming of hydrocarbons to produce mixtures of CO and H_2 is more attractive, especially if the process is operated with the autocatalytic reforming regeneration of the gases in the reducing reactor.

CHAPTER 6

CONCLUSIONS

6. CONCLUSIONS

Under similar operating conditions, the rate of reduction of a Brazilian hematite ore in a rotary kiln is more rapid when the kiln is unrestricted than when a choke is inserted to increase the depth of the ore bed at the discharge end. When the reducing atmosphere is generated within the kiln using the beneficial effect of autocatalytic reaction between a hydrocarbon and a gaseous oxidant on the surface of the DRI, less carbon is deposited on the ore from the carbon monoxide (after the reforming) when the kiln is unrestricted, thus promoting the autocatalytic reaction.

The microscopic structural observation showed a porous sponge iron which indicated that the uniform internal reduction predominated until limited at the temperature where sintering commenced. After sintering commenced the rate of uniform internal reduction decreased and a limited mixed control determined the extent of reduction. This can be concluded also from the results of porosimeter measurements and the findings of percentage reduction obtained for different temperatures, for both modes of kiln operation.

A straight line relationship was found for the amount of hydrocarbon in the input gas and percentage reduction achieved as $\%R = a + bV_{C_4H_{10}}$, where V = volume of hydrocarbon (butane), a and b are constants. Also, from the results, a series of data emerged for the effect of different H_2/CO ratios upon percentage reduction, which gave a straight line relationship as $\%R = a + b(\%H_2)$, where $\%H_2$ = the overall concentration of hydrogen in the mixture of hydrogen

and carbon monoxide after autocatalytic reforming of hydrocarbon within the kiln, a and b are constants. From the above equations can be found any H_2/CO ratio for a desired percentage reduction and vice versa.

Considering only the kinetics of the reduction process it was found that pure hydrogen as reducing agent gave a higher extent of reduction than a mixture of $CO-H_2$ after autocatalytic reforming of hydrocarbon (butane) within the kiln. It is apparent, however, that until a plentiful and cheap supply of hydrogen is available, it is practically and economically advantageous to use a $CO-H_2$ mixture as the gaseous reducing agent, especially if the reducing agents are generated by autocatalytic reaction within the kiln.

A straight line relationship was also found between percentage reduction or a function of it and each individual operating variable, or a function of it, when the other variables were fixed. The operating variables were temperature, the particle size and particle volume, the residence time. From the equations can be found any desired percentage reduction for a given set of variables and vice versa.

Sulphur and phosphorus are partially removed in gaseous form from the ore; within the temperature range examined, sulphur removal increased with increase in temperature, whereas phosphorus removal was favoured at lower temperature. The sulphur and phosphorus removal were examined also during the different stages of reduction (i.e. from iron ore to a desired sponge iron) for one run series and the results showed that the removal in the early stage of reduction was appreciable. The overall removals were in agreement with the above observations.

The carbon content of the sponge iron varied non-linearly with the temperature. In general, the concentration decreased with increase in temperature, but there was a rapid increase in carbon content at an intermediate temperature range. Microscopical examination revealed no evidence of carbon as pearlite, cementite or graphite in the iron, so this increase could not be attributed to changes in carbon solubility consequent upon the α-γ transformation in the iron. The carbon must have been present as a soot deposit and the increase in the concentration in the intermediate temperature range is tentatively ascribed to the increase in pore surface area which also occurred in that temperature range. This was in accord with the experimental results when the kiln was used with chokes but, without chokes, there was no rapid increase in carbon content at an intermediate temperature range. An examination of the carbon content during the different stages of reduction (i.e. from iron ore to a desired sponge iron) for a run series showed that some of the carbon left in the sponge iron can be gasified by hydrogen as methane in the cooling zone of the kiln.

The effect of oxidant content in the mixture of input gas upon the quality of the product (i.e. sponge iron) showed that for a lower oxidant content (compared with the optimum amount needed for autocatalytic reforming of the hydrocarbon make up in the mixture of input gas), a higher carbon deposition was obtained in the sponge iron from the partial cracking of the hydrocarbon. From the economic point of view, the higher carbon content (caused by the partial cracking of the expensive hydrocarbon compared with carbon additions to the steelmaking bath) would not be advantageous even in the alternative

steelmaking process.

The reducing capacity (optimum flow rate of the gas which is above the critical flow rate) was found for similar conditions to those which apply in commercial practice, i.e. use of multiparticle size and the progressive appearance of oxidant in the mixture of proceeding reducing gas, which is completely different from single particle practice (i.e. use of a thermobalance).

CHAPTER 7

RECOMMENDATIONS FOR FUTURE INVESTIGATIONS

7. RECOMMENDATIONS FOR FUTURE INVESTIGATIONS.

As is with any research investigation only a limited study could be performed in the time available, and some new questions remain to be answered. It would be advantageous for upscaling the proposed SDR process to do some more tests on the following aspects.

(i) The result of experiments without chokes in position in the kiln showed a considerable improvement in the extent of reduction. A few test runs for different ore sizes (preferably nearer to the sizes used commercially) and residence times would give useful data, which also may be compared on the same feedstock with the results of a rotary kiln[158] used with baffles. Using the baffle in the kiln gave a better gas to solid contact and required a lower residence time to reach a given per cent reduction.

(ii) A study of the effect of different hydrocarbons[122] (preferably the ones which could be used in commercial practice) and different iron ores or pellets on the reforming and the autocatalytic activity.

(iii) A study of the experiments with recycling the actual experimental kiln off-gases, and adding only hydrocarbon for the recycle regeneration, in order to check methane build up when recycling off-gases.

(iv) An examination of the optimum amount of breeze coal content in ore pellets, to limit ash contamination and avoid an excess of coal in the sponge, or alternatively injection of an optimum amount of high volatile coal (e.g. sub-bituminous)

to compensate some of the make up hydrocarbon usage, while using the autocatalytic effect of hydrocarbon (some comes from the volatile's in the coal) on the surface of the partially reduced ore. This would reduce the high cost of gaseous reducing reactant, which is in shortage in some regions, bu using cheap coal available there, and provide more flexibility for the process.

ACKNOWLEDGEMENT

I would like to express my gratitude to my supervisor, Professor C. Bodsworth, for his extensive valuable advice and encouragement at different stages of this work.

The author is also gratefully indebted to Mr I. G. Nixon, one of the authorities in this field, for his external interest in guiding the project towards further improvement.

And last, but not least, I am particularly thankful to Mrs Valerie Short, for her patience and care in typing the thesis.

REFERENCES

1. E.T. Turkdogan "Physical chemistry of high temperature technology" 1980, New York, Academic Press.

2. Von Bogdandy and H.J. Engell "The reduction of iron ores" 1971, Berlin, Springer-Verlog.

3. J. Szekely, J.W. Evans and H.Y. Sohn "Gas-Solid Reactions" 1976, New York, Academic Press.

4. Robert L. Stephenson (Ed.) "Direct reduced iron", 1980, The Iron and Steel Society of AIME.

5. Terence E. Dancy, Met. Trans. B., 1977, Vol. 8B, p.201.

6. Direct Reduction of Iron Ore : a bibliographical survey, 1979, The Metals Society, London.

7. J.R. Monson: The operation of the blast furnace - theory and practice Vol. 1 - 3 (Proc. Conf.) Arles, France 2 - 4 June, 1980, Vol. 1, P.II.1.1.

8. Dartnell, J. Ironmaking & Steelmaking, 1978, Vol. 5, No. 1, p.18.

9. E.T. Turkdogan Met. Trans. B., 1978, Vol. 9B, p.163.

10. A.K. Gabee, (Proc. Conf.) Arles, France, 2 - 4 June 1980, Vol. 3, P.II.4.1.

11. J.R. Monson and D.S. Gathergood, Ironmaking and Steelmaking, 1981, Vol. 8, No. 3, p.101.

12. C.M. Hemming and G.C. Carter ibid p.104.

13. I. Nishida, T. Uenaka, I. Mizuguchi, (Proc. Conf.) Arles, France, 2 - 4 June 1980, Vol. 1, P.IV.1.1.

14. Y. Ishikawa, Revue de Metallurgie - Mars, 1976, p. 283.

15. A.H. Dixon and D.W. Brooks : Ironmaking and Steelmaking 1981, Vol. 8, No. 4, p.145.

16. A. Ghiglione et al. (Proc. Conf.) Arles France 2 - 4 June 1980, Vol. 3, P.IV-3-1.

17. I.F. Carmichael et al. ibid Vol. 1, p.1-1.

18. M. Kondoh et al. ibid Vol. 1, p.1 - 3.

19. "Decade of growth makes deceptive start" Iron and Steel International, June 1980, Vol. 53, p.121-122.

20. "Steel Production" Iron & Steelmaker, March 1982, p.20.

21. "Direct from Midrex" 2nd Quartar 1982, Vol. 7, No. 3.

22. S. Eketorp, O. Wijk and S. Fukagawa, Proc. Conf. "Extraction Metallurgy 1981", p.184.

23. R.L. Stephenson, Iron and Steelmaker, February 1982, p.40.

24. G.S.F. Hazeldean and R.B. Smith "Mini-Mills" The Institution of Metallurgists, March 1978, Series 3, No. 9, p.14.

25. F. Avila and H.L. Ramos "Raw Materials, Feed and Energy Sources for the Iron and Steel Industry" (Proc. Conf.) Philippines 9-13 Oct., 1978, South East Asia Iron and Steel Institute, Singapore 1978, p.463.

26. M. Motlagh, "Techno-Economic Evaluation of Direct Reduction throughout the World" M.Sc. thesis, 1977, University of Aston in Birmingham.

27. J. Celada and G.E. McCombs I & S.M. October 1976, p.18.

28. Direct from Midrex, Fall 1981, Vol. 7, No. 1.

29. C.W. Sanzenbacher, D.C. Meissner, Can. Min. Metall. Bull., Apr., 1976, p.120.

30. (Prof. Conf.) Philippines 9 - 13 Oct. 1978, South East Asia Iron and Steel Institute. Singapore 1978, p.447.

31. J.E. Bonestell and W. Pietsch "Proceedings of the third international Iron and Steel Congress" 16 - 20 April, 1978, Chicago, Illinois, p.186.

32. "Electrothermal Direct Reduction Process Introduced" Iron and Steelmaker, April 1981, p.27.

33. A.B. Crestani, C.L. Cruse and J.W. Neumann, Industrial Heating, Sept. 1974, Vol. 41(9), p.60.

34. "HyL direct-reduction ironmaking moves to continuous production" Metals and Materials, May/June 1981, p.45.

35. G.G.W. Thom and K. Wilson, Iron and Steelmaker, Oct. 1976, p.30.

36. V. Venkateswaran and J.K. Brimacombe, Met. Trans. B., Sept. 1977, Vol. 8B, p.387.

37. R. Rangel, W. Schnabel and H. Serbent, Proc. Conf. "Extraction Metallurgy '81", London 21 - 23 Sept. 1981, p.193.

38. V.P. Keran, A.C. Baker et al. ISS-AIME, Ironmaking Proceedings, 1980, Vol. 39, p.412.

39. H.A. Kulberg, "Current status of the FIOR of Venezuela start up" AIME Ironmaking Proceedings, Vol. 35, 1976, p.381.

40. Anon, Eng. Min. J., 1972, No. 8, p.78.

41. BISITS. (British Industrial & Scientific International Translation Service), The Metals Society, No. 18979.

42. "Direct Reduction as an Ironmaking Alternative in The United States", Nov. 1981, Fordham University, U.S.A.

43. Metals and Materials, March 1981, p.27.

44. E.T. Turkdogan and R.G. Olsson, Ironmaking and Steelmaking, 1978, Vol. 5, No. 4, p.168.

45. John F. Elliott, Iron & Steelmaker, April, 1981, p.32.

46. R.S. Barnes, Ironmaking and Steelmaking (quarterly) 1975, Vol. 2, No. 2, p.82.

47. J.W. Harrington, Ironmaking & Steelmaking, 1980, No. 7, No 2, p.76

48. F. Fitzgerald, Ironmaking and Steelmaking, 1976, No. 6, p.337.

49. G.S.F. Hazeldeanand R.B. Smith "Mini-Mills", The Institution of Metallurgists, March 1978, p.14.

50. "Direct Reduction a review of the Commercial Processes", (U.S.) Industrial Environmental Research Lab., Research Triangle Park, Nc, Jan., 1980.

51. U.Kalla and R. Steffen, Iron and Steel International, October 1977, p.307.

52. J.R. Miller, Ironmaking and Steelmaking, 1977, No. 5, p.257.

53. M.L. Shrikant, Ironmaking and Steelmaking, 1974, No. 2, p.78.

54. J. Astier, Lim K. Bin, Proc. SEAISI Conference on "Prospects for Mini-Steel Mills" Singapore 8 - 12 Sept. 1980, p.13.

55. K.P. Shaver, S.B. Lasday, SEAISI Quarterly, Jan. 1976, p.29.

56. W. Korf., Direct from Midrex, 1979, Vol. 5, No. 1, p.10.

57. U. Kalla and R. Steffen, Iron and Steel International, Oct. 1977, Vol. 50, p.5.

58. S.J. Ahier and A.R.E. Singer ibid December 1979, p.381.

59. J.R. Miller, Iron and Steelmaker, 1976, Vol. 3, p.12.

60. L.S. Darken and R.W. Gurry, J. Amer. Chem. Soc., 1946, Vol. 68, p.798.

61. B. Phillips and A. Muan, J. Phys. Chem. 1960, Vol. 64, p.1451.

62. O.N. Salmon, J. Phys. Chem. 1961, Vol. 65, p.550.

63. R. Sifferlen, C.R. Bebd. Seances Acad. Sci., 1957, Vol. 244, p.1192.

64. M. Wiberg, Jernkontorets Ann. 1940, Vol. 124, p.179.

65. J.O. Edstrom, J. Iron Steel Inst., Lon., 1953, Vol. 175, p.289.

66. N.A. Hovgard and P.N. Jensfelt, Jernkontorets Ann., 1956, Vol. 140, p.467.

67. C. Bodsworth and H.B. Bell, Physical Chemistry of Iron and Steel Manufacture, 1972, London, Longman.

68. M. Tenebaum, and T.L. Joseph, Trans. Amer. Inst. Min. (Metall.) Engrs. 1940, Vol. 140, p.106.

69. N. Towhidi and J. Szekely, Ironmaking and Steelmaking, 1981, Vol. 8, No. 6, p.237.

70. Q.T. Tsay, W.H. Ray and J. Szekely, A.I.Ch.E. Journal, 1976, Vol. 22, No. 6, p.1064 and 1072.

71. E.T. Turkdogan and J.V. Vinters, Canadian Metallurgical Quarterly, 1973, Vol. 12, No. 1, p.9.

72. J. Szekely and Y. El-Tawil, Metallurgical Transaction B, Sep. 1976, Vol. 7B, p.490.

73. T.S. Yun, Trans. Amer. Soc. Metals, 1961, Vol. 54, p.129.

74. W. Baukloh and R. Durrer: Arch. Eisenhuttenwes (1930/31), Vol. 4, p.455.

75. B.G. Baldwin, J. Iron Steel Inst., 1955, Vol. 179, p.306.

76. S.Y.M. Ezz, R. Wild: J. Iron Steel Inst., 1960, Vol. 194, p.211.

77. T.L. Joseph, Trans. A.I.M.E., 1936, Vol. 120, p.72-98.

78. E.T. Turkdogan and J.V. Vinters, Met. Trans. 1972, Vol. 3, p.1561.

79. E.T. Turkdogan and Vinters, Met. Trans. 1971, Vol. 2, p.3175.

80. E.T. Turkdogan, R.G. Ölsson and J.V. Vinters, Met. Trans. 1971, Vol. 2, p.3189.

81. R.G. Olsson and W.M. McKewan, Trans. Met. Soc. AIME, 1966, Vol. 236, p.1518, Met. Trans. 1970, Vol. 1, p.1507.

82. F. Fitzgerald, Ironmaking and Steelmaking (Quarterly), 1976, Vol. 3, No. 6, p.337.

83. W.M. McKewan, in Steelmaking, The Chipman Conference, 1965, p.141, MIT Press.

84. R.H. Tien and E.T. Turkdogan, Met. Trans., 1972, Vol. 3, p.2039.

85. E.W. Thiele, Ind. Eng. Chem. 1939, Vol. 31, p. 916.

86. J. Szekely and J.W. Evan, Met. Trans. 1971, Vol. 2, p.1691 and 1699.

87. J. Szekely "Blast Furnace Technology Science and Practice", 1972, New York.

88. N.B. Gray and J. Henderson, Trans. TMS-AIME, 1966, Vol. 236, p.726.

89. W.M. McKewan, Trans. TMS-AIME, 1962, Vol. 224, p.2.

90. R.H. Spitzer, F.S. Manning and W.O. Philbrook, Trans. TMS-AIME, 1966, Vol. 236, p.1715.

91. B.B.L. Seth and H.U. Ross, Can. Met. Quarterly, 1966, Vol. 5, No. 4, p.315.

92. J.T. Moon and R.D. Walker, Ironmaking and Steelmaking (Quarterly) 1975, Vol. 2, No. 1, p.30.

93. W. Wenzel et al : Aufbereitungstechnik, 1970, Vol. 11, p.154 (BISITS 9398).

94. R.L. Bleifuss, Trans. AIME, 1970, Vol. 247, p.225.

95. T. Fuwa and S. Ban-ya : Trans. I.S.I. Japan 1969, Vol. 9, p.137.

96. W-K. Lu, Proc. 33rd Ironmaking Conference, Atlantic City, April, 1974, p.61.

97. A.N. Pokhvisnev, A.N. Spektor et al., Stal in English, Feb, 1970, p.85.

98. P.A. Ilmoni, B. Bjorkvall : Ironmaking Proceedings A.I.M.E., 1977, Vol. 36, p.366.

99. H. Vom End, K. Grebe and S. Thomalla, Stahl Eisen, 1970, Vol. 90, No. 13, p.667.

100. R.L. Bleifuss, Trans. AIME, 1970, Vol. 247, p.225.

101. L. Granse, Trans. Iron Steel Inst. Jpn., 1971, Vol.11, p.45.

102. E.E. Hoffman, H. Rausch and W. Thumm, Stahl Eisen, 1970, Vol. 90, p.676.

103. Y.K. Rao, Met. Trans. 1971, Vol. 2, p.1439.

104. M.C. Abraham and A. Ghosh, Ironmaking and Steelmaking, 1979, Vol. 6, No. 1, p.14.

105. K.I. Otsuka and D. Kunll, J. Chem.Eng. Jpn. 1969, Vol. 2, No. 1, p.46.

106. J.B. Lewis "Modern aspects of graphite technology (Ed. L.C.F. Blackman); 1970 London Academic Press.

107. L.S. Darken and E.T. Turkdogan "Heterogeneous kinetics at elevated temperatures" (Eds. G.R. Belton and W.L. Worrell), 1970, New York, Plenum Press.

108. R.J. Fruehan, Met. Trans. B. 1977, Vol. 8B, p.279.

109. R.H. Tien and E.T. Turkdogan, Met. Trans. B., 1977, Vol. 8B, p.305.

110. H.Y. Sohn and J. Szekely, Chem.Eng. Sci., 1973, Vol. 28, p.1789.

111. O.A. Stepanov, S.T. Rostovtsev, and O.L. Kostelov, Steel in U.S.S.R., June 1971, p.430.

112. O.A. Stepanov, et al. ibid August 1971, p.595.

113. B.A. Borok, V.G. Voskoboinikov, et al. ibid, May 1973, p.356.

114. M.A. Qayyum, D.A. Reeve, The Metallurgical Society of CIM, Annual Volume, 1977, p.237.

115. M.A. Qayyum and D.A. Reeve, Carbon, 1976, Vol. 14, p.199.

116. B. Von Ilschner, Tech. Mitt. Krupp, Dec. 1959, Vol. 17, No. 6, p.318.

117. P.K. Strangway and H.U. Ross, Canadian Metallurgical Quarterly, 1966, Vol. 5, No. 3, p.221.

118. M.A. Qayyum, Metallurgija, Sisak, Yugoslavia, Broj., 1971, Vol. 3-4, p.3.

119. W.A. Mullett, I.G. Nixon and J.D. Smith, Journal of the Iron and Steel Institute, April 1973, Vol. 211, No. 4, p.278.

120. I.G. Nixon, Ironmaking and Steelmaking 1980, Vol. 7, No. 1, p.2.

121. I.G. Nixon, British Patent No. 1213641, 1970.

122. I.G. Nixon, Inst. Chem. Eng. Symp., Harrogate, 1975, Series No. 43, 13-7f.

123. I.G. Nixon, C.F. Simpson and J.D. Smith, Ironmaking and Steelmaking, 1976, Vol. 3, No. 2, p.106.

124. R.R. Rogers (Ed.) "Iron ore reduction", 1962, London Pergamon Press.

125. J. MacKenzie, JISI, 1969, Vol. 207, p.765.

126. Juan F. Price - Falcon et al, United States Patent Mar. 3, 1981, 4253867.

127. Technique of organic chemistry volume III, Part II Laboratory Engineering 1957, London.

128. Chemical Procedure DR-4, DR-5, Midrex Corporation, U.S.A.

129. Methods of chemical analysis of iron and steel, British Steel Corporation, 1974.

130. T.S. Harrison "Handbook of analytical control of iron and steel production" British Steel Corporation, 1979.

131. T. Rigg, Can. J. Chem. Eng., 1964, Vol. 42, p.247.

132. W-K.lu and G. Bitsianes, Can. Met. Quart., 1968, Vol.7, No. 1, p.3.

133. D.J. Hucknall "Selective oxidation of hydrocarbons", 1974, London, Academic Press.

134. Catalyst handbook, 1970, Wolfe Scientific Books, London.

135. S. Taniguchi, M. Ohml and H. Fukuhara, Trans. Iron Steel Inst. Jpn, 1978, Vol. 18, No. 10, p.633.

136. M.W. Pepper, K. Li and W.O. Philbrook, Canadian Metallurgical Quarterly, 1976, Vol. 15, No. 3, p.201.

137. K.A. Shehata and S.Y. Ezz, Trans. Inst. Min. Met., 1973, Vol. 82 PTC, p.C38.

138. C. Wagner, J. Metals, 1952, Vol. 4, p.214, Trans. AIME, 1952, Vol. 194, p.214.

139. R. Nicolle and A. Rist, Met. Trans. B., Sept. 1979, Vol. 10B, P.429.

140. R.D. Walker, Metallurgical Journal, 1970, Vol. 20 PT, P.14.

141. C.G. Davis, J.F. McFarlin, and H.R. Pratt, Ironmaking and Steelmaking, 1982, Vol. 9, No. 3, p.93.

142. H.J. Donald, "An Annotated Bibliography" Mellon Inst. Ind. Res. Pittsburgh, Pennsylvania, 1956.

143. P.L. Walker, J.F. Rakszawski and G.R. Imperial, J. Phys. Chem. 1959, Vol. 63, p.133, 140.

144. E.T. Turkdogan and J. V. Vinters, Metall. Trans., 1974, Vol. 5, p.11.

145. S. Klemantaski, J. Iron and Steel Inst., 1952, Vol. 171, p.176.

146. J. Taylor, Ibid, 1956, Vol. 184, p.1.

147. P.C. Kapur, R.P. Goel et al, Ibid, Sept 1972, Vol. 210, p.698.

148. O. Kubaschewski, C.B. Alcock "Metallurgical Thermochemistry" 5th Edition, Pergamon Press 1979.

149. British Standard, 1975, 4250.

150. I.S. Rozenkrants and M.O. Dembo, Russ. Pat. 31.1.1939 No. 54364.

151. Inorganic and Theoretical Chemistry, Vol. VIII, Supplement III Phosphorus, 1971, Longman.

152. A.P. Dunaev, J. Chem. Ind. U.S.S.R., 1931, Vol. 8, No. 14, p.35.

153. J. MacKenzie, Journal of the Iron and Steel Inst., June 1969, Vol. 207, p.765.

154. "Direct from Midrex" Winter 1982, Vol. 7, No. 2, p.8.

155. D. Lihou, "Heaters for chemical reactors" 1975, London Institution of Chemical Engineers, p.2.

156. M. Smith, G. Rasmussen and D. Merrick, Energy exploration and Exploitation, Jan. 1982, Vol. 1, No. 1, p.29.

157. F.D. Rossini, K.S. Pitzer, R.L. Arnett, et al "Selected values of physical and thermodynamic properties of hydrocarbons and related compounds", 1953, Pitsburgh, Carnegie Press.

158. I.G. Nixon, U.K. Patent Application GB, 2 076858 A, 1980, p.1 - 21.

159. K.P. Shaver, Stanley B. Lasday, S.E.A.I.S.I. Quarterly, Jan. 1976, p.29.

APPENDIX I

THE CALCULATION OF NITROGEN CALIBRATION

1. The capillary flowmeter specification:

The capillary flowmeter's zero was set at 2.8 cm on the ruler.

The capillary flowmeter's angle, measured as Sinα, equalled 0.2387.

Density of oil in the flowmeter was 1.042 - 1.045 grams/$_{cm^3}$ at 20^{o}C.

Size of jet installed in capillary flowmeter was 0.8 mm.

2. Experimental functions:

Room pressure - 757.15 mm Hg

Jet temperature - 24^{o}C

Water temperature (in displacement apparatus) - 23^{o}C

Height of conical flask mouth from water surface - 7 cm

Volume of measuring flask - 1000 cc

The gas was collected in a one litre conical flask by displacement of water. Six runs were made with different flow rate measurements as follows:

Run No.	Pm (cm)	ΔP_m (cm)	t (Sec.)	Notes
1	9.0	6.2	125.2	Pm is flow reading from capillary flowmeter $\Delta Pm = Pm - Po$ Po is flowmeter zero ΔP_m is actual flow reading t is time for collection of one litre in measuring flask.
2	12.0	9.2	101.8	
3	14.3	11.5	91.3	
4	19.0	16.2	76.4	
5	21.7	18.9	70.5	
6	24.0	21.2	66.1	

Calculation is shown for first run as follows:

<u>Calculations</u>:

The volume of N_2 at $T^{\ominus}, P^{\ominus}$ is as follows:

$$PN_2 = P_{atm} - P_{H_2O} - P_{hH_2O}$$

PN_2 is nitrogen pressure in flask

P_{atm} is atmospheric pressure (barometer)

Ph_{H_2O} is water height pressure in displacement apparatus

$PN_2 = 757.15 - 21.07 - 5.14 = 730.94$

$$\frac{P\ominus V\ominus}{T\ominus} = \frac{P_2V_2}{T_2}$$

$$\frac{760 \times V\ominus}{273} = \frac{730.94 \times 1000}{296} \quad \text{then } V\ominus = 887.02^{cc} \text{ at } T^{\ominus}, P^{\ominus}$$

$V\ominus$ volume at a standard temperature and pressure, $T^{\ominus}$, $P^{\ominus}$

ΔP actual $= \Delta Pm \cdot \sin\alpha$

ΔP actual is vertical height of oil equivalent with mercury

$$\Delta P \text{ actual} = \frac{62 \times 1.0435 \times 0.2387}{13.6} = 1.1355 \text{ mm Hg.}$$

$$Q\Theta = \frac{V\Theta}{t}$$

$Q\Theta$ = flow rate of the gas ($^{cc}/_{sec}$) at T^{Θ}, P^{Θ}

$$Q\Theta = \frac{887.02}{125.2} = 7.084\ ^{cc}/_{sec}\ \text{at}\ T^{\Theta},\ P^{\Theta}$$

$$Qm = Q\Theta\left(\frac{T_1}{T\Theta}\right)\frac{2P\Theta}{P_1 + P_2}$$

Qm = gas flow (in ^{cc}/sec) at temperature T_1 and any average pressure in mm. Hg.

T_1 is flowmeter temperature at degrees ^{O}K.

P_1 is inlet gas pressure into the jet.

P_2 is outlet gas pressure from the jet.

$P_2 = PM + P_{atm.}$

$P_1 = P_2 + \Delta P$ actual

PM is difference manometer height of oil equivalent with mercury.

$$PM = \frac{240 \times 1.0435}{13.6} = 18.41 \text{ mm Hg}$$

$P_2 = 18.41 + 757.15 = 775.56$ mm Hg

$P_1 = 775.56 + 1.1355 = 776.70$

$$Qm = 7.084 \times \frac{297}{273} \times \frac{2 \times 760}{776.70 + 775.56}$$

$Qm = 7.5465\ ^{cc}/sec$ at room temperature and average pressure

$$\Delta P/Qm = \frac{6.2\ (cm)}{7.5465\ ^{cc}/_{sec}} = 0.82156$$

For all other runs the calculations are the same as above and results are shown in Table 62. These results were used to plot $\Delta P/Qm$ against $Q\Theta$, which gives a straightline (Fig. 73), and from the equation (A) which by statistical calculation can easily find the constants $a\mu$ and $b\rho\Theta$ as follows:

$$Y = \frac{\Delta P}{Qm} = 0.10604\ Q\Theta\ (x) + 0.07339 \qquad (A)$$

$$Y = b\rho\Theta Q\Theta + a\mu \qquad (B)$$

From comparison of equation A and B, a_μ and $b\rho\theta$ are found

$$b\rho\theta = 0.10604$$

$$a_\mu = 0.07339$$

These constants are specific for this particular gas, flowmeter and jet. Now by using these constants in the general formula (Equation 12), it is possible to find very accurately the flow rate $Q\theta$ for every flowmeter reading ΔPm.

$$Q\theta = \left[\tfrac{1}{4}\left(\frac{0.0734}{0.10604}\right)^2 + \frac{\Delta Pm(cm)}{0.10604}\left(\frac{\dfrac{\Delta Pm \times 1.0435 \times 10 \times 0.2387}{13.6}}{2 \times 760} + \frac{2(18.4147 + Patm.)}{2 \times 760}\right)\left(\frac{273}{273 + t_{jet}}\right)\right]^{\frac{1}{2}} - \tfrac{1}{2}\left(\frac{0.0734}{0.10604}\right)$$

NOTES: Hydrocarbons are soluble in water, thus water in displacement apparatus should be saturated with butane for calibration measurements. Carbon dioxide is soluble in water, it was best measured by absorption, standard U column of sofnolite (preferably two in series) and from the difference in measured weights and time of collection the calibration was calculated.

APPENDIX NO. II

Chemical Analysis

The sponge iron was analysed for determination of total iron, metallic iron, carbon, sulphur and phosphorus content as follows.

Total Iron.

Determined by the standard method[128] based on the following principles: the dissolution of sponge iron by concentrated hydrochloric acid to which is added a few drops of hydrofluoric acid, followed by the reduction of the ferric ions to ferrous ions by using stannous chloride, excess of which is removed by mercuric chloride and finally the oxidation of the ferrous ions to ferric ions by titrating with standard potassium dichromate, after the addition of a few mls. of sulphuric-phosphoric acid and the endpoint being detected by the addition of diphenylamine sulphonate as an indicator which turns purple.

Reproducibility: Replicate determination, at 100 per cent ± 0.05 per cent.

Metallic Iron.

Determined by the standard method[128] based on the following principles: the sponge iron is boiled with mercuric chloride and filtered. The filtrate is titrated with standard potassium dichromate ($K_2 Cr_2 O_7$) after the addition of a few mls. of sulphuric-phosphoric acid and the end point is detected by the addition of a few drops of diphenylamine sulphonate which turns purple at the end point.

Reproducibility: Replicate determination, at 100 per cent ± 0.05 per cent.

Carbon (Non-Aqueous Titration Method)[129]

Principle: Carbon is oxidised to CO_2 by high temperature combustion of the sample in purified oxygen. The exit gases are passed through manganese dioxide, to remove sulphur gases before absorbing the CO_2 in a mixture of Dimethyl Formamide [$H{\cdot}CO{\cdot}N(CH_3)_2$] and ethanolamine (2 - Hydromyethylamine ($CH_2OH{\cdot}CH_2{\cdot}NH_2$)). The carbon content of the sample is determined by titration with Tetra-n-butyl ammonium hydroxide ($[CH_3(CH_2)_3]_4$ NOH.)

Reproducibility: At the 0.37 per cent ± 0.002 per cent

At the 0.5 per cent ± 0.01 per cent.

Sulphur (Combustion method)[129]

Principle: The sample is ignited in oxygen using tin powder as flux. Sulphur is oxidised to, SO_2, and possibly some, SO_3. These oxides are absorbed in H_2O_2, and the sulphuric acid so formed is titrated with Borax solution. The relationship between the titrate volume and the sulphur content is empirical but constant if the procedure is strictly followed.

Reproducibility: At the 0.009 - 0.03 per cent ± 0.001 per cent

Phosphorus (Nitric Acid Solution Method)[129]

Principle: The sample is dissolved in diluted nitric acid and after oxidation of carbonaceous matter, phosphorus is precipitated as the yellow phosphomolybdate complex. The precipitate is collected and washed and the determination is completed volumetrically by titration with standard alkali and acid solutions.

Reproducibility: Replicate determination on 2, grams sample ± 0.0025.

Phosphorus (Titrimetric Method for Iron Ores)[130]

Principle: The sample is dissolved in hydrochloric acid, oxidized with nitric acid and evaporated to fumes with perchloric acid. After removal of silica by filtration, hydrobromic acid is added and the solution fumed to expel arsenic. Ammonium nitrate and nitro-molybdate reagent are added and the phosphomolybdate is precipitated by vigorous shaking. Following filtration it is dissolved in standard sodium hydroxide solution, the excess being titrated with standard nitric acid, with phenolphthalein as indicator.

Reproducibility: Replicate determination on 2, grams sample ± 0.003.

APPENDIX III

EXAMPLE OF GAS BALANCE CALCULATION.

The calculation for Run No. 10 of the first series was as follows:

The measured amount of inlet gases at T^{Θ} P^{Θ} was:

H_2 - 2.45 mole per hour

CO_2 - 0.9251 mole per hour

C_4H_{10} - 0.2225 mole per hour

C_3H_8 - 0.02473 mole per hour

(The butane supply contained 10% propane) See also Table 63.

Off gas measurement: The time for collection of two litres of residual gas (after absorption of water and carbon dioxide) was 100 seconds, the temperature and atmospheric pressure were respectively 16.5^{o}C and 756 mm Hg. Converted to T^{Θ}, P^{Θ}, this residual volume was 1876.084 cc at 100 seconds. Thus the measured volume in moles per hour of residual gas was 3.0135 assuming residual gases are CO, H_2, and CH_4. The difference in weight of the absorption column for water was 0.71 grams at 100 seconds and from this figure the amount of water was calculated as 1.42 mole/hour. The amount of carbon dioxide was found in the same manner as for water; the weight of CO_2 absorbed at 100 seconds was 0.798 grams and hence the moles per hour of CO_2 is 0.6529. The amount of carbon transferred to the sponge iron sample was measured as 0.0166 moles/hour. The amount of unreacted hydrocarbons was taken to be methane and measured 10% of the residual gases in mole per hour. From a carbon balance on the in-put and out-put,

the amount of carbon monoxide in the off gases could be found and the amount of hydrogen in the outlet was found by difference. The molecular and atomic balances are shown in the Table 63. Note the small error in inlet and outlet balances for hydrogen and also in calculation of the percentage reduction by gas balances in comparison with the sponge iron analysis. The small difference was caused by the following:

1. Total hydrocarbons in the outlet were assumed to be present as methane, but there were some hydrocarbons with higher C/H ratios.

2. Part of the small difference may also be due to leakage from equipment.

APPENDIX IV

Date: 15.2.79 *Run No.* 10 *Angle of Kiln:* 1°11" *Size of Ore:* 2.36-3.35mm *Type of Ore:* Brazilian *Size of Chokes:* *Top:* 17mm *Exit:* 20mm

Time	Hopper Tem.	Eurotherm Max. Tem. Zones			Ampere			Axial-Thermocouple Max. Tem. (°C) Zones			Ore Feeding Rate			Flowing of gases Flowmeters reading (cm)					Notes
		L.H.	Mid.	R.H.	L.H.	Mid.	R.H.	L.H.	Mid.	R.H.	Input grams	Output grams	Speed Sec.	N_2	H_2	CO_2	CO	C_4H_{10}	
1200	75	890	890	905	3.7	0.5	3.7	886	884	920	100	-	29	-	25.2	29.5	-	52.4	Gases were fed at 1155. R.H. 5°C up at 1230. L.H. 5°C up at 1230
1300	80	895	890	910	3.7	0.5	3.7	894	889	929	100	65	29	-	25.4	29.3	-	52.3	
1400	80	895	890	910	3.7	0.5	3.8	893	891	929	100	70.8	29	-	25.4	29.3	-	52.4	L.H. 5°C off at 1415
1500	91	890	890	910	3.6	0.5	3.8	888	891	930	100	70	28.8	-	25.4	29.4	-	52.3	L.H. and Mid. 20°C off at 1530 because of stickiness avoidance.
1600	87	875	870	910	3.6	0.5	3.8	874	882	927	100	70.8	29	-	25.3	29.3	-	52.2	L.H. 5°C up at 1555 L.H. & R.H. 5°C up at 1620
1700	97	880	870	915	3.6	0.5	3.8	882	889	935	100	69.3	28.8	-	25.3	29.2	-	52.3	
1800	92	880	870	915	3.6	0.5	3.8	883	887	933	100	69.5	29	-	25.3	29.4	-	52.4	
1900	90	880	870	915	3.6	0.5	3.8	884	890	934	100	69.6	29	-	25.2	29.3	-	52.4	Gas and sponge sample were taken.

An example of a Run Report Sheet.

Experimental results for first series of runs with ore size 2.36 - 3.35 mm and average residence time of 220 mins.

(Code No. RP_1S_1)

Run No.	Table No. 1		Table No. 2		Table No. 3		
	Temp. (T^{o}_{C})	Reduction (%R)	Log %R	$10^4/TK^{o}$	Length of Hot Zone(cm)	Amount of ore in Hot Zone (grams)	Residence time (R.t) mins.
1	856.3	89.27	1.9507	8.855	54	394.7	236.8
2	829.0	85.45	1.9317	9.0744	51	372.7	223.6
3	809.6	81.66	1.9120	9.237	47.5	347.0	208.3
4	773.0	69.61	1.8426	9.5602	46	336.2	201.7
5	743.3	62.31	1.7945	9.8396	40.7	297.8	178.7
6	761.0	64.34	1.8084	9.6711	43.7	319.7	191.8
7	887.6	97.49	1.9889	8.6162	55.0	401.9	241.2
8	878.0	98.28	1.9924	8.688	52.5	383.7	230.2
9	899.3	98.67	1.9941	8.53	55.2	403.8	242.3
10	903.6	98.93	1.9953	8.499	56.5	414.99	249.0

Table 4. Continuation of experimental results for first series (CodeNo. RP_1S_1)

Run No.	% Fe Metallic	Metallization	%R by weight sponge out	%R by oxygen balance	$\frac{CO}{CO_2}$	$\frac{H_2}{H_2O}$	$\frac{CO + H_2}{CO_2 + H_2O}$
1	77.52	83.61	96.48	85.84	1.41	1.41	1.41
2	71.49	78.43	93.38	83.71	1.35	1.52	1.46
3	65.68	73.31	86.83	87.3	1.28	1.47	1.41
4	48.25	55.95	73.39	65.81	1.25	1.43	1.36
5	38.42	46.36	60.30	67.88	1.27	1.31	1.29
6	41.11	48.67	57.54	69.01	1.21	1.32	1.28
7	91.15	95.1	103.37	93.0	1.51	1.31	1.37
8	92.49	95.40	102.34	95.93	1.45	1.28	1.34
9	93.16	96.30	106.13	100.8	1.46	1.23	1.30
10	93.60	96.87	104.75	98.97	1.41	1.26	1.31

Table 5. The carbon content in the sponge iron for each run of first series (Code No. RP_1S_1)

Run No.	Temperature ^{o}C	% Carbon
5	743.3	0.678
6	761.0	0.540
4	773.0	0.561
3	809.6	0.666
2	829.0	0.636
1	856.3	0.426
8	878.0	0.165
7	887.6	0.168
9	889.3	0.204
10	903.6	0.138

Experimental results for second series of runs with ore size 3.35-4.75 mm and average residence time of 106.8 mins.

(Code No. RP_1S_2)

Run No.	Table No. 6		Table No. 7		Table No. 8		
	Temp. (To) c	Reduction (%R)	Log %R	$10^4/T_K o$	Length of Hot Zone (cm)	Amount of ore in Hot Zone (grams)	Residence Time (R.t) mins.
11	804.3	65.84	1.8184	9.2822	45.0	157.5	94.5
12	831	75.77	1.8795	9.0579	48.2	168.9	101.3
13	852	76.85	1.8856	8.8888	49.7	174.1	104.5
14	879.3	87.3	1.9410	8.6780	51.0	178.5	107.1
15	900.3	90.11	1.9547	8.5227	54.7	191.6	114.9
16	931	93.38	1.9702	8.3056	58.5	204.7	122.8
17	912	92.71	1.9671	8.4388	56.2	196.8	118.1
18	855.6	83.14	1.9198	8.8600	51.2	179.4	107.6
19	843	78.15	1.8929	8.9605	49.0	171.5	102.9
20	814	72.17	1.8583	9.1996	45.7	160.1	96.1
21	870	84.15	1.9250	8.7489	50.0	175.0	105

Table 9. Continuation of experimental results for second series (Code No. RP_1S_2)

Run No.	% Fe Metallic	Metallization	%R by weight sponge out	%R by oxygen balance	$\frac{CO}{CO_2}$	$\frac{H_2}{H_2O}$	$\frac{CO + H_2}{CO_2 + H_2O}$
11	43.12	51.60	67.74	64.89	1.49	1.348	1.3969
12	56.97	65.38	74.62	80.14	1.51	1.21	1.29
13	58.53	67.17	77.37	80.62	1.58	1.31	1.40
14	74.39	81.51	87.68	88.97	1.69	1.22	1.36
15	78.86	85.88	92.84	94.61	1.73	1.27	1.40
16	84.22	90.40	96.97	94.50	1.95	1.11	1.34
17	83.10	89.2	95.25	88.95	1.60	1.55	1.57
18	67.91	74.69	80.81	81.04	1.64	1.28	1.39
19	60.43	68.48	80.81	77.95	1.43	1.28	1.33
20	51.82	59.79	75.65	70.06	1.53	1.30	1.37
21	69.47	76.41	87.68	81.98	1.69	1.29	1.41

Table 10. The carbon and sulphur content in the sponge iron for each run of second series (Code No. RP_1S_2)

Run No.	Temp. ^{o}C	% Carbon	% Sulphur
11	804	0.515	0.0031
20	814	0.509	0.0020
12	831	0.377	0.0017
19	843	0.389	0.0020
13	852	0.371	0.0020
18	855	0.491	0.0017
21	870	0.545	0.0020
14	879	0.467	0.0013
15	900	0.431	0.0017
17	912	0.203	0.0010
16	931	0.197	0.0020

Table 11. The phosphorus content in the sponge iron for three different run temperatures of second series (Code No. RP_1S_2)

Run No.	Temp. ^{o}C	% Phosphorus
11	804	0.015
18	855	0.034
16	931	0.075

Experimental results for third series of runs with ore size 1.7-2.36 mm and average residence time of 163.9 mins.
(Code No. RP_1S_3)

Run No.	Table No. 12		Table No. 13		Table No. 14		
	Temp. (T_c)	Reduction (%R)	Log %R	$10^4/T_K$ o	Length of Hot Zone (cm)	Amount of ore in Hot Zone (grams)	Residence Time (R.t) mins.
22	831.33	86.16	1.9353	9.0552	50	283.8	170.3
23	855	88.71	1.9479	8.8652	51	289.5	173.7
24	867	92.16	1.9645	8.7719	54.5	309.4	185.6
25	805.6	77.46	1.8890	9.2712	45.2	256.8	154.0
26	756.66	64.41	1.8089	9.7119	40	227	136.2

Table 15. Continuation of the third series (Code No. RP_1S_3)

Run No.	% Fe Metallic	Metallization	%R by weight sponge out	%R by oxygen balance	$\frac{CO}{CO_2}$	$\frac{H_2}{H_2O}$	$\frac{CO + H_2}{CO_2 + H_2O}$
22	72.60	78.88	88.35	83.30	1.39	1.35	1.36
23	76.62	83.45	90.07	90.70	1.44	1.36	1.38
24	82.21	87.41	92.82	92.08	1.29	1.46	1.40
25	59.42	66.83	78.04	77.76	1.42	1.43	1.43
26	41.21	49.2	63.94	65.38	1.35	1.42	1.40

Experimental results for fourth series of runs with ore size 1.7-2.36 mm and average residence time of 227.7 mins.

(Code No. RP_1S_4)

Run No.	Table No. 16		Table No.17		Table No.18		
	Temp. (To) C	Reduction (%R)	Log %R	$10^4/T_K o$	Length of Hot Zone (cm)	Amount of ore in Hot Zone (grams)	Residence Time (R.t) mins.
27	756	68.80	1.8375	9.7181	44	347.5	208.5
28	777.3	75.61	1.8785	9.5210	44.75	353.4	212.0
29	806.3	82.10	1.9143	9.2652	48	379.0	227.5
30	831.3	90.24	1.9553	9.0552	50.75	400.8	240.5
31	855.3	94.46	1.9752	8.8626	52.75	416.6	250.0

Table 19. Continuation of the fourth series (Code No. RP_1S_4)

Run No.	% Fe Metallic	Metallization	%R by weight sponge out	%R by oxygen balance	$\frac{CO}{CO_2}$	$\frac{H_2}{H_2O}$	$\frac{CO + H_2}{CO_2 + H_2O}$
27	47.13	55.09	68.75	67.15	1.43	1.37	1.39
28	56.74	64.30	75.29	75.67	1.29	1.43	1.39
29	66.34	73.69	81.48	82.19	1.31	1.41	1.37
30	79.08	85.30	90.42	90.32	1.49	1.41	1.43
31	86.01	90.3	94.20	90.96	1.46	1.40	1.43

Experimental results for fifth series of runs with ore size 3.35-4.75 mm and average residence time of 290 mins.
(CodeNo. RP_1S_5)

Run No.	Table No. 20		Table No. 21		Table No. 22		
	Temp. (T_o)$_c$	Reduction (%R)	Log %R	$10^4/T_K o$	Length of Hot Zone (cm)	Amount of ore in Hot Zone (grams)	Residence Time (R.t) mins.
32	754.66	66.17	1.8206	9.7308	42	451.2	270.7
33	784.33	75.38	1.8772	9.4577	45	483.4	290.0
34	828.66	84.44	1.9265	9.0772	48	515.6	309.4

Table 23. Continuation of the fifth series (Code No. RP_1S_5)

Run No.	% Fe Metallic	Metallization	%R by weight sponge out	%R by oxygen balance	$\frac{CO}{CO_2}$	$\frac{H_2}{H_2O}$	$\frac{CO + H_2}{CO_2 + H_2O}$
32	43.56	51.45	64.63	66.71	1.28	1.42	1.37
33	56.40	64.41	72.19	75.88	1.36	1.35	1.35
34	69.92	77.09	86.98	83.04	1.59	1.24	1.34

Experimental results for sixth series of runs with ore size 3.35-4.75 mm and average residence time of 201 mins.
(Code No. RP_1S_6)

Run No.	Table No. 24		Table No.25		Table No. 26		
	Temp. (T_o) °C	Reduction (%R)	Log %R	$10^4/T_K^o$	Length of Hot Zone (cm)	Amount of ore in Hot Zone (grams)	Residence Time (R.t) mins.
35	761.6	62.81	1.7980	9.6655	38.5	310.4	186.2
36	792.3	70.21	1.8463	9.3870	40.5	326.5	195.9
37	831.3	80.55	1.9060	9.0552	46.25	372.8	223.7

Table 27. Continuation of the sixth series (Code No. RP_1S_6)

Run No.	% Fe Metallic	Metallization	%R by weight sponge out	%R by oxygen balance	$\frac{CO}{CO_2}$	$\frac{H_2}{H_2O}$	$\frac{CO + H_2}{CO_2 + H_2O}$
35	39.09	47.16	64.28	63.87	1.34	1.52	1.45
36	49.03	56.57	70.47	71.50	1.32	1.47	1.42
37	64.0	71.26	81.47	80.02	1.44	1.34	1.37

Table 28. The data and equations show the relationship between percentage reduction and temperature at (^{o}C), for all series of experiments with chokes in position.

Series Code No.	Data Equation No.	Particle size mm	Temperature range ^{o}C	% R = a T^{o}C - b		r^2
				a	b	
RP_1S_2	19	3.35 - 4.75	804 - 931	0.234	119.4	0.955
RP_1S_3	21	1.7 - 2.36	756 - 867	0.251	124.97	0.984
RP_1S_4	23	1.7 - 2.36	756 - 855	0.260	127.71	0.992
RP_1S_5	25	3.35 - 4.75	754 - 828	0.243	116.90	0.985
RP_1S_6	27	3.35 - 4.75	761 - 831	0.255	131.45	0.999

Table 29. The data and equations show the relationship between logarithm of percentage reduction and a function of temperature at K^o for all series of experiments with chokes in position.

Series Code No.	Data Equation No.	Particle size mm	Temperature range ^oC	$\log \%R = -a(\frac{10^4}{T_{K^o}}) + b$		r^2
				a	b	
RP_1S_2	20	3.35 - 4.75	804 - 931	0.1630	3.349	0.977
RP_1S_3	22	1.7 - 2.36	756 - 867	0.1657	3.423	0.983
RP_1S_4	24	1.7 - 2.36	756 - 855	0.1618	3.415	0.991
RP_1S_5	26	3.35 - 4.75	754 - 828	0.1599	3.382	0.981
RP_1S_6	28	3.35 - 4.75	761 - 831	0.1770	3.509	0.999

Table 30. Data and residence time calculation for the different run series of experiments with chokes in position.

Series Code No.	The last run No. in the series	The amount of reduced ore in the heating length of the kiln (choke to choke) grams	Length of the kiln (choke to choke) cm	Residence time for the last run minutes	Average residence time for all the runs in a series minutes
RP_1S_2	21	252.2	89.5	105	106.8
RP_1S_3	26	427.9	89.5	136.0	163.9
RP_1S_4	31	526.7	85	249.9	227.7
RP_1S_5	34	690	80	309	290
RP_1S_6	37	522.5	80	223.7	201.9

Data to indicate the relationship between % reduction and average particle sizes at the identified temperatures.

Table No. 31

Temp (°C)	Average Size (mm)	Reduction (%)
830	2.03	88.67
830	2.855	84.79
830	4.05	80.03

Table No. 32

Temp (°C)	Average Size (mm)	Reduction (%)
800	2.03	80.85
800	2.855	76.79
800	4.05	72.39

Table No. 33

Temp (°C)	Average Size (mm)	Reduction (%)
770	2.03	73.03
770	2.855	68.78
770	4.05	64.74

Data to indicate the relationship between % reduction and logarithm of average particle volume, at the identified temperatures.

Table No. 34

Temp (°C)	Ln(volume) cm^3	Reduction (%)
830	- 4.9547	88.67
830	- 4.1799	84.79
830	- 3.2322	80.03

Table No. 35

Temp (°C)	Ln (volume) cm^3	Reduction (%)
800	- 4.9547	80.85
800	- 4.1799	76.79
800	- 3.2322	72.39

Table No. 36

Temp (°C)	Ln (volume) cm^3	Reduction (%)
770	- 4.9547	73.03
770	- 4.1799	68.78
770	- 3.2322	64.74

Table No. 37 Data taken to show the relationship between % reduction and residence time.

Run No.	Temperature ^{o}C	Residence time (Minutes)	Reduction (%)
24	831	101.3	75.77
69	831.3	223.7	80.55
64	828.6	309.4	84.44

Table No. 38. Hydrocarbons (H.C.) Analysis in Off Gases by Chromotography

Temperature (^{o}C) / % H.C $_{(Co-H_2 basis)}$	746	800	851	876	902	917	930
CH_4	3.278	3.264	3.224	3.104	2.845	3.178	3.189
C_2H_6	4.1	3.362	1.751	0.702	0.229	0.1344	0.0654
C_3H_8	0.436	0.0214	0.0044	0.0012	0.0002	0.0001	-
C_4H_{10}	0.202	0.0106	0.0018	0.0004	-	-	-
Total H.C. (basis CH_4)	17.64	12.34	9.01	6.48	4.29	4.46	3.98

Series VII (RP_2S_7)

Table 39

Ore Size 3.35 - 4.75 mm

Average residence time 92 minutes

Run No.	Temp. °C	% Reduction by Analysis	% Reduction by weight sponge out	% Reduction by oxygen balance	$\frac{H_2}{H_2O}$	$\frac{CO}{CO_2}$	$\frac{CO + H_2}{CO_2 + H_2O}$
38	900	90.66	92.82	90.50	1.88	2.33	2.03

Series VII (Contd.)

Table 40

Distance of the sample from the sponge exit end	Run Sample	10	20	30	40	50	60	70	80	90	100	110
Temperature ^{o}C	-	360	591	777	875	897	900	898	904	869	740	385
% Total Iron	93.83	92.49	93.16	92.71	93.60	90.70	83.77	79.31	76.18	72.83	73.05	70.15
% Metallic Iron	79.75	77.52	77.52	76.18	78.41	67.47	38.20	21.22	8.71	2.90	0.894	0.670
% Metallization	84.99	83.81	83.21	82.17	83.77	74.38	45.60	26.75	11.44	3.98	1.22	0.955
% Carbon	0.128	0.137	0.160	0.096	0.032	0.006	0.006	0.019	0.013	0.013	0.013	0.038
% Sulphur Analysed	0.003	0.0023	0.003	0.003	0.0017	0.0017	0.0017	0.003	0.0023	0.0035	0.003	0.0041
Zero Sulphur lost	0.0125	0.0123	0.0124	0.0124	0.0125	0.0121	0.0111	0.0106	0.0101	0.0097	0.0097	0.0093
Difference & Sulphur Removal	0.0095	0.01	0.0094	0.0094	0.0108	0.0104	0.1093	0.0076	0.0078	0.0062	0.0067	0.0052

Series VII (Contd.)

Table 41

Distance of sample from sponge exit end	Analysed	Assuming zero phosphorus removal	Difference & Phosphorus removal	% Total Iron
Run sample	0.062	0.097	0.035	93.83
40	0.058	0.0970	0.039	93.60
60	0.055	0.0868	0.031	83.77
90	0.058	0.075	0.017	72.83

Tables 42, 43, 44.

Series VIII (RP_2S_8)
Ore Size 3.35 - 4.75 mm
Average residence time 97 minutes.

Run No.	Table No. 42			Table No. 43		Table No. 44		
	Temp(T°C)	Reduction (%R)	% Carbon	Log % R	$10^4/T_{KO}$	Length of hot zone (cm)	Amount of ore in hot zone (grams)	Residence Time (R.t) mins.
39	752	61.79	0.3403	1.7909	9.756	42	137.5	82.5
40	819	79.87	0.2761	1.9024	9.157	48.5	158.8	95.3
41	820	81.81	0.2632	1.9128	9.149	48.5	158.8	95.3
42	845	88.01	0.1926	1.9445	8.944	49.5	162.1	97.3
43	870	94.06	0.1413	1.9734	8.749	51	167.0	100.2
44	872	93.38	0.1733	1.9702	8.734	51	167.0	100.2
45	899	95.26	0.1605	1.9789	8.532	53.5	175.2	105.0
46	902	97.36	0.1156	1.9884	8.511	53.5	175.2	105.0

Series VIII (Contd.)

Table 45

Run No.	%Fe Metallic	Metallization	%R by weight sponge out	%R by oxygen balance	$\frac{CO}{CO_2}$	$\frac{H_2}{H_2O}$	$\frac{CO + H_2}{CO_2 + H_2O}$
39	37.75	44.95	63.60	65.40	1.98	1.79	1.86
40	62.99	70.68	80.79	80.19	1.98	1.96	1.97
41	65.90	73.20	82.51	81.99	2.36	1.66	1.88
42	75.50	81.05	89.38	89.39	2.55	1.74	1.98
43	85.34	90.30	94.54	95.49	2.21	1.70	1.86
44	84.22	88.50	94.54	93.88	2.36	1.75	1.94
45	87.35	92.0	92.82	96.06	2.05	1.74	1.84
46	90.92	95.54	97.98	97.57	2.25	1.70	1.87

Table 46. The measured total pore volume by the mercury penetration porosimeter for run series (RP_2S_8).

Run No.	Temp. °C	% Reduction	% Total Iron	% Metallic Iron	V_1 Calculated total vol. of sponge iron assuming zero pore content c.c./grm.	V_2 Measured total pore volume c.c./grm.	V_t Overall vol. of sponge iron ($V_t = V_1 + V_2$) c.c./grm.	% Swelling
45	899	95.26	95.16	87.35	0.1346	0.115	0.2496	14.67
44	872	93.38	94.94	84.22	0.1397	0.113	0.2527	15.87
42	845	88.01	93.15	75.50	0.1503	0.111	0.2613	19.26
40	819	79.87	88.91	62.99	0.1603	0.116	0.2763	25.64

Table 47

Series IX (RP_2S_9)

Ore size 3.35 - 4.75 mm
Average residence time 103 minutes

Run No.	Temp. °C	% Reduction	% Carbon	% Hydrocarbon in off gases	Input Gases							Overall H_2/CO	Reducing Capacity Mole/h
					H_2Mole/h	CO_2Mole/h	C_4H_{10}Mole/h	Reforming		Cracking		Total			
								H_2Mole/h	CO Mole/h	H_2Mole/h	Carbon grms.	H_2mole/h	CO mole/h		
47	867	92.57	7.004	1.6	2.550	0.2886	0.2451	0.3607	0.5772	0.8647	8.373	3.683	0.5770	6.383	1.38
48	867	94.59	2.202	1.51	2.550	0.5169	0.2451	0.6460	1.0336	0.5795	5.562	3.775	1.0336	3.652	1.55
49	867	94.86	1.002	2.30	2.449	0.7431	0.2434	0.9285	1.4856	0.2885	2.766	3.665	1.4856	2.467	1.63
50	867	94.72	0.1605	1.05	2.448	1.033	0.2434	1.2560	2.0096	-	-	3.761	2.0096	1.871	1.78
43	870	94.06	0.1413	2.0	2.505	0.9371	0.2512	1.2170	1.9472	-	-	3.665	1.9472	1.882	1.84

Series IX (Contd.)

Table 48

Run No.	%Fe Metallic	Metallization	%R by weight sponge out	%R by oxygen balance	$\frac{CO}{CO_2}$	$\frac{H_2}{H_2O}$	$\frac{CO + H_2}{CO_2 + H_2O}$
47	82.88	87.70	89.38	95.47	1.87	1.39	1.45
48	86.23	90.61	96.26	94.58	2.81	1.98	2.16
49	86.68	91.08	97.98	94.98	2.31	1.99	2.08
50	86.45	90.84	96.26	91.80	2.30	1.91	2.04
43	85.34	90.30	94.54	95.49	2.21	1.70	1.86

Table 49

Series X (RP_2S_{10})

Ore Size 3.35 - 4.75 mm
Average residence time 99 minutes

Run No.	Temp. °C	% Reduction	Reducing capacity Mole/h	% Carbon	Input Gases			Overall H_2/CO after reforming
					H_2 Mole/h	CO_2Mole/H	C_4H_{10}Mole/H	
51	874	78.07	1.454	0.2247	1.403	0.9286	0.2457	1.338
52	874	84.74	1.576	0.2247	1.768	0.9281	0.2457	1.524
53	875	86.03	1.576	0.2439	1.753	0.9280	0.2466	1.513
54	875	88.99	1.675	0.1733	2.063	0.9259	0.2466	1.670
44	872	93.38	1.786	0.1733	2.471	0.9223	0.2447	1.887
43	870	94.06	1.837	0.1413	2.505	0.9370	0.2512	1.871

Series X (Contd.)

Table 50

Run No.	%Fe Metallic	Metallization	%R by weight sponge out	%R by oxygen balance	$\frac{CO}{CO_2}$	$\frac{H_2}{H_2O}$	$\frac{CO + H_2}{CO_2 + H_2O}$
51	60.32	67.68	84.23	77.62	2.03	1.89	1.95
52	70.37	76.46	85.94	84.72	1.89	1.77	1.82
53	72.38	78.64	87.66	87.95	1.85	1.74	1.78
54	77.07	83.13	89.38	93.43	1.83	1.70	1.75
44	84.22	88.50	94.54	93.88	2.36	1.75	1.93
43	85.33	90.30	94.54	95.49	2.21	1.70	1.86

Table 51

Series XI (RP_2S_{11})

Ore Size 3.35 - 4.75 mm
Average residence time 97 minutes

Run No.	Input gases (Mole/h)			After reforming		Reducing Capacity	$\frac{CO}{CO_2}$	$\frac{H_2}{H_2O}$	$\frac{CO + H_2}{CO_2 + H_2O}$
	C_4H_{10}	CO_2	H_2	% CO	% H_2				
55	0.2588	0.9319	2.475	35.45	64.54	1.867	2.33	2.22	2.26
56	0.2565	0.9063	2.435	35.56	64.43	1.869	2.21	1.94	2.03
57	0.2043	0.7696	2.995	28.92	71.07	1.783	2.29	1.75	1.89
58	0.2022	0.7611	2.917	29.16	70.83	1.750	1.98	1.82	1.87
59	0.1507	0.5699	3.753	21.10	78.89	1.798	1.82	1.83	1.83
60	0.1021	0.3825	4.554	13.88	86.11	1.834	2.86	1.91	2.0
61	zero	-	5.802	-	100%	1.934	-	2.09	-

Series XI (Contd.)

Table 52

Run No.	Temp. °C	% Metallic Iron	% Metallisation	% Reduction by Analysis	% Reduction by weight sponge out	% Reduction by oxygen balance	% Carbon
55	849	78.19	82.74	89.69	89.38	89.24	0.1862
56	849	78.41	83.76	89.83	92.82	91.96	0.1926
57	849	81.76	87.76	91.89	91.10	93.66	0.192
58	849	80.87	86.80	91.34	91.10	92.81	0.1764
59	849	83.10	88.14	92.71	92.82	92.86	0.2724
60	849	85.11	89.64	93.92	94.54	94.89	0.2712
61	849	88.46	91.87	95.91	96.26	96.15	-

Table 53

Series XII (RP_2S_{12})

Ore size 4.75 - 6.70 mm
Average residence time 63 minutes

Run No.	Input gases (Mole/h)			After reforming		Reducing Capacity	$\frac{CO}{CO_2}$	$\frac{H_2}{H_2O}$	$\frac{CO + H_2}{CO_2 + H_2O}$
	C_4H_{10}	CO_2	H_2	% CO	% H_2				
62	0.3620	1.366	2.560	39.85	60.14	2.290	2.76	2.65	2.69
63	0.2407	0.9155	3.986	27.06	72.93	2.225	3.68	2.07	2.39
64	0.1265	0.4527	5.567	14.03	85.96	2.251	6.63	2.20	2.45
65	Zero	-	5.786	-	100	1.928	-	2.48	-

Series XII (Contd.)

Table 54

Run No.	Temperature °C	% Metallic Iron	% Metallization	% Reduction by Analysis	% Reduction by weight sponge out	% Reduction by oxygen balance	% Carbon
62	900	81.76	86.52	92.09	90.41	91.12	0.2547
63	900	91.59	93.81	97.98	96.26	98.15	0.1860
64	900	92.26	95.16	98.37	96.26	101.12	0.1920
65	900	93.38	96.31	99.02	92.82	97.91	-

Table 55. The data which were taken to find the residence time for the different run series of experiments without chokes in position.

The end term of residence time measurement Code No.	The last run No. in the term.	The amount of reduced ore in the heating length of the kiln. grams	The heating length of the kiln. cm	The length of the hot zone. cm	The amount of unreduced ore in the hot zone. grams	Residence time minutes
RP_2T_1RT	38 (Just one Run in series RP_2S_7)	206.7	90	53.0	153.8	92.0
RP_2T_2RT	61	230.5	90	49.5	162.1	97.0
RP_2T_3RT	65	134.9	90	54.5	105.2	63.0

Table 56. The average residence time for the series of experiments without chokes in position.

Series Code No.	Average hot zone length cm.	The amount of unreduced ore in the hot zone grams	Average residence time for the series minutes
RP_2S_8	49.68	162.7	97.00
RP_2S_9	52.5	171.9	103.00
RP_2S_{10}	50.5	165.4	99.00
RP_2S_{11}	49.5	162.0	97.00
RP_2S_{12}	54.5	105.2	63.0

Table 57. The relationship between percentage reduction and the variable factor for each series of runs.

Series No.	Temperature °C	Particle Size mm	Equations		
			No.	The relationship between paired values of the variables.	r^2
VIII RP_2S_8	752 - 902	3.35 - 4.75	36	$\%R = 0.2683(T_{^oC}) - 139.45$	0.994
			37	$\text{Log}\%R = -0.1556(\frac{10^4}{T_{K^o}}) + 3.325$	0.962
XI RP_2S_{11}	849	3.35 - 4.75	38	$\%R = -23.79\ V_{C_4H_{10}} + 96.17$	0.978
			39	$\%R = 0.170\ (\%H_2) + 79.169$	0.972
XII RP_2S_{12}	900	4.75 - 6.7	40	$\%R = -17.62\ V_{C_4H_{10}} + 100.07$	0.722
			41	$\%R = 0.158(\%H_2) + 84.260$	0.710

Table 58. Distribution of the amount (grams) of inventory along the kiln length at 10 cm. interval.

Series Code No.	Cooling Zone		Reducing Zone								← Ore Inlet
	0 - 10	10 - 20	20 - 30	30 - 40	40 - 50	50 - 60	60 - 70	70 - 80	80 - 90	90 - 100	100 - 110
RP_1S_2	In choke 21.5		67.5	49	40.7	30	22	14	11	10	8
RP_2S_{8-11}	8	10.7	12.5	18	20	24	23	28	32	33	40
RP_2S_7	9	13.5	14	18	17	20.7	24.5	24	29	32	27.5

Table 59.

Brazilian Iron Ore Analysis
Mainly Hematite, loss on ignition 2%
Fe = 67 to 68% (FeO - 1.3%)
SiO_2 = 1%
Al_2O_3 = 1.3%
P = 0.06 to 0.08%
S = 0.009%

Table 60. Data to show the thermodynamic equilibrium for sulphur removal in comparison with the amount in the sponge.

Run No.	Temp. in K^o	ΔG^o in J	H_2 mole/hour	H_2s mole/hour	Equilibrium Constant K	S, removal at equilib. grams/h	%S content in sponge	
							Assuming zero sulphur loss	Analysed
11	1077	56281.2	1.5863	0.00294	0.00186	0.09421	0.01113	0.0031
20	1087	55842.7	1.6348	0.00338	0.00207	0.1083	0.01139	0.0020
12	1104	56215.9	1.6791	0.00366	0.00219	0.1172	0.01154	0.0017
19	1116	56188.4	1.6718	0.00393	0.00235	0.1257	0.01165	0.0020
13	1125	56167.9	1.6688	0.0041	0.00247	0.13135	0.01159	0.0020
18	1128.6	56159.9	1.4504	0.00367	0.00252	0.1174	0.01187	0.0017
21	1143	56129	1.6761	0.00456	0.00272	0.1461	0.01192	0.0020
14	1152.3	56109.8	1.7172	0.00490	0.00286	0.1568	0.01206	0.0013
15	1173.3	56067.6	1.8566	0.00593	0.00319	0.1899	0.01220	0.0017
17	1185	55822.6	1.8808	0.0065	0.00346	0.2083	0.01232	0.0010
16	1204	55773.7	1.6464	0.0062	0.00381	0.1994	0.01235	0.0020

Table 61. Data to show the thermodynamic equilibrium for phosphorus removal in comparison with the amount in the sponge.

Run No.	Temp. (^{o}K)	Hydrogen Moles per hour	Equilibrium Constant of formation of PH (K')	Phosphorus removal per hour at equilibrium grms/h.	%Phos. Content in Sponge	
					Assuming zero Phos. loss.	Analysed
11	1077	1.5863	0.00248	0.1215	0.0865	0.015
18	1128.6	1.4504	0.00217	0.09765	0.0923	0.034
16	1204	1.6464	0.00178	0.0908	0.0961	0.075

Table 62.

The Results which were taken to calculate the equation ($\frac{\Delta P}{Qm}$ = 0.10604Qo + 0.07339)								
Run No.	Time Second	ΔP actual mm H_9	P_2 P_M + P atm.	P_1 P_2 + ΔP actual	Qm cc/sec	Qo = x cc/sec	$\Delta P/_{Qm}$ = Y	ΔP_{cm}
1	125.2	1.1355	18.4147 + 757.15 = 775.56	776.70	7.5465	7.084	0.82157	6.2
2	101.8	1.6849	775.56	777.249	9.2789	8.7133	0.99149	9.2
3	91.3	2.1062	775.56	777.670	10.3433	9.7154	1.11183	11.5
4	76.4	2.9670	775.56	778.531	12.3537	11.6102	1.31134	16.2
5	70.5	3.4615	775.56	779.026	13.3833	12.5818	1.4122	18.9
6	66.1	3.8827	775.56	779.447	14.2703	13.4193	1.4856	21.2

Table 05

Gaseous Condition in Run No. 10 Series: First Case Ore Sized: 2.36-3.35mm Date: 15.2.79

IN					OUT							
Comp.	Grm. Moles/ Hour	C Grm. Atoms/ Hour	H Grm. Atoms/ Hour	O Grm. Atoms/ Hour	Comp.	Meas. Grm./ Moles/ Hour	Conversion H.C.	Conversion C	C Grm. Atoms/ Hour	H Grm. Atoms/ Hour	O Grm. Atoms/ Hour	Notes
H_2	2.4549	-	4.9098	-	H_2O	1.42		1.42		2.84	1.42	CO/CO_2 = 1.4066
CO_2	0.9251	0.9251	-	1.8502	CO_2	0.6529		0.6529	0.6529		1.3058	
C_4H_{10}	0.2225	0.890	2.225	-	CH_4	3.0135	0.3013	0.3013	0.3013	1.2052		H_2/H_2O = 1.2632
					CO		2.7122	0.9184	0.9184		0.9184	
					H_2			1.7938		3.5876		$\frac{CO + H_2}{CO_2 + H_2O}$ = 1.308
C_3H_8	0.02473	0.07419	0.19784	-	C	0.0166		0.0166	0.0166			
					Loss	-		-				%R Oxygen Balance = 98.68
TOTAL	3.6272	1.8892	7.3326	1.8502	Total	5.103		5.103	1.8892	7.6328	3.6442	%R Analysis = 98.92

Differences Between Inlet and Outlet

C Grm.Atoms/Hour	H Grm.Atoms/Hour	O Grm.Atoms/Hour
0	+ 0.3002	1.794

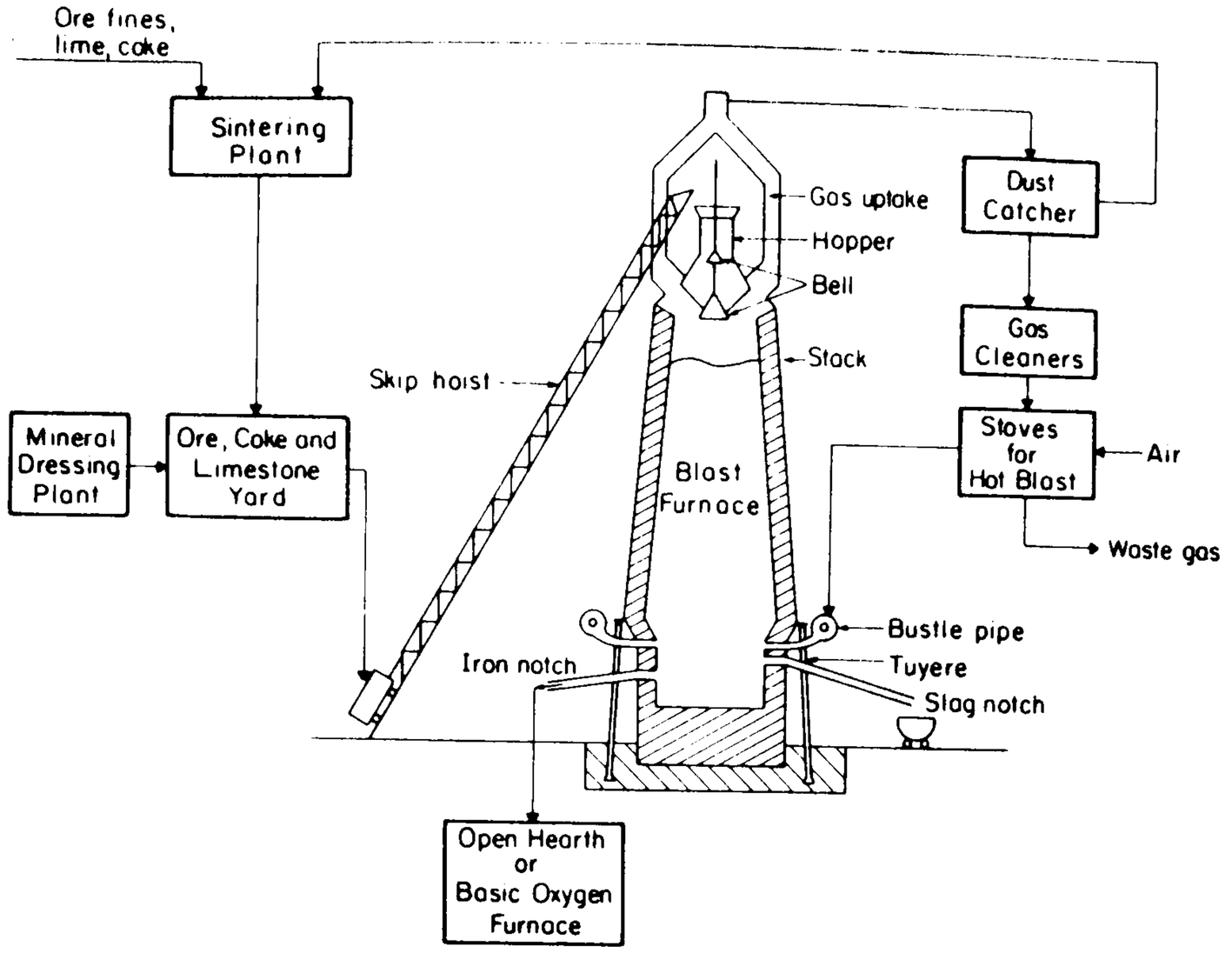

Fig. 1. Schematic diagram of an iron blast furnace and associated plant.

Elred

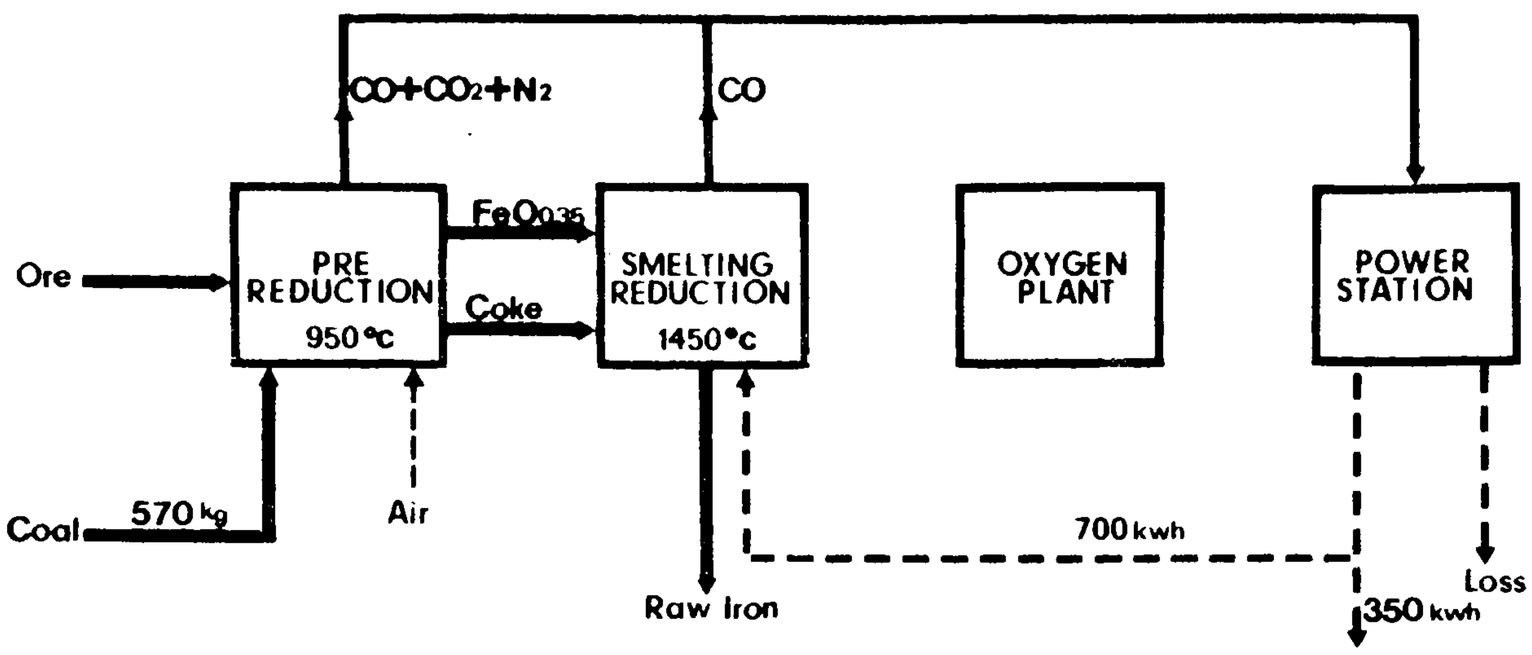

Inred

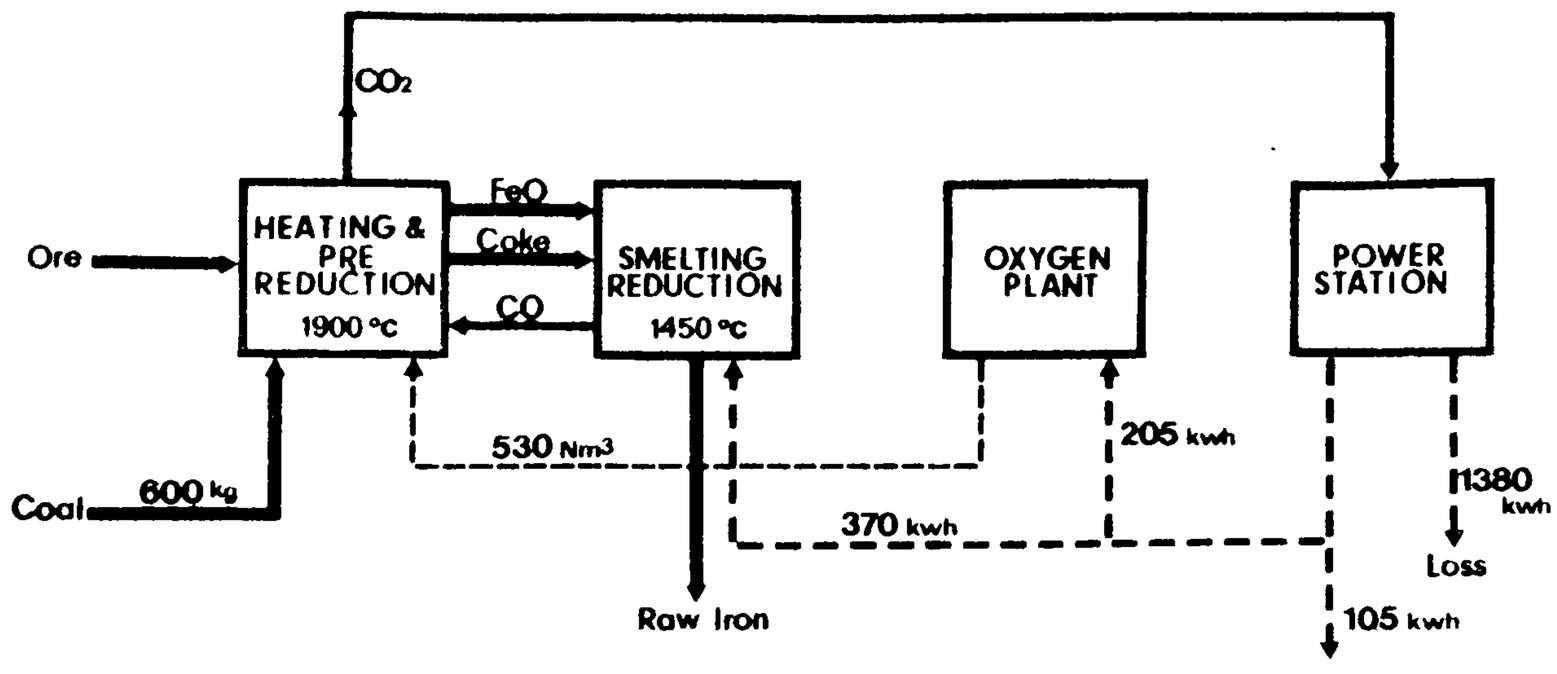

Plasmamelt

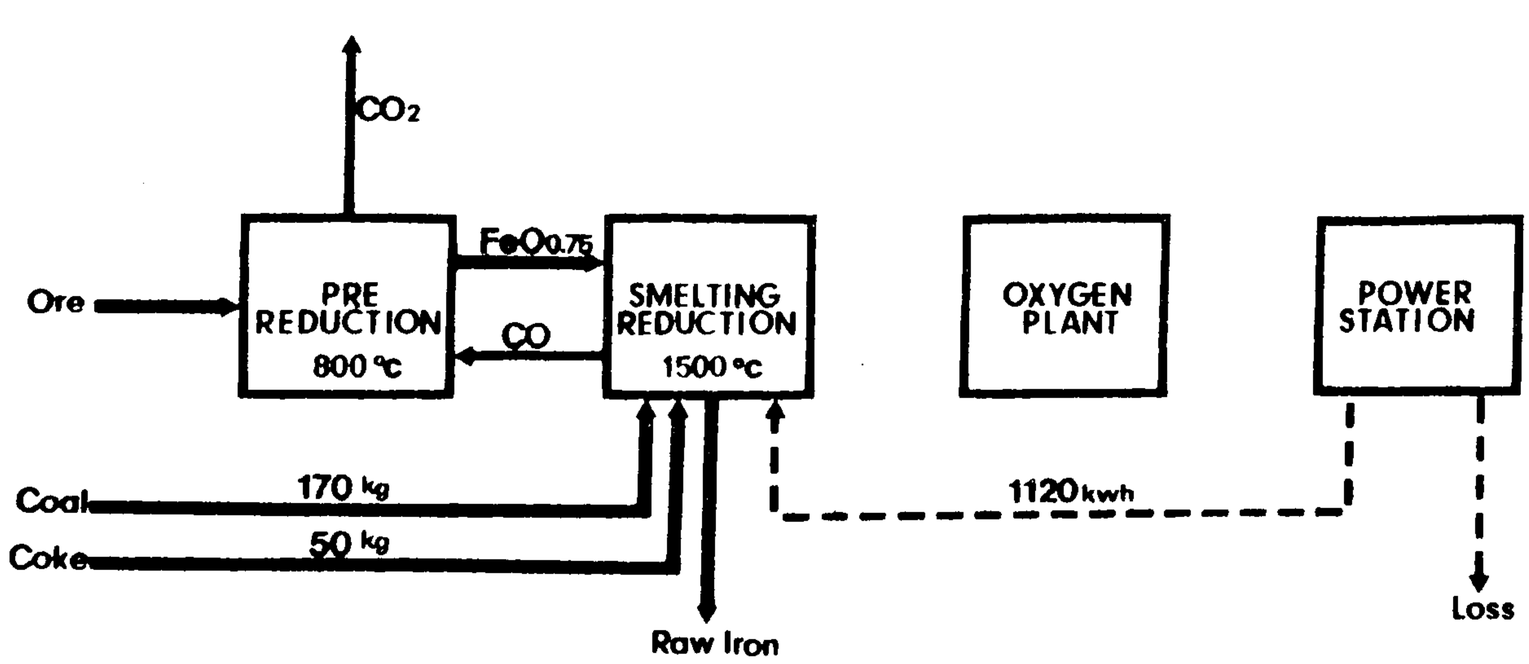

Fig. 2. The principle of the Elred, Inred, plasmamelt systems.

Fig. 3. **Flowsheet for the Batch-Type HYL Process**

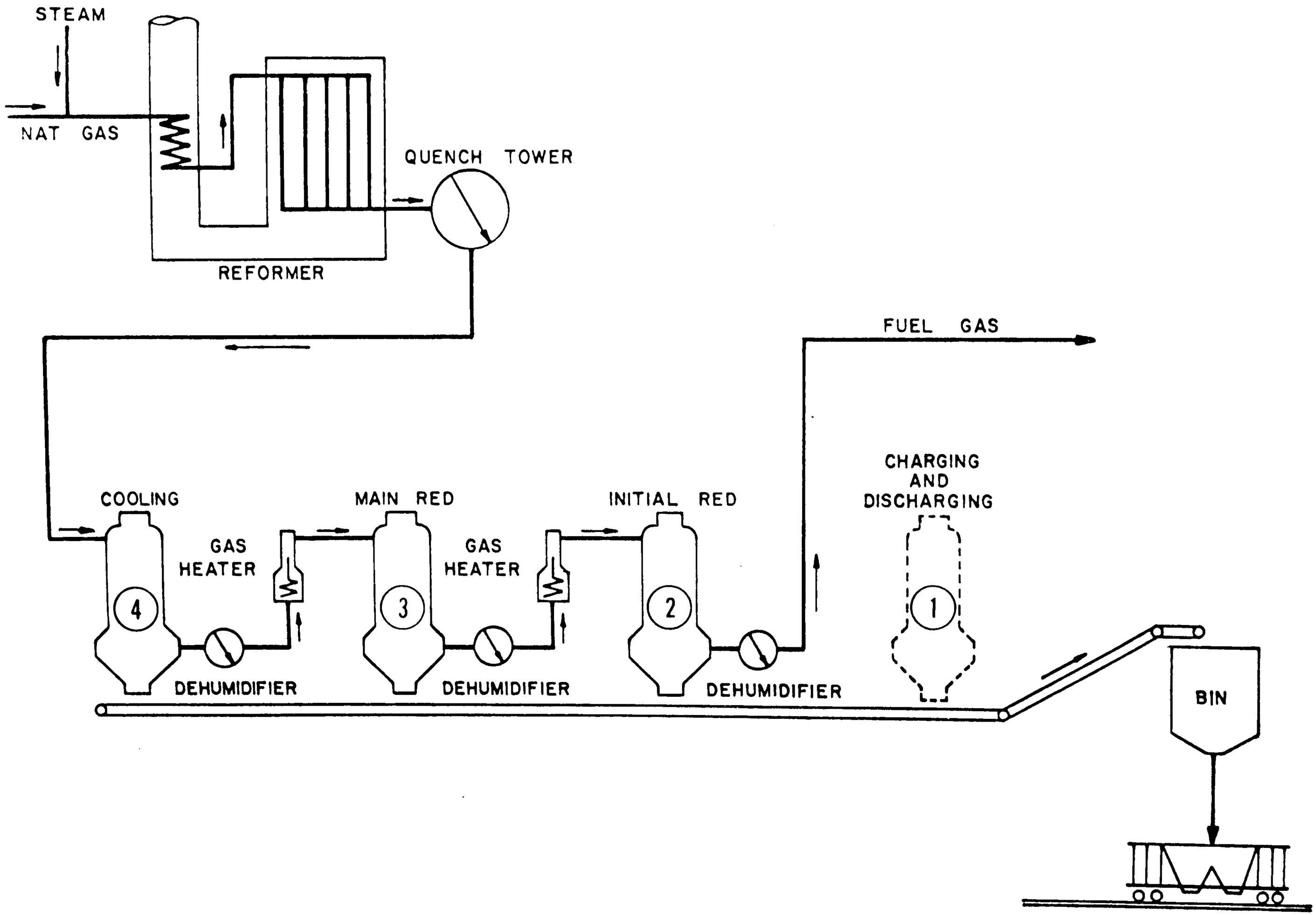

Fig. 4. **Standard Flowsheet for the Midrex Process**

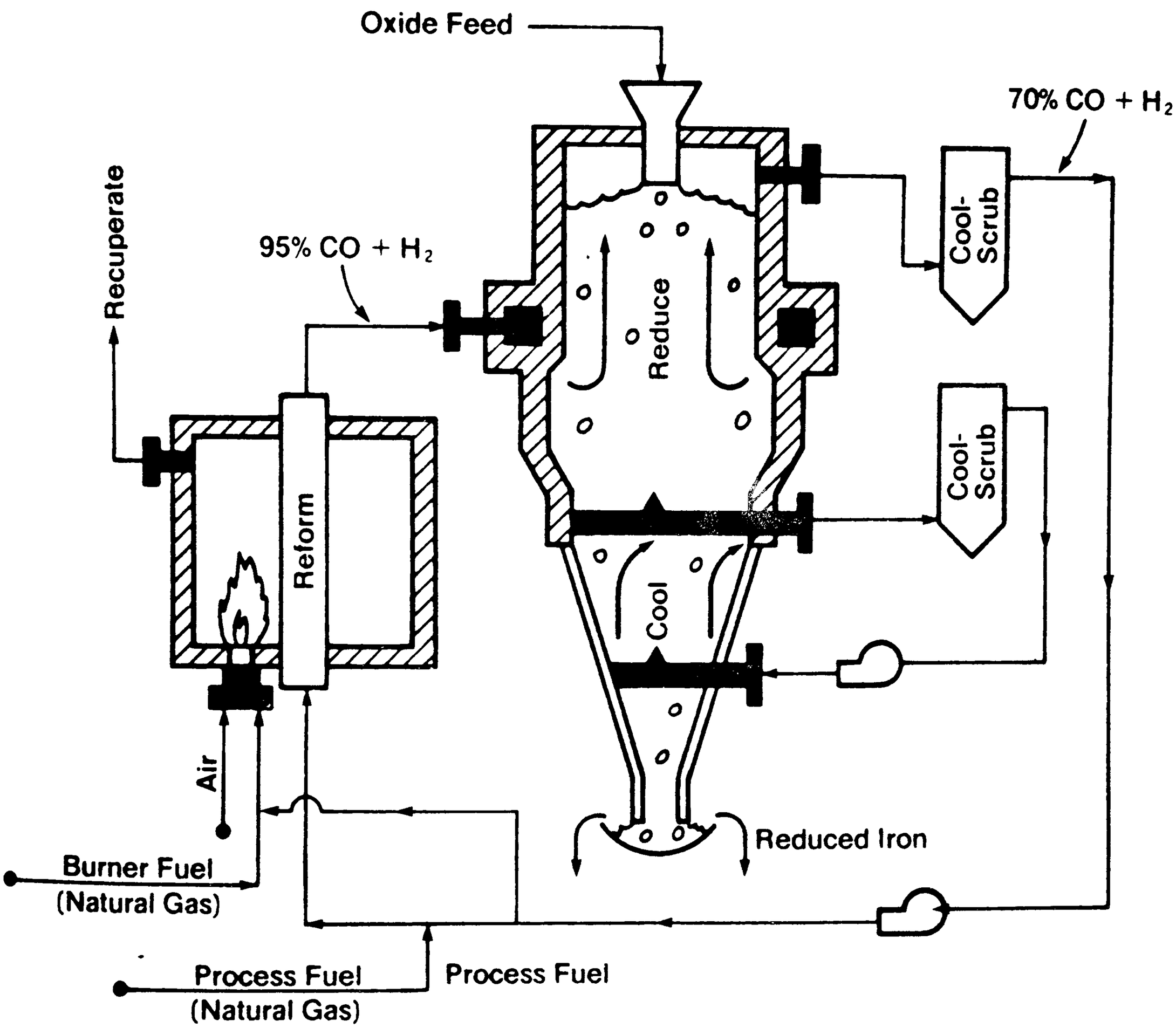

Fig. 5. The Midrex EDR Process Flowsheet With Export Fuel Gas Option

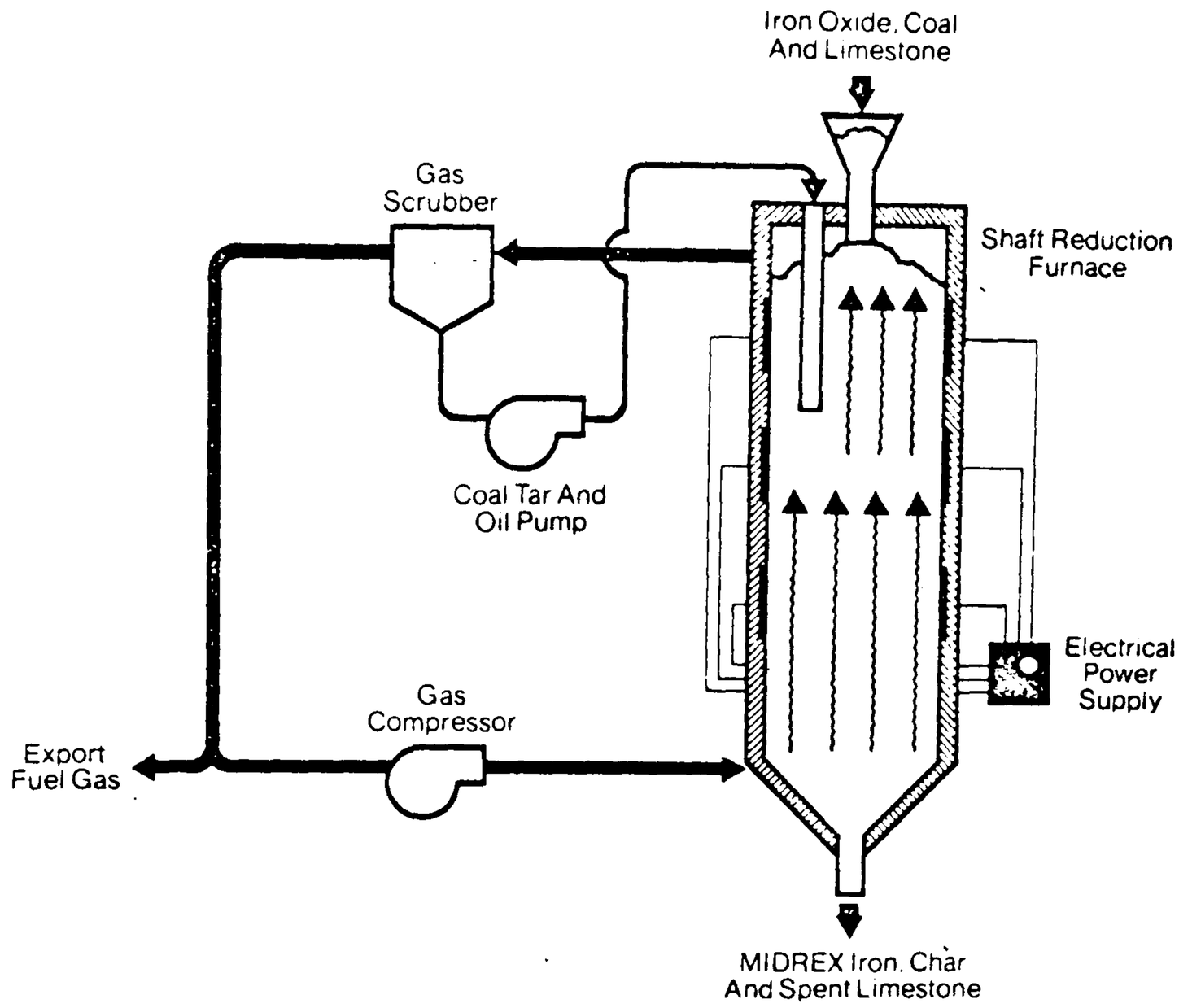

Fig. 6. Flowsheet for the Armco Process

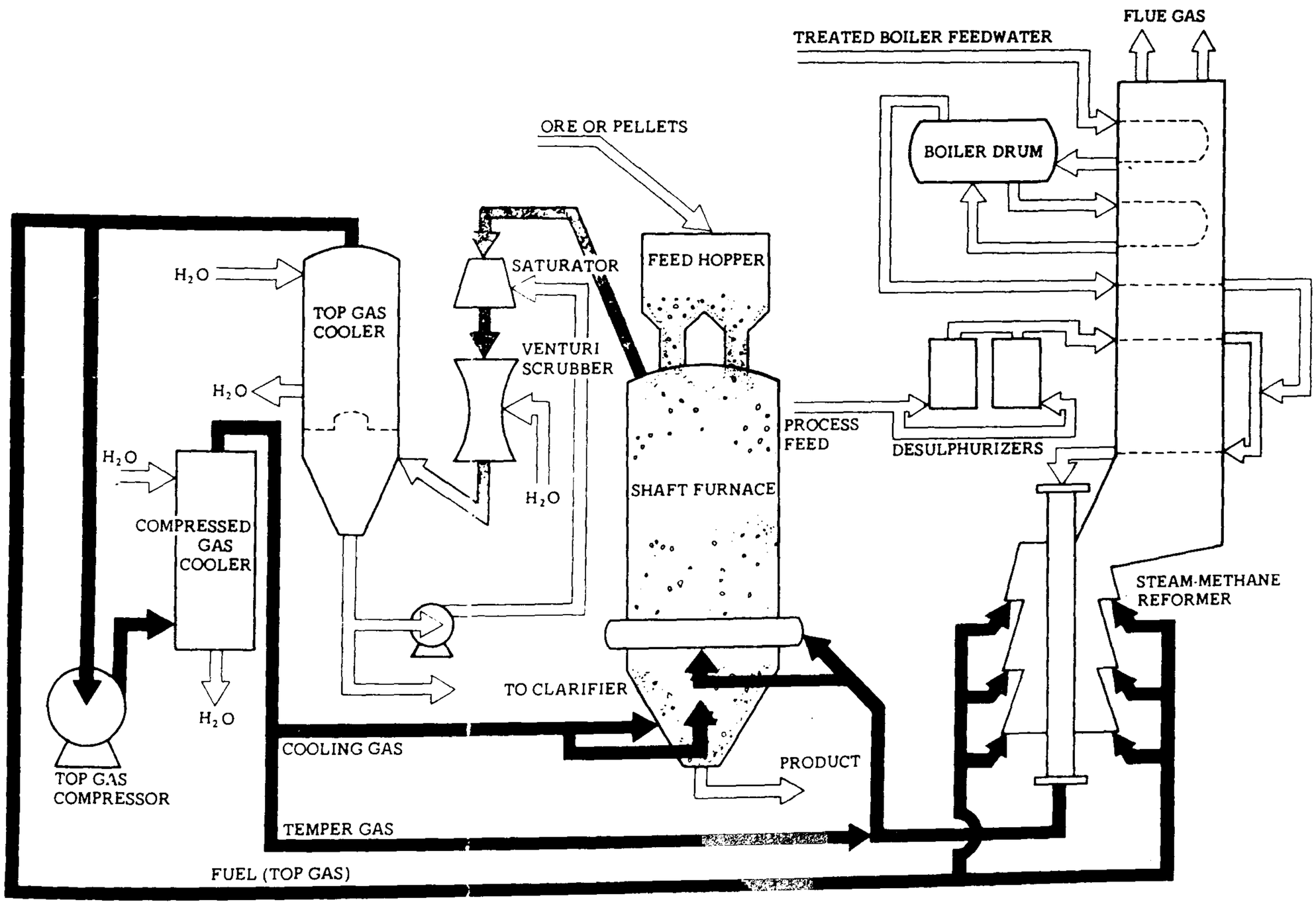

Fig. 7. **Flowsheet for the Continuous HYL III Process**

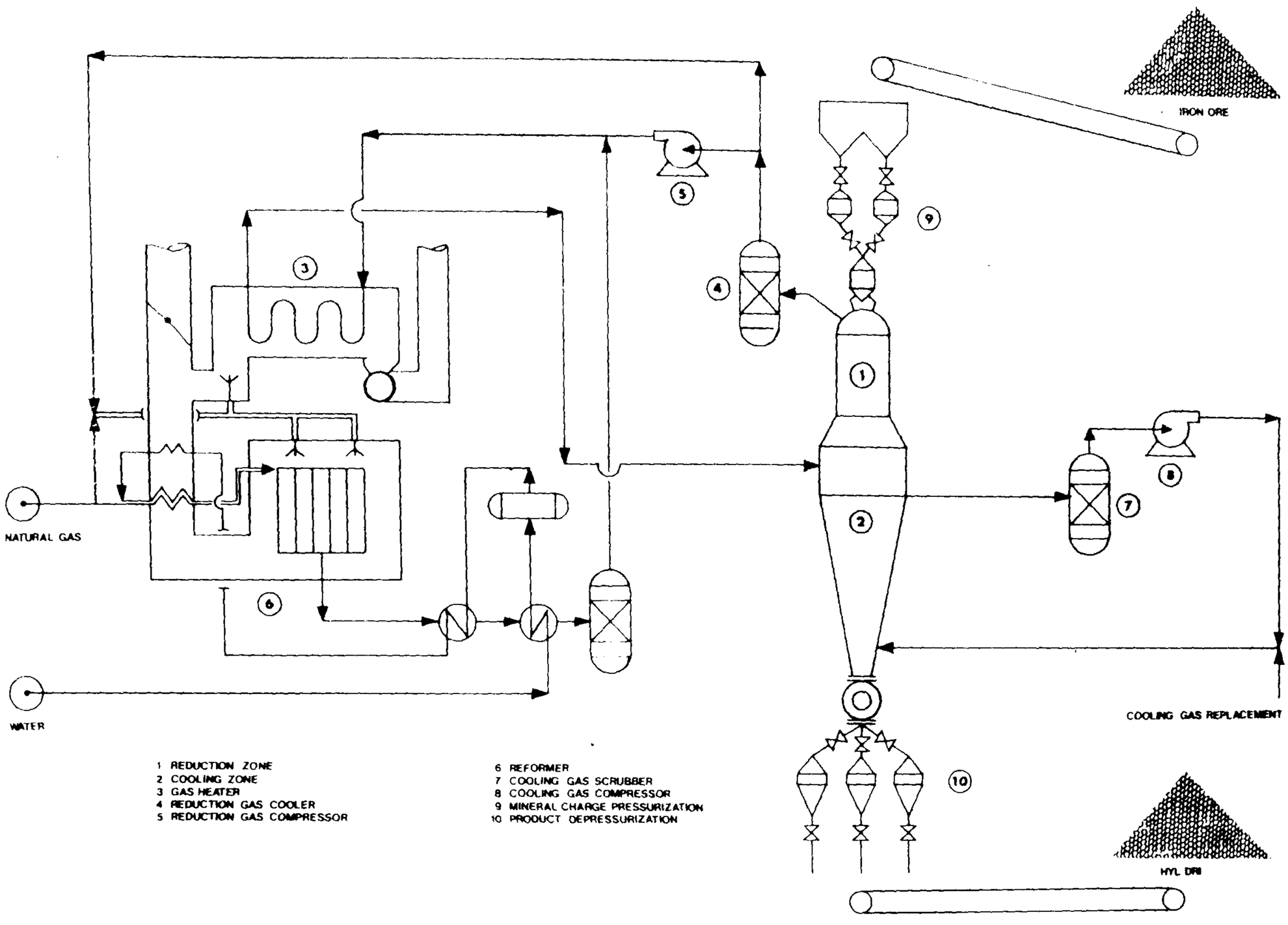

Fig. 8. **SL/RN DR process flowsheet**

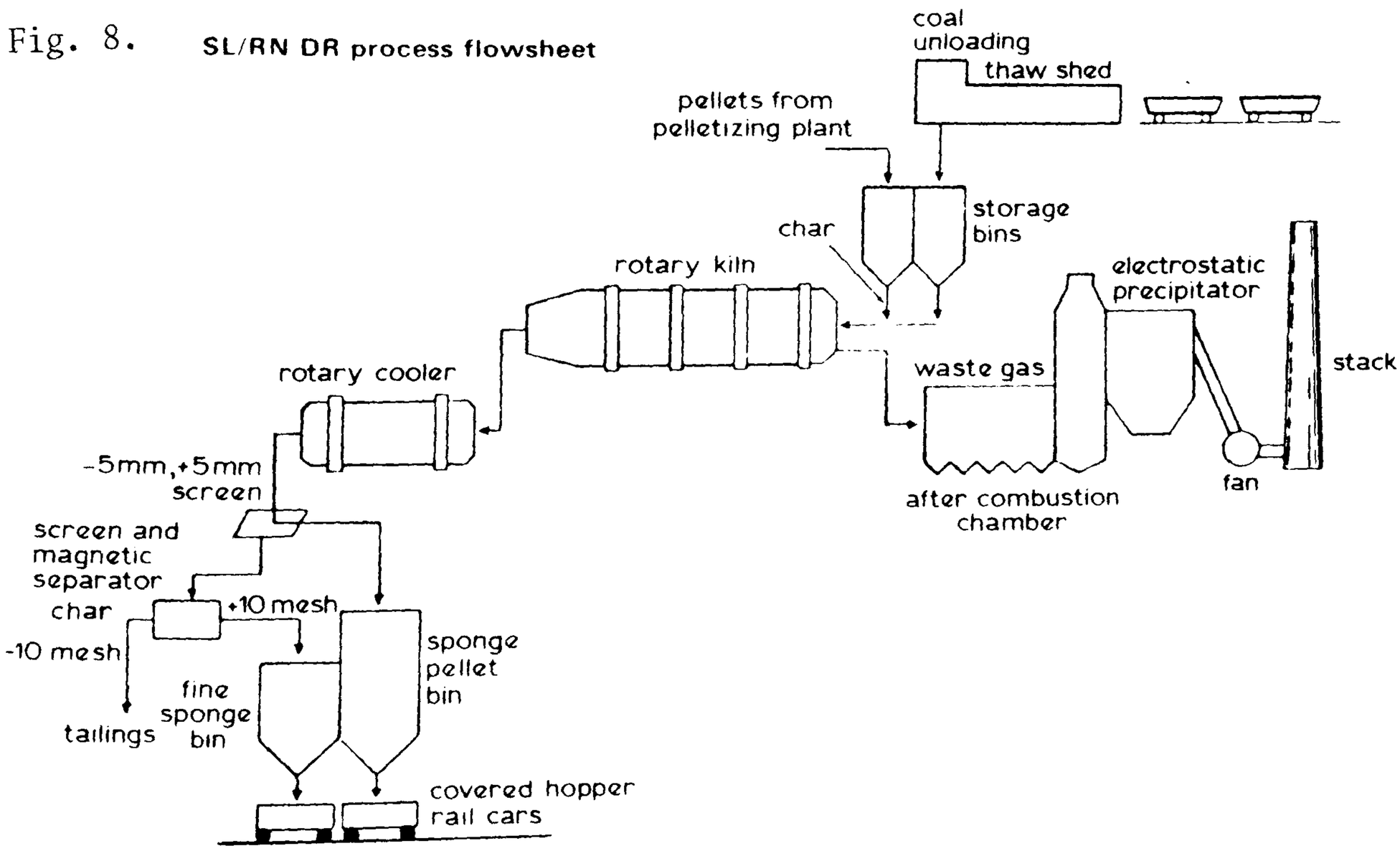

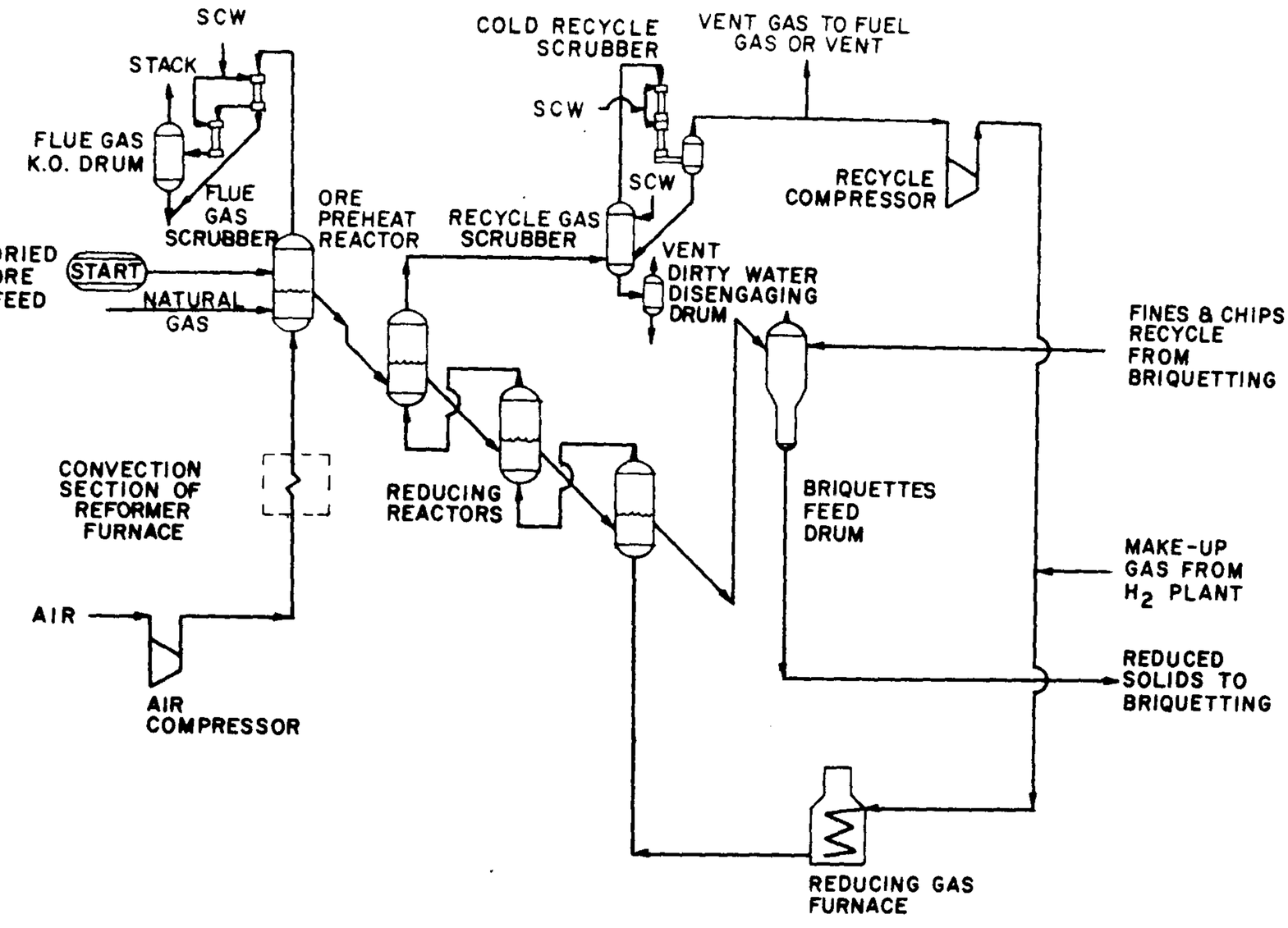

Fig. 9. Schematic arrangement of the equipment for the FIOR process

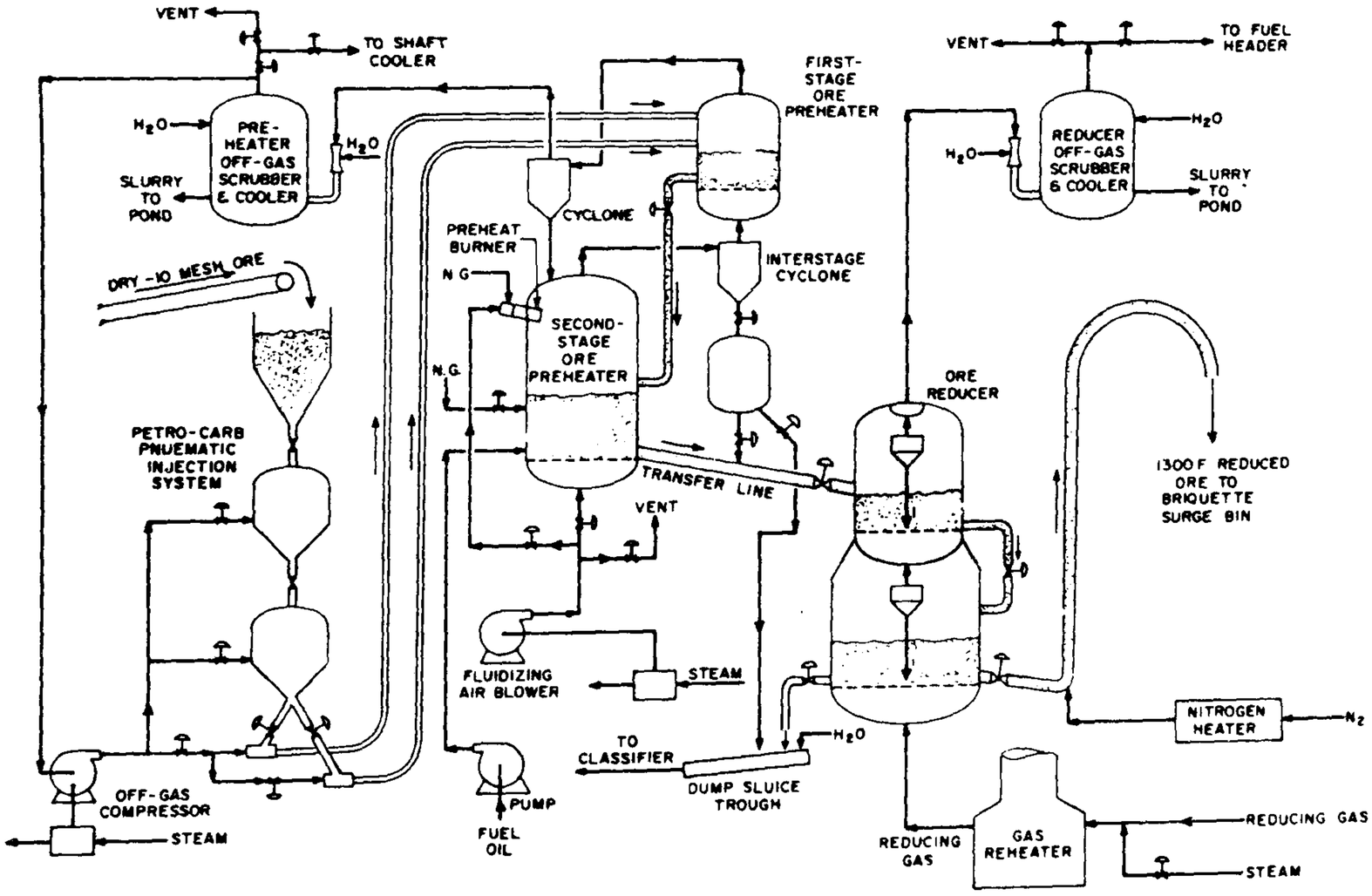

Fig. 10 Ore preheating and reduction section of the HIB plant

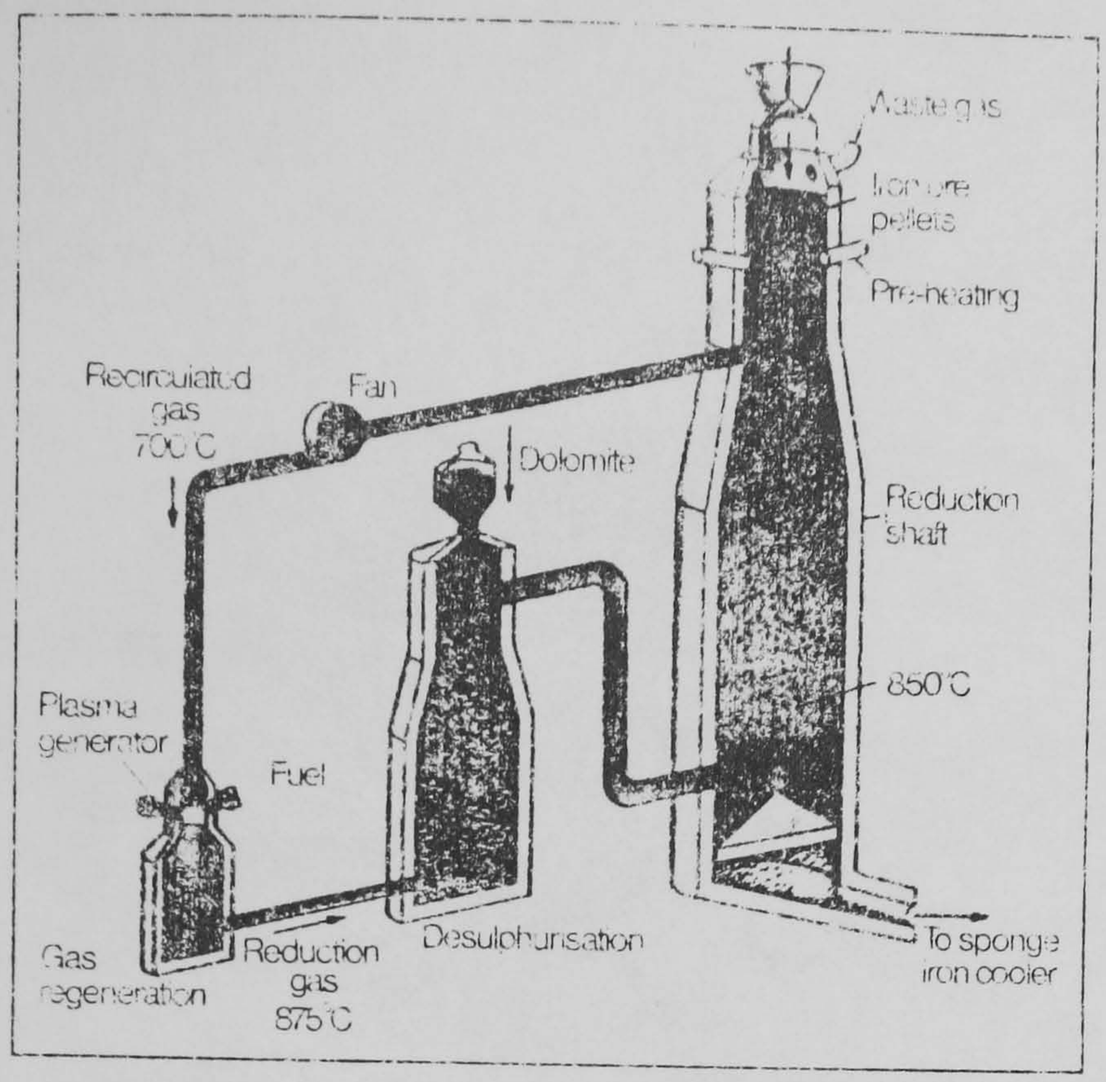

Fig. 11. *Schematic diagram of the Plasmared direct-reduction sponge-iron process.*

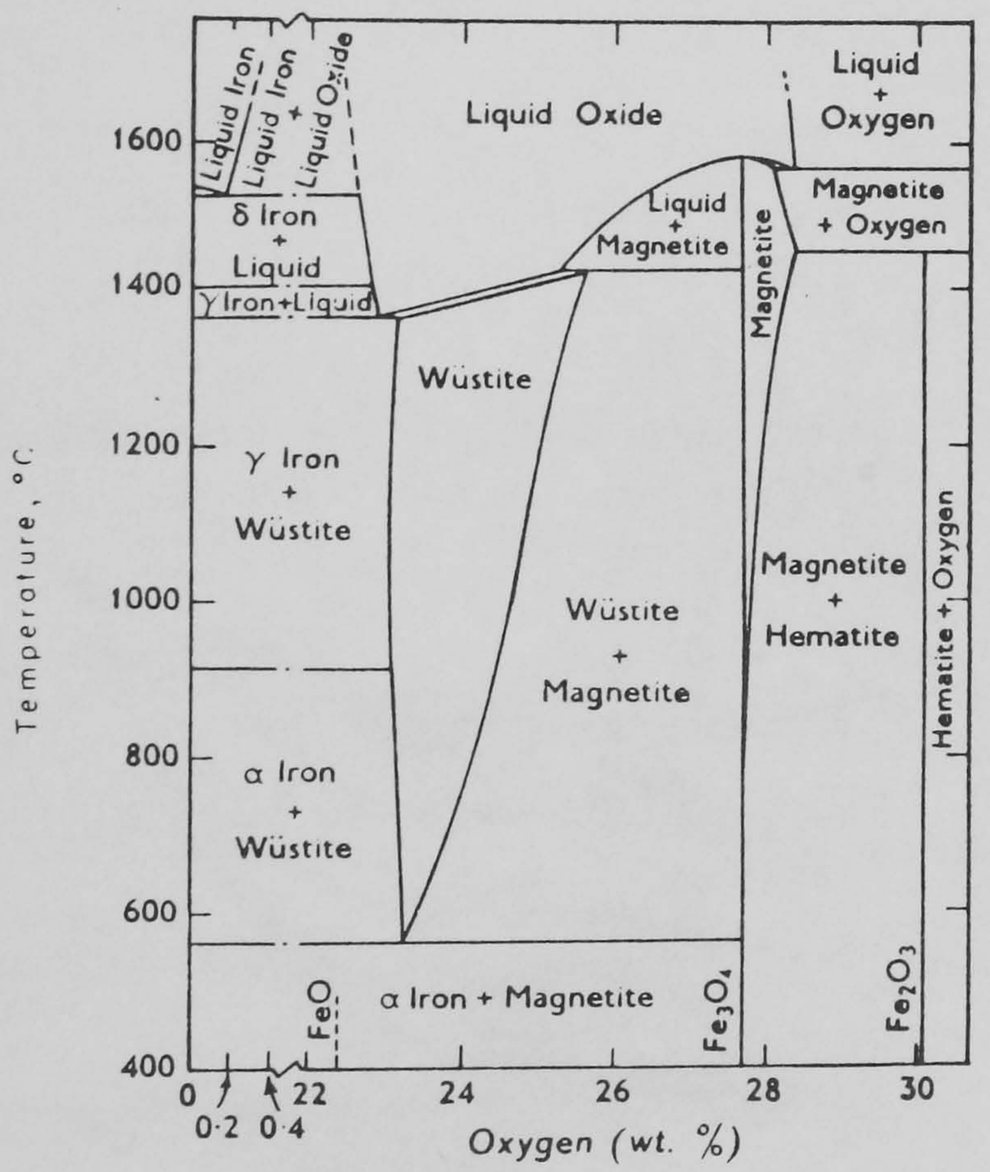

Fig. 12 **The binary system iron-oxygen at a total pressure of one atmosphere.** (After Darken and Gurry

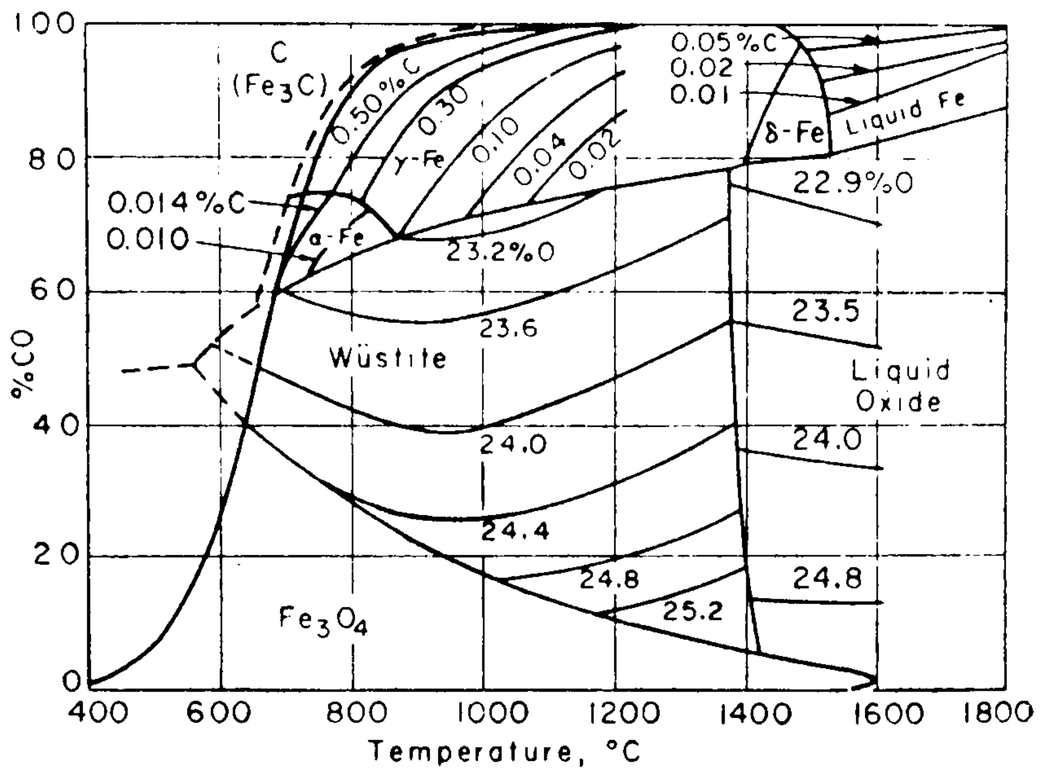

Fig. 13. Complete Fe—C—O diagram.

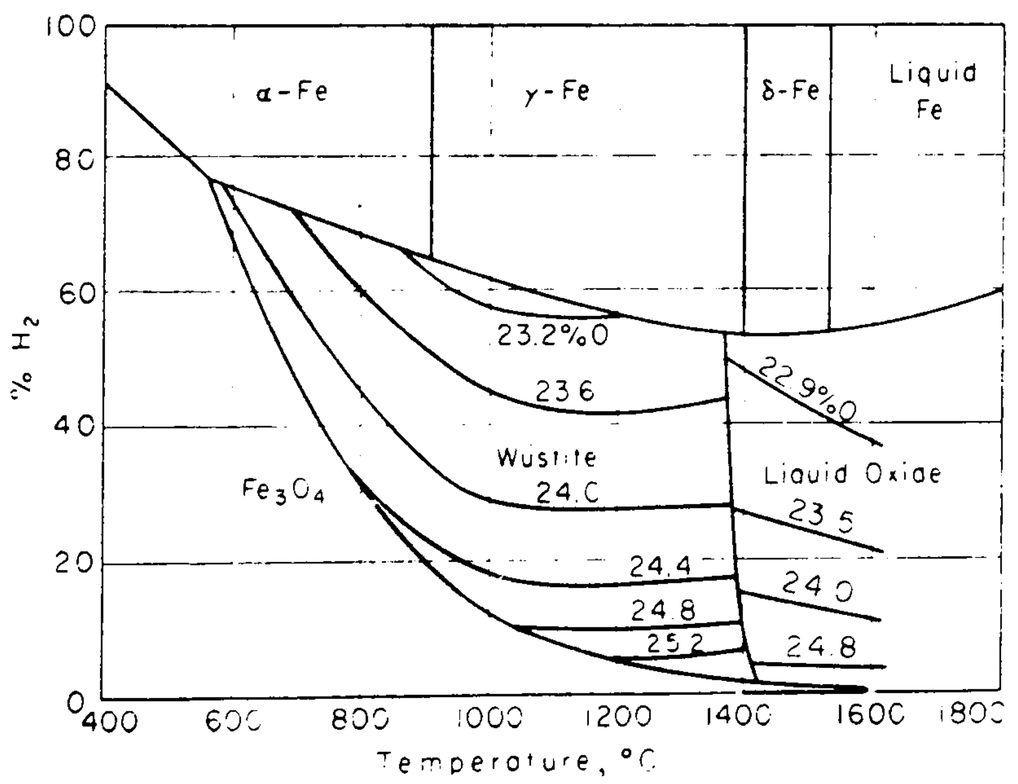

Fig. 14. Complete Fe—H—O diagram.

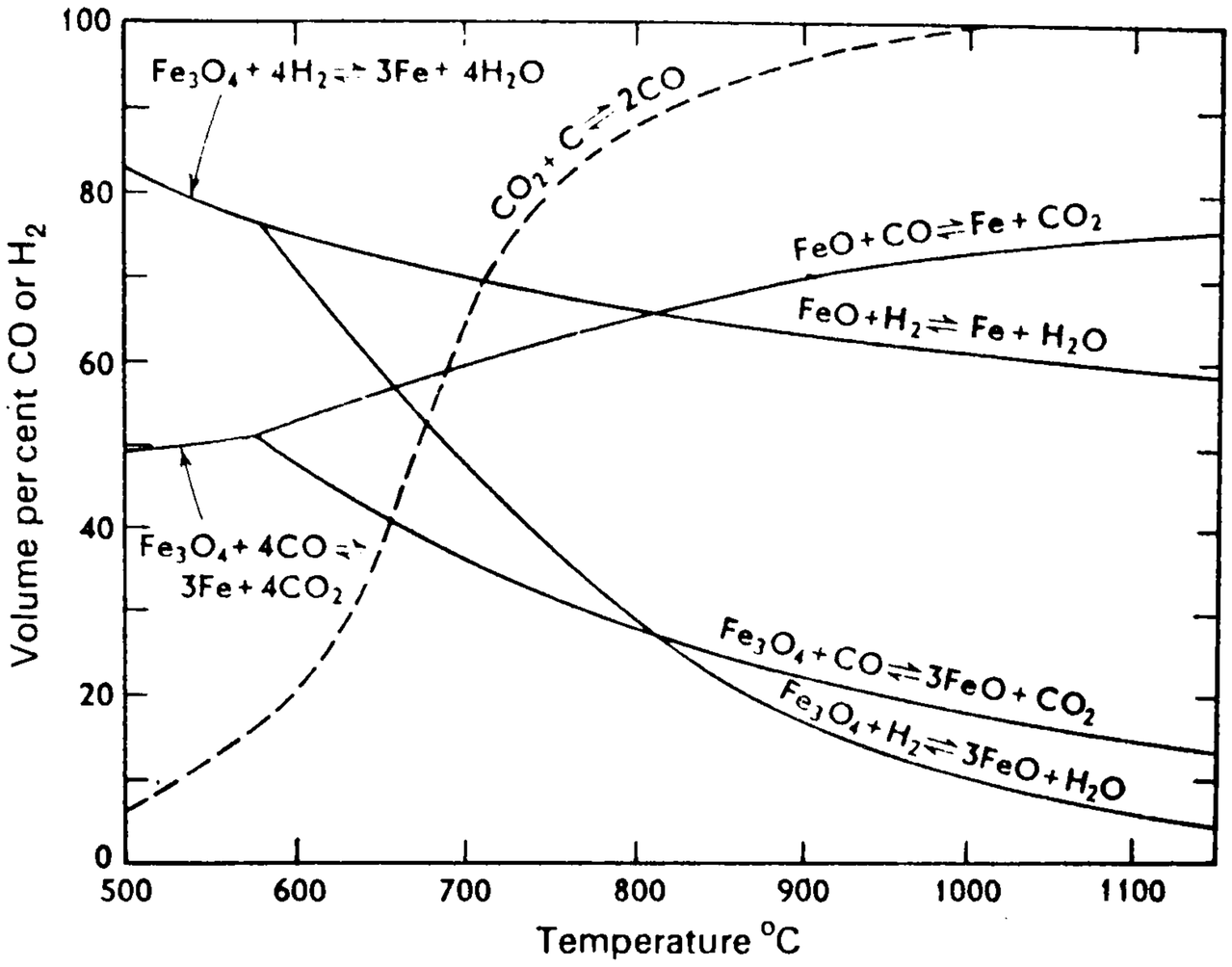

Fig. 15. **Equilibrium relations in the systems iron–carbon–oxygen, iron–hydrogen–oxygen and carbon–oxygen.**

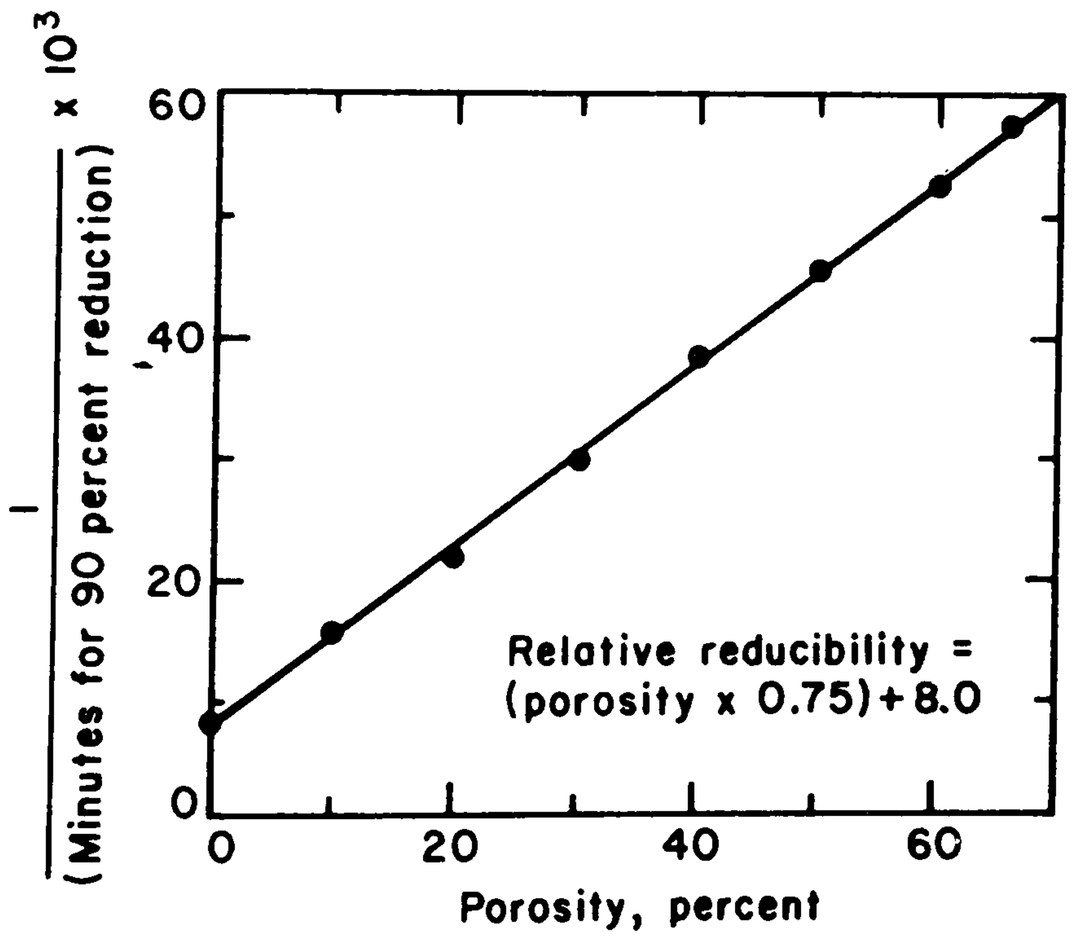

Fig. 16. **Relation between porosity and relative reducibility of iron ore (after Joseph)**

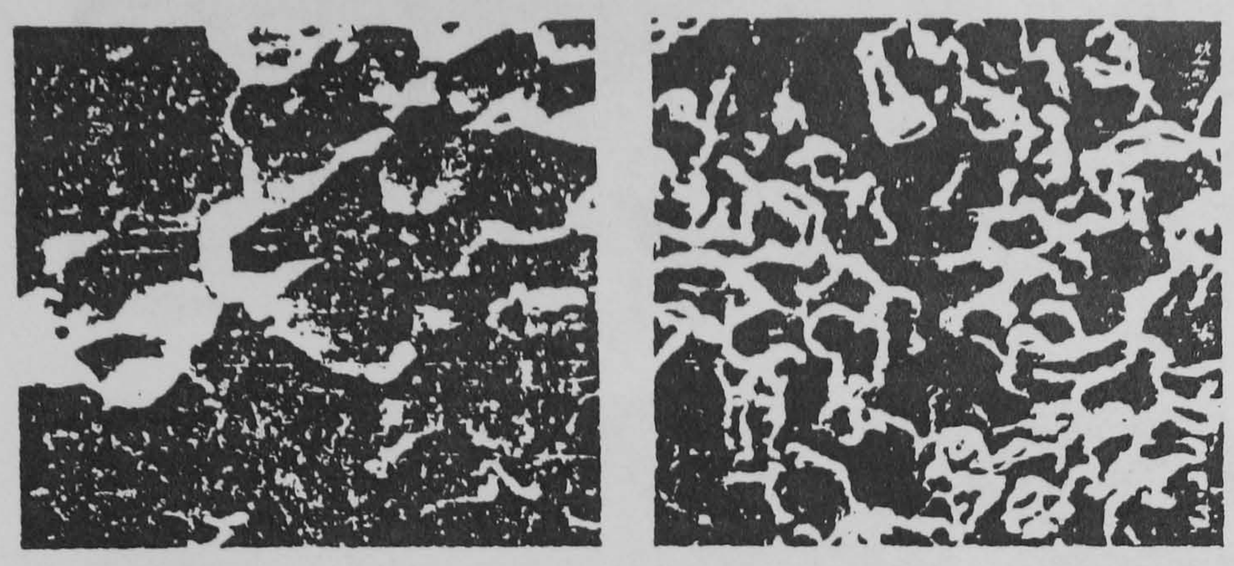

FIG. 17 Scanning electron micrographs. (a) Fracture surface of sintered Fe_2O_3 pellet before and after H_2 reduction. (b) Outer surface of dense wustite before and after H_2 reduction.

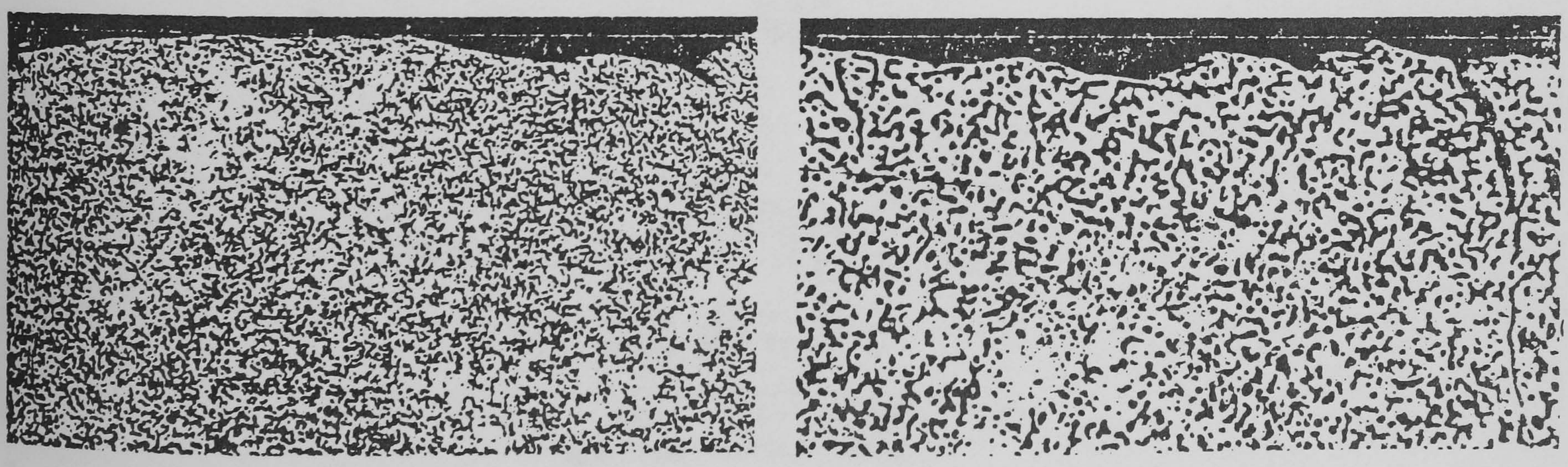

FIG. 18. -Polished sections showing network of pores in the iron formed by H_2 or CO reduction of dense wustite at 1200°C.

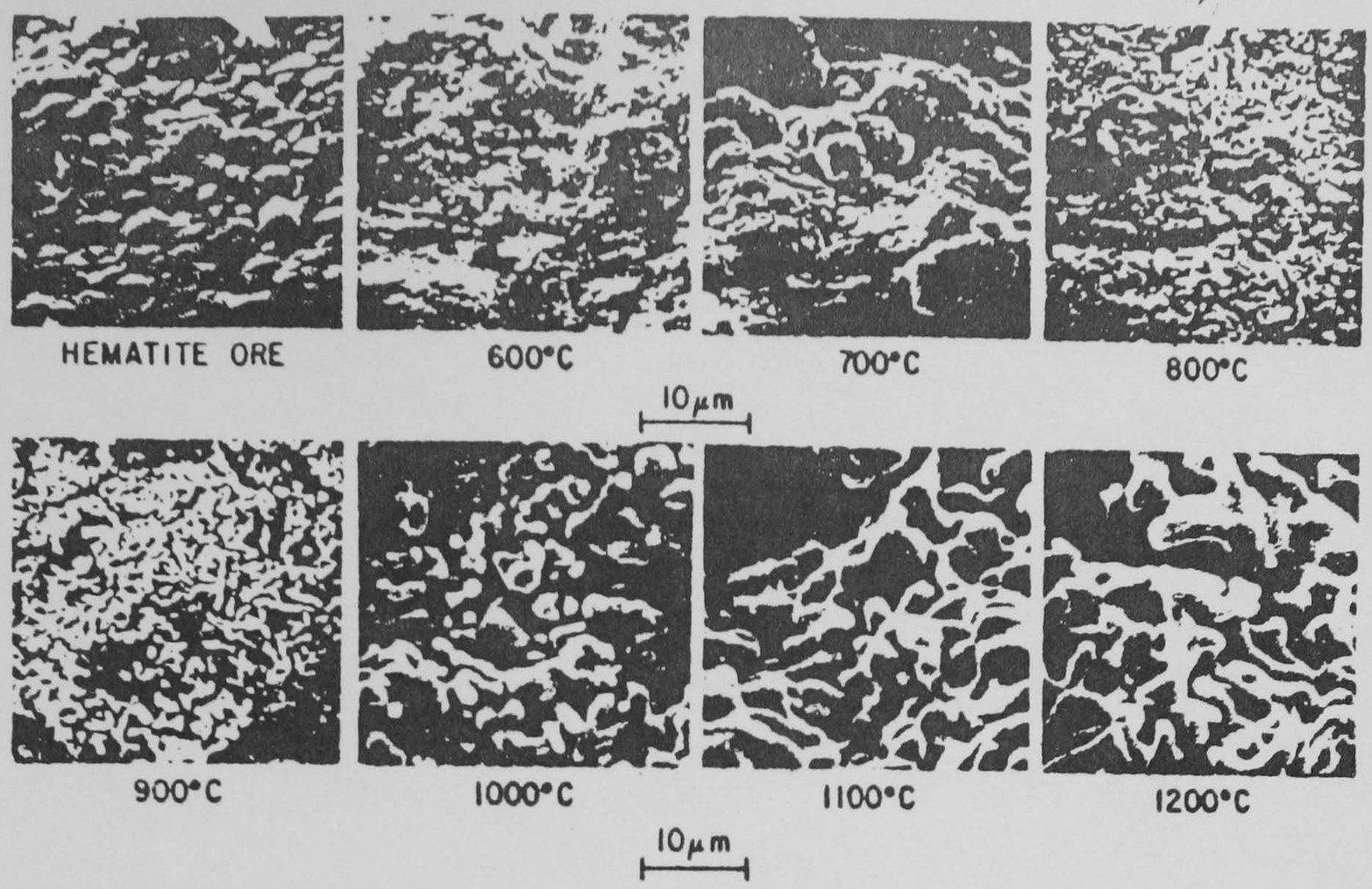

FIG. 19. Fracture surfaces of lump hematite ore and porous iron reduced in hydrogen at indicated temperatures as viewed in the scanning electron microscope.

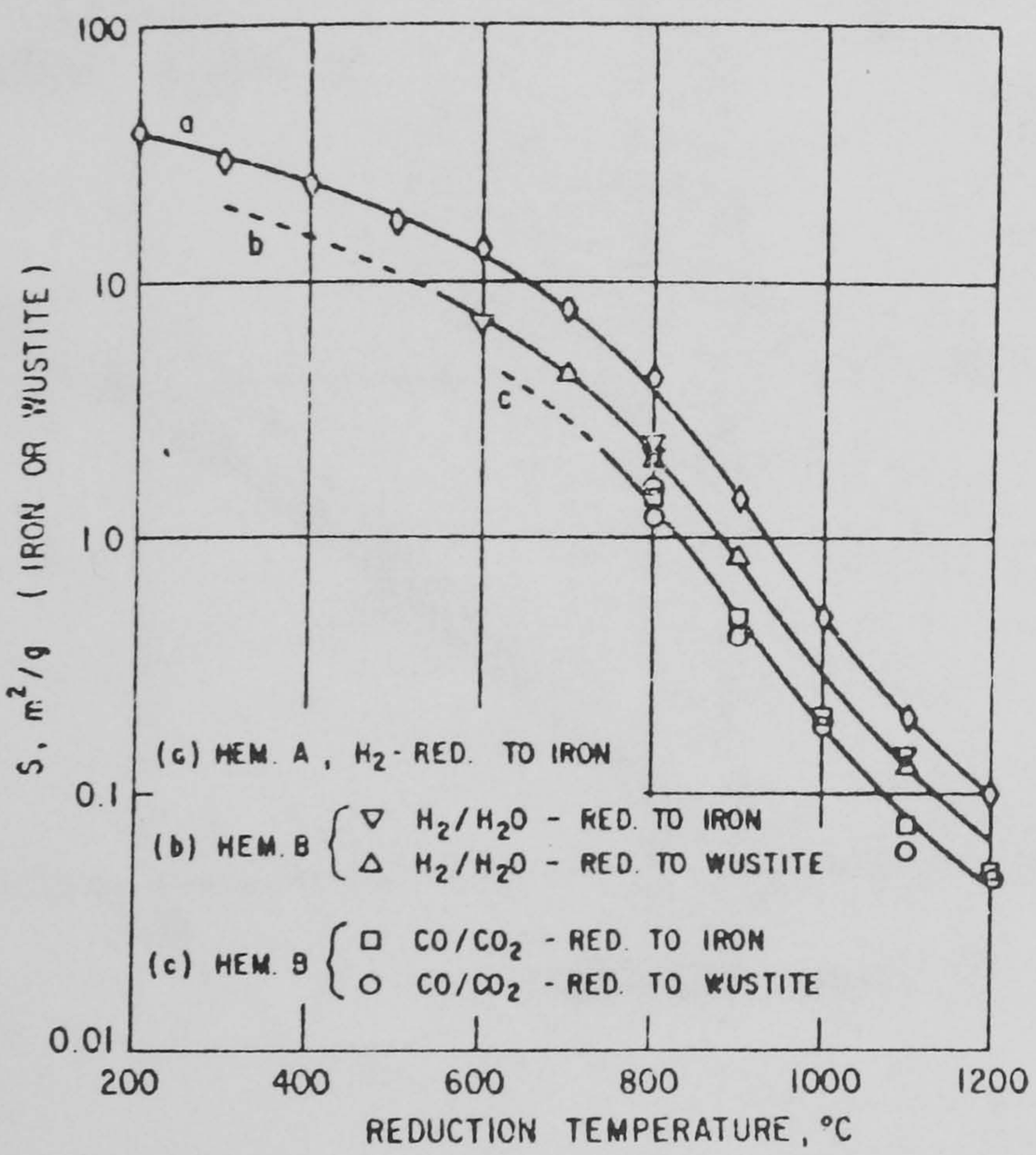

FIG.20 Internal pore surface area of iron and wustite formed by reduction of hematite ores A and B as a function of reduction temperature.

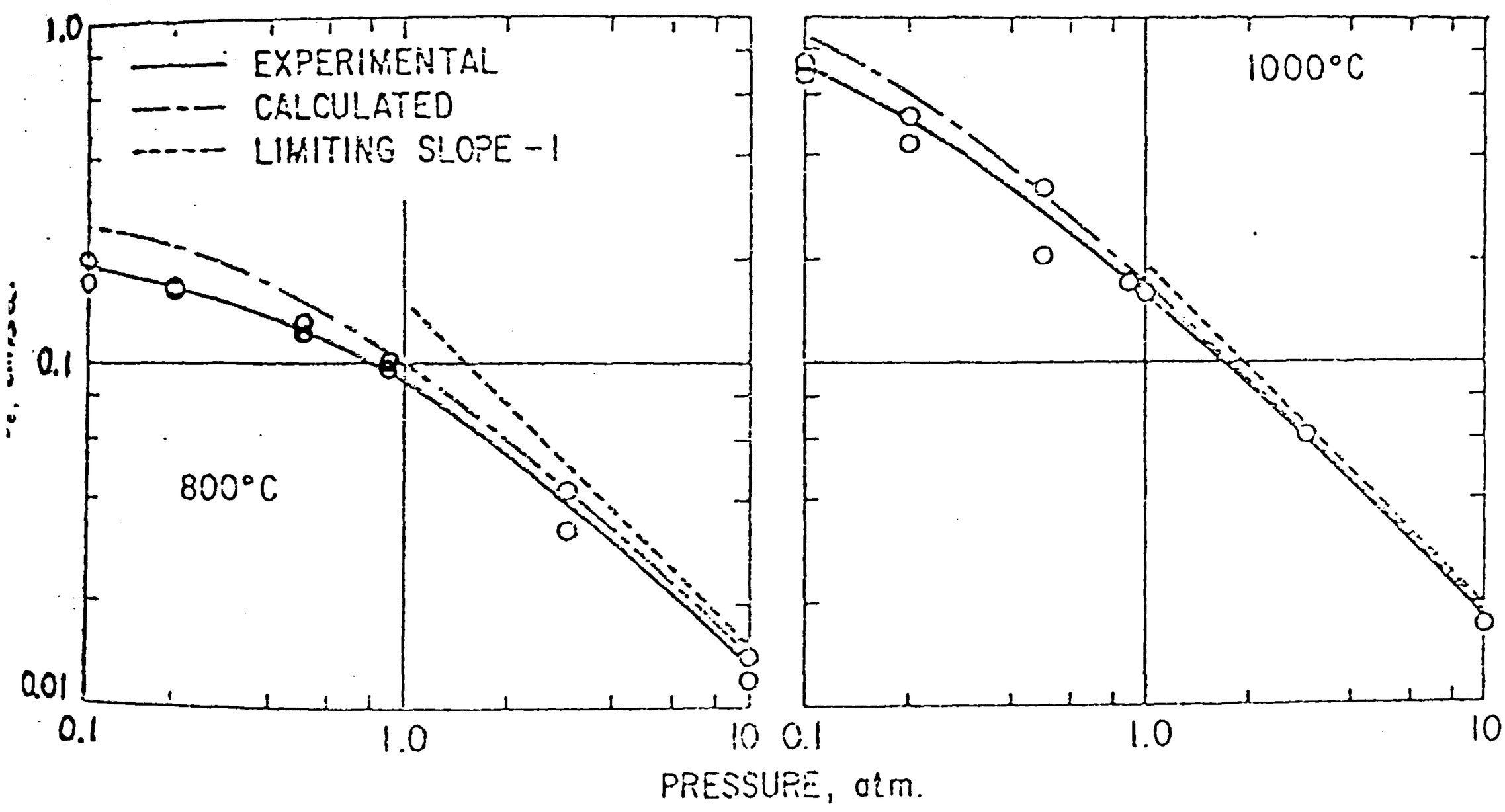

Fig. 21 - Pressure dependence of effective diffusivity He-CO_2 at 20°C in iron reduced from hematite ore in hydrogen at indicated temperatures.

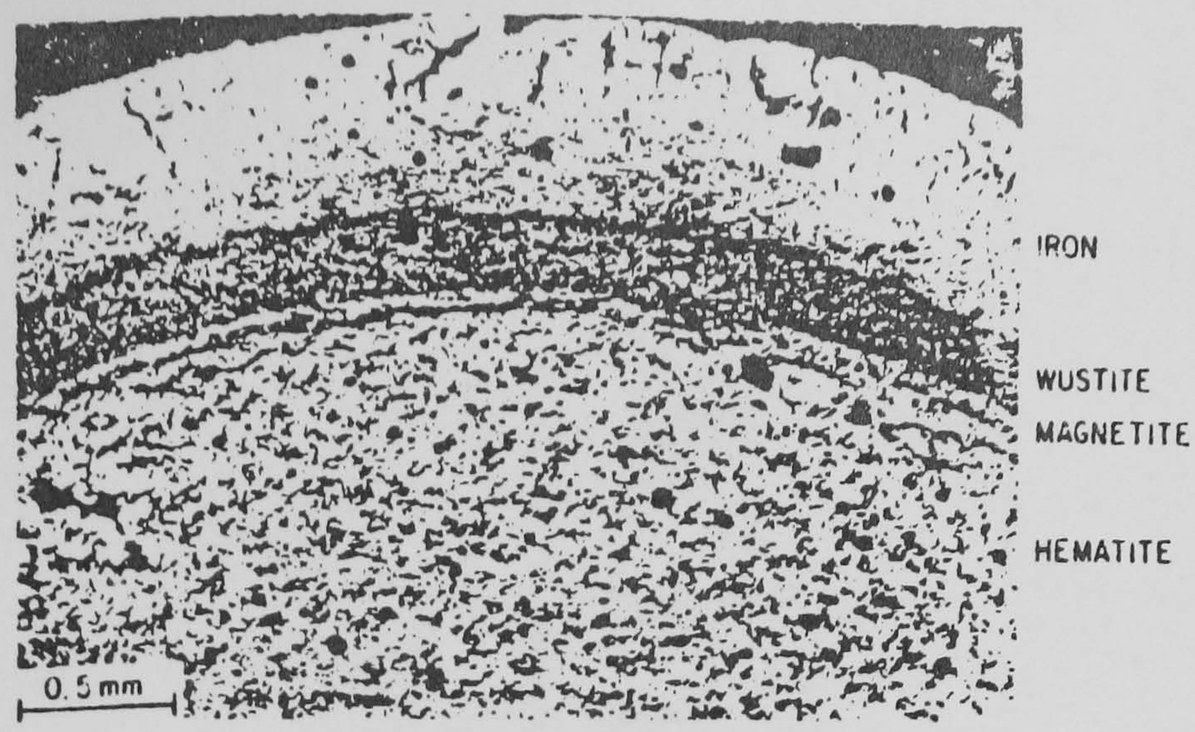

FIG. 22. Polished section of a partially H_2-reduced (900°C) sintered Fe_2O_3 pellet (4.8 g/cm^3 and 12 mm dia) showing product layers.

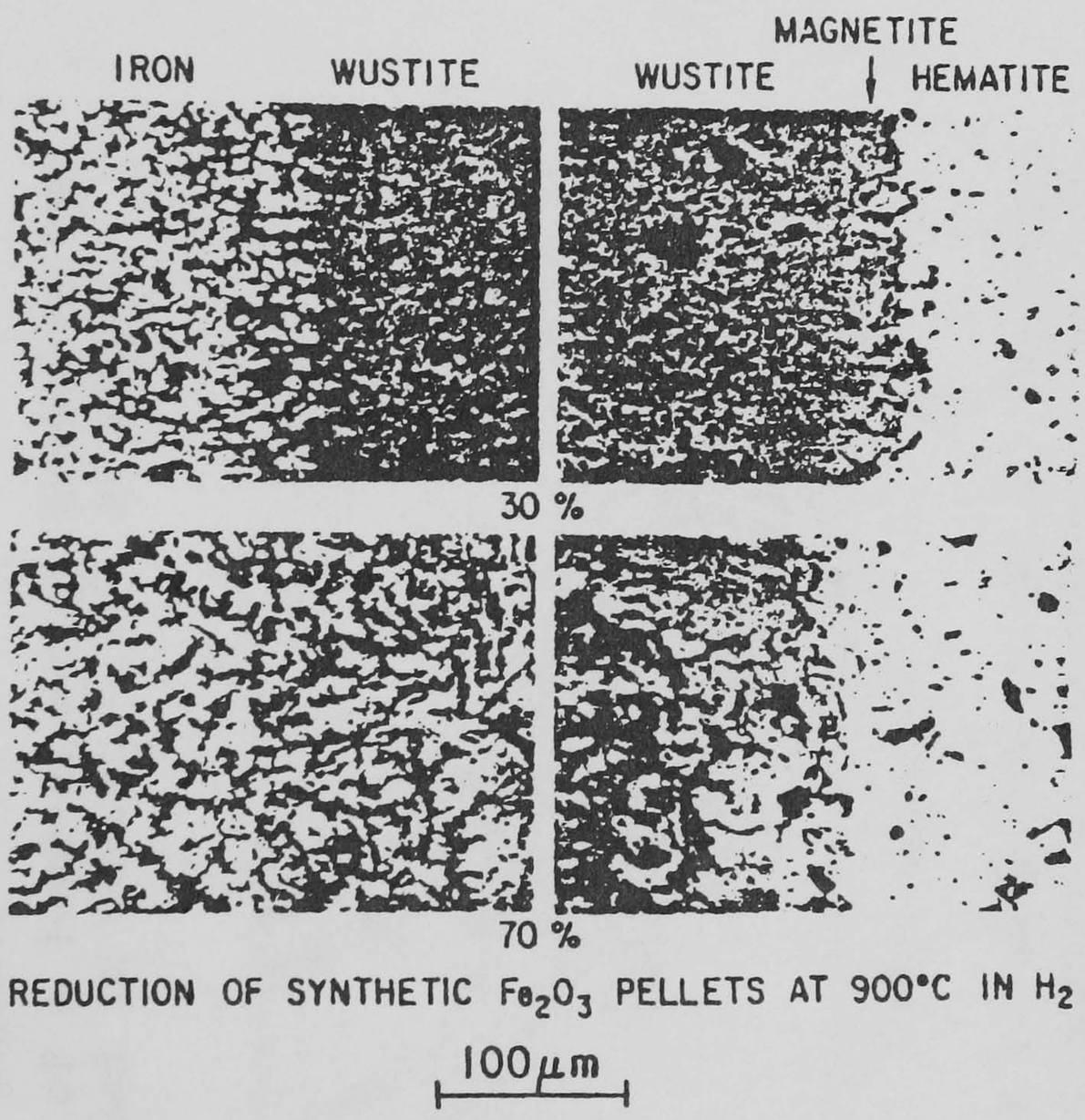

REDUCTION OF SYNTHETIC Fe_2O_3 PELLETS AT 900°C IN H_2

FIG. 23. Sections of partially H_2 reduced (900°C) sintered Fe_2O_3 pellets (4.8 g/cm^3 and 12 mm dia) showing diffuse iron/wustite interface and less irregular interfaces of magnetite with wustite and hematite.

FIG 24.

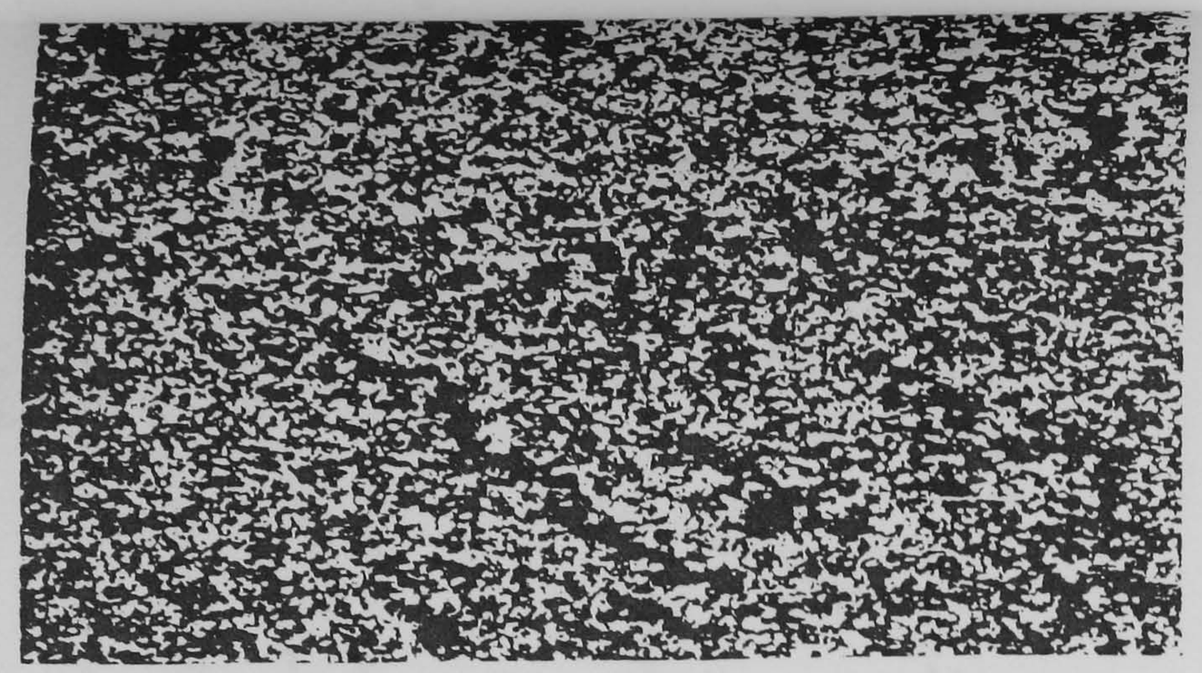

20 µm

Polished section of a 1-mm-diameter hematite ore granule 60% reduced in CO/Co_2 = 9/1 at 800°C.

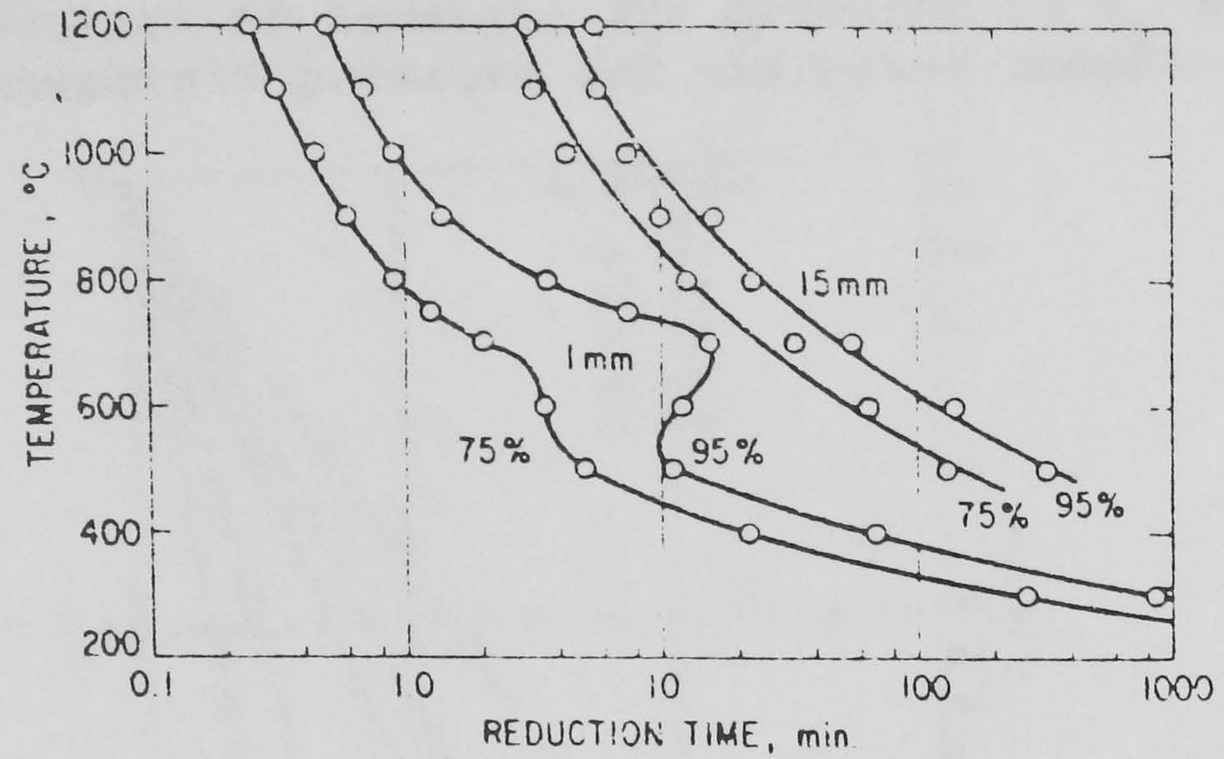

FIG 25

Temperature effect on reduction time of hematite ore, 1 and 15-mm diameter, in atmospheric pressure of hydrogen.

FIG 26.

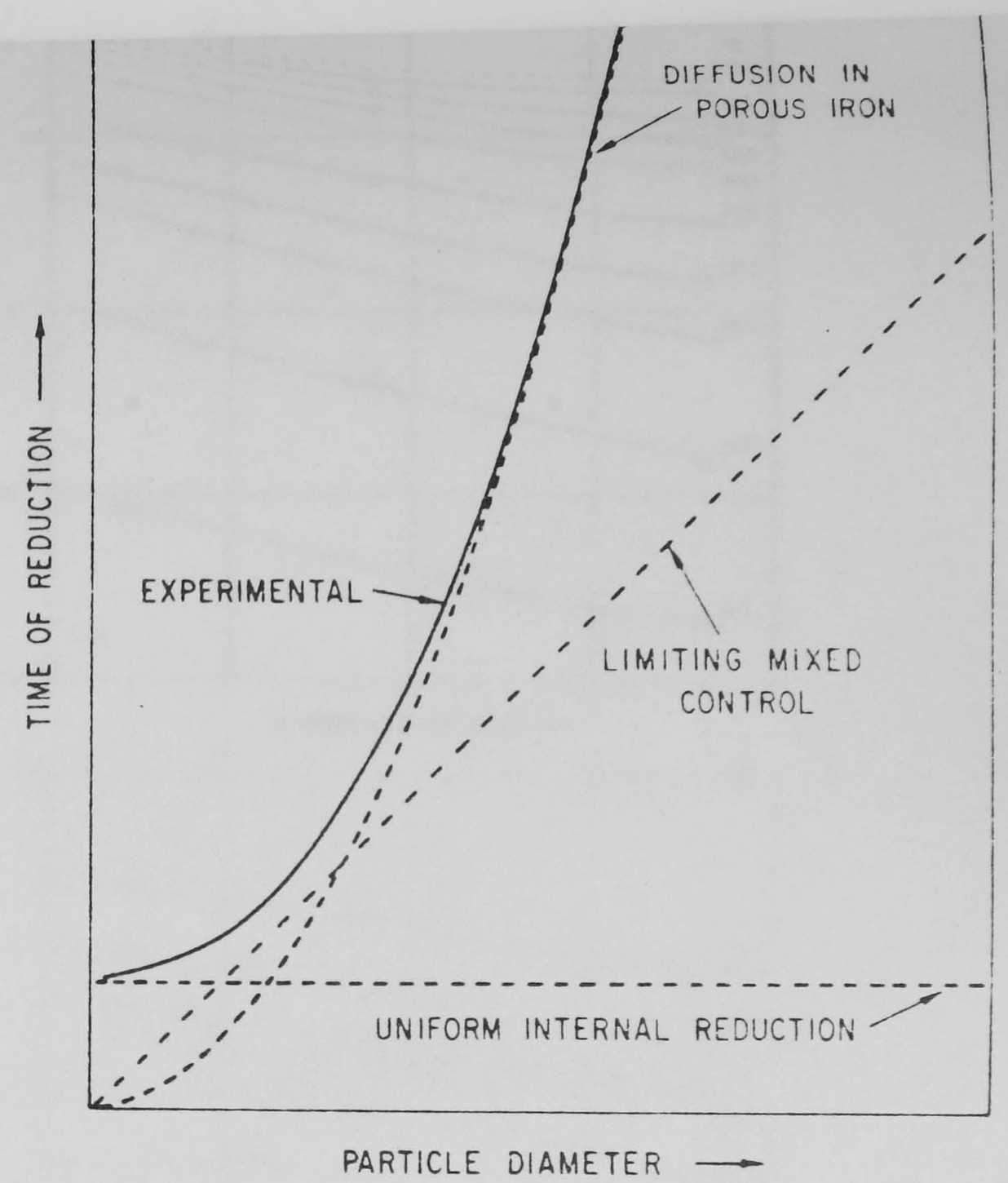

Schematic representation of time of reduction (for a given percent oxygen removal) as a function of particle size.

FIG 27.

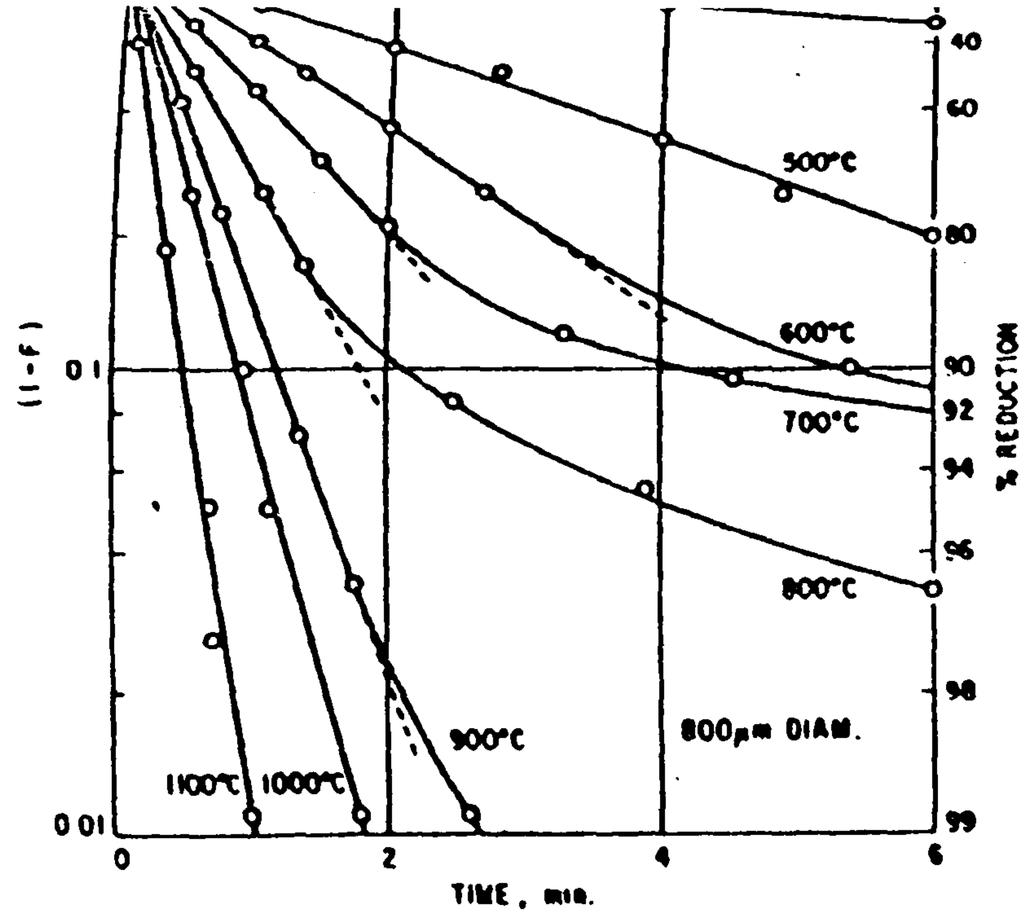

Reduction of hematite (B) granules in H_2 at atmospheric pressure and indicated temperatures.

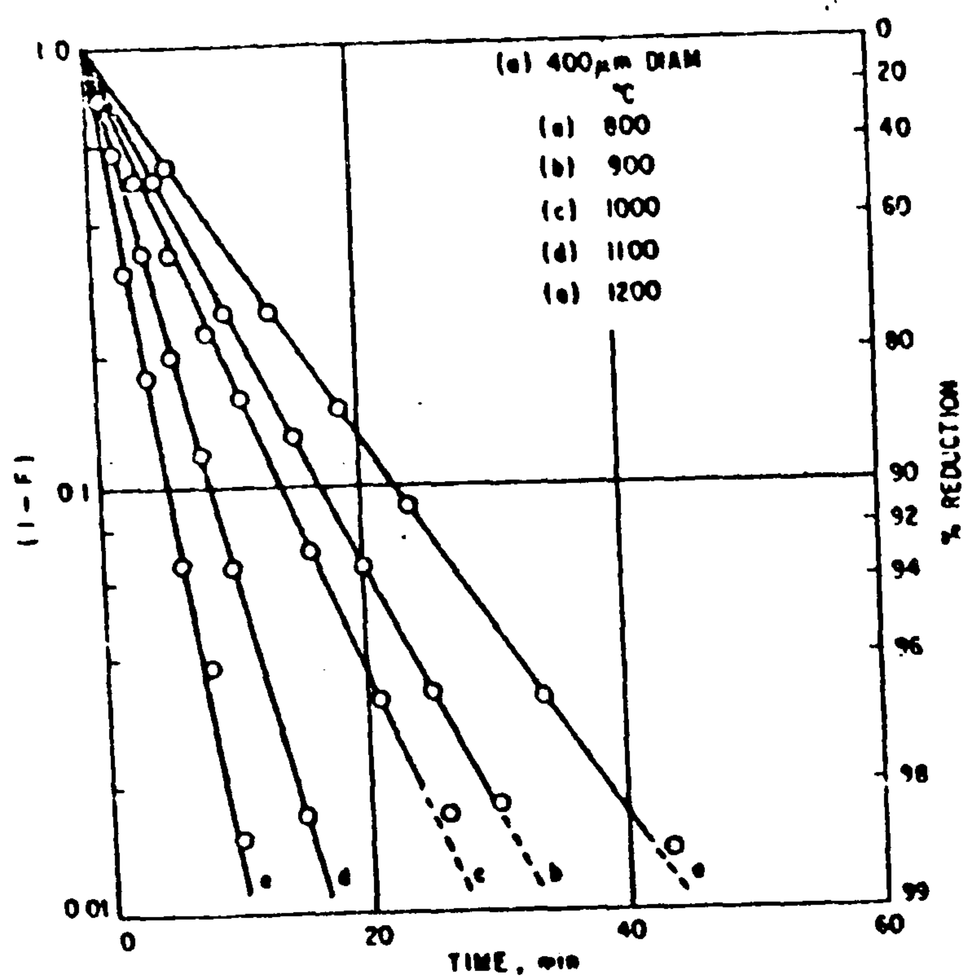

FIG.28. Reduction of hematite (B) granules in a 90% CO + 10% CO_2 mixture at atmospheric pressure and indicated temperatures.

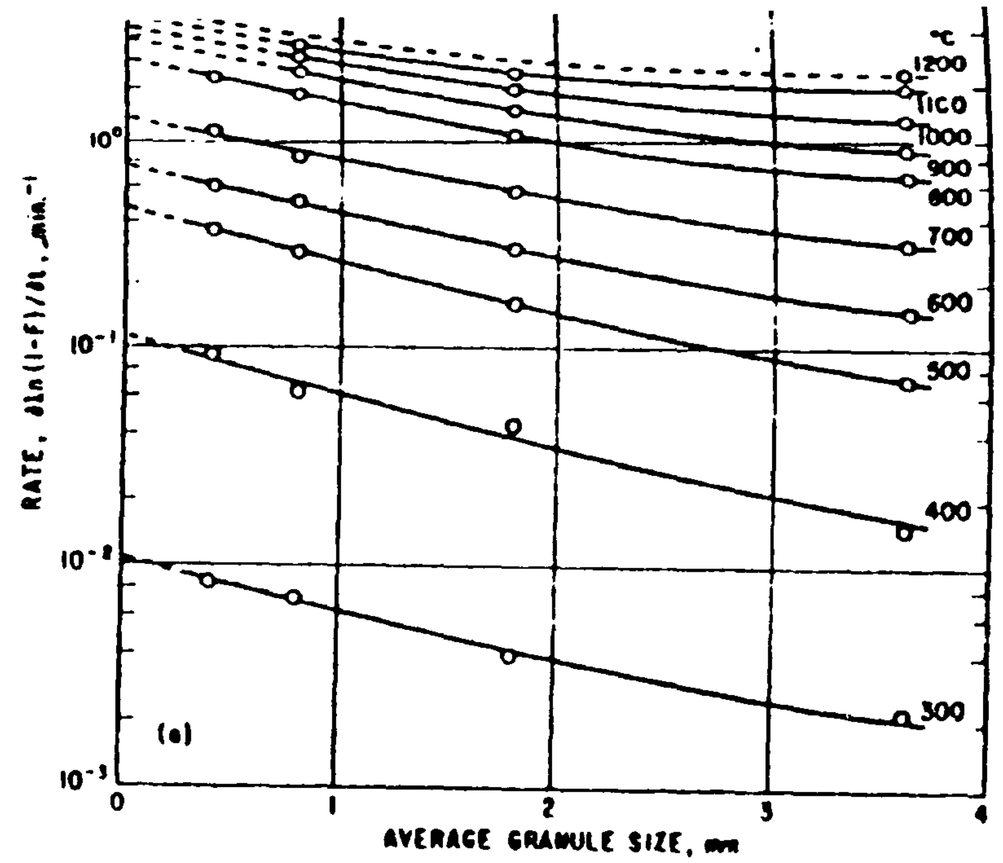

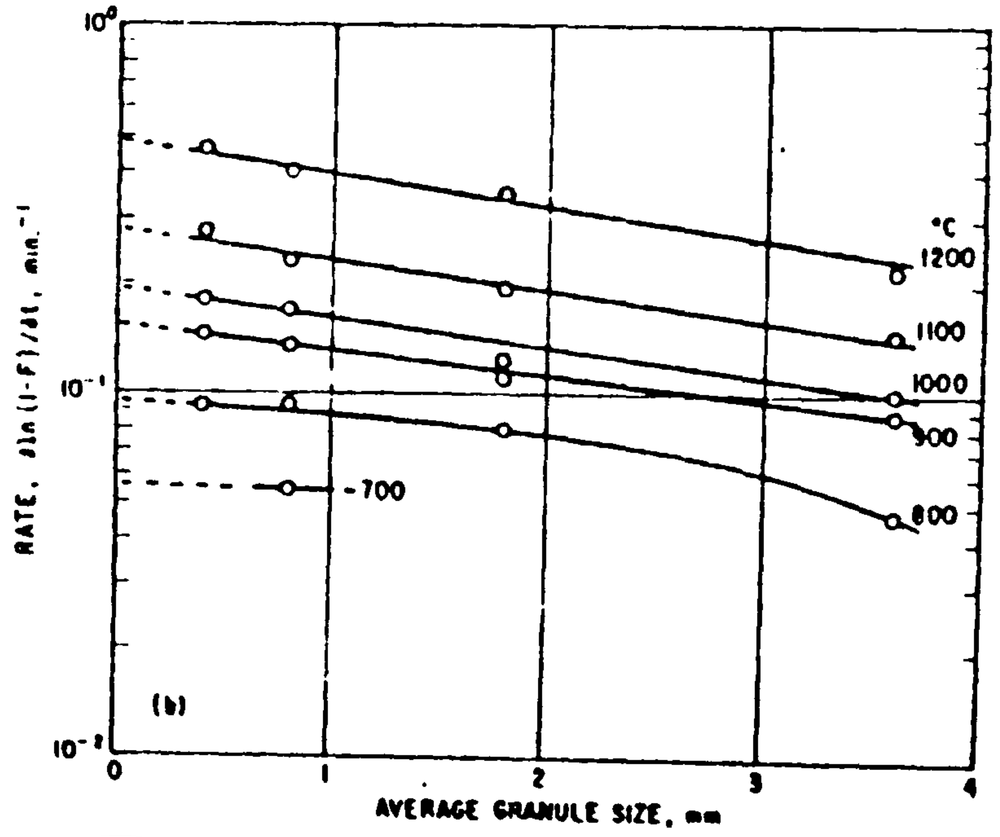

FIG. 29. Effect of granule size on the rate of internal reduction of hematite (B) granules in

(a) 100% H_2 and
(b) 90% CO^2+ 10% CO_2 at atmospheric pressure.

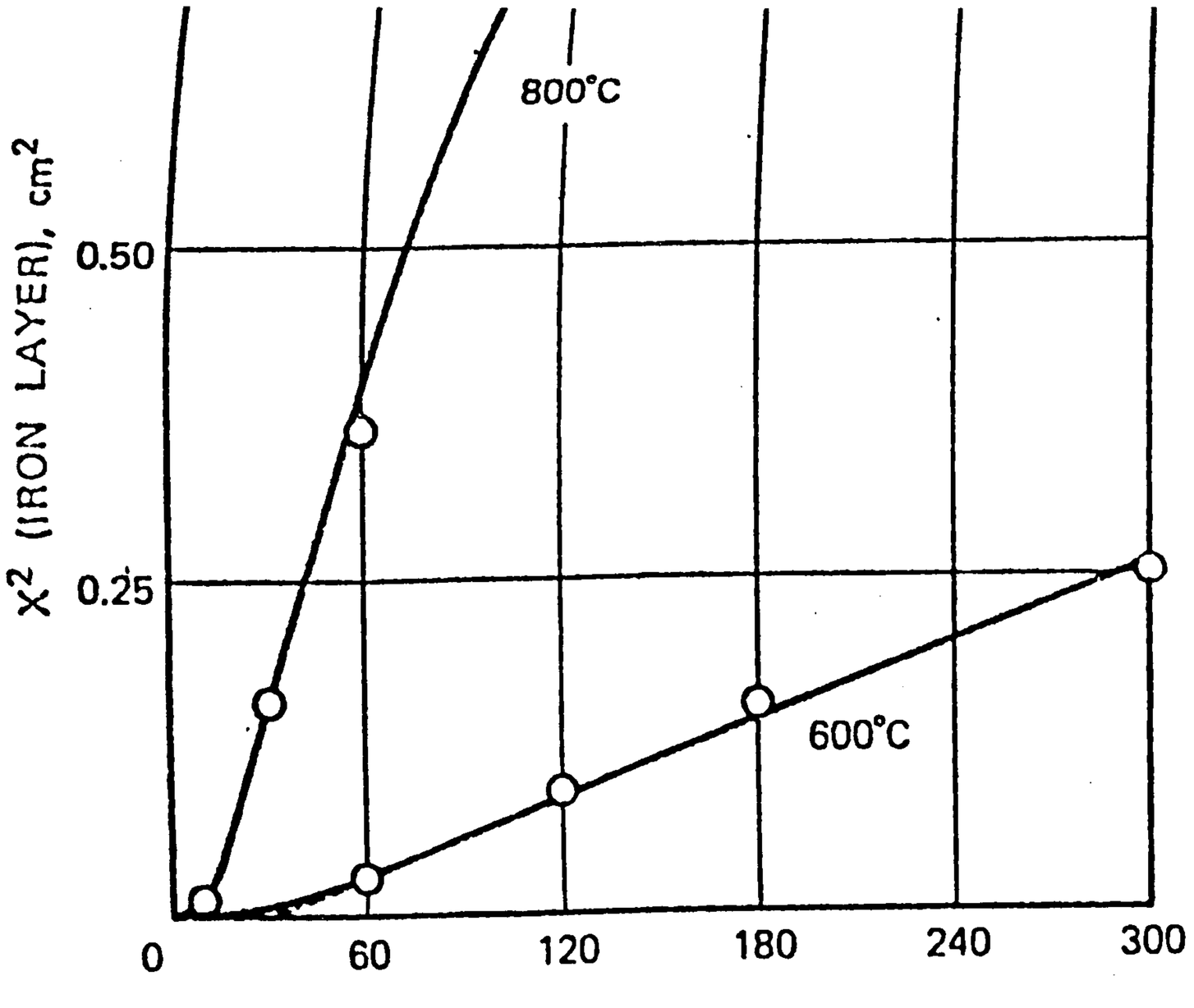

FIG. 30. Parabolic growth of reduced porous iron layer in unidirectional reduction of cylindrical rod of hematite ore in hydrogen at atmospheric pressure.

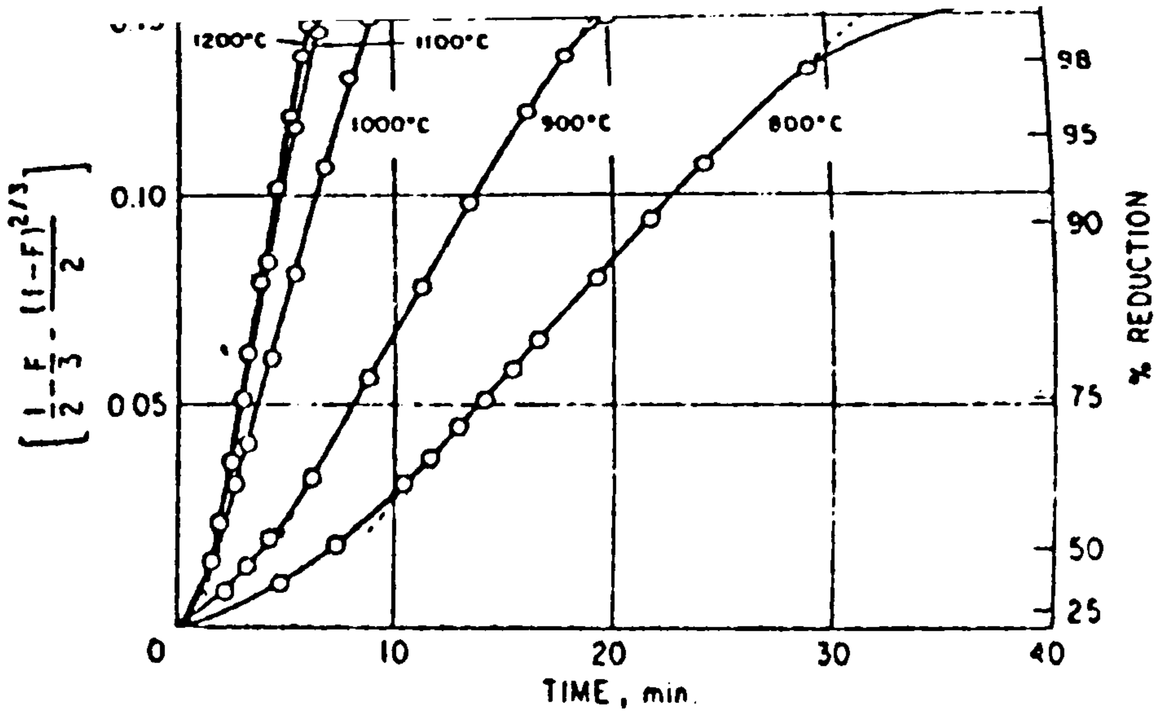

FIG. 31. Diffusion plot of reduction data for 15 mm diameter spheroidal hematite ore and atmospheri pressure of hydrogen.

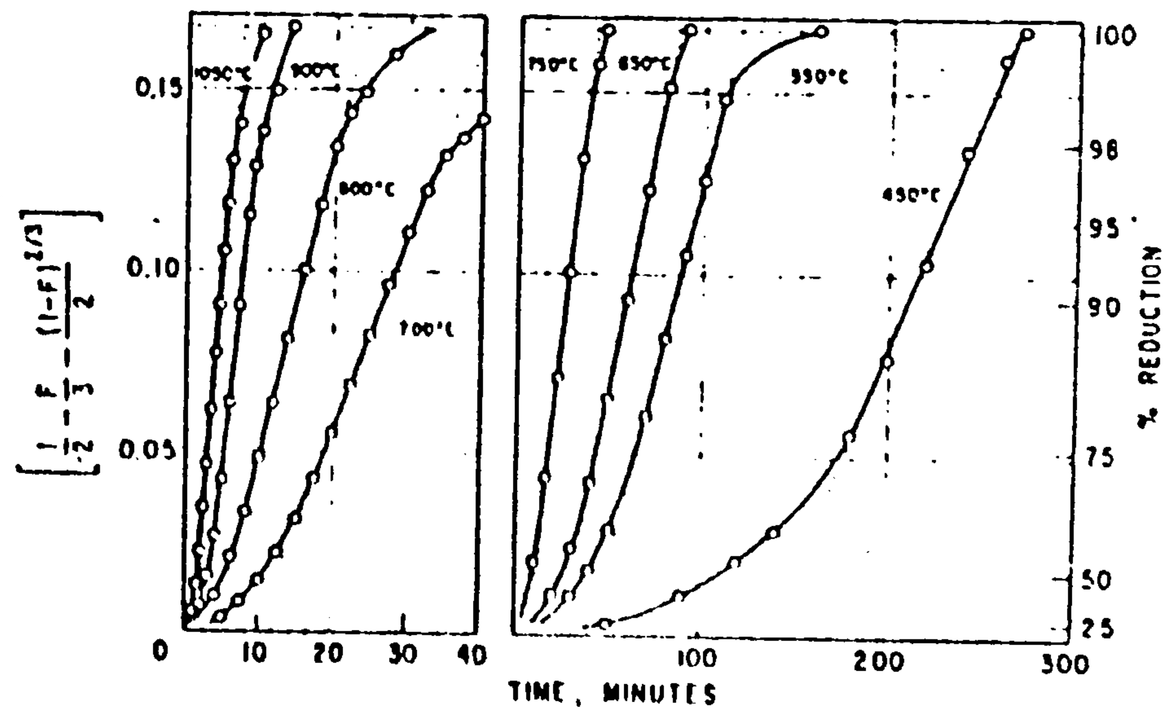

FIG. 32. Data for sintered synthetic hematite pellets (8- to 11-mm-diameter) for atmospheric pressure of hydrogen, using McKewan's data[76].

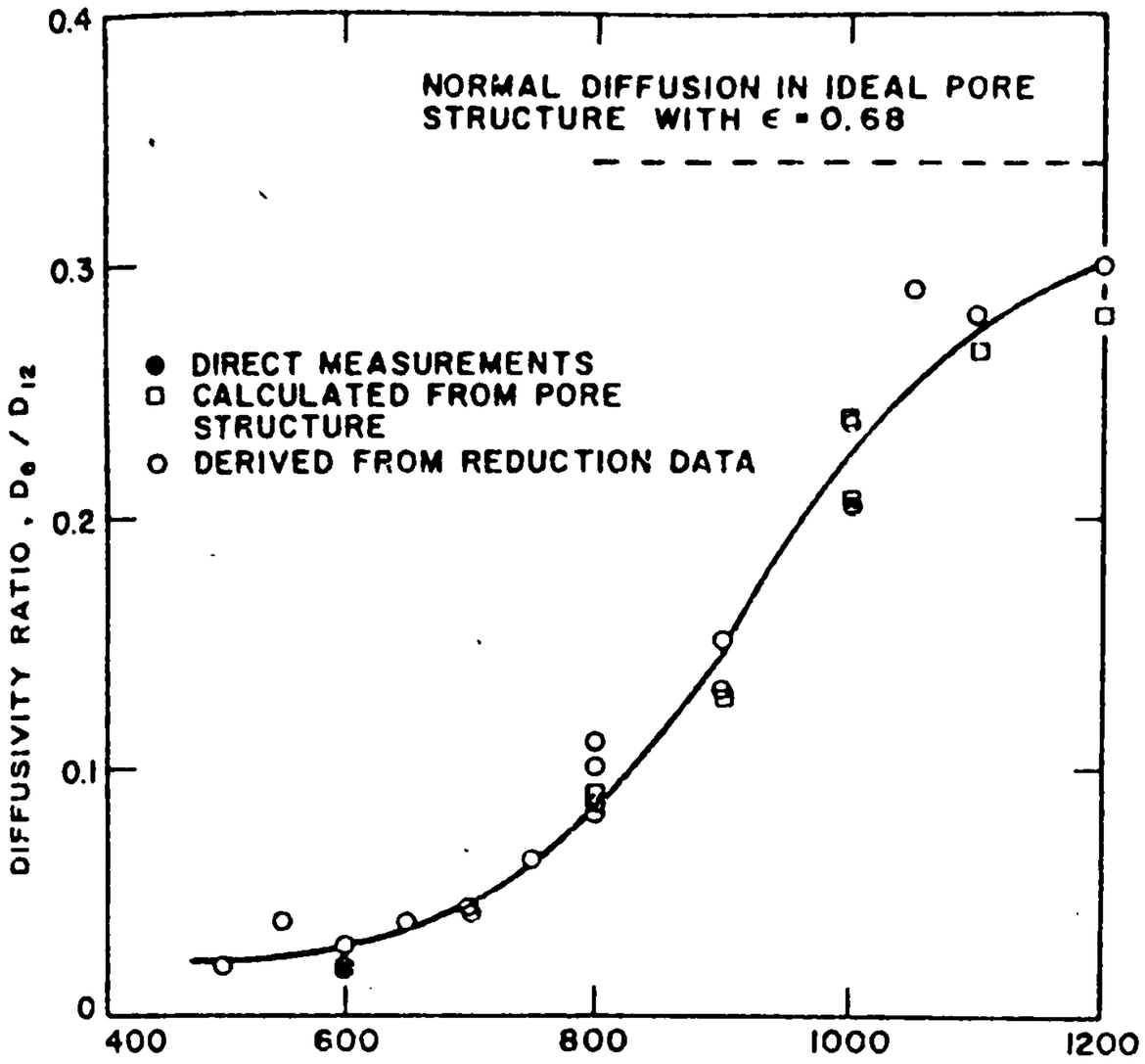

Fig. 33

Diffusivity ratio D_e/D_{12} for porous iron as a function of reduction temperature.

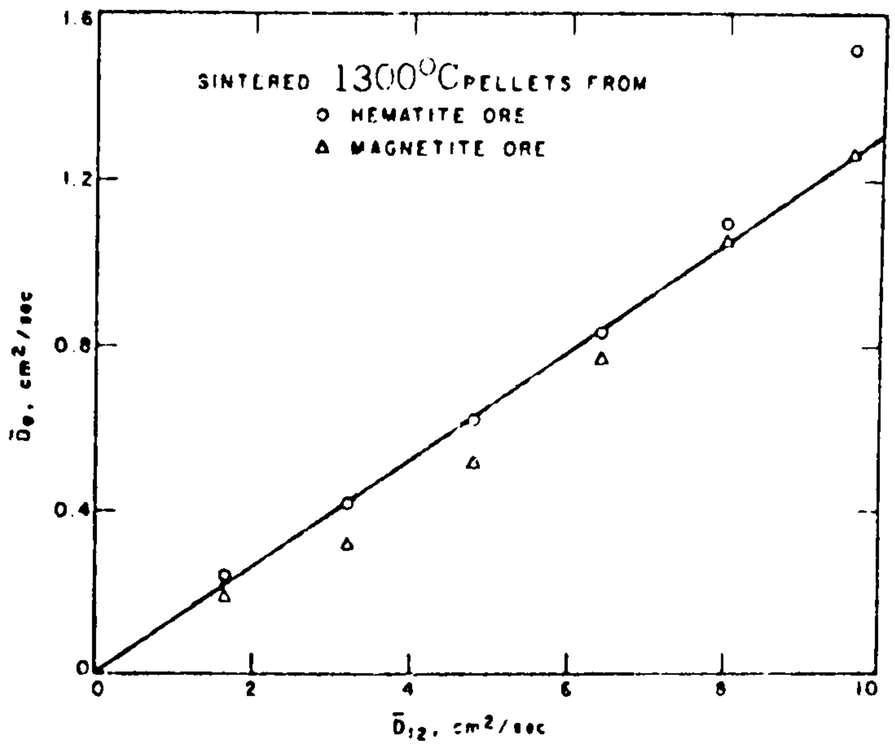

Fig. 34.

Effective diffusivity $\bar{D}_e$ in porous iron from reduction data (using H_2-CO mixtures) related to approximate molecular diffusivity for gas mixtures at atmospheric pressure and 900°C.

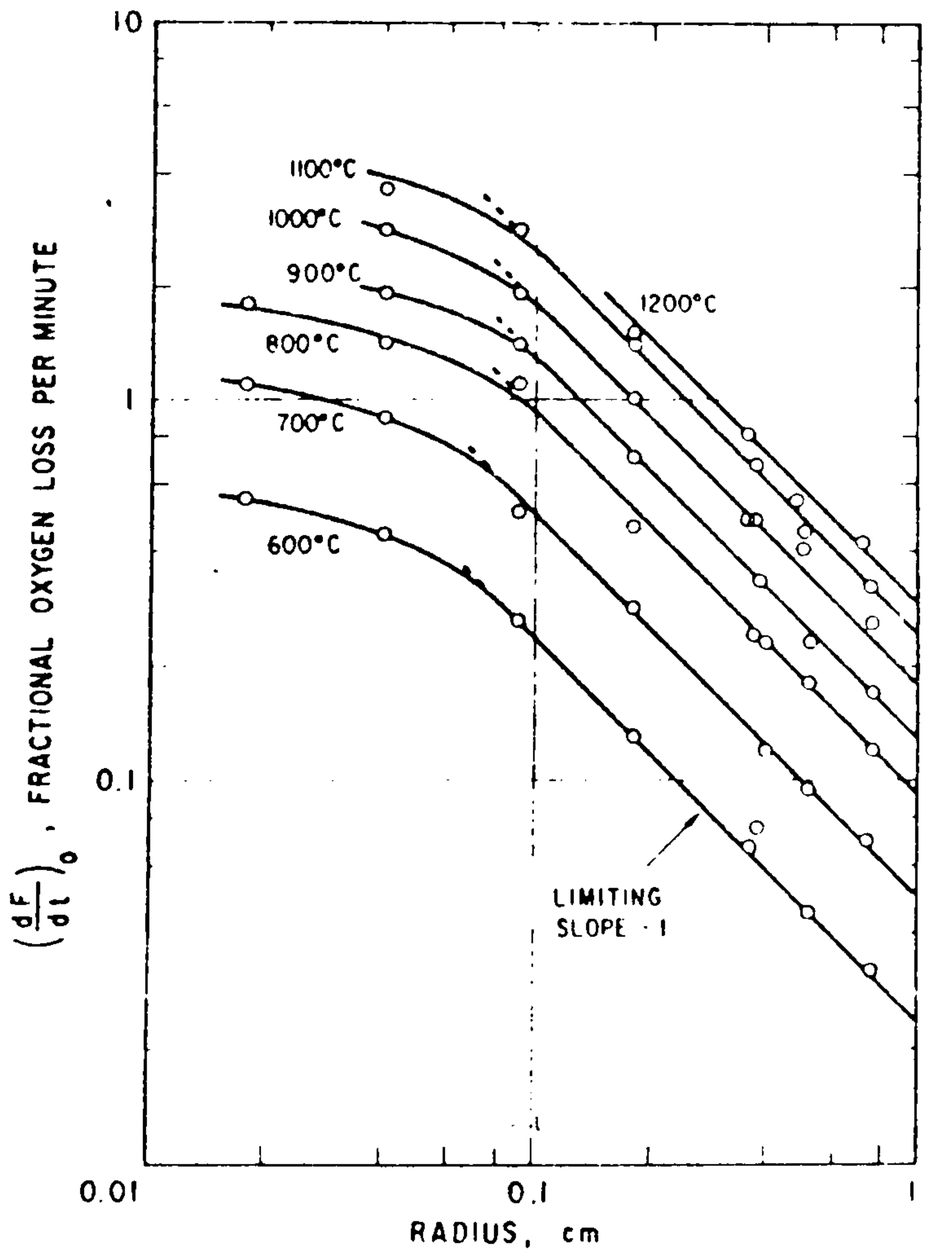

Fig. 35. Initial rate in hydrogen at atmospheric pressure as a function of particle radius at indicated temperatures.

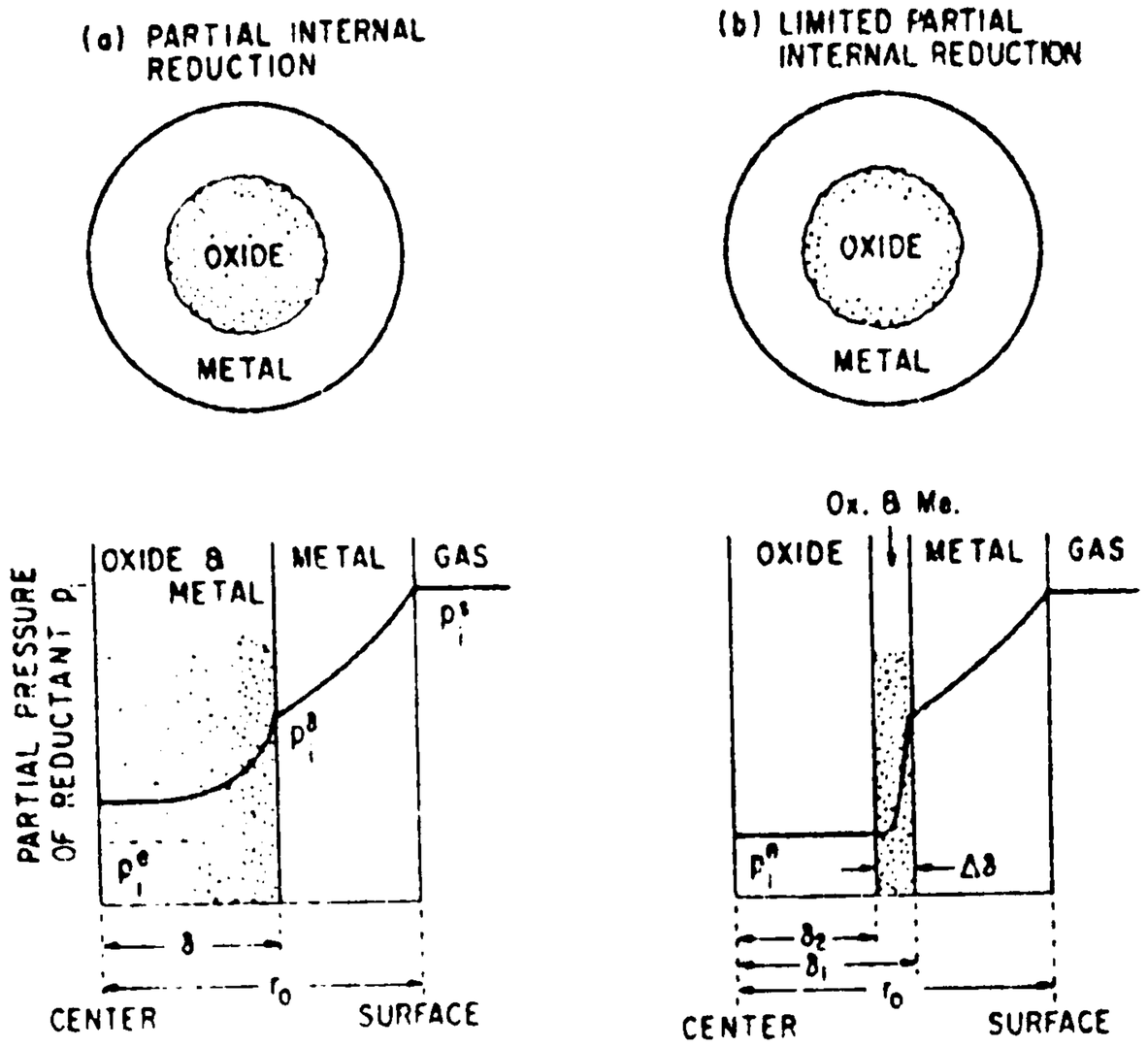

FIG. 38. Schematic representation of a) partial internal reduction, b) limited partial internal reduction, in the oxide core surrounded by porous metal shell.

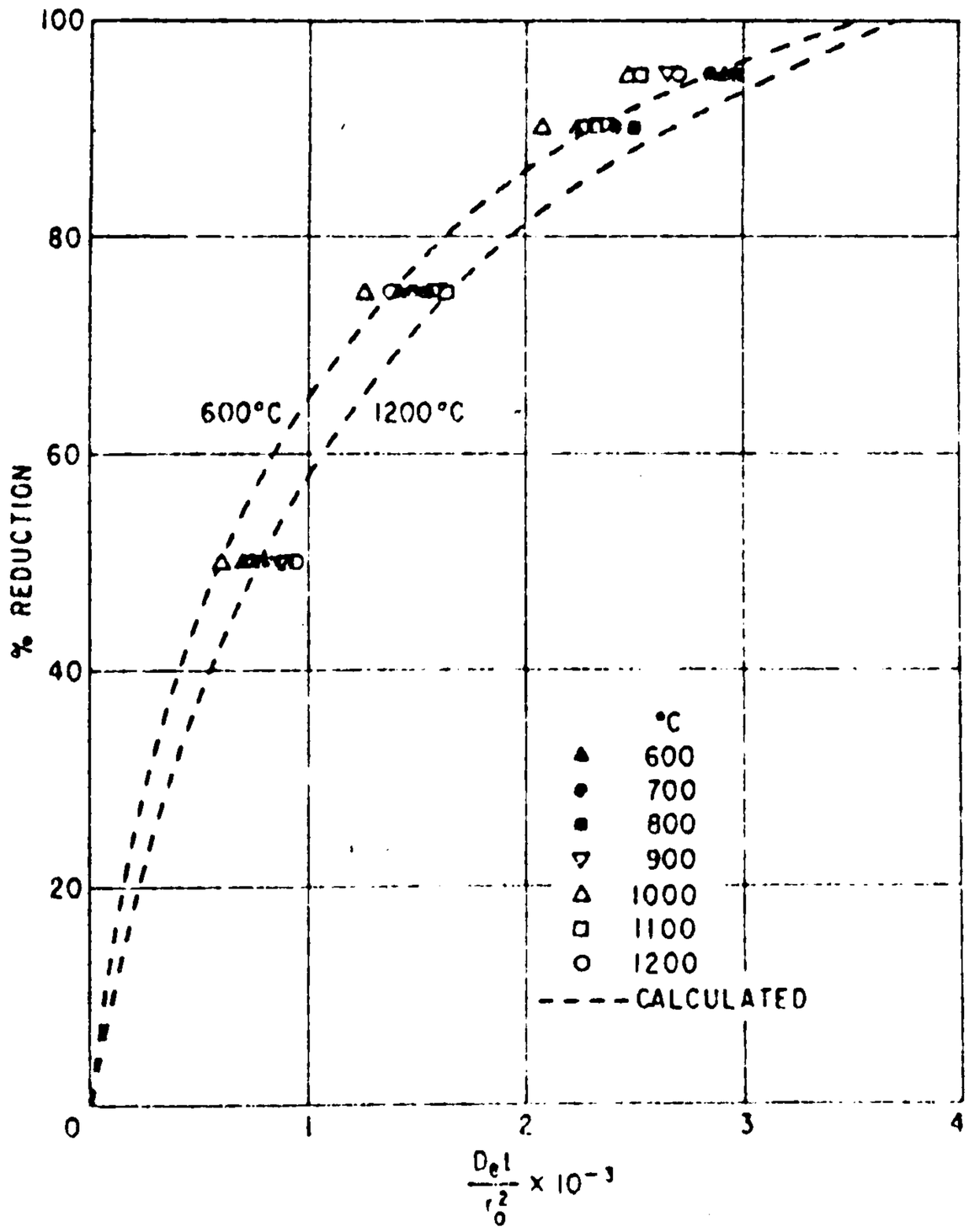

FIG. 39. Experimental results for H_2 reduction of hematite ore spheroids (10 mm dia) are compared with those calculated using three-zone model.

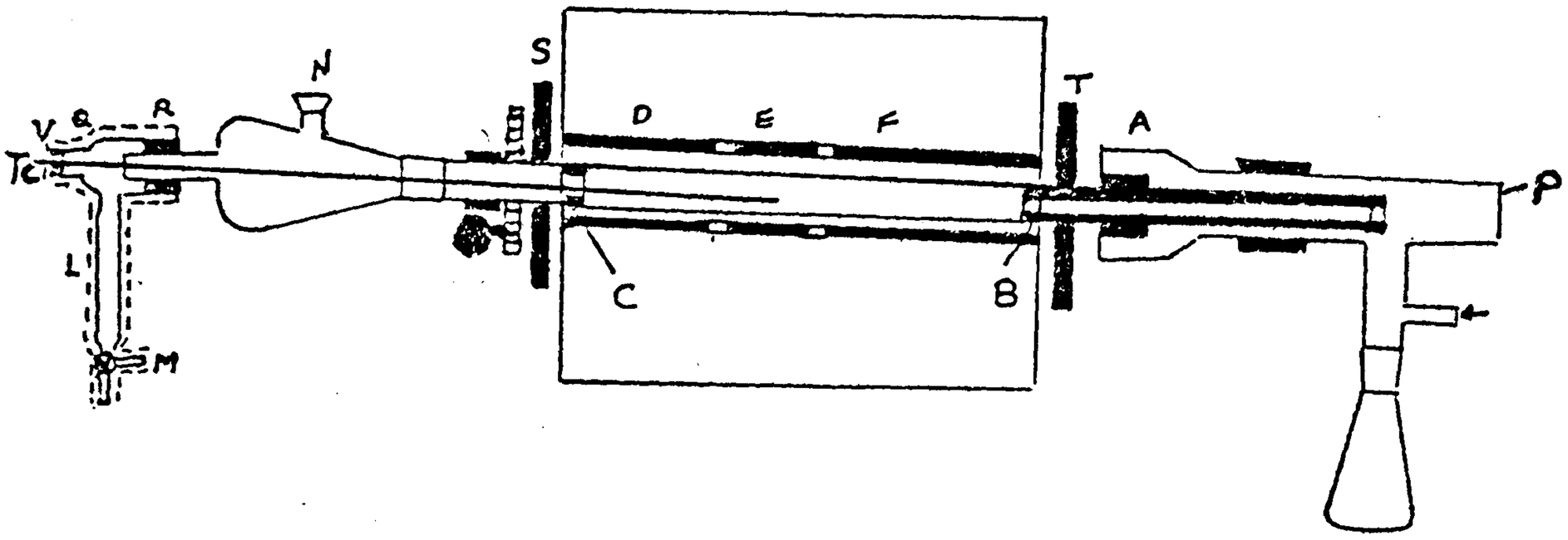

Fig. (40) Schematic drawing of the kiln.

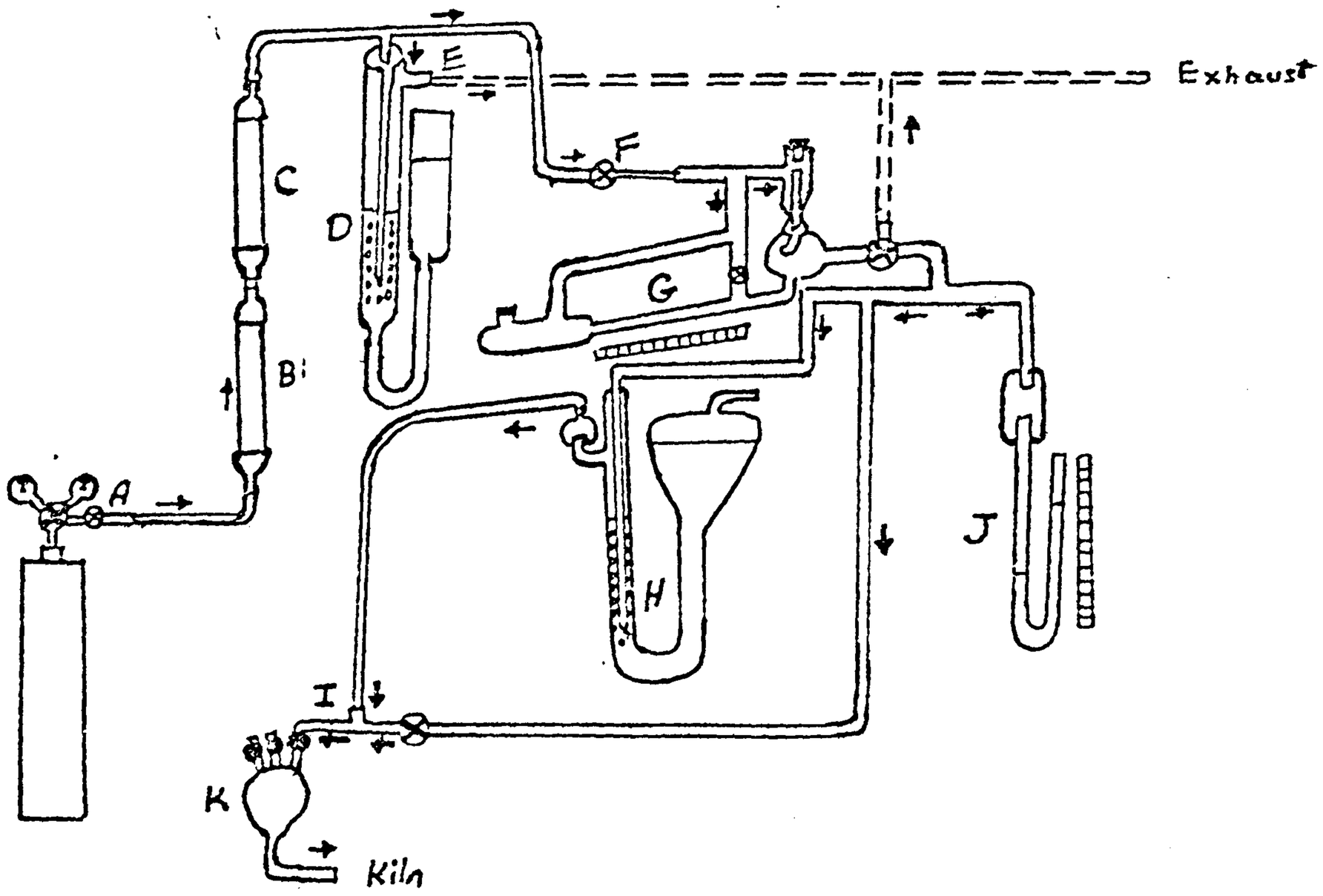

Fig. (41). Schematic drawing of the gas system.

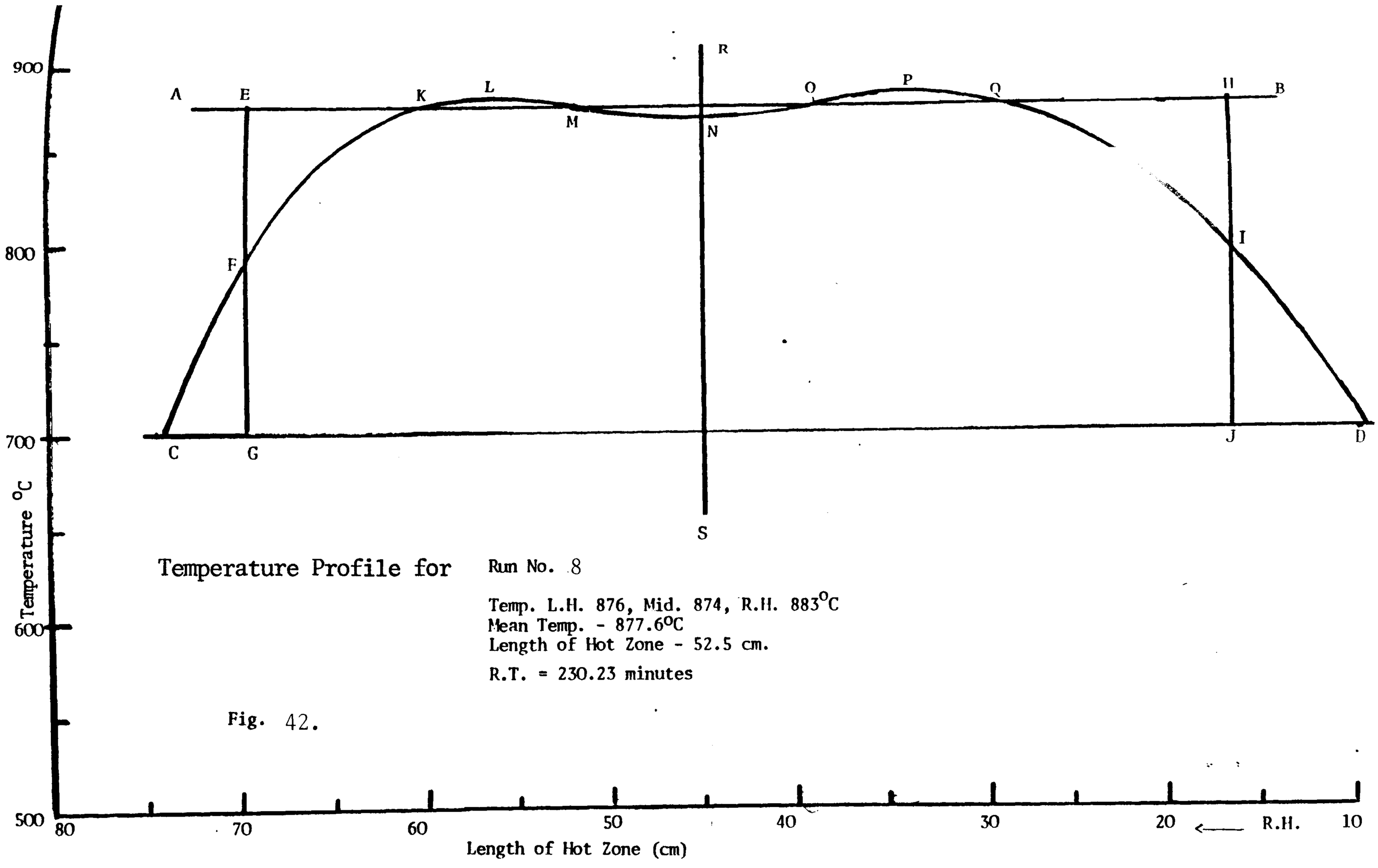

Temperature Profile for Run No. 8

Temp. L.H. 876, Mid. 874, R.H. 883°C
Mean Temp. - 877.6°C
Length of Hot Zone - 52.5 cm.

R.T. = 230.23 minutes

Fig. 42.

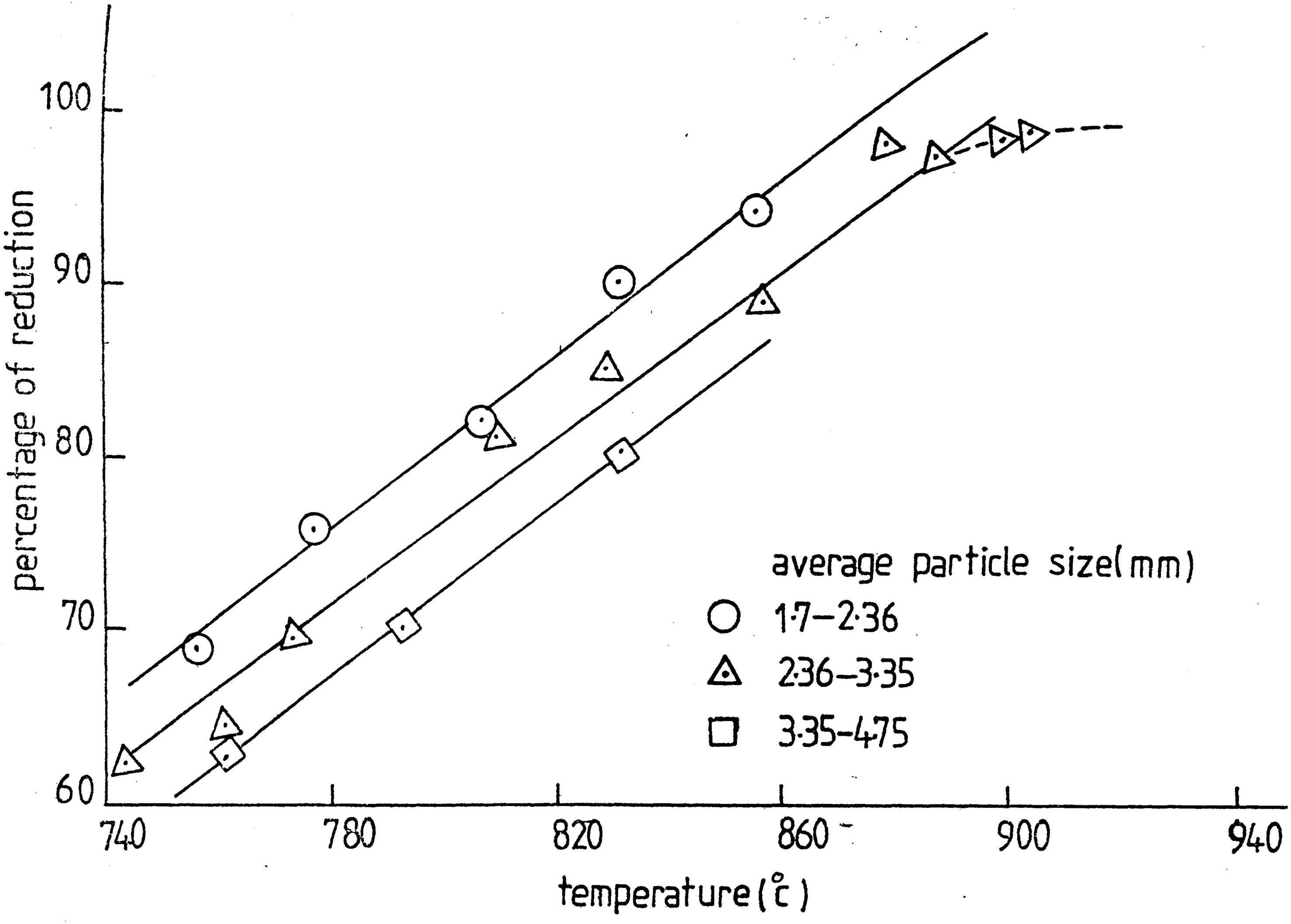

FIG. 43. THE EFFECT OF THREE DIFFERENT PARTICLE SIZES UPON PERCENTAGE REDUCTION FOR RUNS OF THE 1ST, 4TH AND 6TH SERIES.

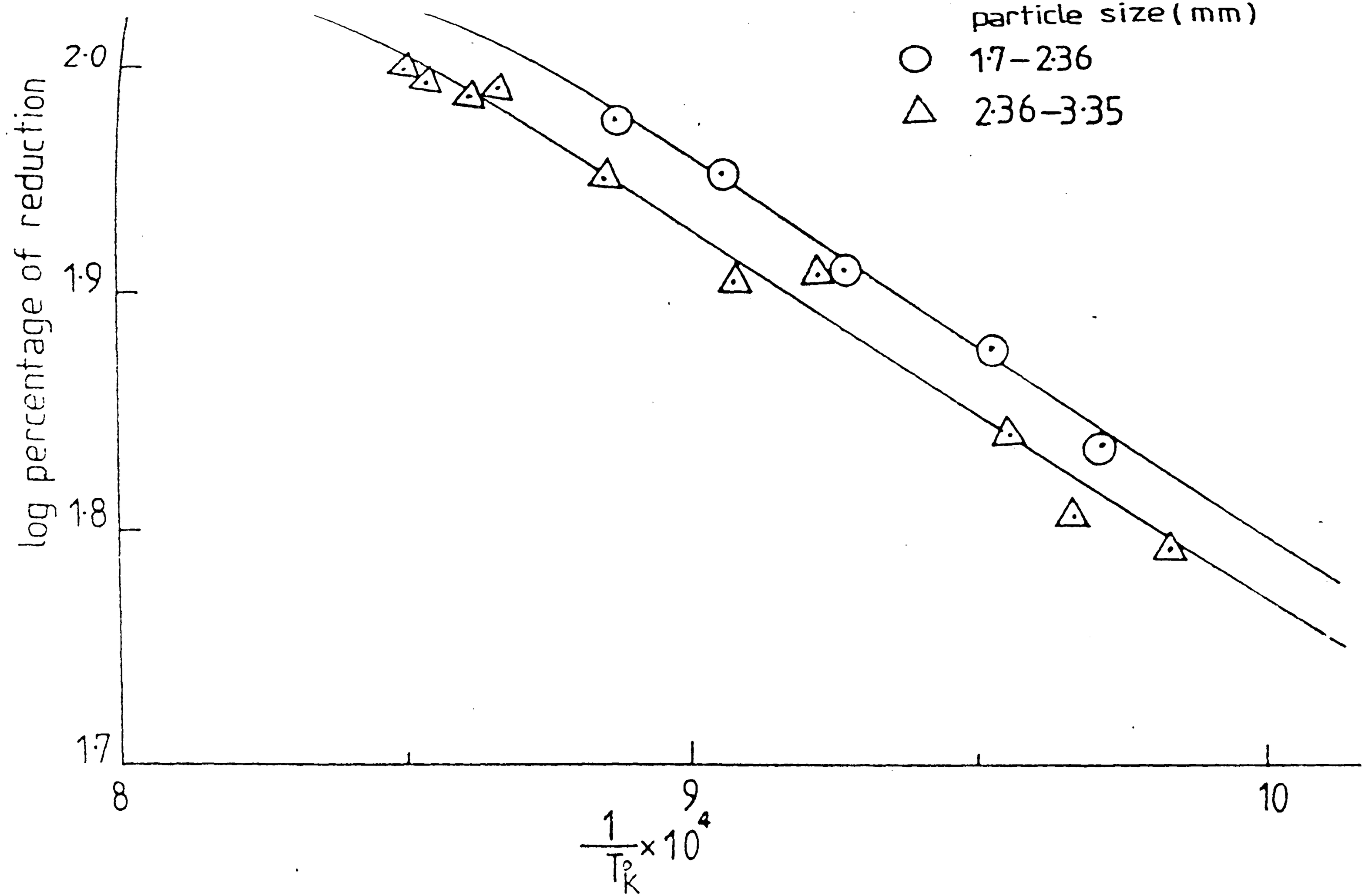

FIG. 44. THE EFFECT OF TWO DIFFERENT PARTICLES SIZES UPON THE LOGARITHM OF PERCENTAGE REDUCTION FOR TWO SERIES OF RUNS WITH ORE SIZES: 1.7-2.36 AND 2.36-3.35 (mm).

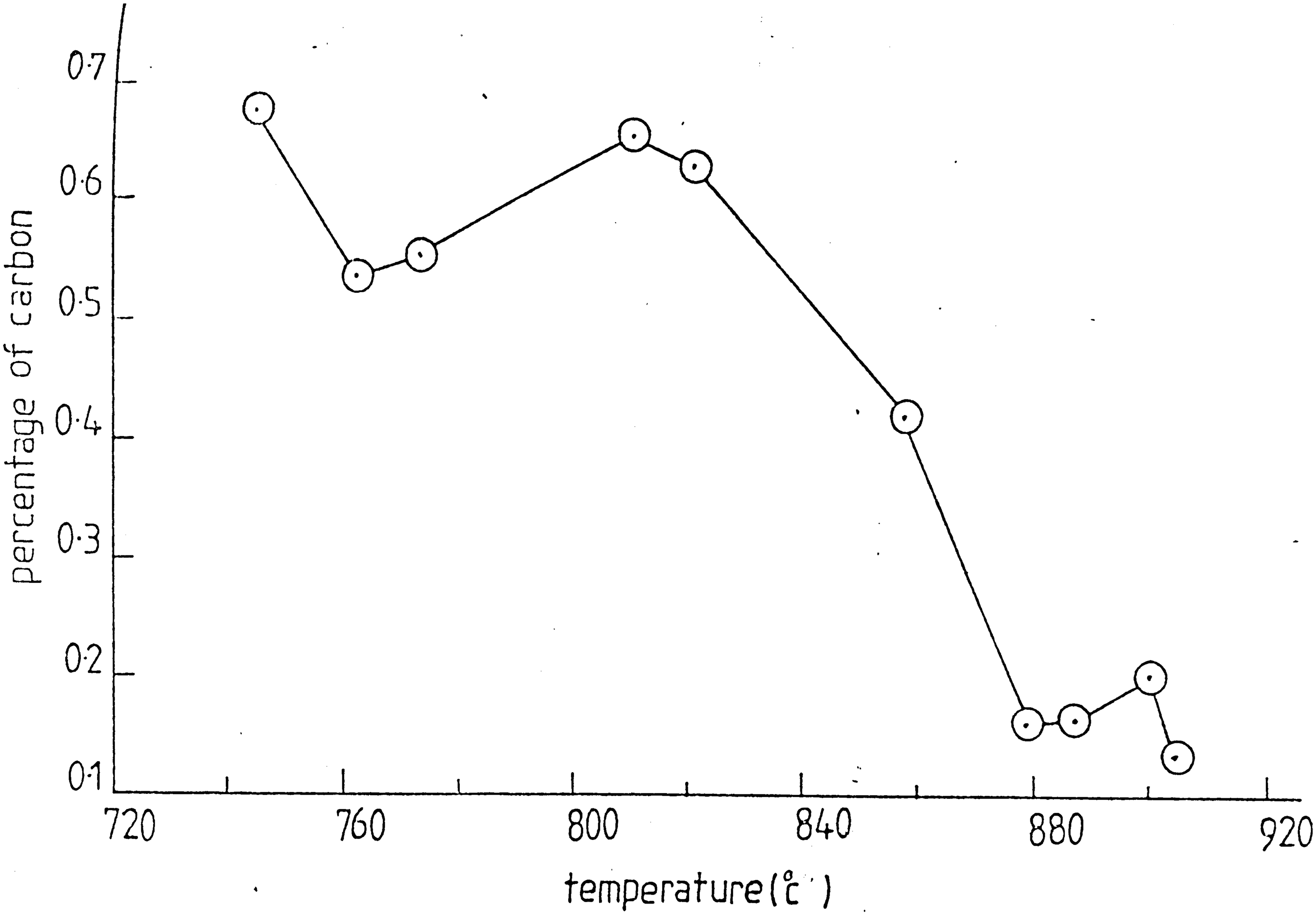

FIG. 45. THE CARBON CONTENT IN THE SPONGE FOR DIFFERENT RUNS OF THE 1ST SERIES WITH ORE SIZE 1.7-2.36 (mm).

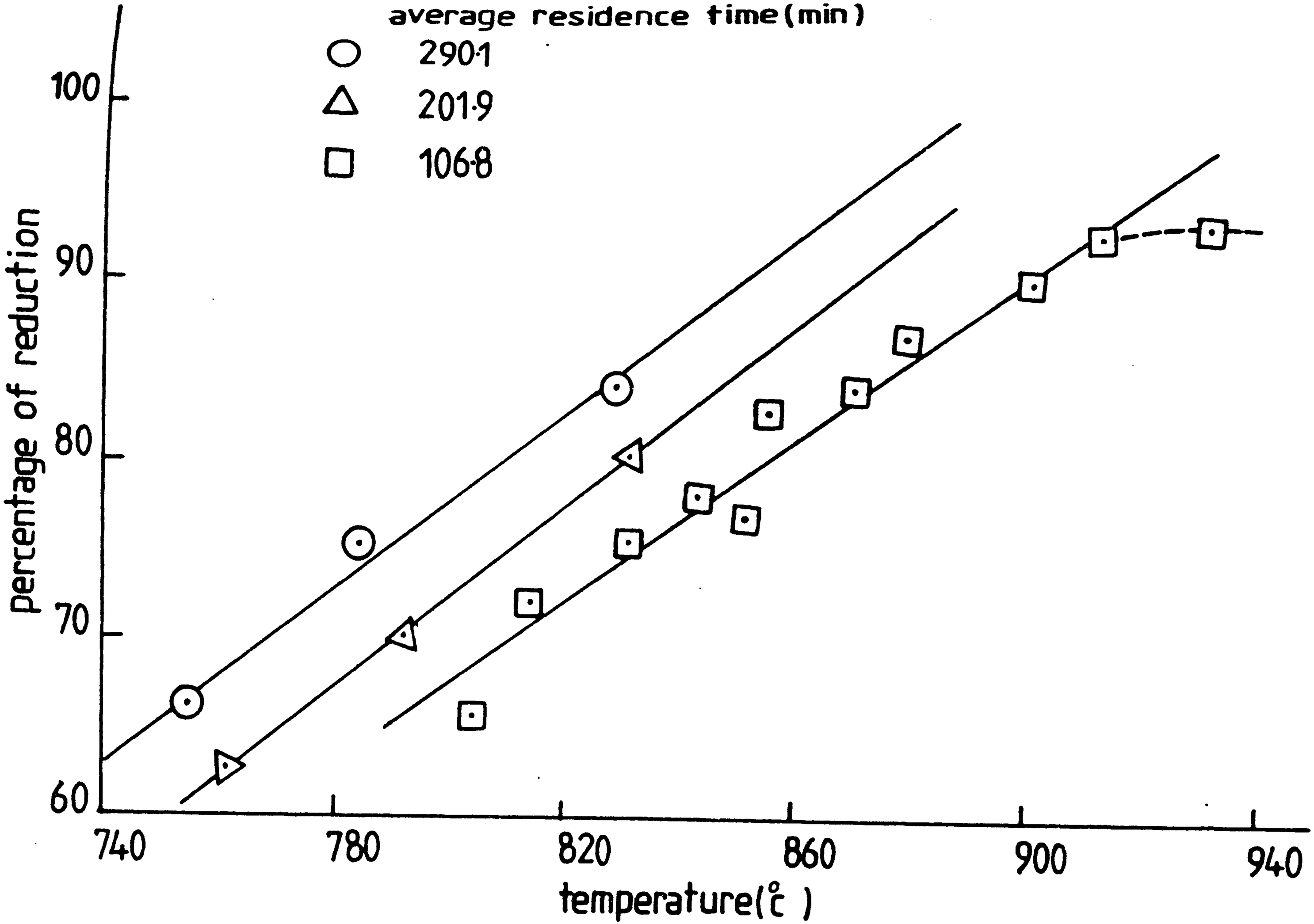

FIG. 46. THE EFFECT OF VARYING RESIDENCE TIME UPON THE RELATIONSHIP BETWEEN PERCENTAGE REDUCTION AND TEMPERATURE FOR THREE SERIES OF RUNS WITH ORE SIZE 3.35-4.75 (mm).

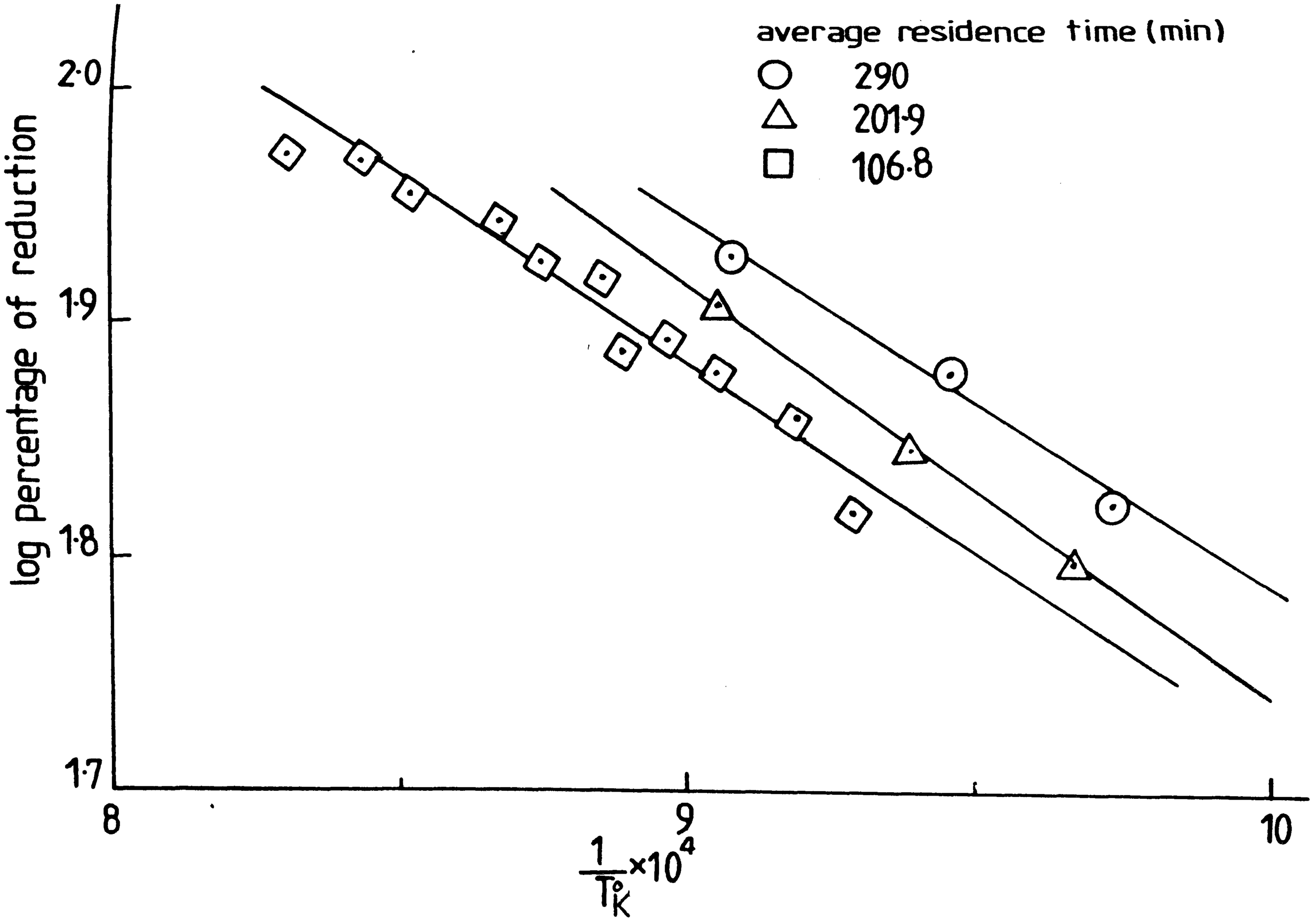

FIG. 47 THE EFFECT OF DIFFERENT RESIDENCE TIMES UPON LOGARITHM OF PERCENTAGE REDUCTION FOR THREE SERIES OF RUNS WITH ORE SIZE 3.35-4.75 (mm).

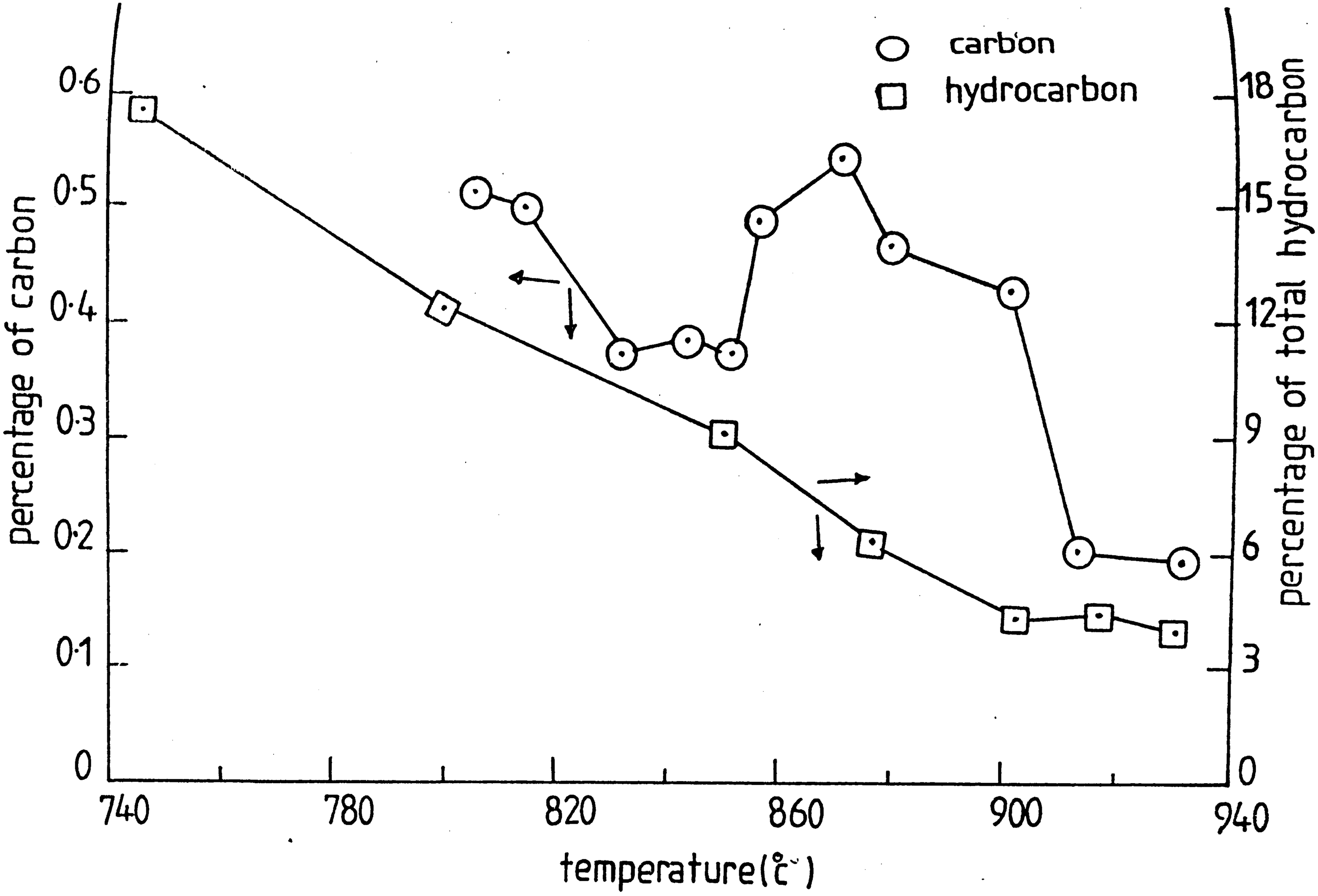

FIG. 48. THE CARBON CONTENT IN THE SPONGE FOR DIFFERENT RUNS OF THE 2ND SERIES WITH ORE SIZE 3.35-4.75 (mm) AND THE AMOUNT OF TOTAL HYDROCARBON IN OFF GASES FOR DIFFERENT TEMPERATURES.

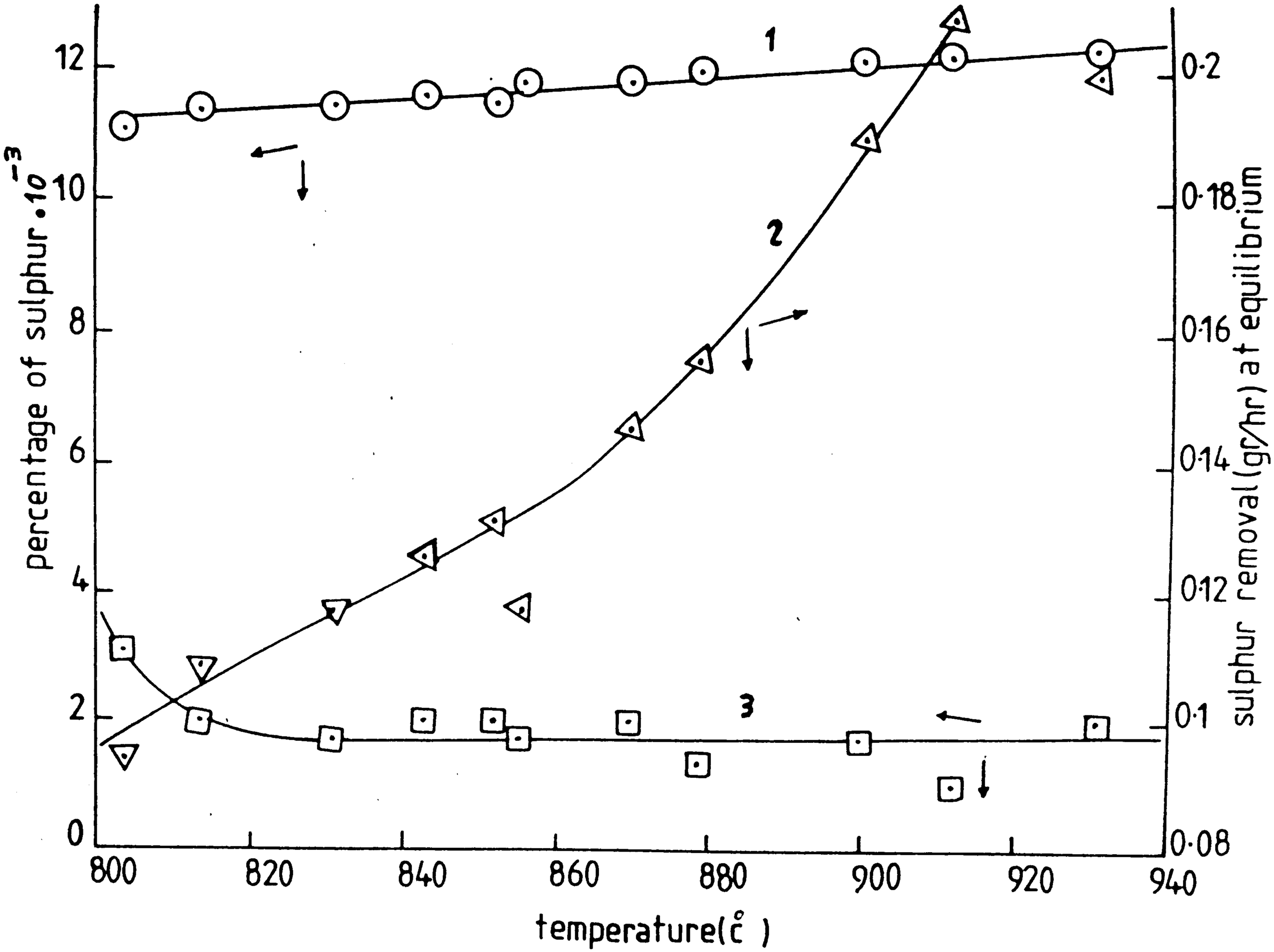

FIG. 49. THE SULPHUR CONTENT IN THE SPONGE FOR DIFFERENT RUNS OF 2ND SERIES WITH ORE SIZE 3.35-4.75(mm), CURVE (1) ASSUMING ZERO SULPHUR LOSS, CURVE (3) ANALYSED, AND CURVE (2) POTENTIAL FOR SULPHUR REMOVAL AT EQUILIBRIUM.

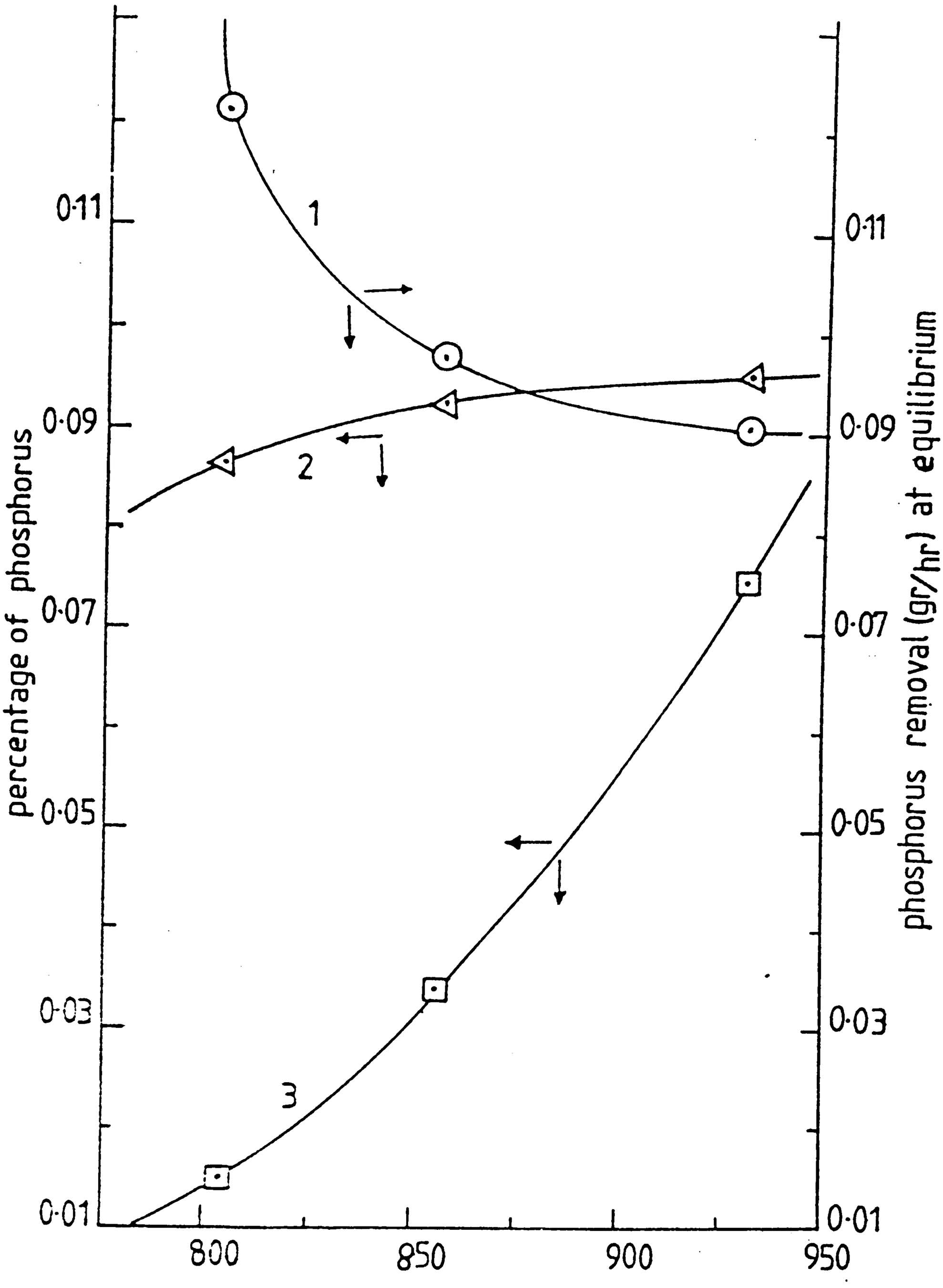

FIG. 50. THE PHOSPHORUS CONTENT IN THE SPONGE FOR THREE DIFFERENT RUN TEMPERATURES FOR THE 2ND SERIES WITH ORE SIZE 3.35-4.75(mm), CURVE (2) ASSUMING ZERO PHOSPHORUS LOSS, CURVE (3) ANALYSED, AND CURVE (1) POTENTIAL FOR PHOSPHORUS REMOVAL AT EQUILIBRIUM.

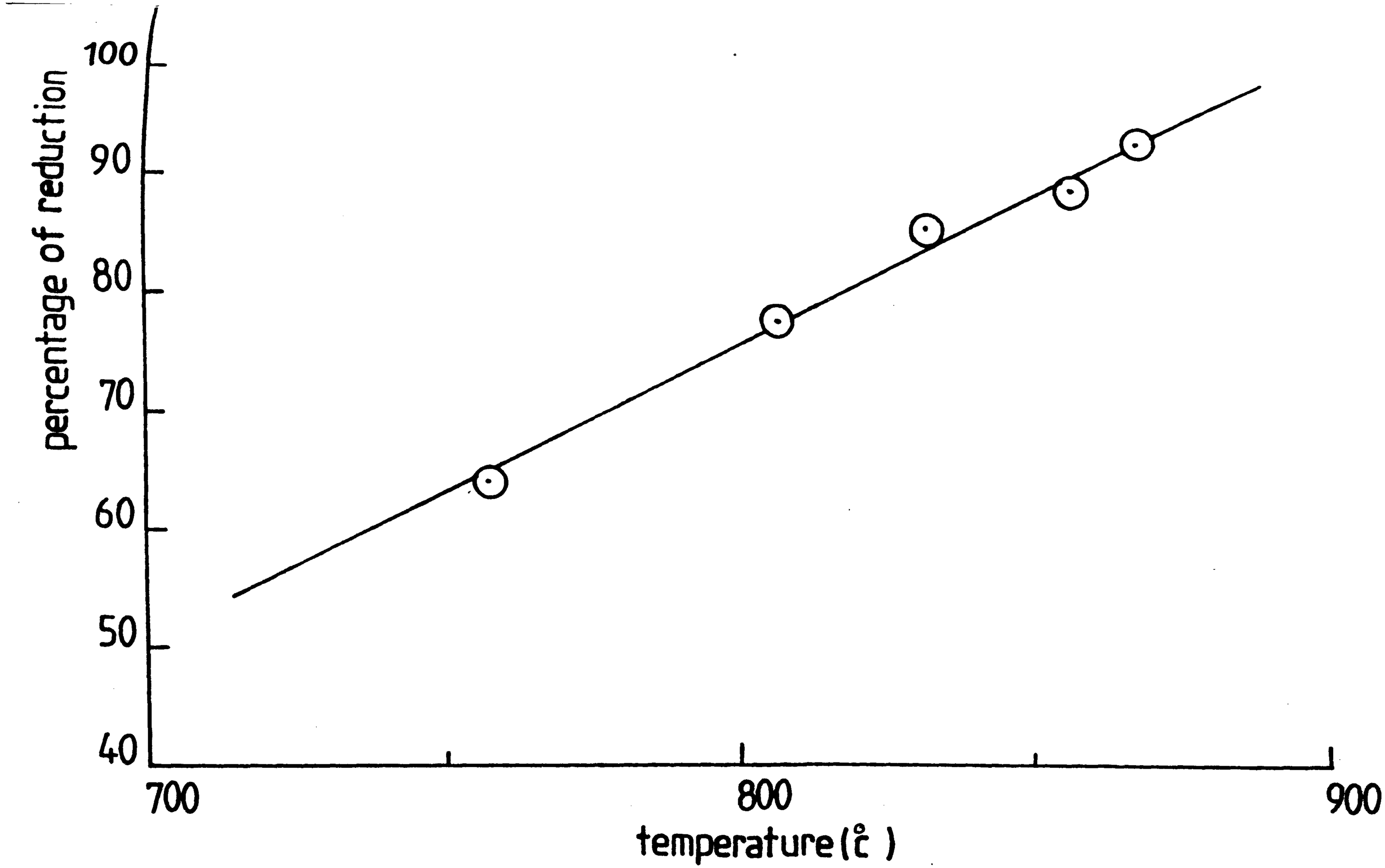

FIG. 51. THE EFFECT OF TEMPERATURE UPON PERCENTAGE REDUCTION FOR RUN SERIES WITH ORE SIZE 1.7-2.36 (mm) AND AVERAGE RESIDENCE TIME OF 164 (MINS.).

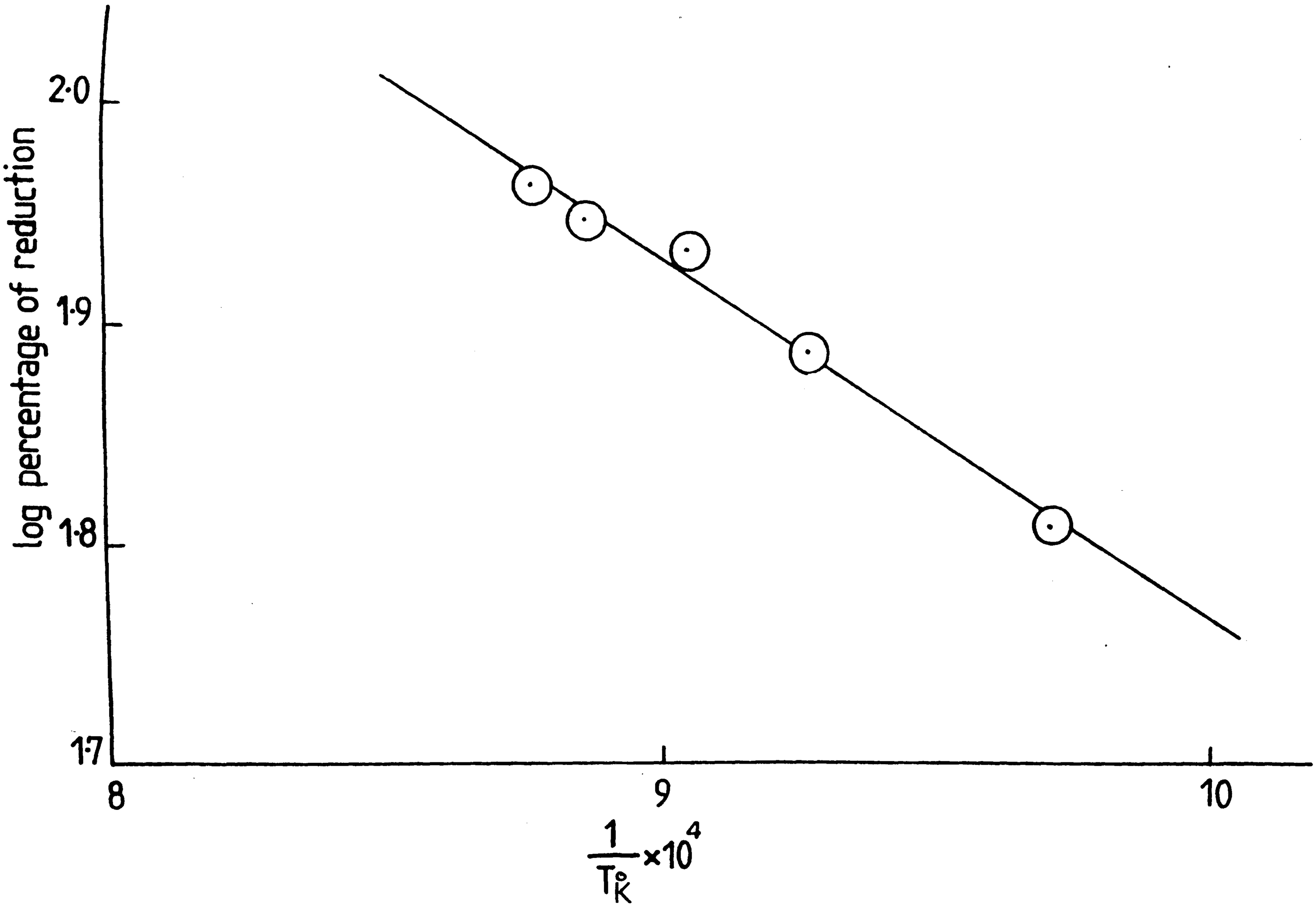

FIG. 52. THE RELATIONSHIP BETWEEN RECIPROCAL TEMPERATURE AND LOGARITHM OF PERCENTAGE REDUCTION FOR RUN SERIES WITH ORE SIZE 1.7-2.36(mm) AND AVERAGE RESIDENCE TIME OF 164 (MINS.).

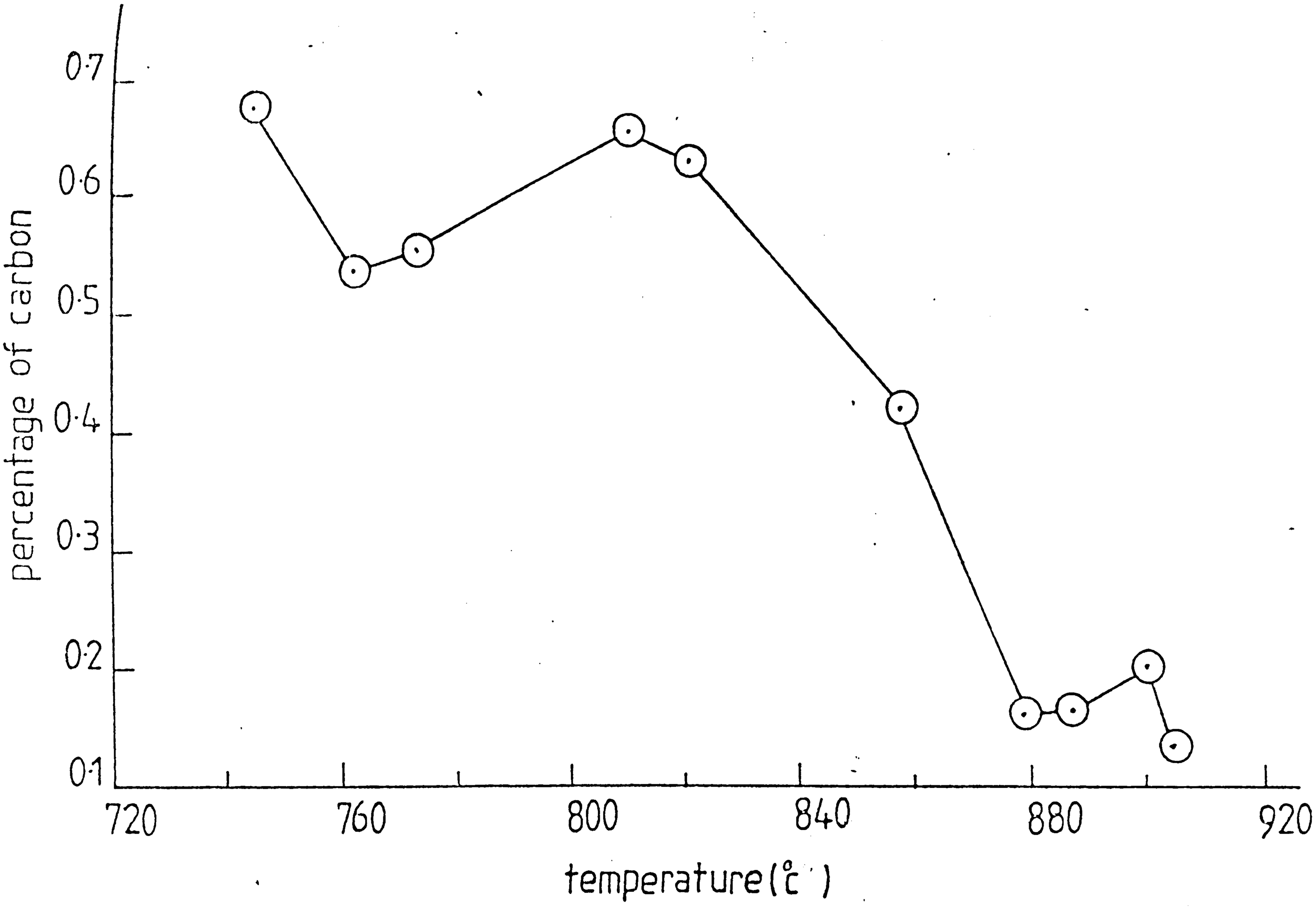

FIG. 45. THE CARBON CONTENT IN THE SPONGE FOR DIFFERENT RUNS OF THE 1ST SERIES WITH ORE SIZE 1.7-2.36 (mm).

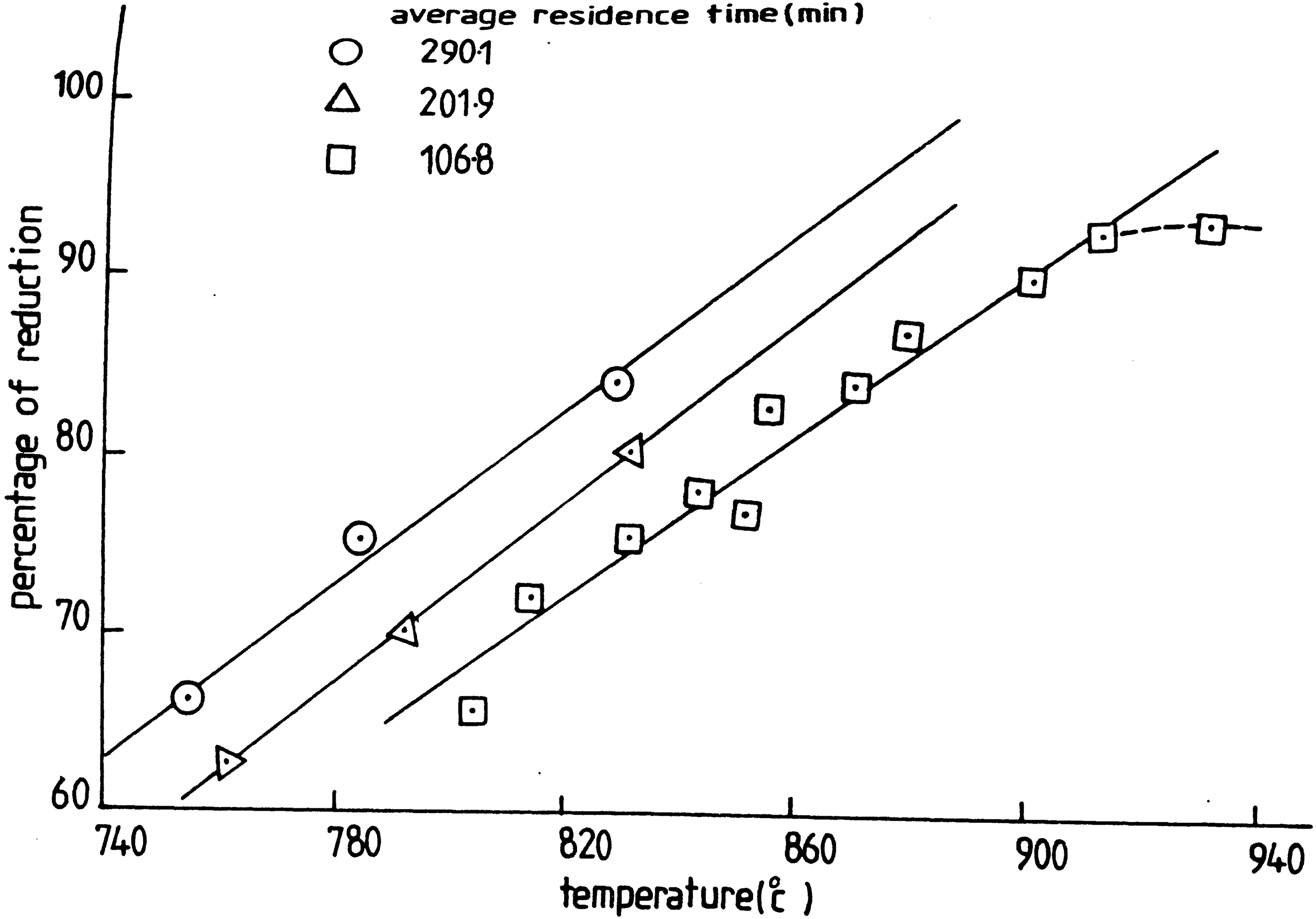

FIG. 46. THE EFFECT OF VARYING RESIDENCE TIME UPON THE RELATIONSHIP BETWEEN PERCENTAGE REDUCTION AND TEMPERATURE FOR THREE SERIES OF RUNS WITH ORE SIZE 3.35-4.75 (mm).

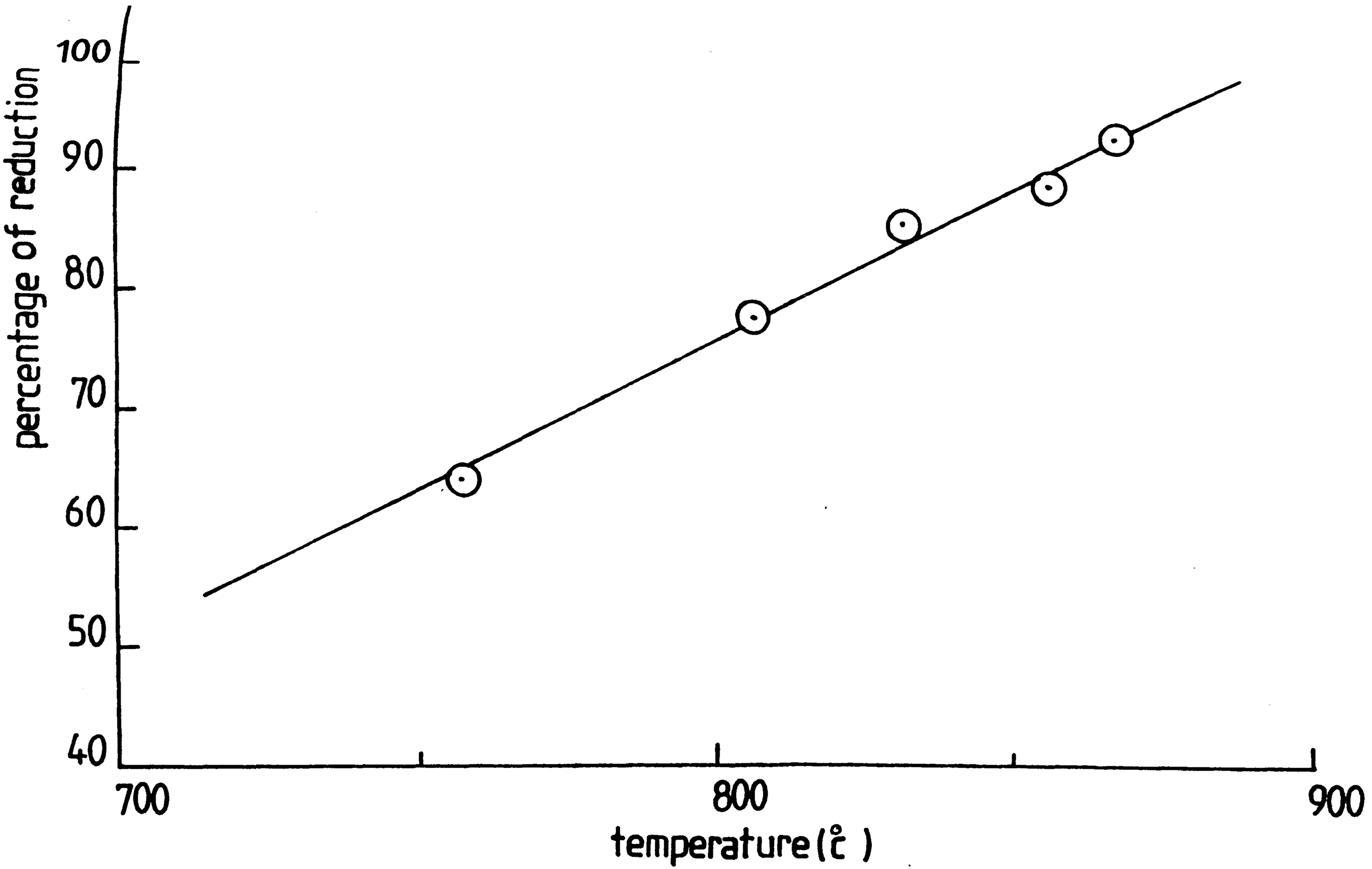

FIG. 51. THE EFFECT OF TEMPERATURE UPON PERCENTAGE REDUCTION FOR RUN SERIES WITH ORE SIZE 1.7-2.36 (mm) AND AVERAGE RESIDENCE TIME OF 164 (MINS.).

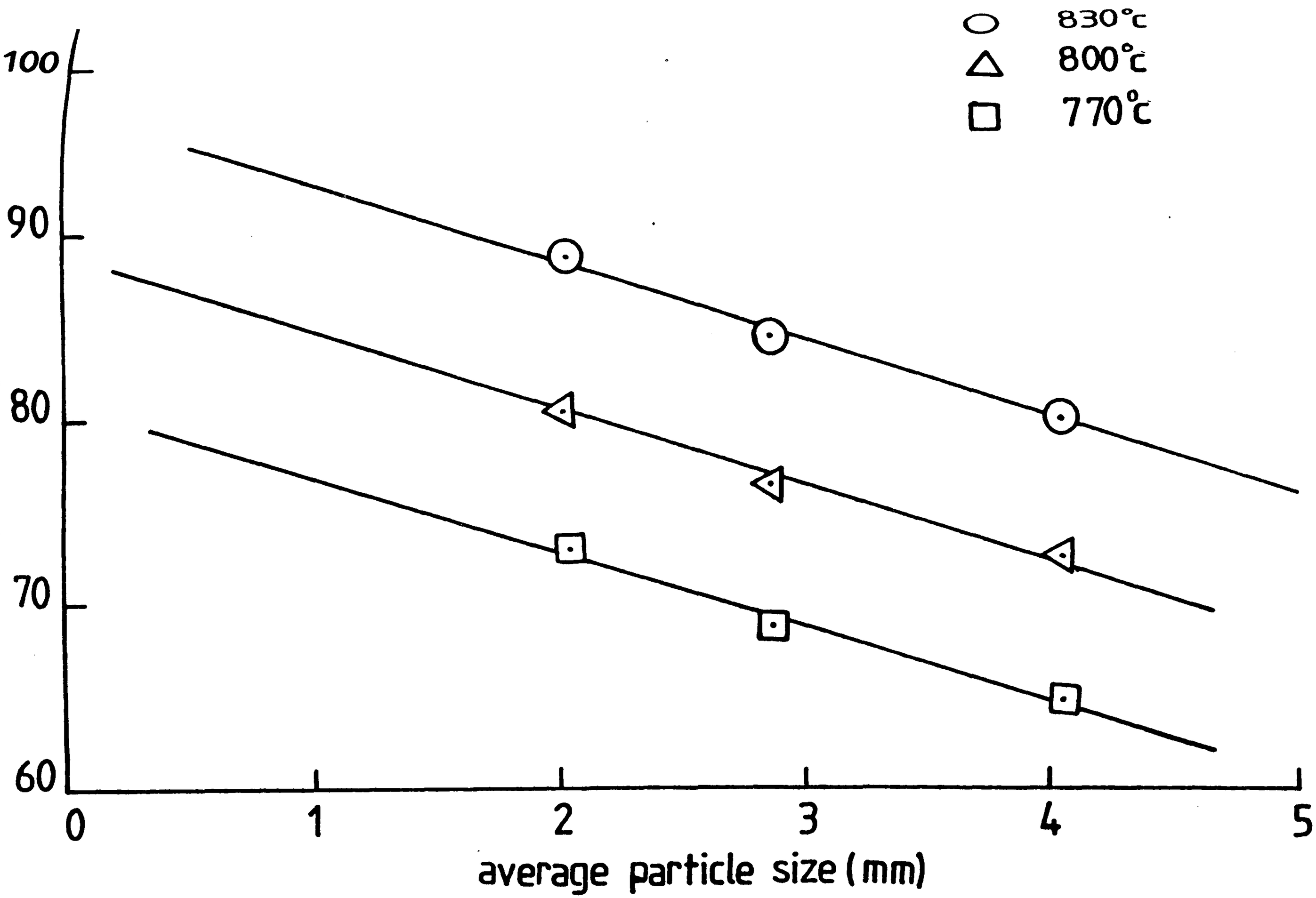

FIG. 53. THE EFFECT OF AVERAGE PARTICLE SIZE UPON PERCENTAGE REDUCTION FOR THREE DIFFERENT TEMPERATURES.

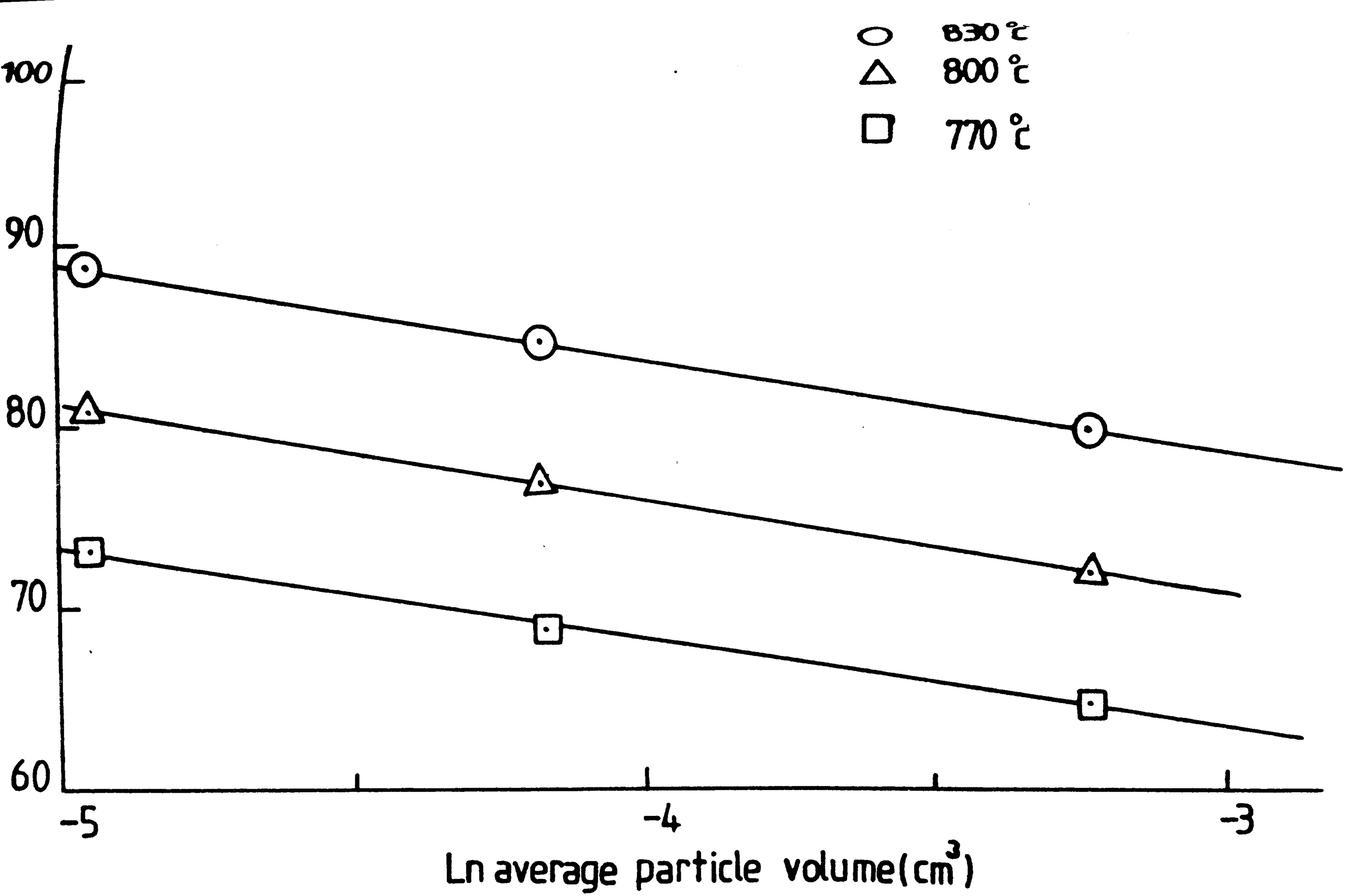

FIG. 54. THE RELATIONSHIP BETWEEN THE AVERAGE PARTICLE VOLUME AND PERCENTAGE REDUCTION FOR THREE DIFFERENT TEMPERATURES.

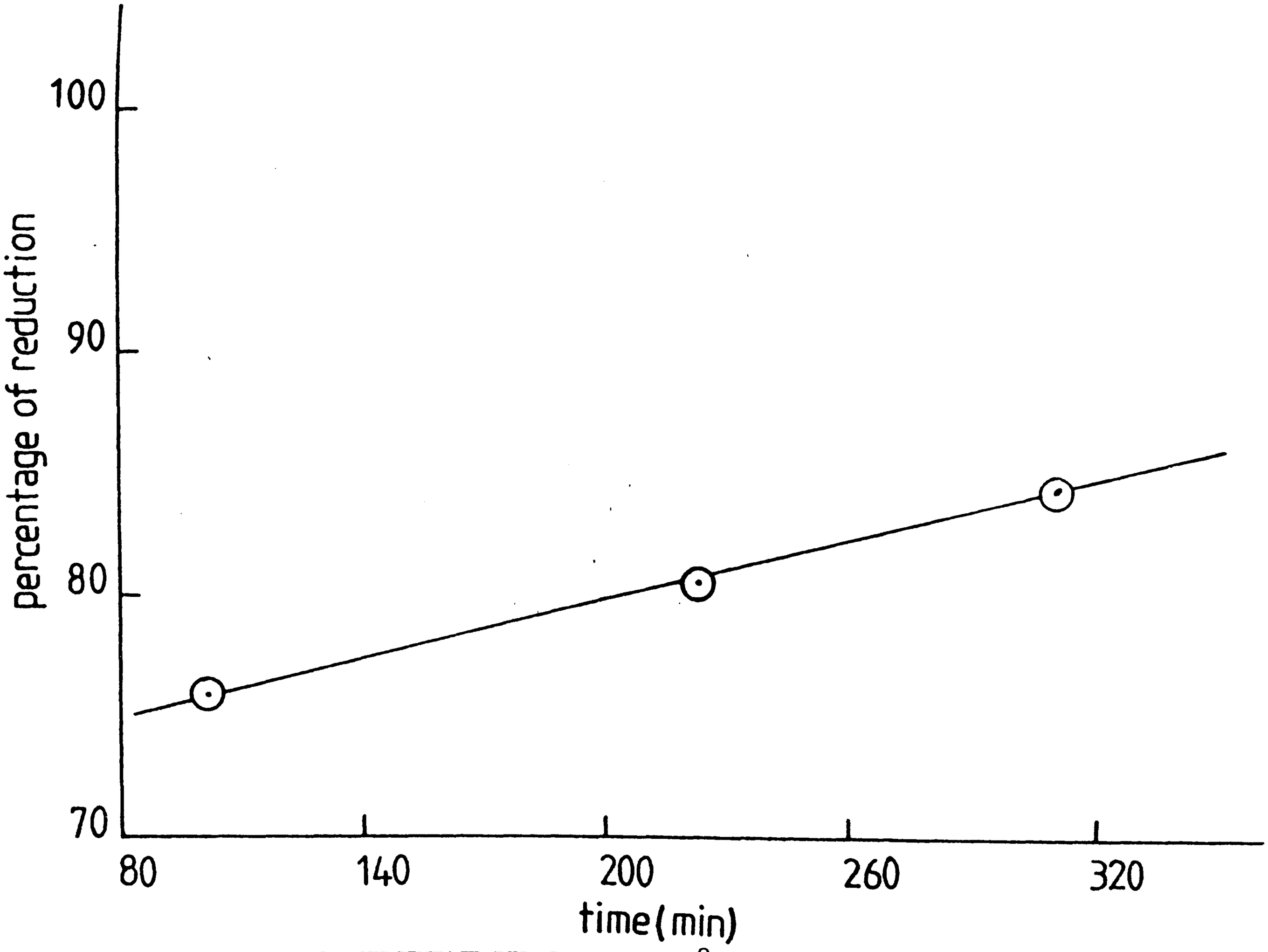

FIG. 55. THE EFFECT OF RESIDENCE TIME UPON PERCENTAGE REDUCTION AT 831°C FOR THREE DIFFERENT SERIES OF RUNS WITH ORE SIZE 3.35-4.75 (mm).

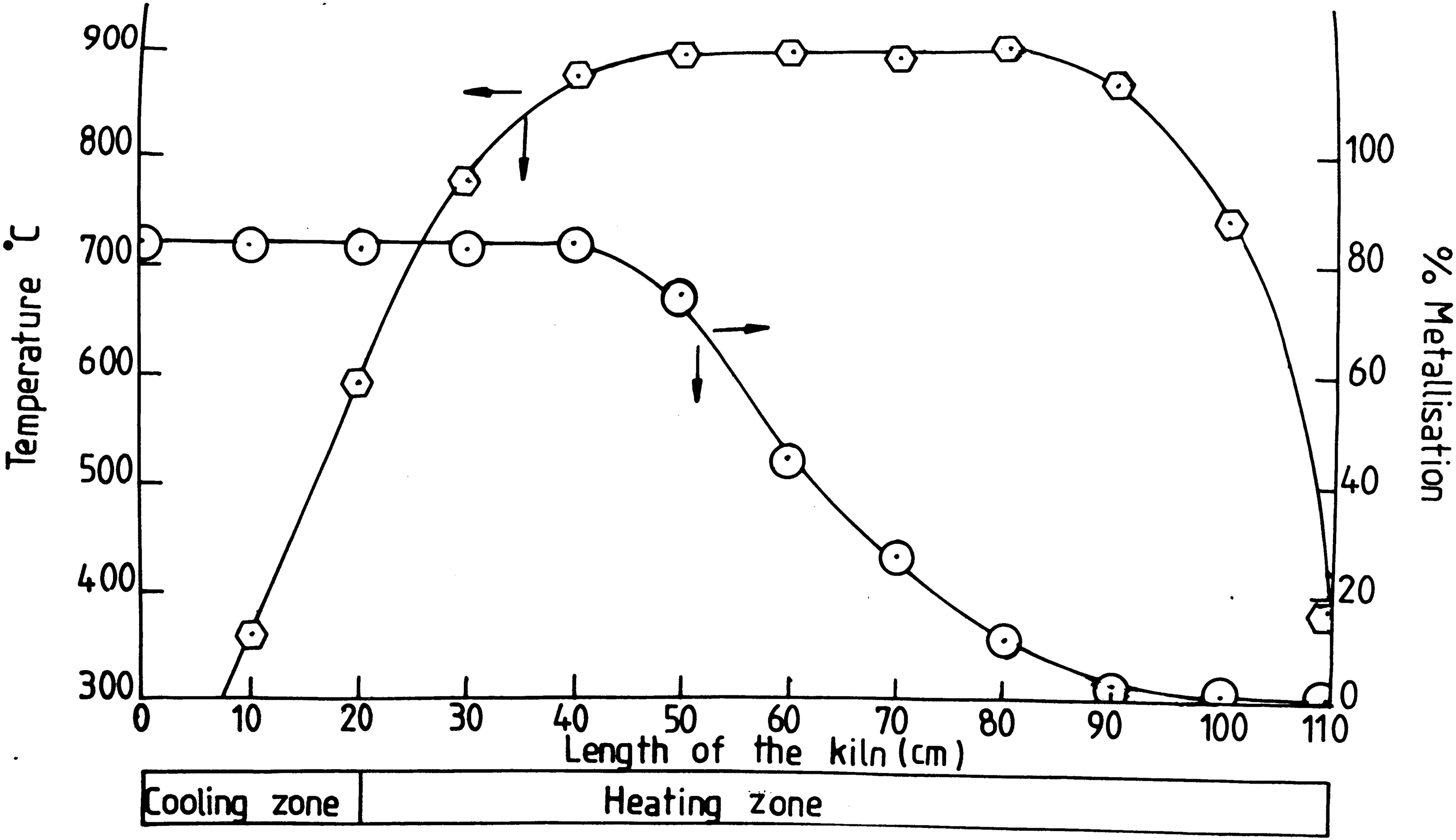

Fig. 56. The progress of metallisation along the kiln length for the run series (RP_2S_7)

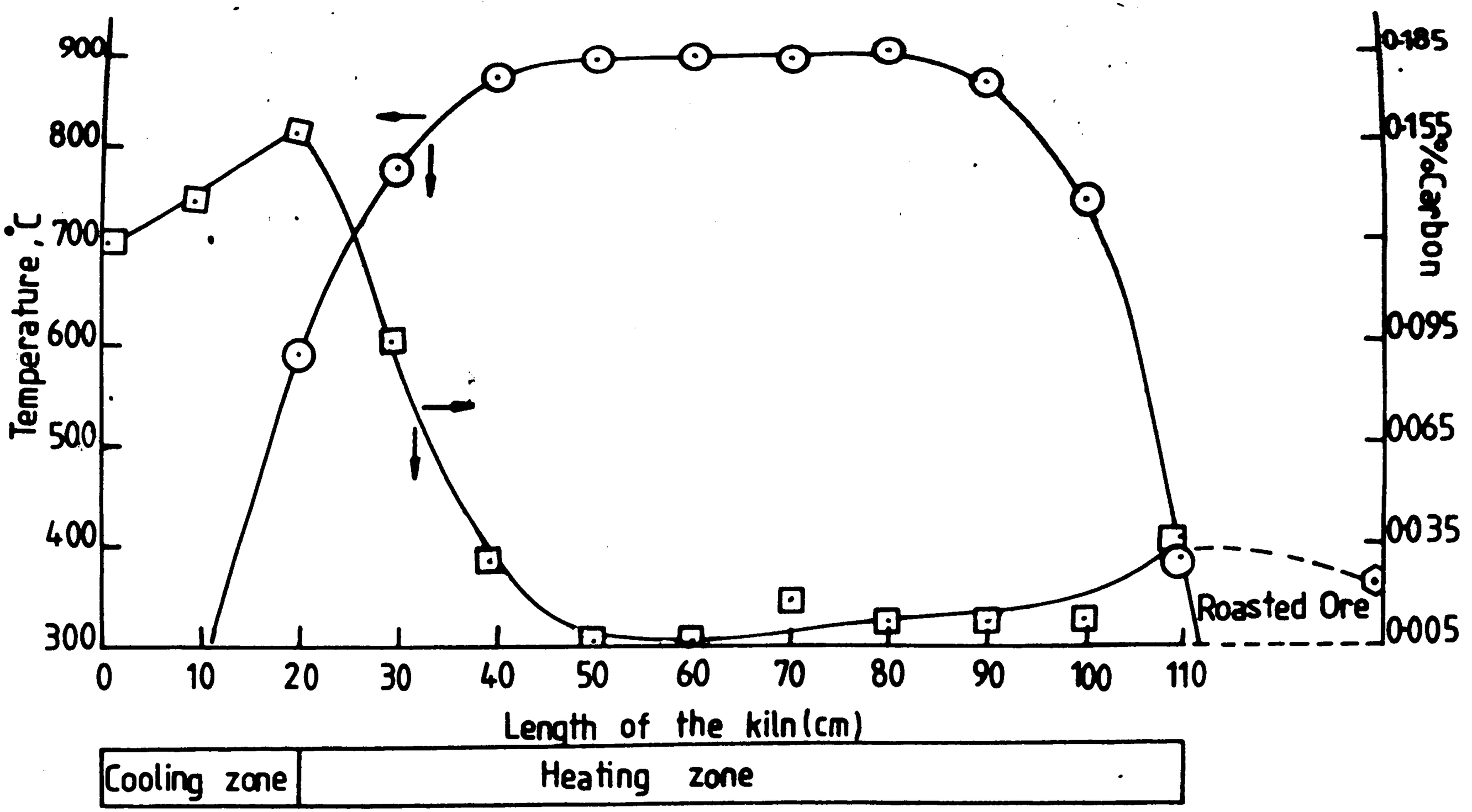

Fig. 57. The carbon content of the sponge iron at different temperature and stage of reduction along the length of the kiln for the run series (RP_2S_7).

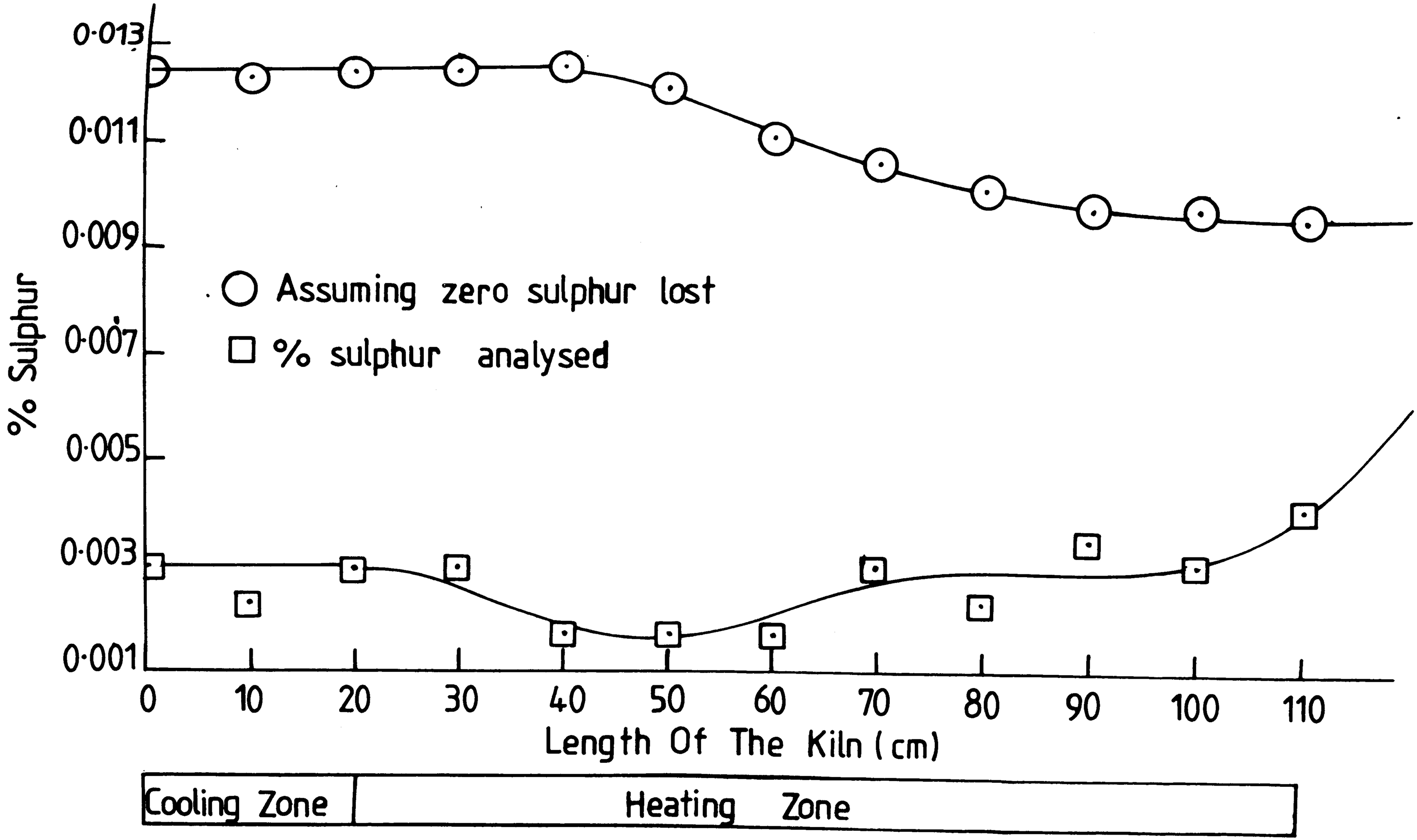

Fig. 58. The sulphur content of the sponge iron along the length of the kiln for the run series (RP_2S_7).

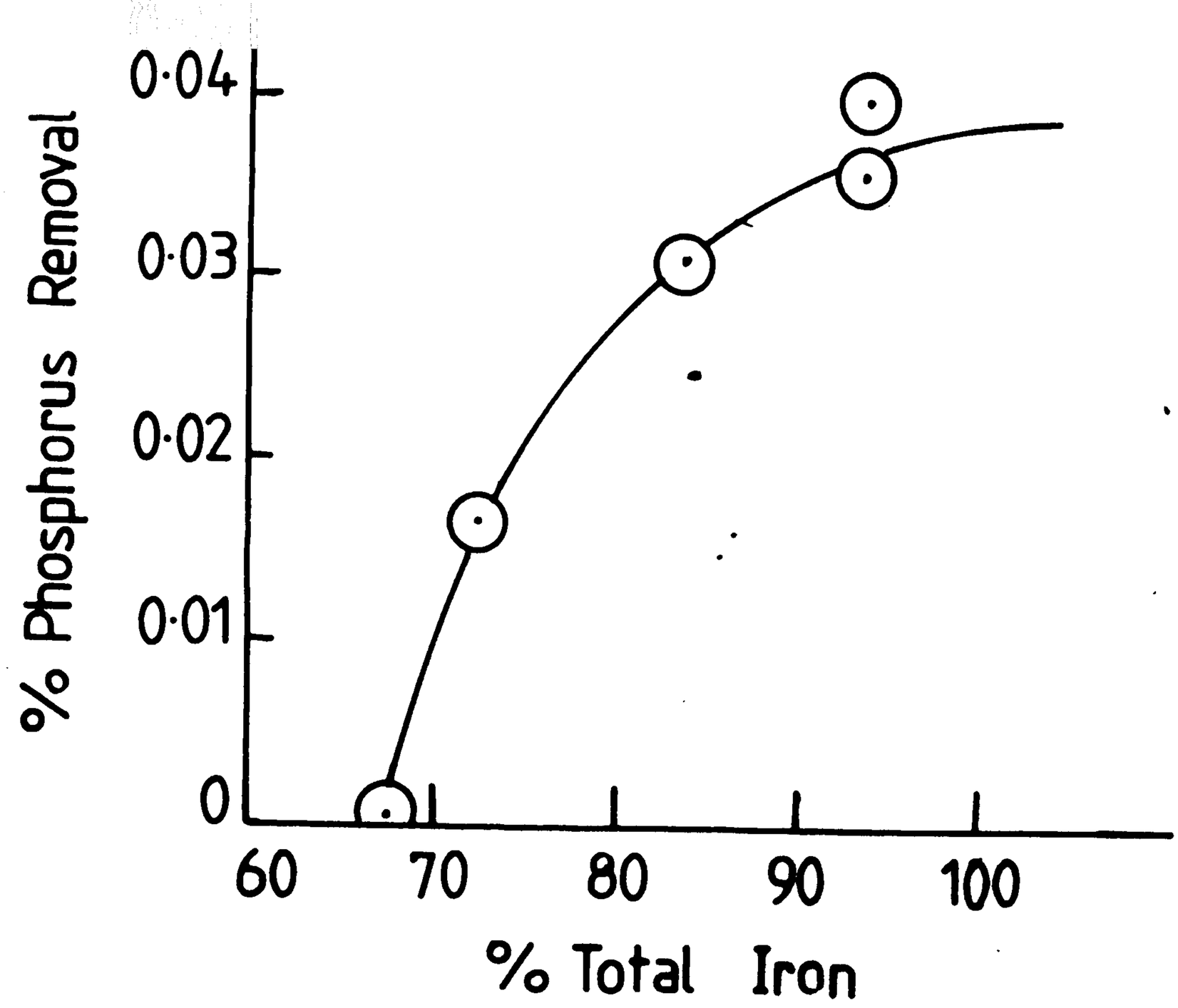

Fig. 60. The relationship between % Total iron and phosphorus removal in the samples along the length of the kiln for run series (RP_2S_7)

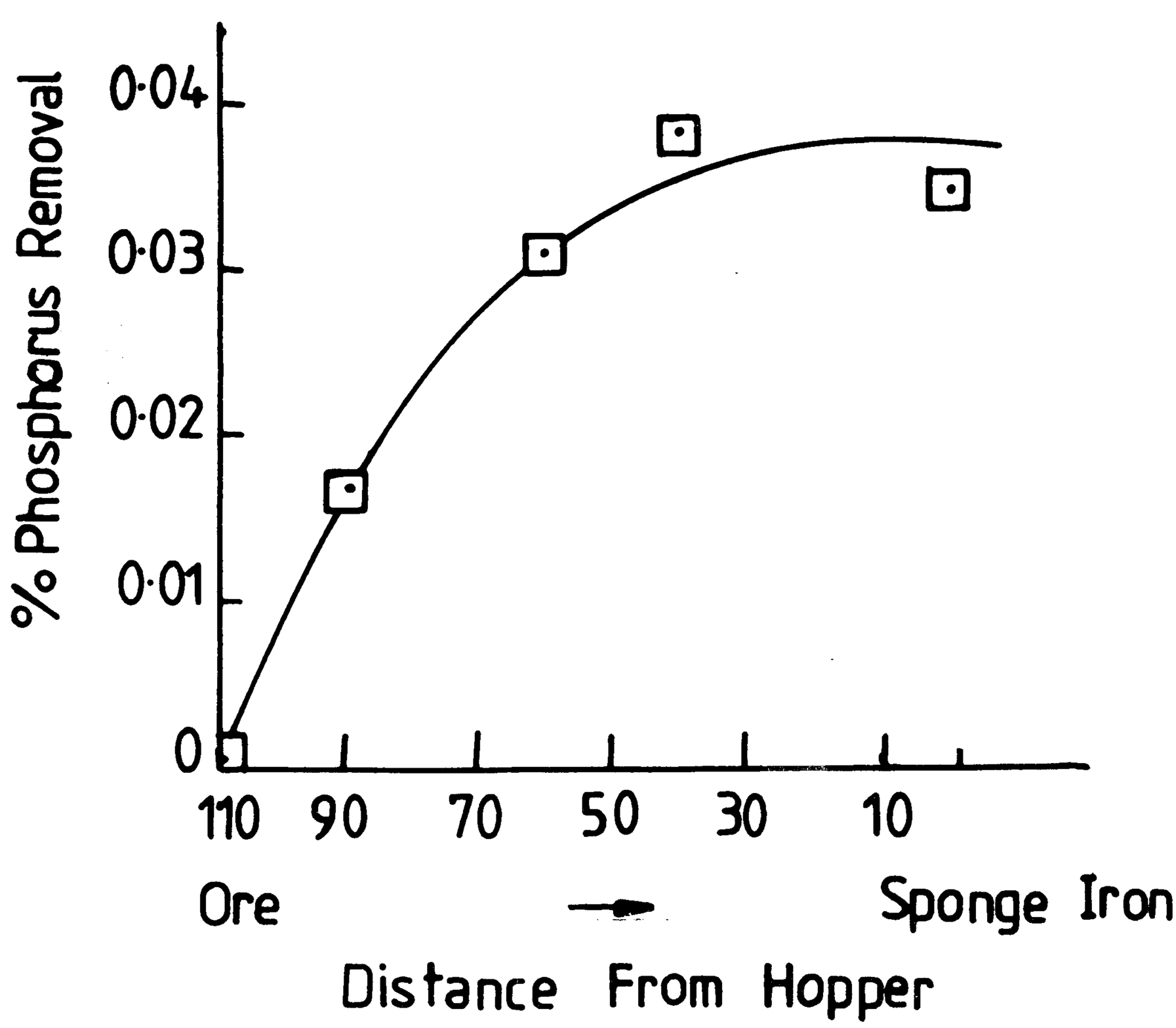

Fig. 59. The phosphorus removal along the length of the kiln for run series (RP_2S_7).

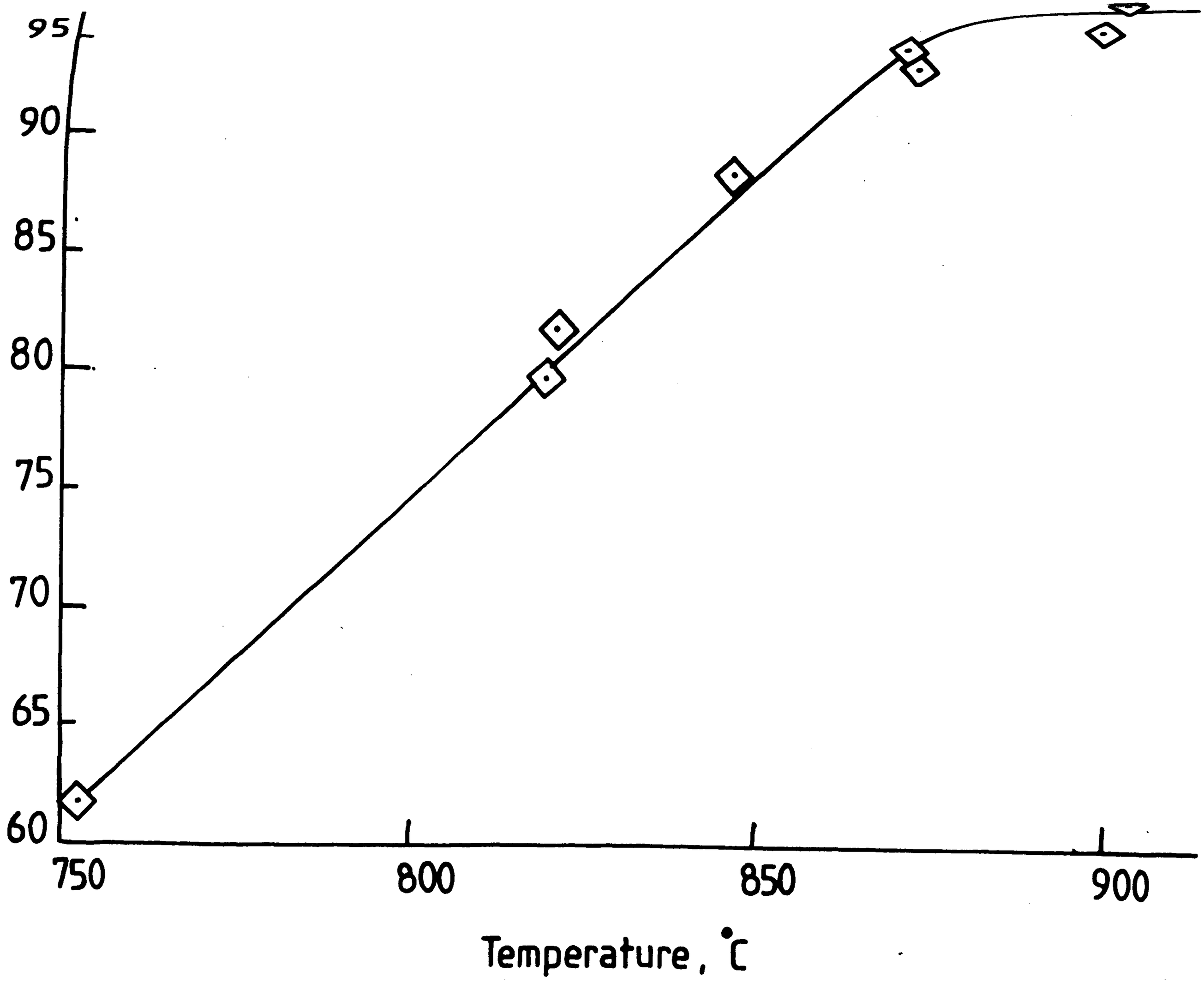

Figure 61. The effect of temperature (^{o}C) upon the percentage reduction for ore sized 3.35 - 4.75 mm, run series (RP_2S_8)

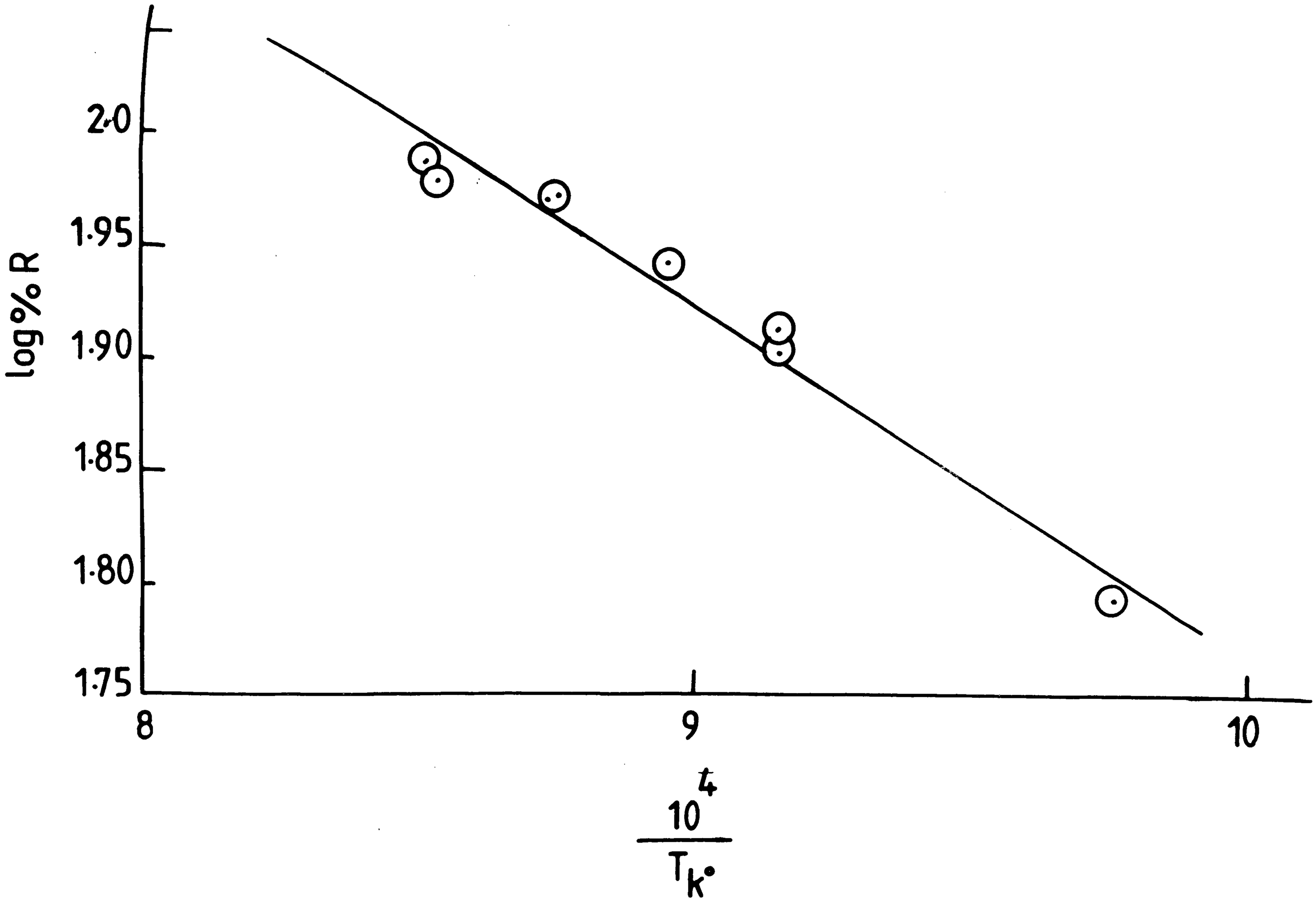

Fig. 62. The relationship between logarithm of percentage reduction and reciprocal of temperature (K^O) for the run series (RP_2S_8).

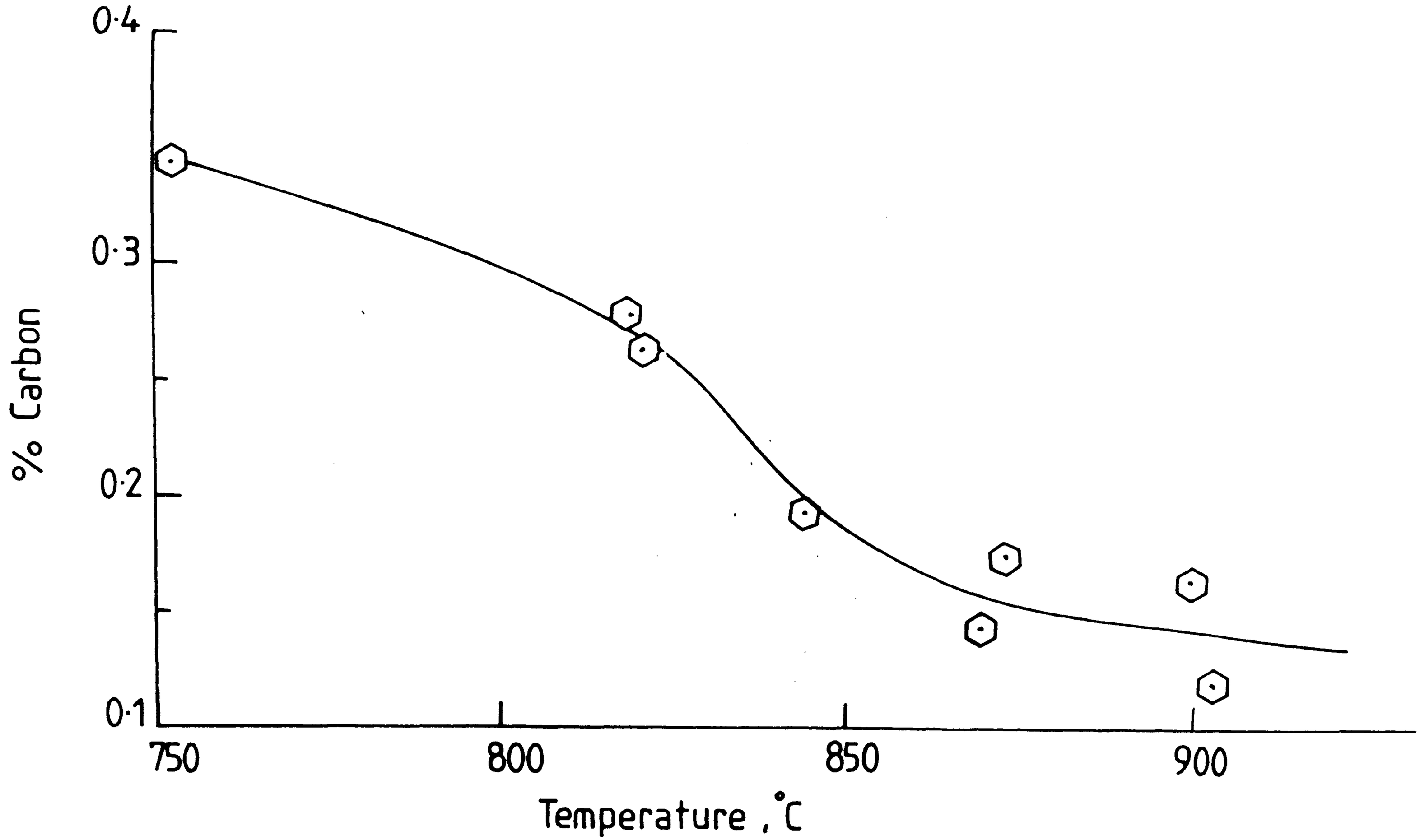

Fig. 63. The effect of temperature upon carbon content in the sponge iron for the run series (RP_2S_8).

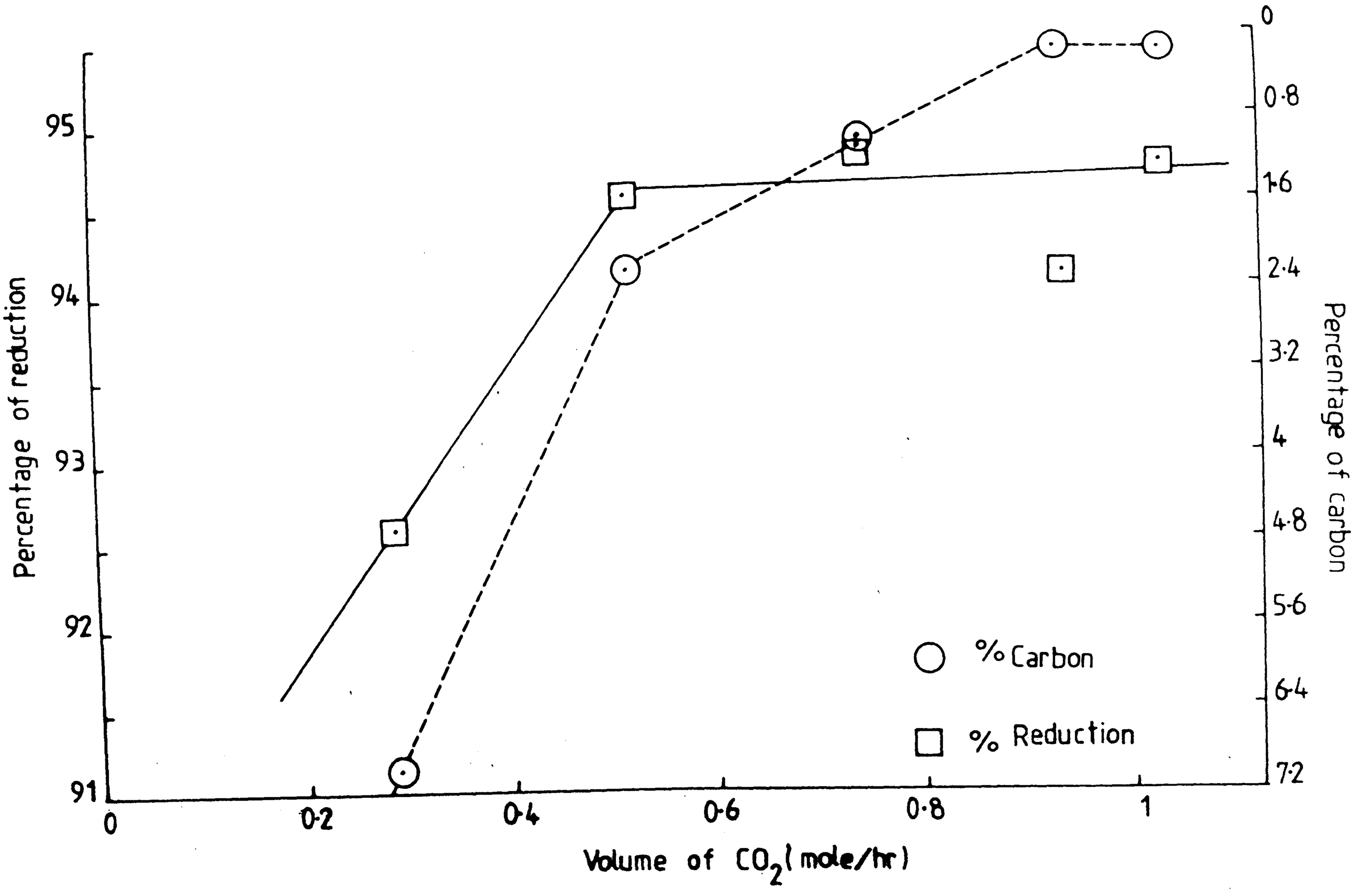

Fig. 64. The effect of amount of oxidant (CO_2) in the mixture of input gases upon the percentage reduction and the amount of carbon content in the sponge iron, for the run series (RP_2S_9).

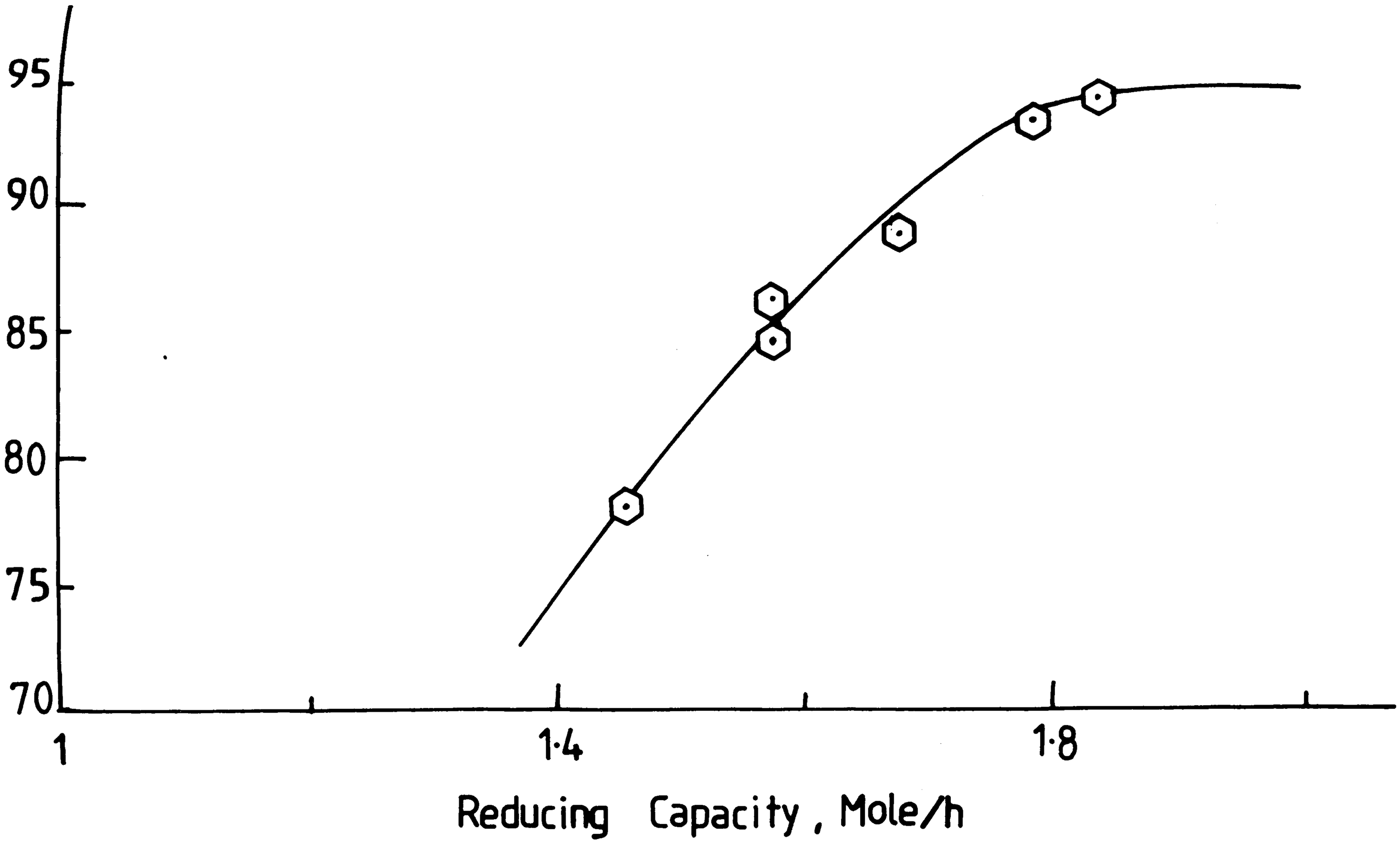

Fig. 65. The effect of the reducing capacity upon the percentage of reduction for run series (RP_2S_{10}).

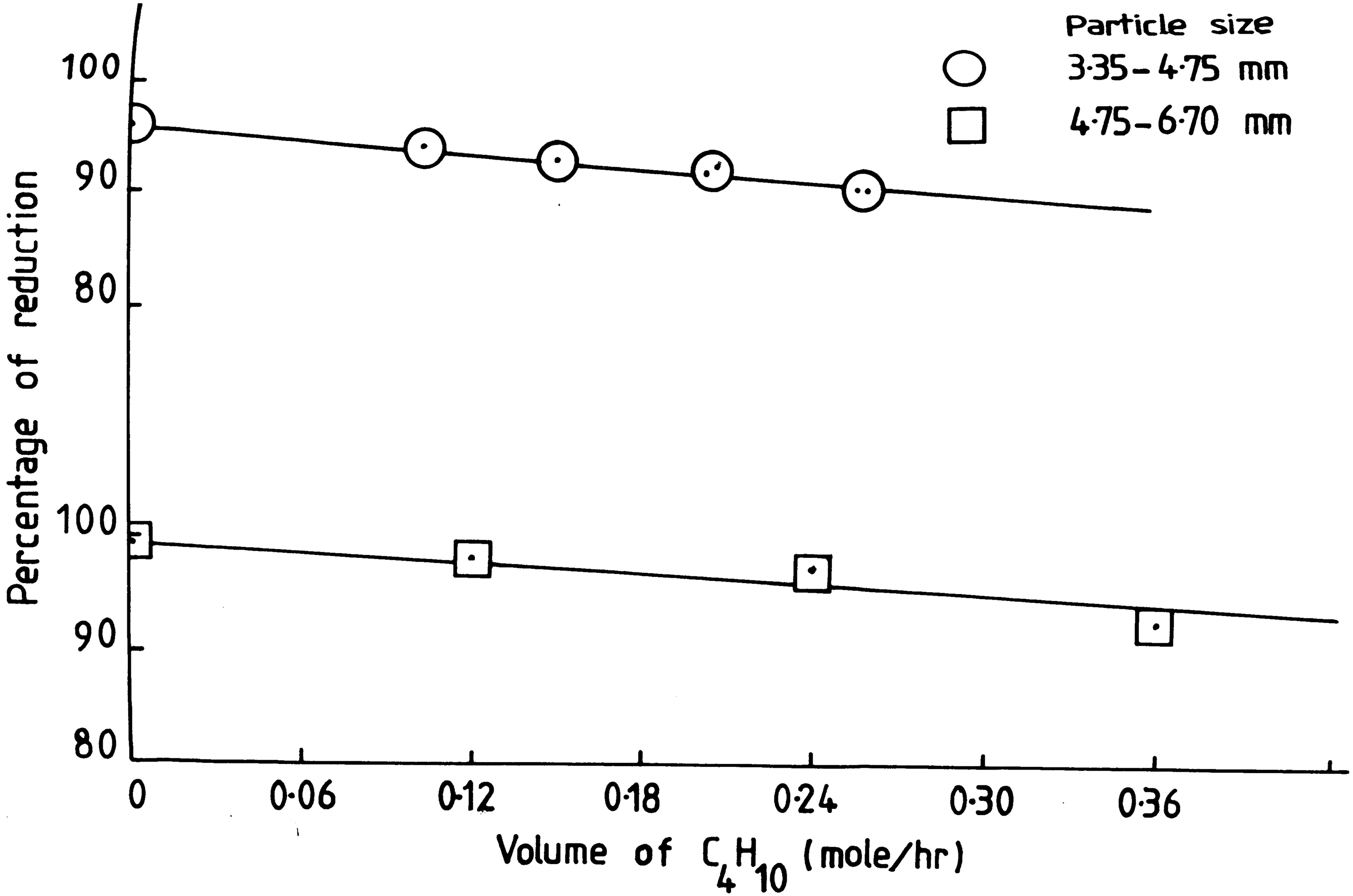

Fig. 66. The effect of amount of hydrocarbon (C_4H_{10}) in the mixture of input gases upon percentage reduction for run series (RP_2S_{11}, RP_2S_{12}).

PAGE NUMBERING AS ORIGINAL

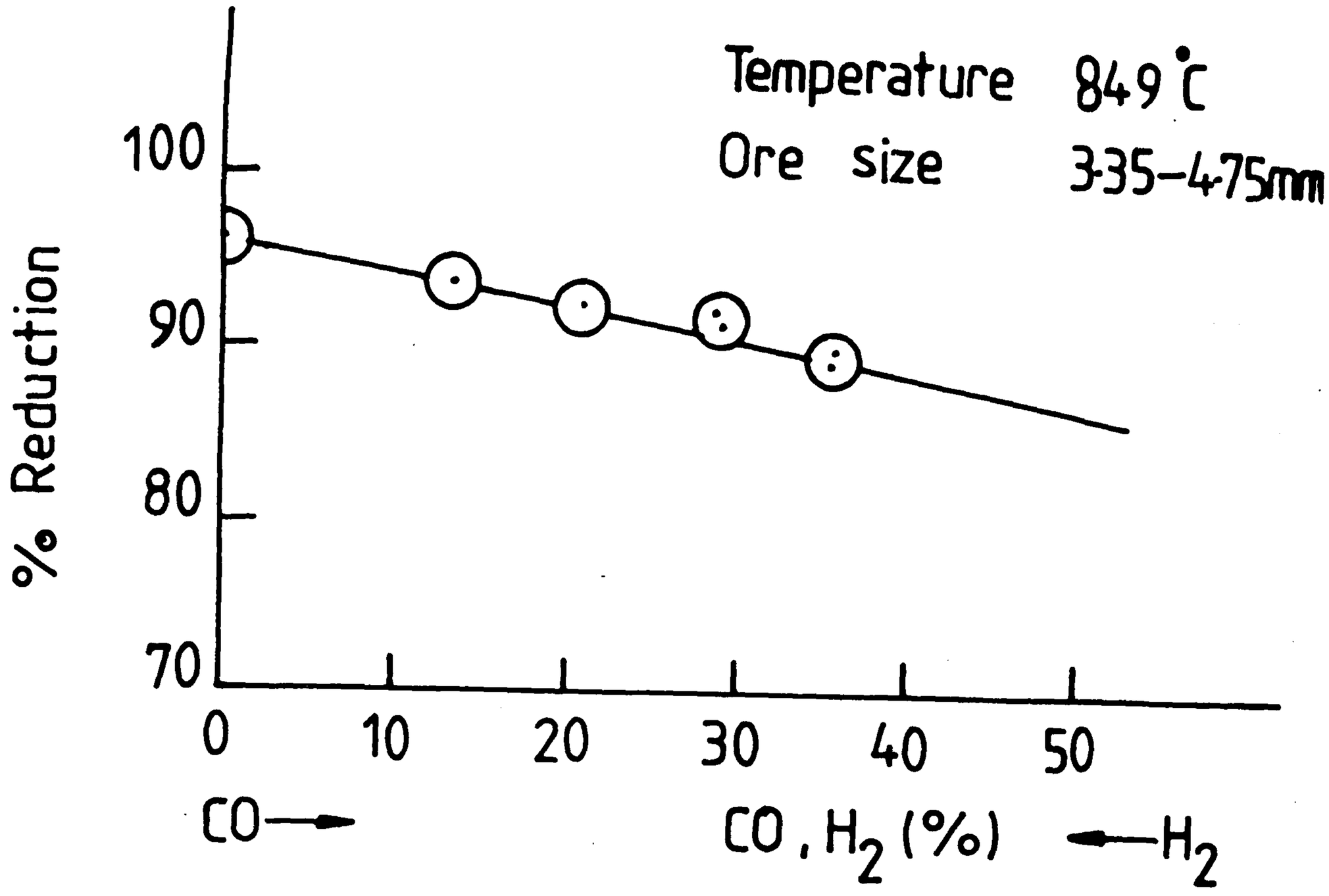

Fig. 67. The effect of ratio of CO/H_2 in the mixture of reducing gas (after autocatalytic reforming of C_4H_{10} in the kiln) upon percentage reduction, for the run series RP_2S_{11}.

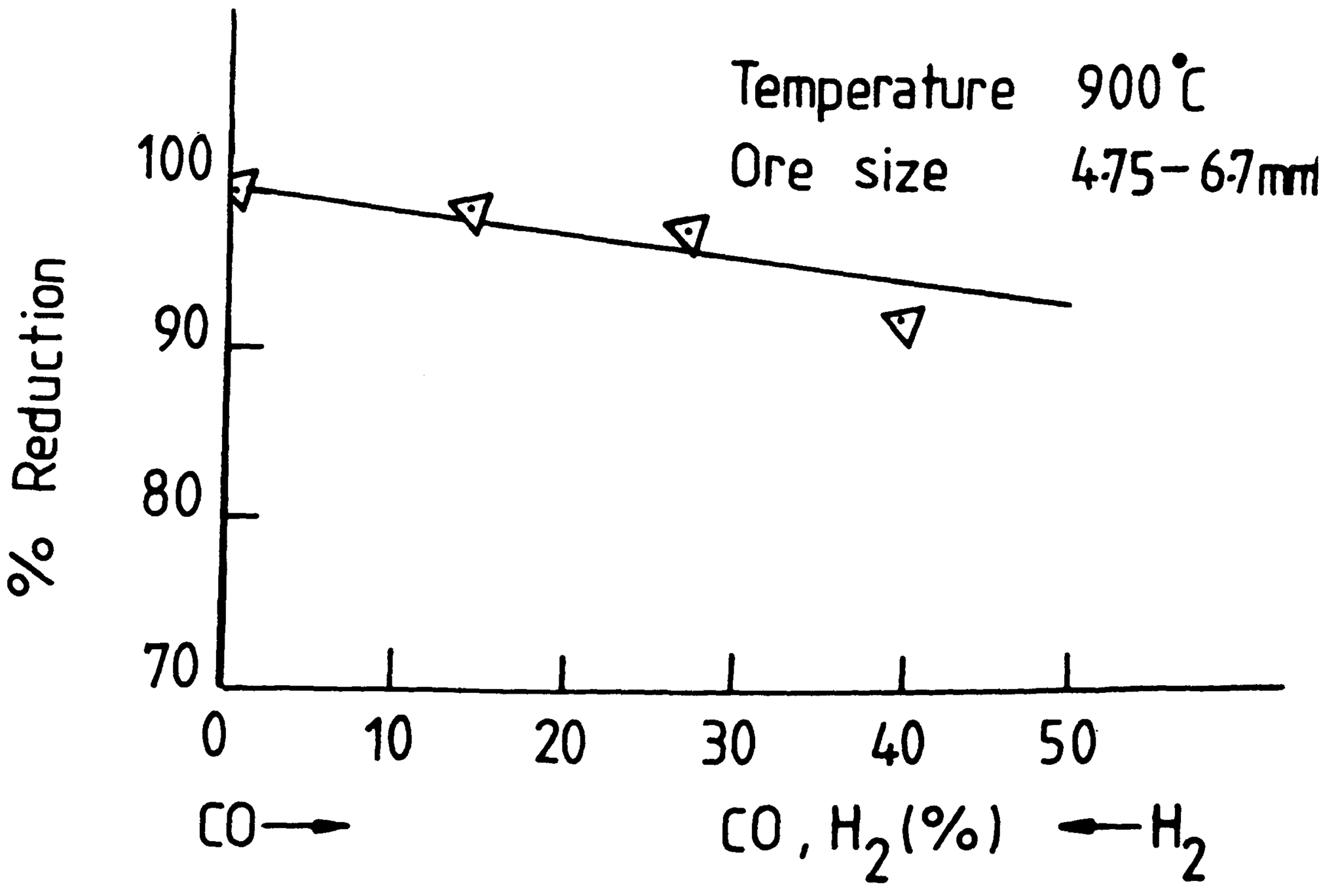

Fig. 68. The effect of ratio of CO/H_2 in mixture of reducing gas (after autocatalytic reforming of C_4H_{10} in the kiln) upon percentage reduction, for the run series RP_2S_{12}.

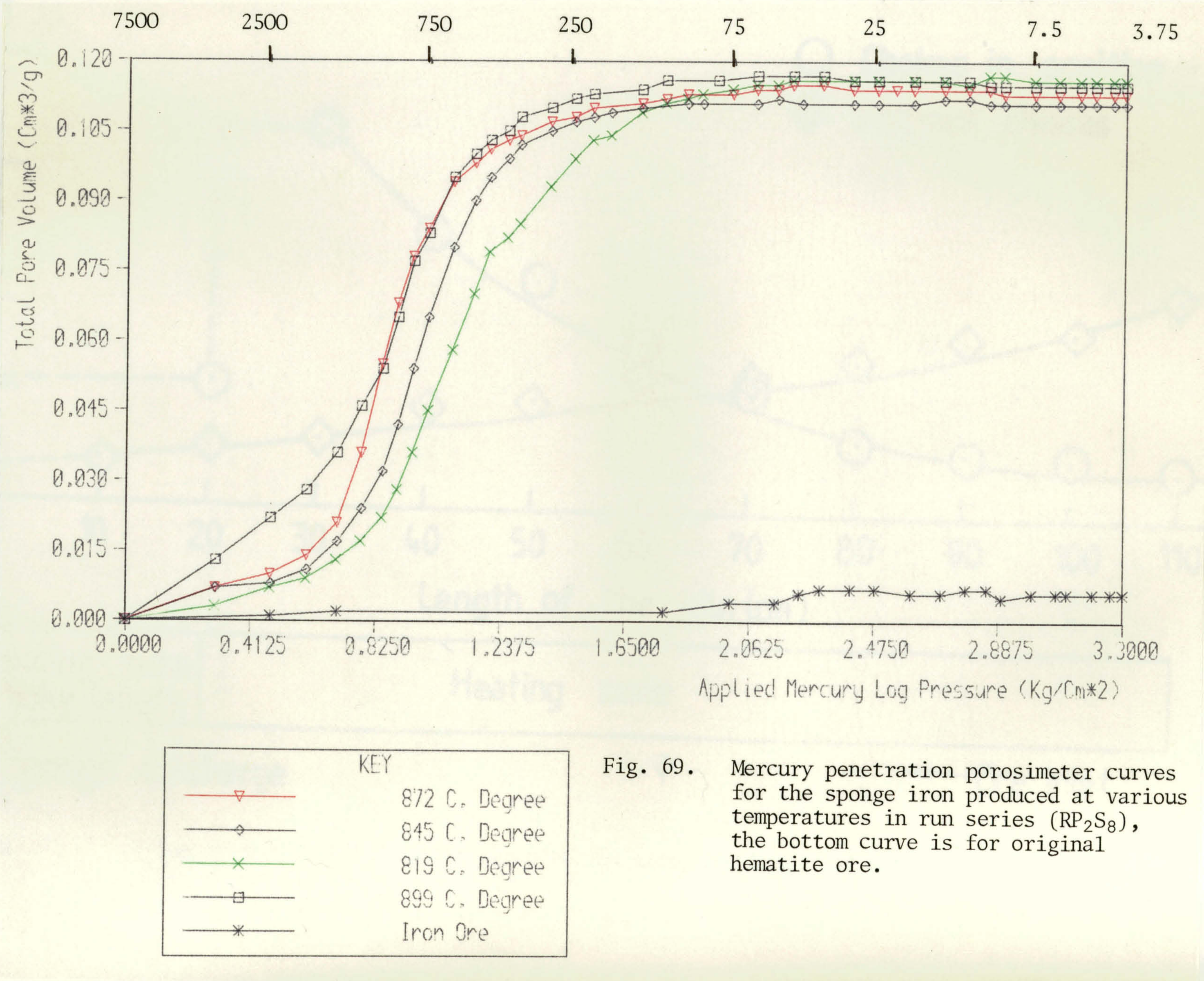

Fig. 69. Mercury penetration porosimeter curves for the sponge iron produced at various temperatures in run series (RP_2S_8), the bottom curve is for original hematite ore.

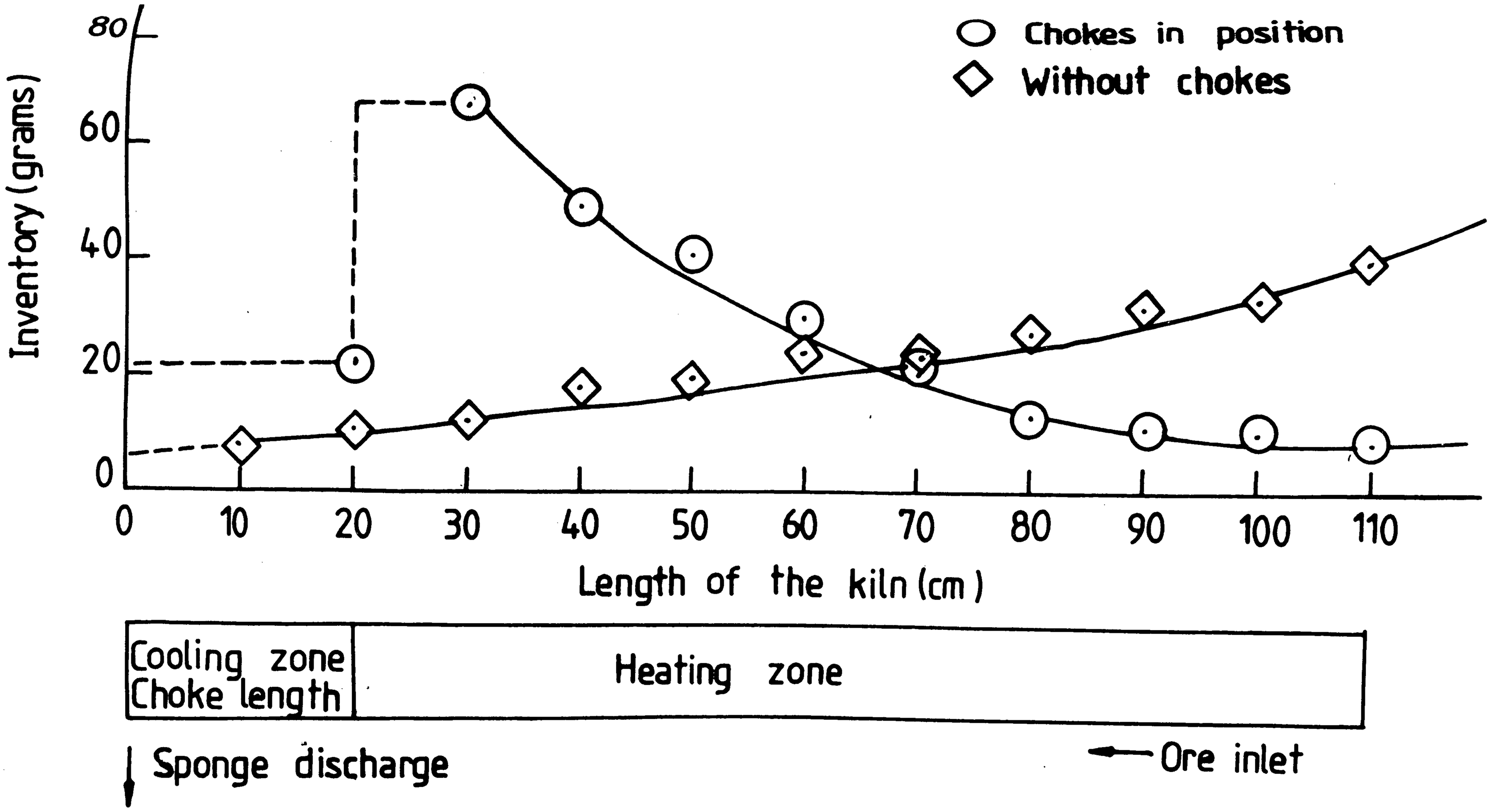

Fig. 70. A comparison of the inventory distribution along the length of the kiln for two manners of experiments.

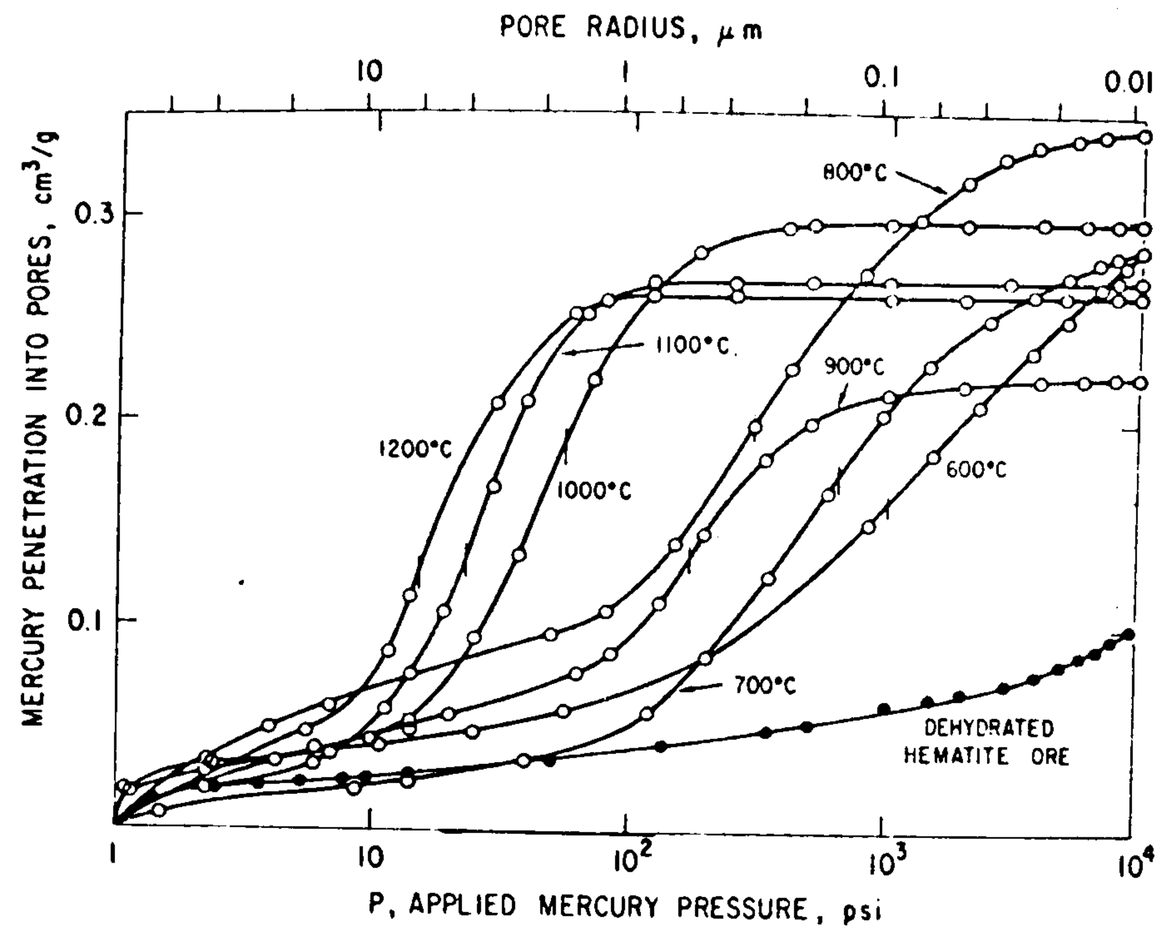

Fig. 71. —Connected (≈total) pore volume of iron reduced from hematite ore in hydrogen at various temperatures; lower curve is for dehydrated hematite ore.

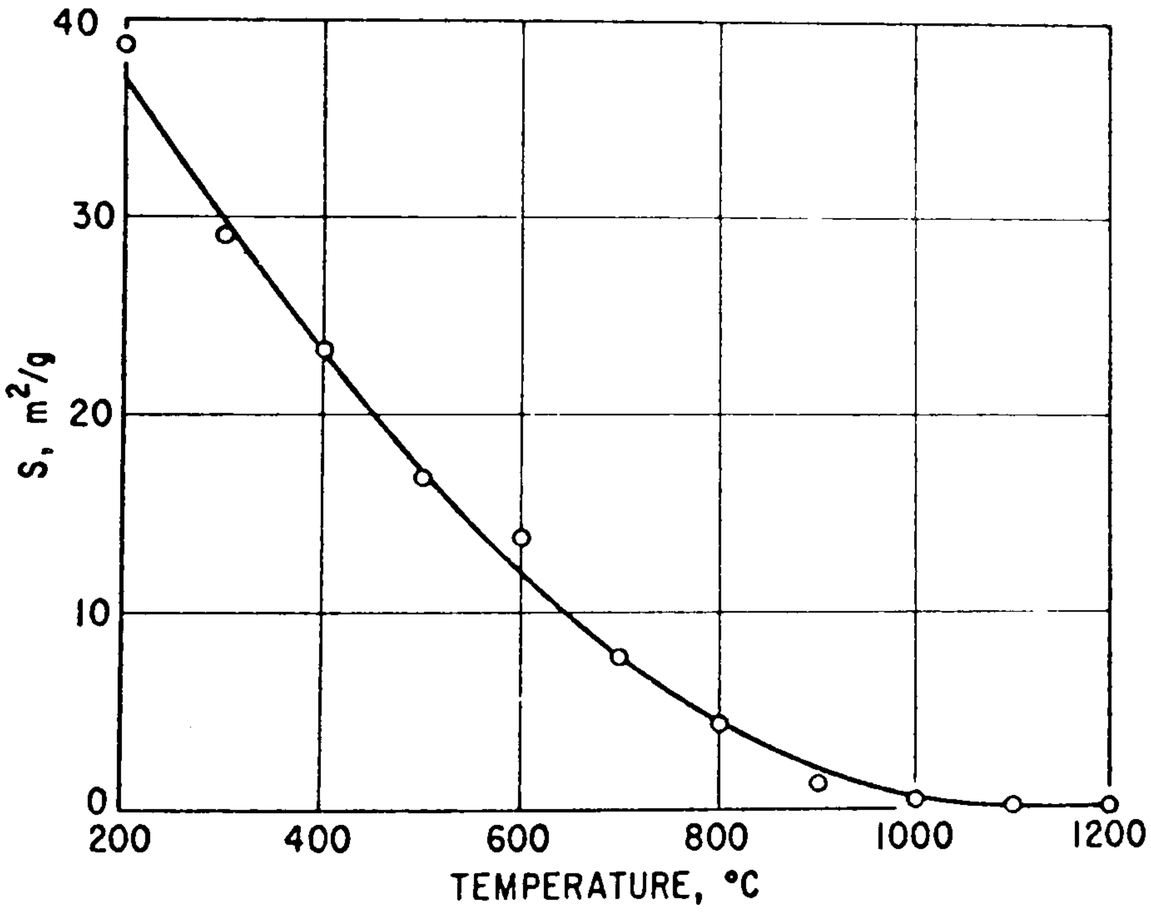

Fig. 72. —Pore surface area of iron reduced from hematite ore in hydrogen as a function of reduction temperature.

Gas Flow Calibration (Nitrogen)

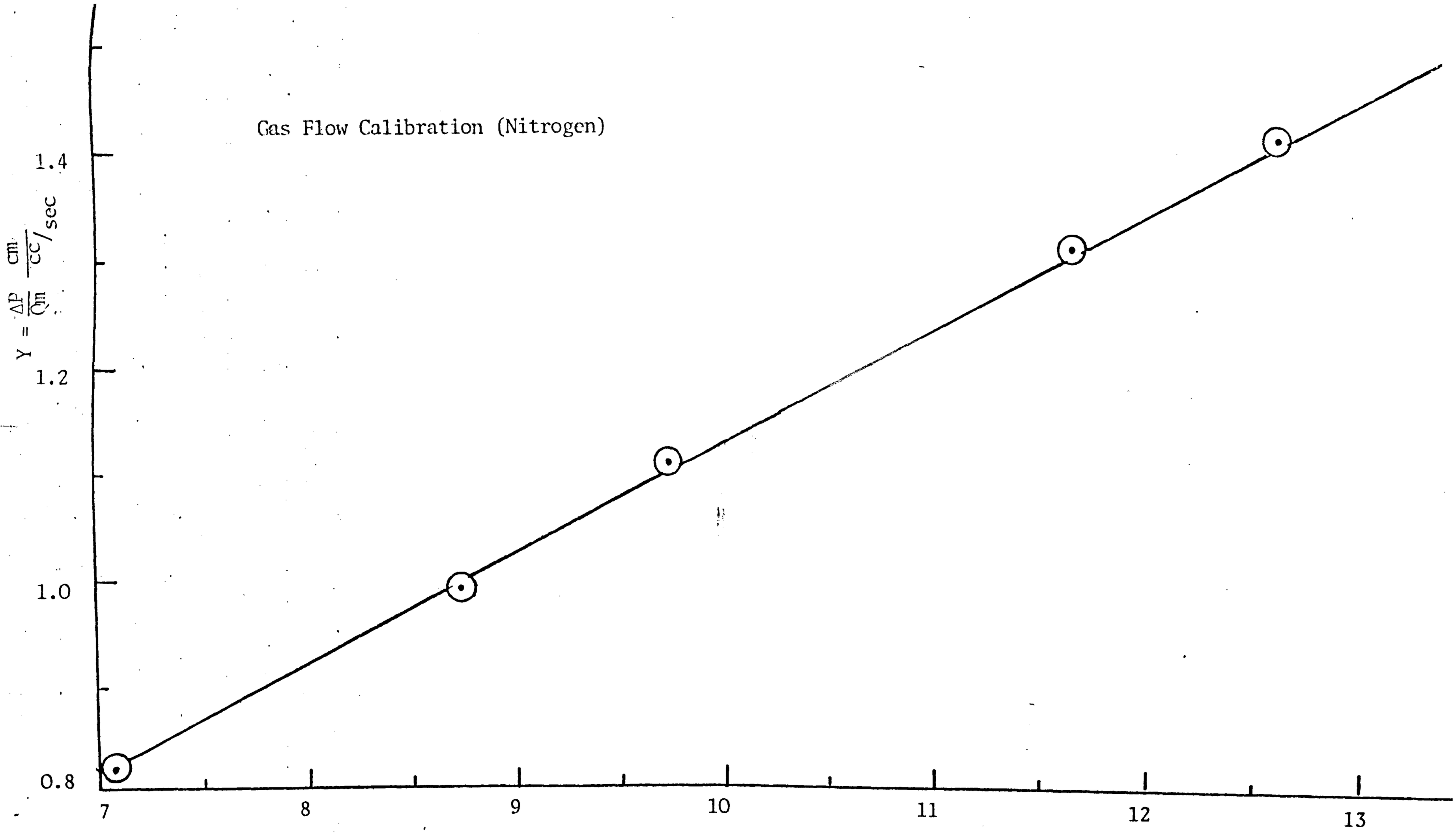

FIG. 73. Showing the straightline relationship of equation $Y = \frac{\Delta P}{Qm} = 0.10604Qo(X) + 0.07339$

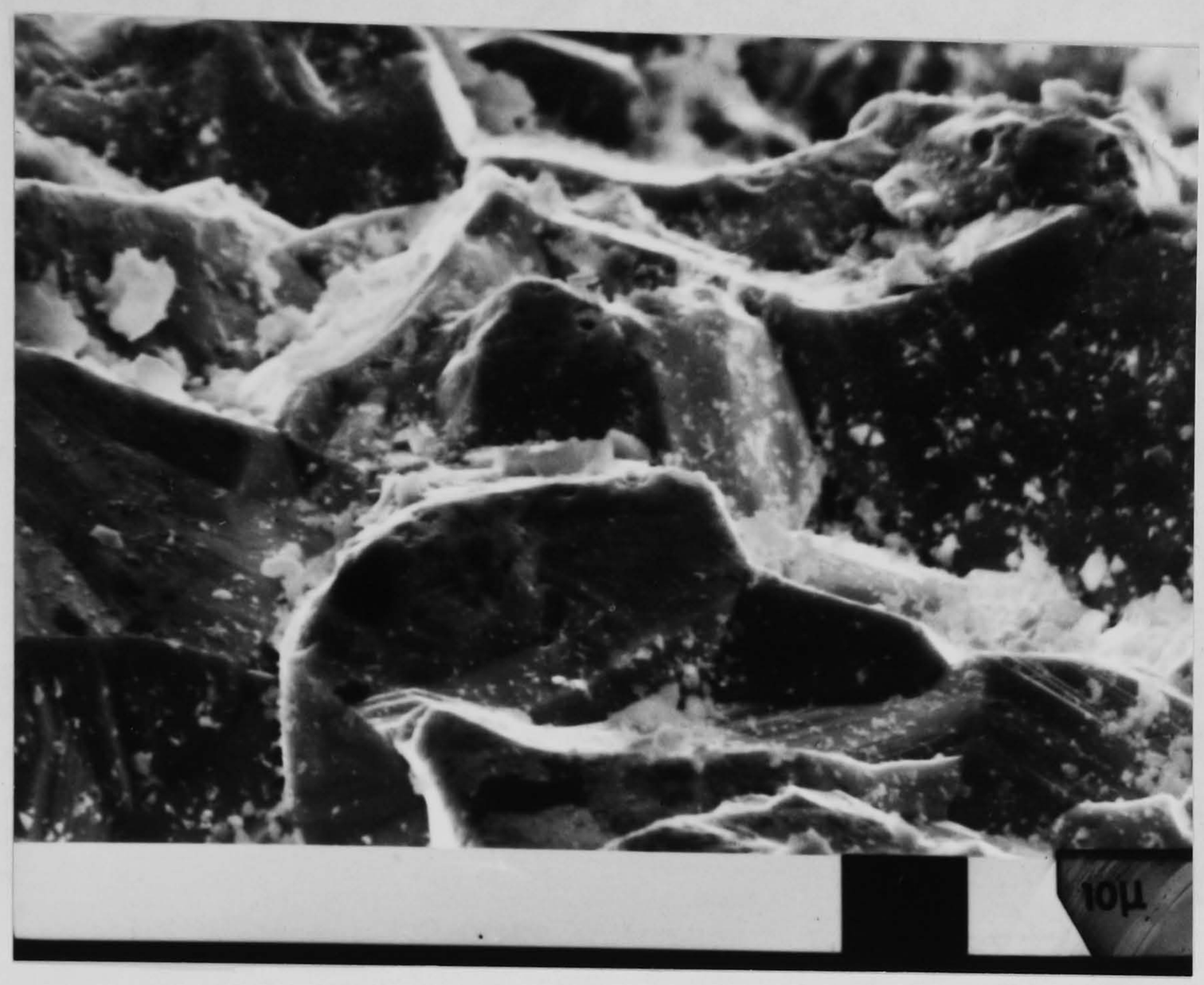

Scanning Electron Micrograph A: The dehydrated original iron ore particle x 2000

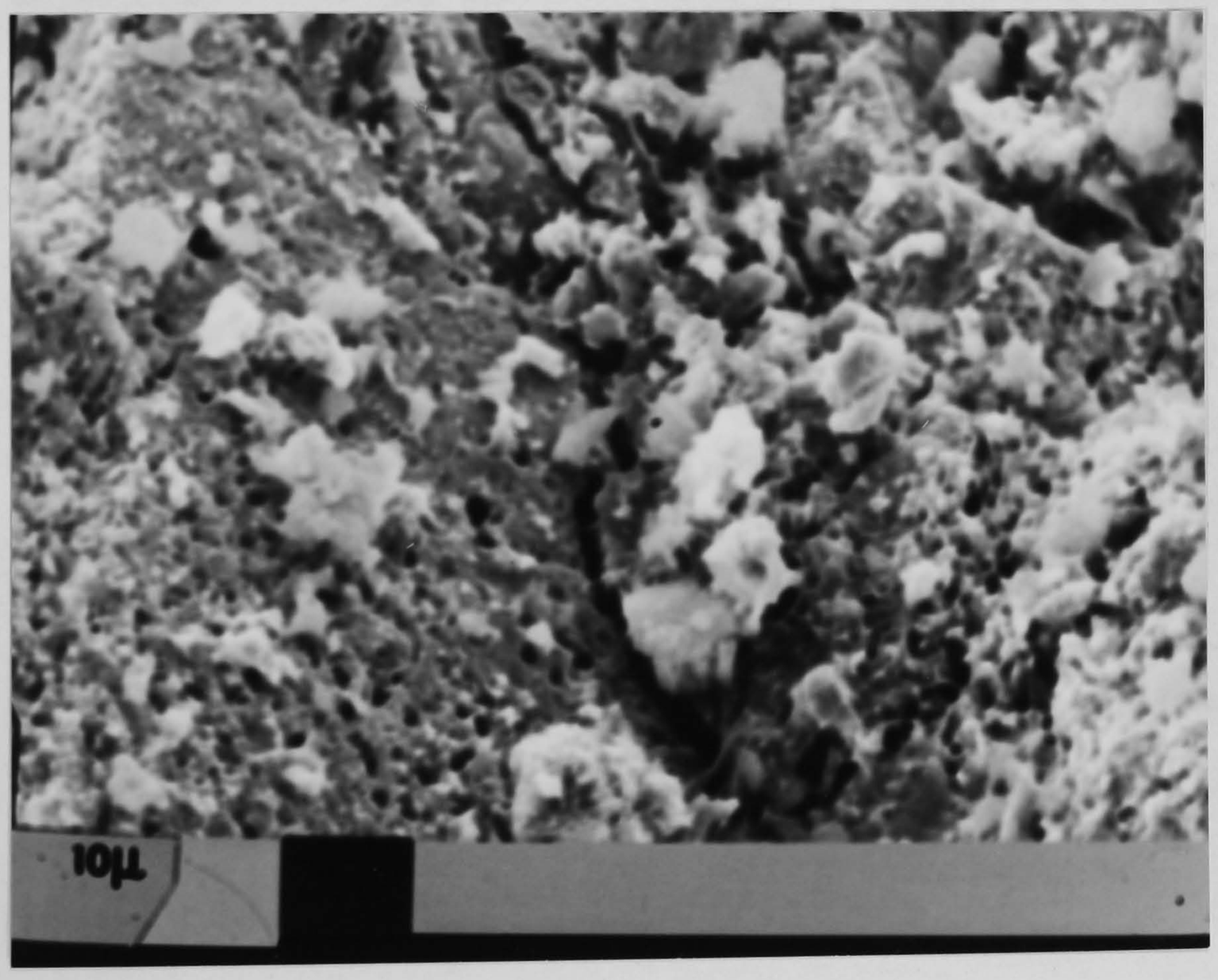

Scanning Electron Micrograph B: Sponge produced at 773°C, Run No. 4. x 2000

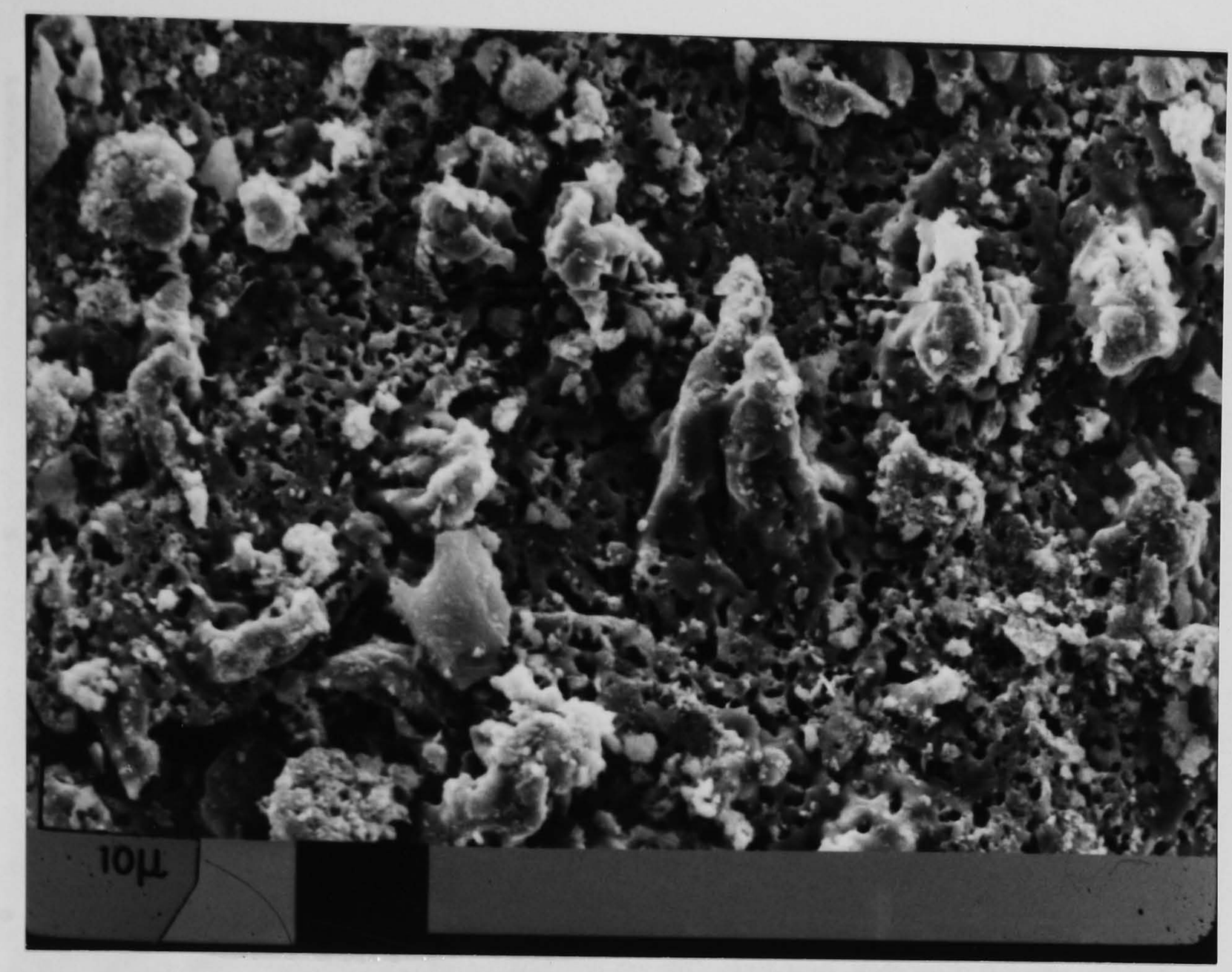

Scanning Electron Micrograph C: Sponge produced at 829°C
Run No. 2. x 2000

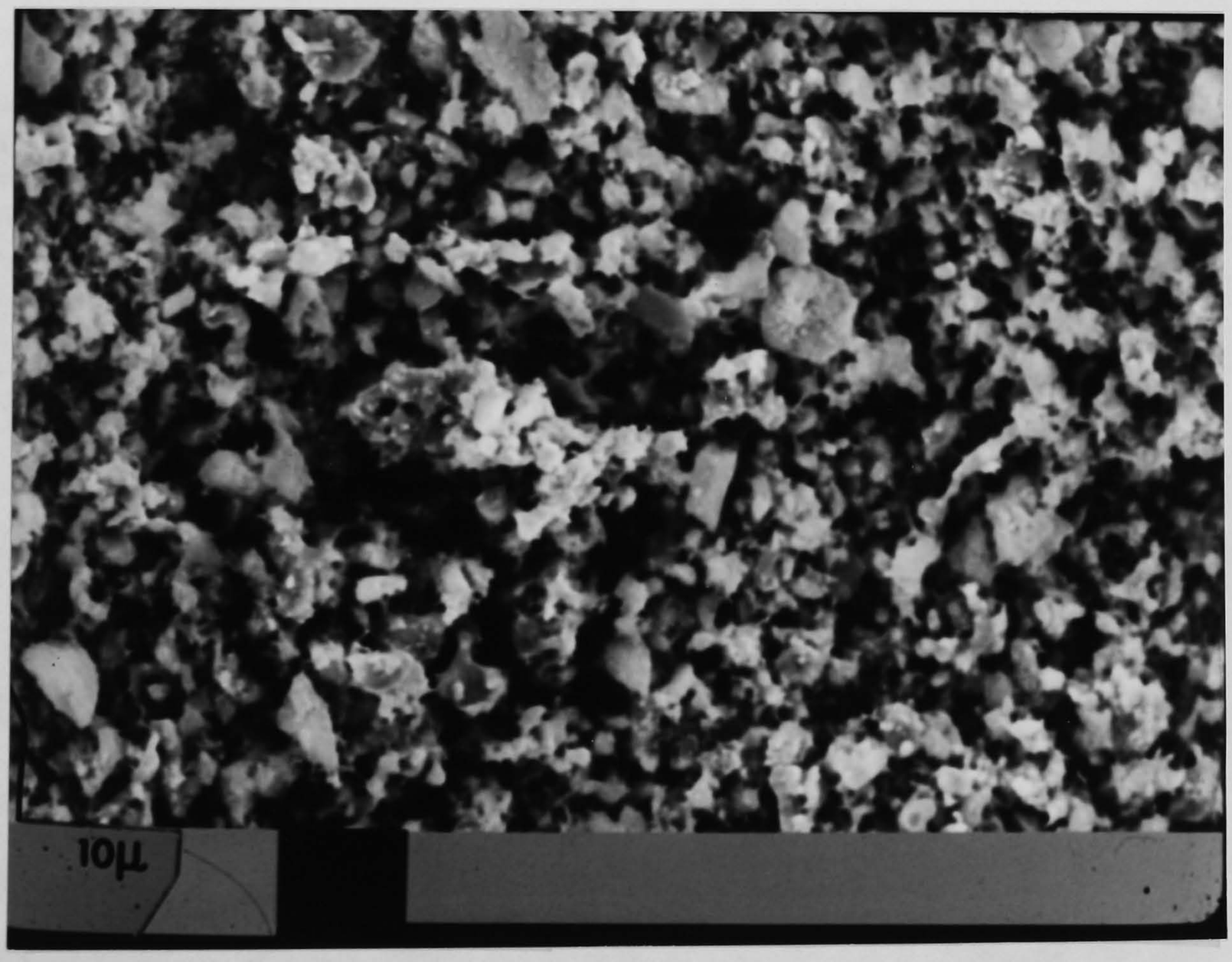

Scanning Electron Micrograph D: Sponge produced at 878°C,
Run No. 8. x 2000

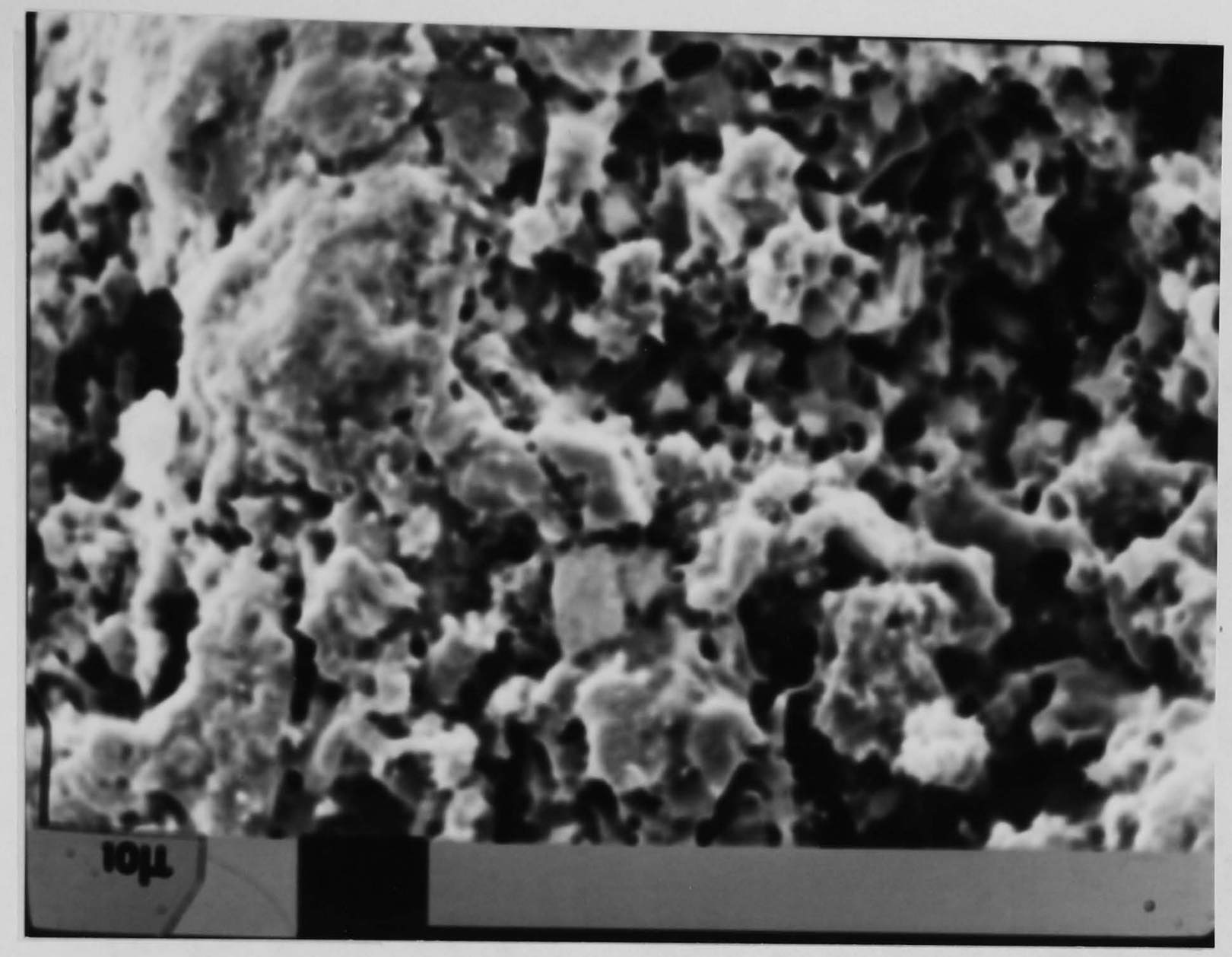

Scanning Electron Micrograph E: Sponge produced at 878°C
Run No. 8. x 2000

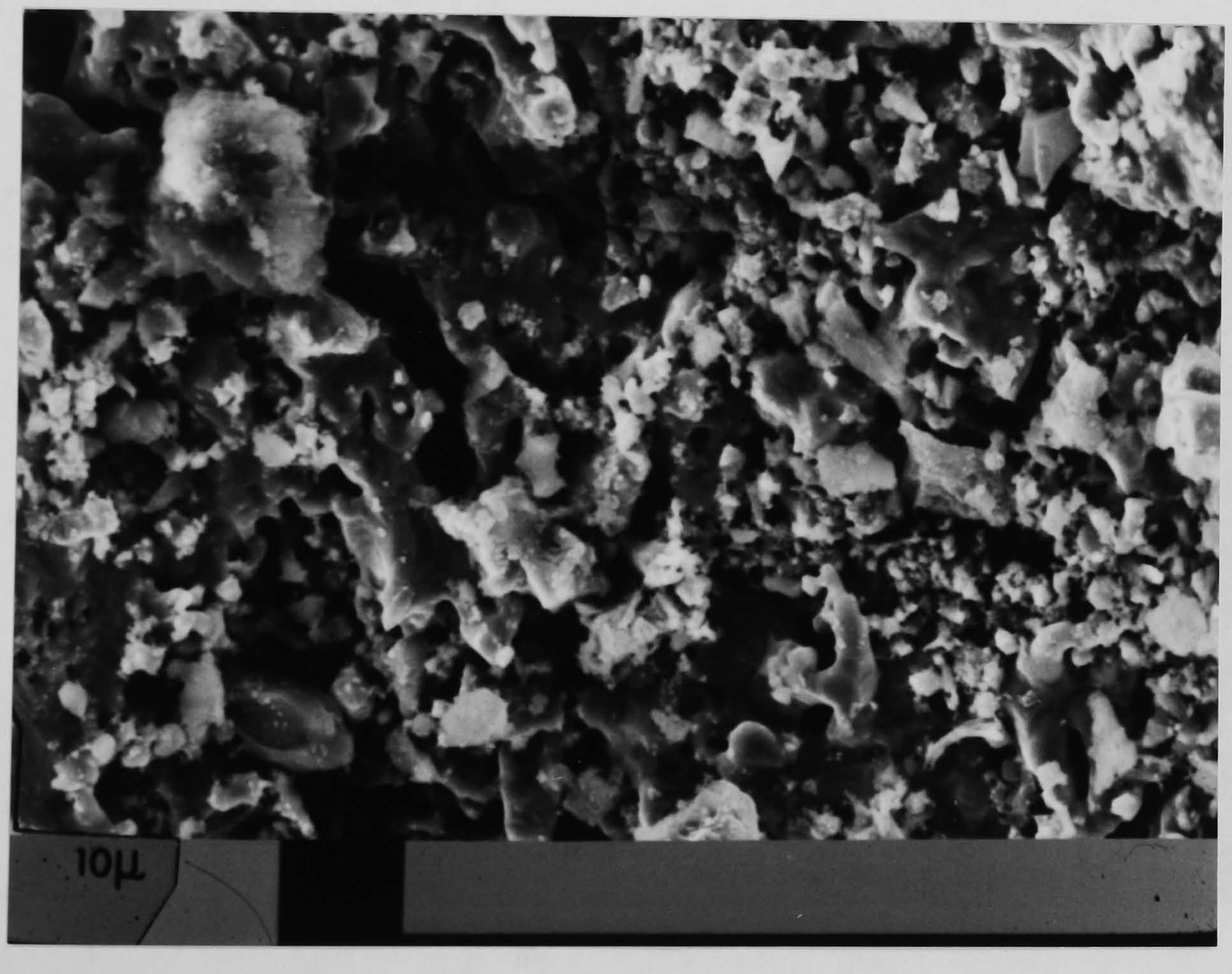

Scanning Electron Micrograph F: Sponge produced at 889°C,
Run No. 9. x 2000

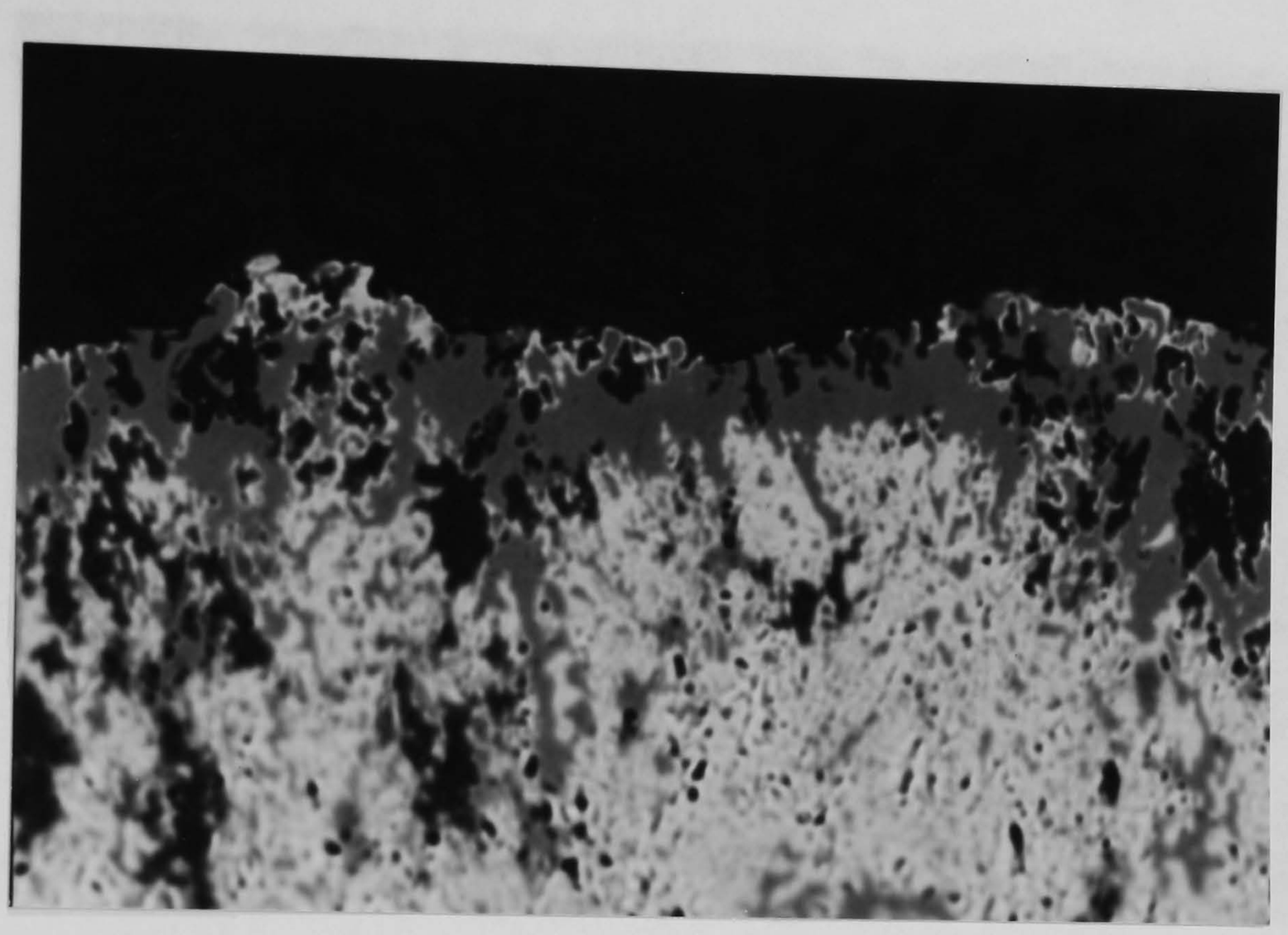

Optical Microscopic Micrograph G: Sponge produced at 870°C
Run No. 21, etched in 2% Nital. x 500

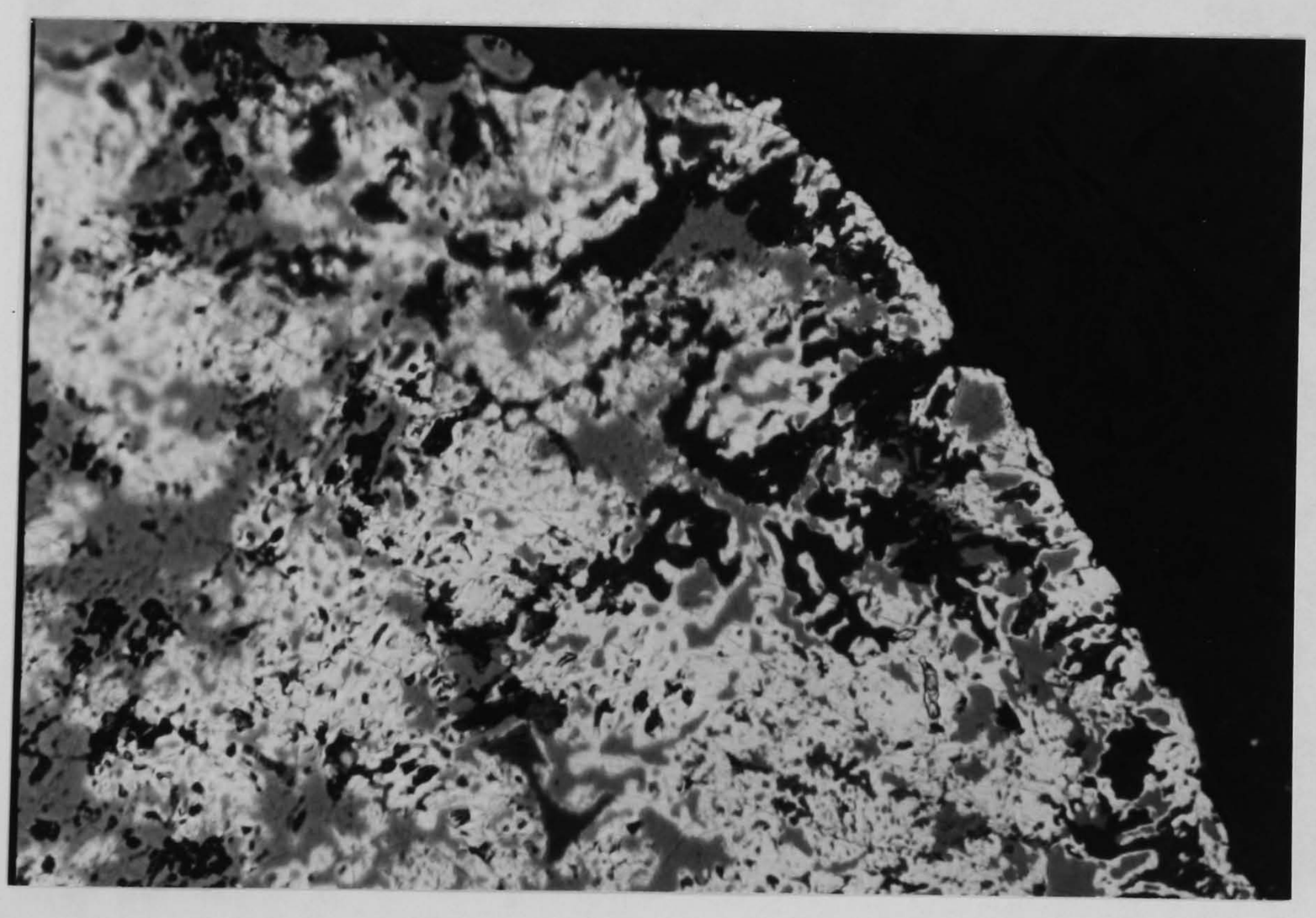

Optical Microscopic Micrograph H: Sponge produced at 870°C,
Run No. 21, etched in 2% Nital. x 500

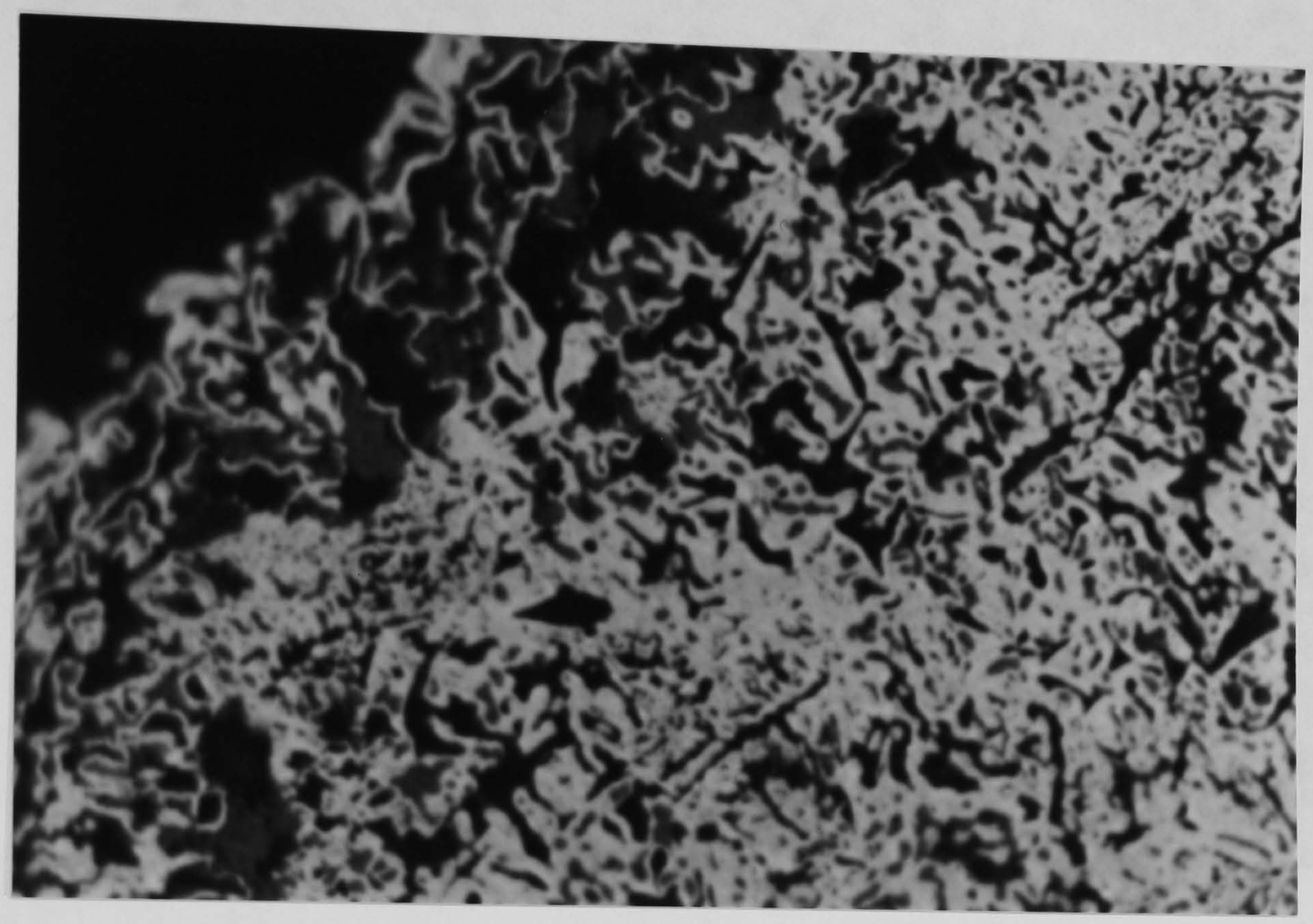

Optical Microscopi Micrograph I: Sponge sample 10 from exit of the kiln, Run No. 38. x 500

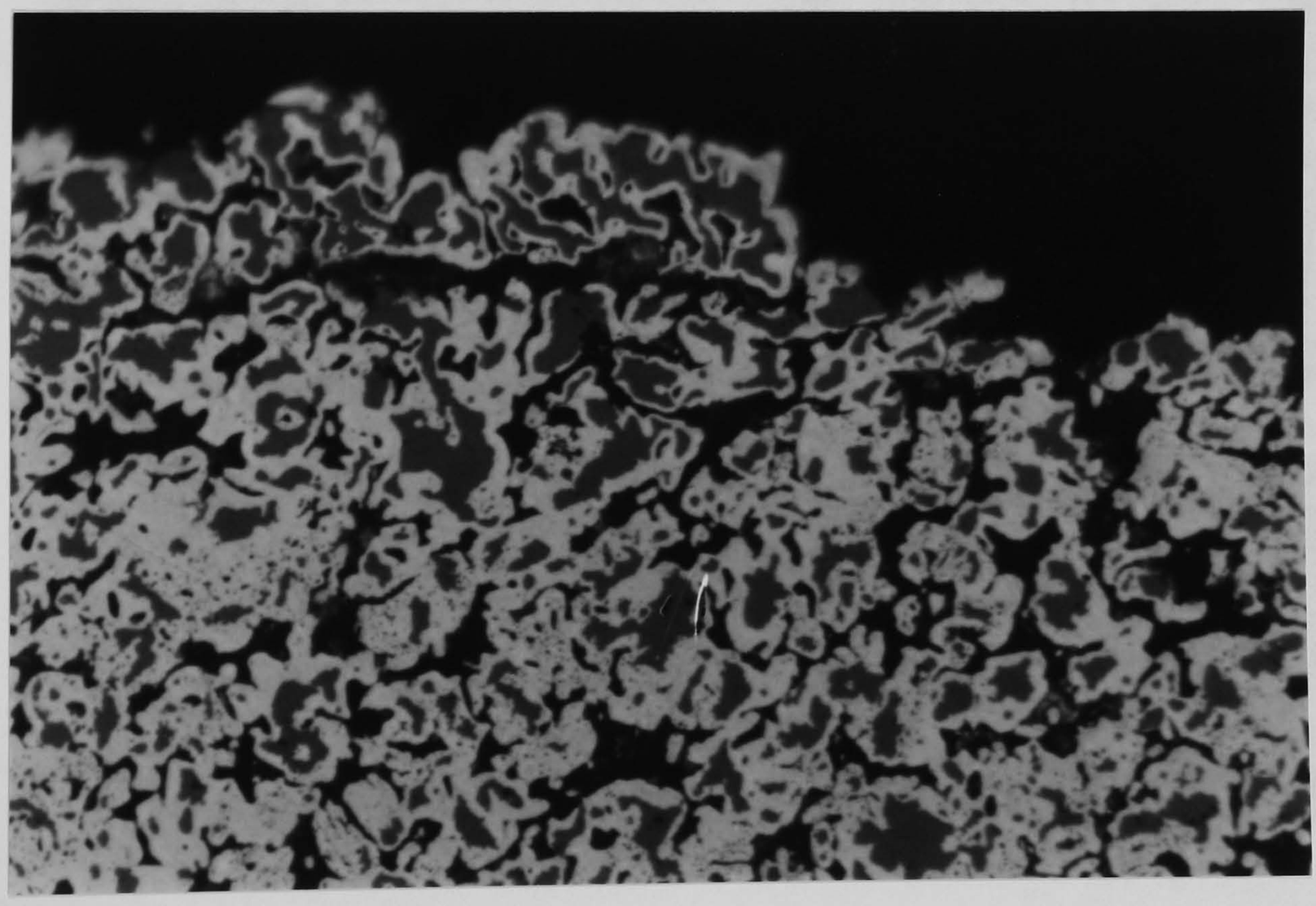

Optical Microscopic Micrograph J: Sponge sample 60 from exit of the kiln, Run No. 38. x 500

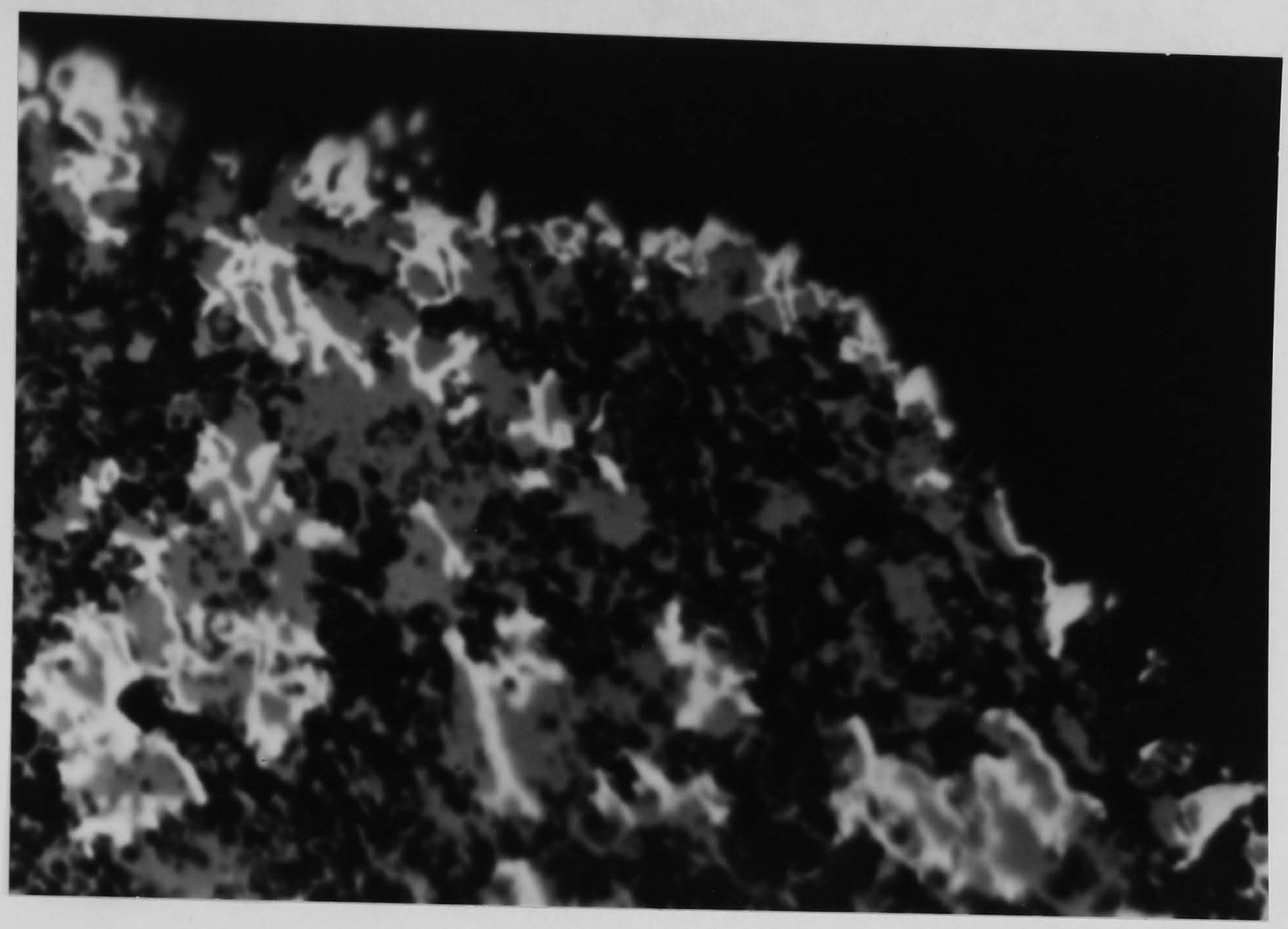

Optical Microscopic Micrograph K: Sponge sample 80 from exit of the kiln, Run No. 38. x 500

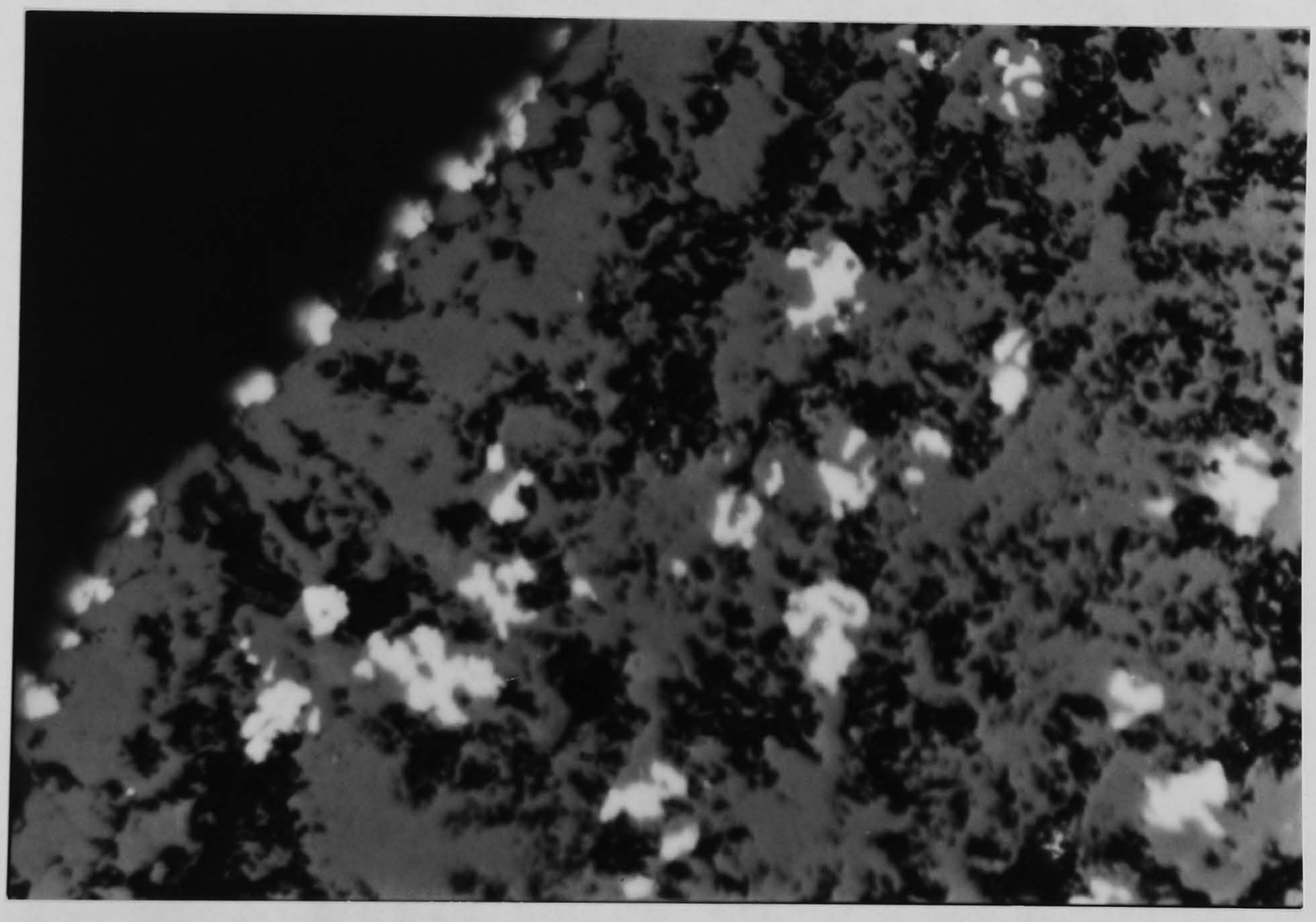

Optical Microscopic Micrograph L: Sponge sample 90 from exit of the kiln, Run No. 38. x 500

Scanning Electron Micrograph M: Sponge produced at 819°C
Run No. 40. x 2000

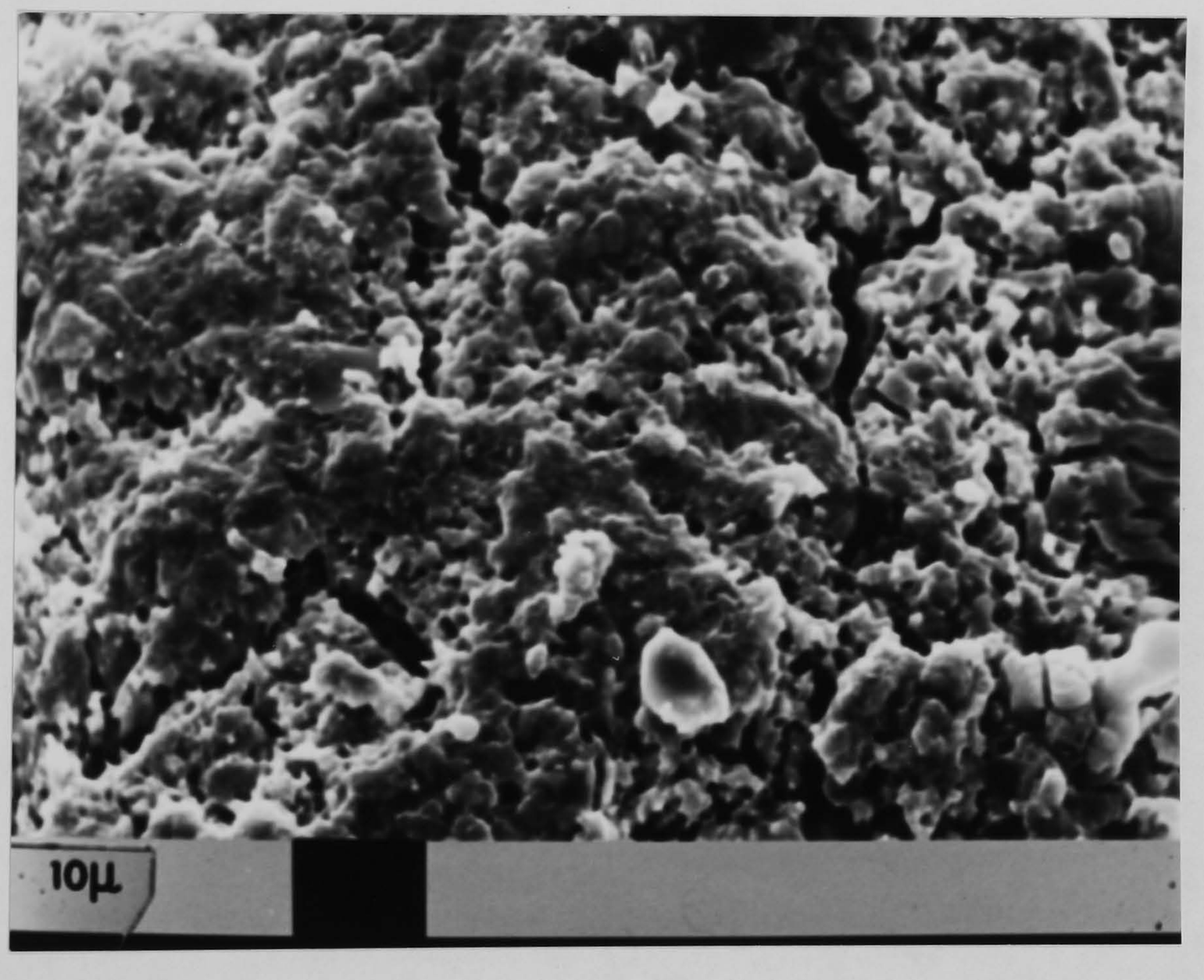

Scanning Electron Micrograph N: Sponge produced at 845°C,
Run No. 42. x 2000

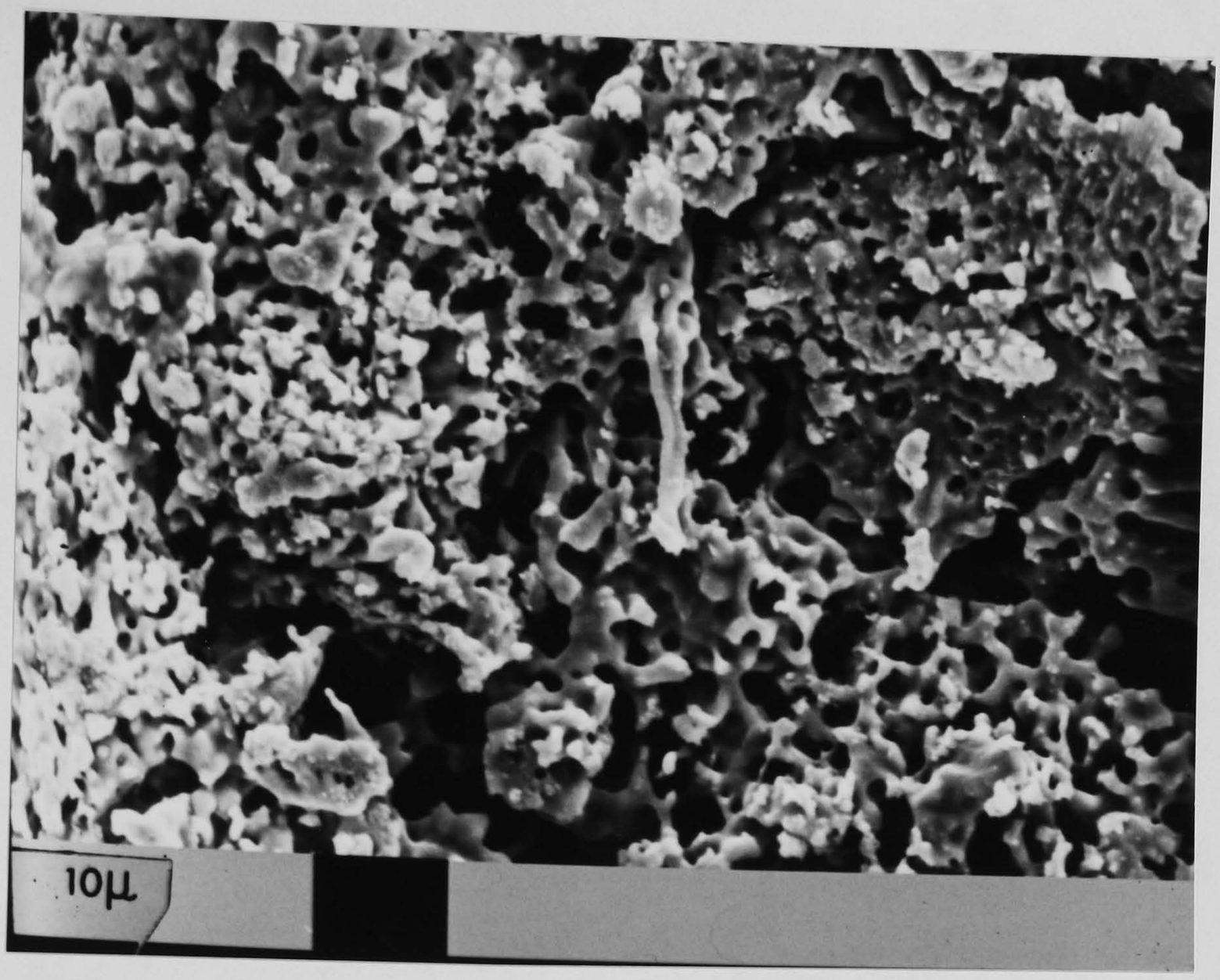

Scanning Electron Micrograph O: Sponge produced at 872°C, Run No. 44. x 2000

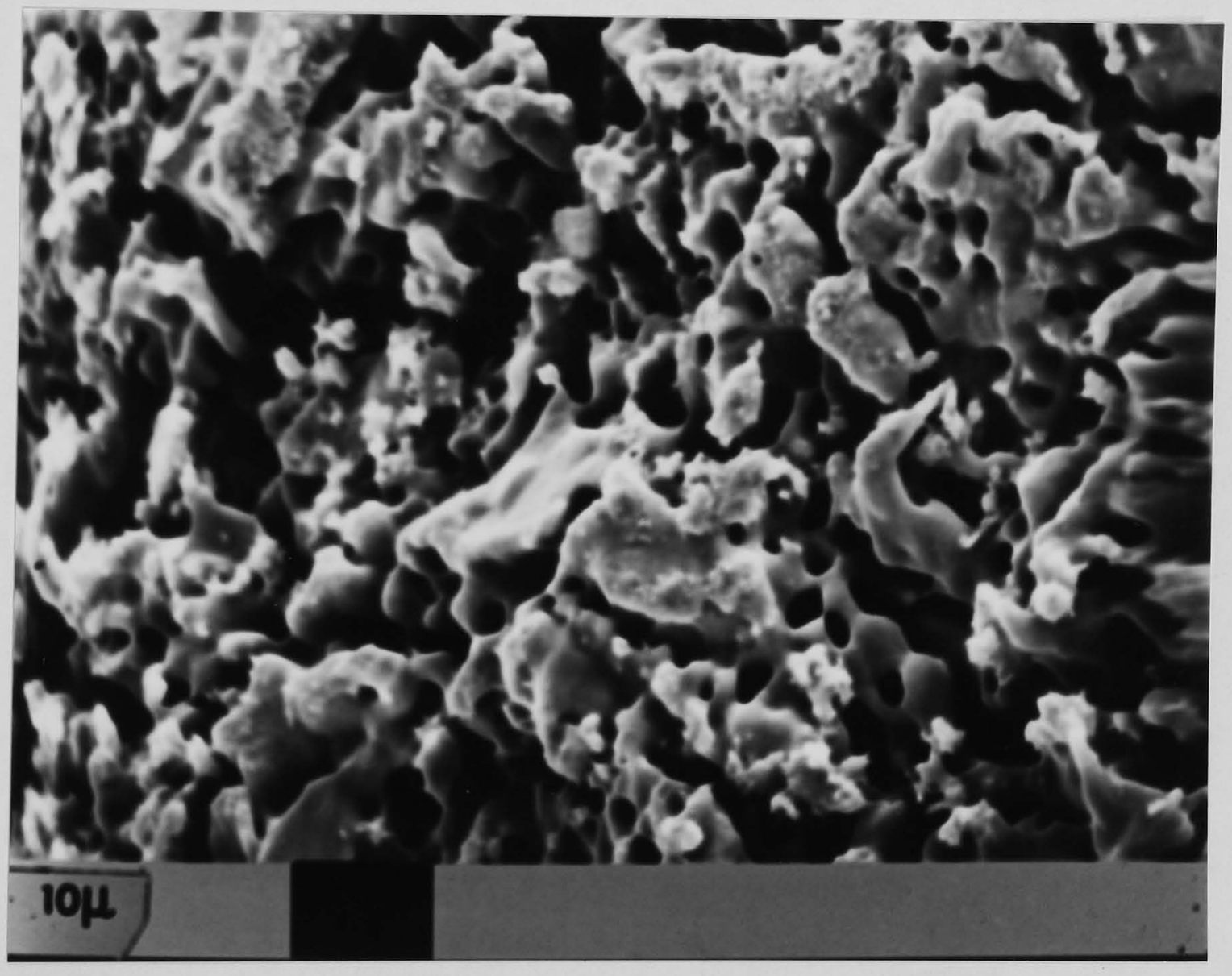

Scanning Electron Micrograph P: Sponge produced at 899°C, Run No. 45. x 2000